Investigating Factors affecting the Development of Wheat Spike Blast Caused by the Triticum and Lolium Pathotypes of *Magnaporthe oryzae*

DISSERTATION

Presented in Partial Fulfillment of the Requirements for the Degree Doctor of Philosophy in the Graduate School of The Ohio State University

By

Karasi B Mills

Graduate Program in Plant Pathology

The Ohio State University

2021

Dissertation Committee

Dr. Laurence V. Madden, Advisor

Dr. Pierce A. Paul, Co-Advisor

Dr. Guo-Liang Wang

Dr. Clay Sneller

Abstract

Wheat blast, caused by the Triticum pathotype of the fungus *Magnaporthe oryzae* (MoT), poses a significant threat to global wheat production, as it is capable of causing 100% yield loss during seasons with highly conducive environmental conditions. Wheat blast has been endemic in wheat growing regions of South America since the 1980's and has recently been reported in Bangladesh (2016), India (2017), and Zambia (2017). Incursion of the wheat blast pathogen into Asia and Africa likely occurred through contaminated grain originating from South America, as results from whole-genome sequencing showed that isolates causing the disease in affected countries were closely related to MoT isolates from South America. Although MoT has not been reported in North America, the Lolium pathotype of *M. oryzae* (MoL) is a native pathogen that causes gray leaf spot on perennial ryegrass that is present in wheat-producing areas of the U.S. One blast-affected spike was found in Kentucky in 2011 and genetic analysis confirmed that it was caused by an isolate of the local MoL pathotype. Prior controlled-environment studies have shown that U.S. wheats are susceptible to both MoT and MoL. To determine the risk posed by MoL to U.S. wheat, two controlled-environment studies were conducted to identify environmental-, pathogen-, and host-related factors that were most conducive for wheat blast development from the native MoL. Additionally, studies were conducted to model the development of spike blast in an area of Bolivia where the wheat blast is endemic

in an effort to quantify the temporal and spatial dynamics of the disease under naturally conducive field conditions.

The objectives of the first controlled-environment study were to quantify the effects of temperature (TEMP) and initial high relative humidity (RH) duration on MoL infection and spread within winter wheat spikes, and to model the temporal change in wheat blast intensity as influenced by TEMP and RH duration. Cohorts of wheat spikes were inoculated at anthesis and immediately subjected to different combinations of TEMP (20, 25, and 30˚C) and high (> 95%) RH duration (0, 3, 6, 12, 24, and 48 h). Blast developed under all tested conditions, with both incidence (INC) and severity (SEV) increasing over time. The highest mean levels of spike blast and the greatest temporal rates of increase in INC and SEV were observed at 25 and 30˚C, with 24 and 48 h of high RH immediately after inoculation. The Gompertz growth model best described epidemics that developed at 25 and 30oC with high RH duration greater than 12 h. In the second growth chamber study, the effects of inoculum density and crop growth stage at time of infection on the development of spike blast on wheat cultivars with different levels of susceptibility were determined. Both tested cultivars were infected with MoL from early spike emergence through watery ripe, developing similar final levels of spike blast INC and SEV. MoL inoculum density and cultivar susceptibility affected spike blast onset and temporal development, with disease intensity and rate of increase per unit increase inoculum density being greater for the highly susceptible (HS) than the moderately susceptible (MS) cultivar. The Gompertz model appropriately described the INC and SEV progress curves for most

combinations of cultivar and inoculum density. The rate of increase in disease intensity was greater on the HS cultivar than on the MS cultivar at high inoculum densities. From these two studies, the conclusions were that the window of wheat susceptibility to MoL was fairly wide, and that MoL-incited blast was a polycyclic-type disease at the spikelet level that poses the greatest threat to US wheat on HS cultivars under warm, humid conditions at high inoculum density.

To address key knowledge gaps in the epidemiology of wheat blast, research was conducted to monitor, model, and compare naturally occurring wheat spike blast epidemics in Bolivia. The objectives of the third study were to quantify the temporal progress of spike blast under different growing conditions, estimate time to specific spike blast severity thresholds as influenced by local conditions, and determine the effect of leaf blast severity (LEAF) on spike blast epidemics. Six plots of the highly susceptible wheat cultivar Atlax were planted at different times (15 April, 20 April, and 8 May) at three locations in the Santa Cruz de la Sierra region of Bolivia, Okinawa 1 (OK1), Okinawa 2 (OK2), and Cuatro Cañadas (CC). Spike and disease emergence were similarly staggered, and disease intensity on leaves and spikes were assessed approximately every three days on a 10 x 10 grid with nodes (sampling locations) approximately 2.55 m apart. Spike blast increased over time for as many as 20-30 days before approaching a final mean incidence (INC) of 100%, and a mean spike severity (SEV) of 60 to 75%. The logistic model was the most appropriate for describing the temporal dynamics of spike blast. The highest absolute rates of disease increase occurred earliest at OK1 and latest at OK2, and in all cases, coincided with major

rain events. Estimated y0 values (initial blast intensity) were significantly ($P < 0.05$) higher at OK1 than at CC or OK2, whereas estimated rL values (the logistic rate parameter) were significantly higher at OK2 than at CC or OK1. It took about 10 fewer days for spike blast SEV to reach thresholds of 10, 15, or 20% at OK1 compared to OK2 and CC. For every 5% increase in LEAF, the chance of SEV reaching the critical thresholds by 21 days after heading increased by 30 to 55%.

In a fourth study, the spatial pattern of wheat blast was analyzed using the same set of data collected form the Bolivian research plots. The objectives were to characterize the spatial patterns of INC, SEV, and LEAF to determine if there was significant clustering or aggregation, ascertain if there were temporal trends of aggregation, and determine if there were different trends in aggregation among INC, SEV, and LEAF. All measures of wheat blast were intensively sampled at a lattice of 100 nodes in every plot. At each rating time (6 for OK1 and OK2, 9 for CC), the Moran's I spatial autocorrelation coefficient was calculated for the logit transformation of each disease variable (INC, SEV, LEAF), and significance was determined using the standard normal statistic (Z). Significant I values indicated that disease intensity values in neighboring sampling nodes were more likely to be similar than values at greater distances, whereas a non-significant I indicated that the pattern was indistinguishable from random. The fit of general linear mixed models indicated that rating time, disease response variable, location, and their interactions had significant effects on I. The least square means for OK1, the earliest planted field, were significantly different from OK2 and CC. Interaction means confirmed that CC had the

lowest means or equal to the lowest means for all measures of disease (0.04, 0.12), and that the highest means were for LEAF at OK1 (0.39) and OK2 (0.25), and SEV at OK1 (0.32). At OK1, 95% of the I values were significant, 66% at OK2, and only 42% at CC, the latest-planted location. There was no overall trend in I with rating time or level of disease within plots, and the interaction means indicated that rating time had only minor impact on the differences in I between measures of disease and locations. Although non-random spatial aggregation was more common at earlier plantings, final INC, SEV, and LEAF levels were lowest at OK1 (86, 57, 37%) than at OK2 (100, 72, 53%) and CC (95, 71, 87%). Results from the temporal and spatial analyses of the natural wheat blast epidemic in Bolivia provide new insight into the epidemiology of this disease and clues as to factors driving epidemics.

I dedicate this dissertation to my companions
who helped me pursue happiness during these many years of research. To my most cherished friend and husband, Matt, who encouraged me to persevere when I was gone for weeks on end, worked late nights without coming home, and spent weekends and holidays by the growth chambers. He celebrated all my successes, small and large, and buoyed my spirit.
I owe him seven years of vacuuming.

To the women with whom I attended classes, shared early morning coffees, attended conferences, and navigated the peaks and valleys of graduate student life. Thank you, my beloved Anna T., Ashley S., Rachel M., Amanda K., and Becca K., for being the best parts of my graduate school experience. It is for you that some of my heart remains in Ohio.

Finally, to my dearest friends who I met through happenstance. Addy and Divya, I cannot wait to pursue our shared passions together and look forward to having you in the next chapters of my life.

Acknowledgements

I would like to express my deepest appreciation for my advisors, Drs. Pierce Paul and Larry Madden. First and foremost, the completion of this dissertation would not have been possible without their intense efforts and patience. More broadly, they enabled my graduate experience to be a series of adventures. They made sure I attended the annual American Phytopathological Society conferences every year, invited me to a wheat blast conference in Brazil, a biosecurity course in Kansas, and sent me to Bolivia to conduct field research. They broadened my horizons as a scientist, encouraged my scholastic efforts, and were a joy to be around. I am humbled by their intellect and passion.

My degree was supported by a USDA NIFA grant awarded to an international team of scientists for "Novel strategies for managing blast diseases on rice and wheat" led by Dr. Barbara Valent. It was wonderful to be a part of this diverse community of scientists and collaborate with them for field work and growth chamber studies. I want to recognize and thank the other members of my Student Advisory Committee, Drs. Tom Mitchell and Clay Sneller. My committee members were excellent resources, happy to help, and I was lucky to attend several conferences with them.

My field work in Bolivia would not have been possible without Dr. Christian Cruz who was an excellent mentor and inspiring field scientist. The relationships he built with agricultural companies and collectives in Santa Cruz de la Sierra, Bolivia, were crucial to the success of our research. I would like to acknowledge our primary collaborator at Anapo, Diego Baldelomar, and the team from Cetabol, Javier Kiyuna, Juan Vasquez Onofre, and Mary Luz Huaynoca who all directly assisted in field preparation, planting, and disease assessments, and were friendly and reliable. I am very grateful for those collaborators who assisted David and I when were in a precarious situation and ensured that we could continue our research. Most importantly, I owe a debt of gratitude to my fellow lab mate, and friend,

Dr. David Salgado who worked alongside me collecting disease assessments, driving more than four hours every day to field sites, and entering hours upon hours of data.

David was also an integral part of the lab in Ohio, and essential in preparing the team for field and lab work. My other lab mates were excellent, and I enjoyed working with Drs. Felipe Dalla Lana de Silva and Wanderson Bucker Morales in various lab capacities. I hope our professional paths cross again. The graduate students in the Plant Pathology department were a pleasure to conduct research alongside and I am proud of the efforts of the Plant Pathology Graduate Student Association.

The Plant Pathology department as a whole was a welcoming and friendly community, and students were routinely encouraged and supported so that they could flourish. Dr. Monica Lewandowski was always approachable, happy to assist, and constantly finding new ways to engage students. I also owe thanks to Nikki Beckrum and Ramona Powell for helping me with the nuances of international travel, and the late Lynn West, all of whom I enjoyed visiting with at the two campuses. My greenhouse and growth chamber work were heavily supported by Lee Wilson and Bob James, and I appreciate all the help they provided and the affable conversations. I am grateful that I was able to work alongside many of these people (Larry, Lee, Tom, Monica, Ramona, Sarah Williams, and Mike Ellis) on the 50th Anniversary celebration.

There are many other unnamed people who have helped me along my journey, and I am thankful for all of you.

Vita

2005.....B. S. Ecology and Evolution, University of Washington

2017.....M. S. Plant Pathology, The Ohio State University

2021.....Ph. D. Plant Pathology, The Ohio State University

Professional Experience

2019 – present .....Research Associate in Dr. Christopher Mundt's Wheat Disease and Epidemiology Lab, Oregon State University

2013 – 2019.....Plant Pathology Graduate Student Association (Vice President, Plant Sale Chair, Social Chair), The Ohio State University

2014 – 2016.....Biotechnology Committee Chair, The American Phytopathological Society

2016 – 2017.....Graduate Student Committee Chair, The American Phytopathological Society

Publications

Contina, J. B., Lantz, R L., Chaulagain, B., Mills, K. B., Tildesley, M., and Mundt, C. C. 2021. The influence of farm connectedness on the foot-and-mouth disease outbreaks in livestock. Ecol. Appl. *In publication.*

Chaulagain, B., Contina, J. B., Mills, K. B., Lantz, R. L., and Mundt, C. C. 2021. Comparing the efficacy of control strategies for infectious disease outbreaks using field and simulation studies. *In preparation.*

Mills, K. B., Salgado, J. D., Cruz, C. D., Valent, B., Madden, L. V., and Paul, P. A. 2021. Comparing the temporal development of wheat spike blast epidemics in a region of Bolivia where the disease is endemic. Plant Dis. 105:96-107. doi: 10.1094/PDIS-04-20-0876-RE.

Mills, K. B., Madden, L. V., and Paul, P. A. 2020. Quantifying the effects of temperature and relative humidity on the development of wheat blast caused by the Lolium pathotype of *Magnaporthe oryzae*. Plant Dis. 104:2622-2633. doi:10.1094/PDIS-12-19-2709-RE.

Mills, K. B., Paul, P. A., Madden, L. V., and Peterson, G. L. 2015. Preliminary assessment of differential susceptibility of northern soft red winter wheat cultivars to Lolium and Triticum pathotypes of *Magnaporthe oryzae*. Phytopathology 105:S4.96.

Fields of Study

Major Field: Plant Pathology
Epidemiology

Table of Contents

List of Tables

List of Figures

Fig. 2.4. Relationships between hours of exposure to high (> 95%) relative humidity immediately after spray inoculation with a spore suspension of an isolate (PL2-1) of the Lolium pathotype of *Magnaporthe oryzae* and arcsine-square root-transformed (**A, C**, and

Chapter 1. Introduction

WHEAT BLAST

Wheat blast is a significant threat to global wheat production since it continues to spread into new wheat growing regions and has the potential to substantially reduce grain yield and quality. The causal agent of this disease is the *Triticum* pathotype of the fungal pathogen *Magnaporthe oryzae*, which infects the wheat spikes, leaves and stems, impedes grain fill, causes characteristic bleaching symptoms, and results in the production of small, shriveled, lightweight kernels (Fig. 1.1.). Wheat blast emerged in the mid-1980s in the grain-producing regions of the state of Parana in southern Brazil and quickly became established as a significant threat to wheat production in South America during the following years (Igarashi, 1986). Although it is not a problem every season, when epidemics do occur, the disease is capable of reducing grain yield by 40 to 100 percent (Goulart, 1992). For instance, in 2002, Paraguay suffered a wheat blast epidemic that resulted in over 70 percent crop loss, and harvested grain lots from most fields were too damaged for human consumption (Kohli, 2011). Similarly, in 2009, wheat blast became the limiting factor for wheat production in Brazil, where over 30 percent of the crop was affected (Duveiller, 2010).

In 2016, wheat blast was observed for the first time in Bangladesh (Malaker et al. 2016), where an estimated 16% of cultivated wheat was affected (Islam et al. 2016) and yield losses as high as 100% were reported in some affected districts (Islam et al. 2016). Following this initial incursion, the disease continued to spread into new regions in the sub-Indian continent, reaching several new Bangladeshi districts in 2017-2018 (Bishnoi et al. 2021). Many measures were taken, including a so-called "wheat holiday" and "no wheat zone" on the border with Bangladesh, to prevent the spread of wheat blast into India and China (Mottaleb et al. 2019), two top producers of wheat globally (Food and Agricultural Organization of the United Nations 2021). However, these efforts were to no avail as the disease was subsequently reported in the state of West Bengal, India, in 2017 (Yesmin et al. 2020). Shortly thereafter, wheat blast was reported for the first time in Zambia, Africa, in research plots and farmers' fields during the 2017-2018 rainy season, with spike blast incidence ranging from 50 to 100% (Tembo et al. 2020).

Wheat blast outbreaks in both South Asian and African were caused by the *Triticum* pathotype of the pathogen (MoT), and results from whole-genome sequencing showed that Bangladeshi isolates were closely related to MoT isolates from South America (Islam et al. 2016). MoT has not yet been reported in the United States (US), but isolates of the local Lolium (MoL) pathotype of the pathogen, which causes gray leaf spot of perennial ryegrass, are also capable of infecting wheat and causing losses. In fact, the first and only confirmed case of wheat blast in the US was caused by MoL, and it is likely that other infections have occurred and gone unnoticed or confused with Fusarium head blight, a

disease of the spike of similar symptomatology (Farman et al. 2017). In 2020, the US produced around 1.83 billion bushels (49.8 million metric tons) of wheat, which represented an almost 9-billion-dollar industry (USDA ERS 2021). To prepare against the possible incursion of MoT or development of wheat blast epidemics from local MoL in the US, it is important to study the epidemiology of the disease caused by both pathotypes, screen for resistant cultivars, identify effective chemical treatment regimes, and develop forecasting systems based on the epidemiology of the disease (Cruz and Valent 2016; Ceresini et al. 2018).

Fig. 1.1. Images of natural wheat blast in Bolivia depicting a blasted spike with characteristic black cuff on rachis (A), field with blasted spikes (B), shriveled grains from blasted spikes (C), and gray sporulating lesions on wheat leaves (D)

PATHOGENICITY OF MAGANPORTHE ORYZAE

Magnaporthe oryzae is pathogenic on more than 50 graminaceous species and has several host-specific pathotypes. Wheat blast is typically caused by the Triticum pathotype (MoT), and genetic analysis has confirmed that the expansion of wheat blast into Asia and Africa was from MoT that was likely introduced from Brazil through trade (Malaker et al. 2016; Tembo et al. 2020). There is an ongoing debate as to whether the wheat blast fungus should be officially named *Magnaporthe oryzae* Triticum pathotype or *Pyricularia graminis-tritici*, but in this study, it will only be referred to as the former, with the MoT

abbreviation (Ceresini et al. 2019; Valent et al. 2019). In the US, two other pathotypes of *M. oryzae* cause commercially important diseases, including the most significant rice disease, rice blast, caused by the Oryzae pathotype (MoO), and gray leaf spot (GLS) of perennial ryegrass caused by the Lollium pathotype (MoL). The single blast-affected wheat spike found in Kentucky in 2011 was found to be caused by a native MoL isolate (Farman 2017).

There have been many tests with isolates of *M. oryzae* on a wide variety of graminaceous crops and weeds to determine host range (Urashima et al. 1993; Murakami et al. 2000; Tosa et al. 2004; Couch et al. 2005; and Yoshida et al. 2016). Weeds commonly bordering or invading cultivated grain fields may harbor isolates of *M. oryzae* that are pathogenic on commercial crops such as rice, barley, and wheat. In pathogenicity tests, rice blast only developed when rice was inoculated with MoO, and not with any other pathotypes of *M. oryzae* (Prabhu et al. 1992). Wheat and barley were more susceptible to a range of pathotypes (including MoT and MoL) when tested under highly disease-conducive conditions. GLS of ryegrass is caused by both host-specific and non-specific forms of the MoL pathogen. The host-specific MoL forms are only pathogenic on rye at low temperatures, while non-specific MoL can be pathogenic on rye or wheat at high temperatures (Tosa, 2004). Pathogenicity studies using US ryegrass isolates indicated that under laboratory conditions, MoL was virulent on hard red winter wheat, soft white winter wheat, soft white spring wheat, triticale, and tall fescue (Viji et al. 2001).

When Urashima et al. inoculated twenty wheat cultivars with the 72 *M. oryzae* isolates collected in 2004, no isolate was pathogenic on all cultivars, and only one cultivar

was susceptible to all isolates (Urashima et al. 2004). This range of responses indicates that there are many partial resistance genes at play in wheat blast epidemics (Urashima et al. 2004; Prestes et al. 2007; Cruz et al. 2010). Studies to identify distinct differentials to define races of MoT have yielded mixed and inconclusive results (Urashima et al. 2004; Cruz et al. 2016; Cruppe et al. 2020). The one wheat cultivar that was found to be susceptible to all 72 isolates by Urashima et al. (2004), Anahuac, was commonly grown during the first major wheat blast outbreak in 1985 and was still widely recommended in Brazil until 1999 (Urashima et al. 2004). This highly susceptible cultivar may have contributed to the evolution of MoT from MoL and the establishment of wheat blast in South America by increasing the proportion of *M. oryzae* that was virulent on wheat in the surrounding environment (Inoue et al. 2017).

DISEASE CYCLE OF WHEAT BLAST

Winter wheat is grown to some extent in 42 states in the US, although most of the production occurs across the Great Plains states and in the Pacific Northwest (USDA 2010). Climate conditions vary greatly across the range of areas that grow winter wheats, and since spike development in winter wheat is strongly correlated with photoperiod and temperature (Baker and Gallagher 1983), wheat growth stages occur earlier or later in different regions. For example, in southern states such as Texas, grain is generally fully mature and ready to be harvested in mid-May, while, in northern states such as Washington, grain is still developing over the summer and is harvested as late as mid-August (USDA

2010). Climate change in the US has resulted in greater variability in both temperature and rainfall across these states (Shafer et al. 2014). Environmental effects have been shown to be responsible for 80% of the variability in wheat grain development and yield (Anderson 2010) so there is variation in timing of wheat growth stages year to year within winter wheat production areas. The most susceptible growth stages of wheat to infection by MoL and MoT are still being defined, but it is generally accepted that spike emergence and anthesis are highly susceptible stages for spike blast and the three-leaf stage has been shown to be susceptible to leaf blast in growth chamber studies (Cruz et al.2015).

In US turf, GLS generally emerges late in the summer when temperatures are high and MoL spores are present in high concentrations (Tosa, 2004). According to North Carolina State Extension (2018), GLS is generally present south of Interstate 80 (I-80), which is approximately the 41st parallel North. USDA wheat production maps (2021) show that the majority of spring wheats are grown north of I-80, but a large proportion of winter wheats are grown below I-80 and overlap with areas where GLS is often present on ryegrass. Although most US wheat is currently harvested before GLS is visible and spore become abundant, shifting climate patterns may reduce this temporal separation, and future coincidence of GLS with wheat anthesis may threaten local wheat crops. Before this study, there has been no epidemiological research to quantify the conditions under which US wheats are most susceptible to wheat blast caused by MoL. There are a few forecasting models available to predict where MoT may enter and infect wheat in the US (Cruz 2016) and we hope to contribute data that can be used to develop models to predict areas and conditions where wheat may be vulnerable to MoL.

The disease cycle for wheat blast is only partially defined and needs to be flushed out to create the most accurate forecasting models and define the most effective integrated management strategies. For example, research still needs to explore the sources of overwintering inoculum, potential alternate hosts, and where sexual recombination occurs. Prior to spike emergence, MoT can cause leaf lesions that are characteristically oblong with a dark border and light center that becomes gray during sporulation. Although foliar lesions often appear before wheat spike blast epidemics occur, spike blast-affected fields have been observed with few if any lesions present below the spike. For fields that do have leaf lesions, there is increasing evidence that these lesions contribute to spike blast development in-field and have been shown produce copious amounts of spores while wheat is at anthesis (Cruz et al. 2015).

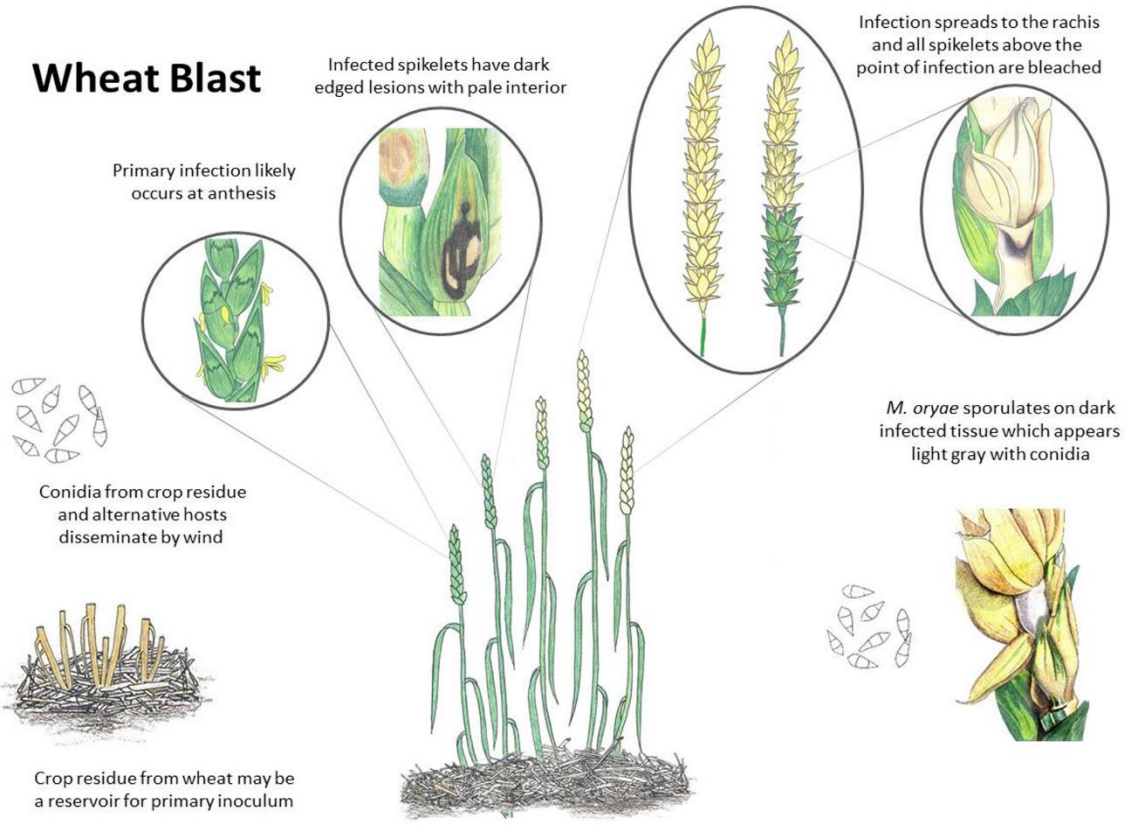

Fig. 1.2. Proposed wheat blast disease cycle showing possible sources of inoculum and typical signs and symptoms on parts of the wheat spike.

Fields that do not have leaf lesions are suspected to be infected by residue-borne and wind-blown primary inoculum (Fig. 1), but quantifying MoT spores present in airflow is challenging as multiple pathotypes or subgroups of *M. oryzae* are usually present concomitantly during a wheat season (Danelli et al. 2019; Pieck et al. 2017). Technology is being developed to differentiate specific pathotypes of *M. oryzae* using Loop-Mediated Isothermal Amplifications (Villari et al. 2016; Yasuhara-Bell et al. 2018). While MoT has been shown to cause lesions on both leaves and spikes, some resistance screenings showed that leaf lesions on seedlings were not consistently correlated with the susceptibility of the

spikes to the same isolates (Cruz et al. 2015). In other words, resistance to leaf blast did not necessarily correspond to resistance to spike blast. Therefore, the relationship between leaf lesions (leaf blast) and spike infection (spike blast) requires additional research to better understand the role of leaf blast in the disease cycle, and consequently, the epidemiology of spike blast.

The basic biology of infection and spread of MoT within a spike is not fully understood. MoT spores that land on anthers or glumes penetrate the cells using appressoria (Wilson and Talbot 20019). The mycelium eventually infects the rachis adjacent to infected glumes, and is visible as a thin, dark cuff around the rachis (Goulart, 1992). Damage to the rachis restricts the flow of nutrients and water to tissues above the point of infection, and as a consequence, spikelets above this point either do not produce grain (early infection) or produce small, shriveled, and lightweight kernels of poor market value (Prabhu 1992; Goulart 2007; Urashima et al. 2009; Gomes 2017; Surovy et al. 2020). Interestingly, kernels below this point of infection may develop to be significantly larger than average kernels and appear swollen in the glumes (Goulart et al. 1992).

Early infection of spikes has the greatest potential to cause yield loss (Goulart, 2007), therefore it is important to quantify disease intensity following early as well as late infections by *M. oryzae*. Vertical spread of the pathogen within the rachis has not been observed or quantified in nature, since there are multiple points of infection in naturally infected wheat fields. Complete bleaching of wheat spikes has anecdotally been observed to occur very quickly, with some reports that a healthy field can appear completely damaged with 100 incidence and severity in only a few days (*CAICO seed co-operative,*

personal communication). However, not all diseased fields within an affected region have the same blast intensity. These differences are likely due to diverse cultivar genotypes, microclimates, and virulence of MoT within the field.

GENETIC DIVERSITY OF *MAGNAPORTHE ORYZAE*

M. oryzae pathotypes have extreme genetic variation, even within a single infected field (Brodani et al. 2000; Tosa et al. 2004; Urashima et al. 2004). For instance, in one area affected by rice blast, at least eight distinct lineages of MoO were identified, and extremely diverse MoO isolates have even been collected from a single plant (Brodani et al. 2000; Correa-Victoria and Zeigler 1993). Polymorphism at simple sequence repeat (SSR) loci can be used to estimate diversity within and between fields (Brondani et al. 2000). A great diversity of MoT isolates have been collected from Brazil, and in one study, 72 genetically discrete isolates were collected in one growing season (Urashima et al. 2004). Conversely, a genetically unique isolate of MoT can be found across a large geographical region, indicating long distance dispersal by natural means or through introduction, as was likely the case with MoT in Asia and Africa (Maciel et al. 2014).

This high level of regional gene flow originates both from sexual recombination and clonal mutations due to a high proportion of transposons (Yoshida et al. 2016). There are two *M. oryzae* mating types, and in areas where mating events are recent, the expected ratio of the two is 50/50. In wheat blast fields there is an extreme mating type disequilibrium and a high clonal fraction of the population, indicating that sexual

reproduction is infrequent, and has not been directly observed in the field (Maciel et al. 2014). With great diversity of MoT within an area, it is unsurprising that there is high evolutionary potential for *M. oryzae* to overcome resistance genes and develop resistance to fungicides (Urashima el al. 2004). This pattern of shifting genetic diversity is common in rice blast, wheat blast, and gray leaf spot. Interestingly, gray leaf spot races in the United States only have one mating type present while the same pathotype in Brazil has both mating types present (Uddin et al. 2003b; Viji et al. 2001).

FACTORS AFFECTING INFECTION, BLAST DEVELOPMENT, AND HOST REACTION

Field observations of conducive environmental conditions for epidemics to develop are similar for all three major diseases caused by *M. oryzae* (rice blast, GLS, and wheat blast). Greenhouse experiments confirm that moderate-to-high temperatures and long wet periods are ideal in most cases (Tosa et al. 2004; Cardoso et al. 2008; Gomes et al. 2012). Wheat blast epidemics have been associated with warm and wet conditions in El Niño years, and often occur when several days of continuous rain are followed by a dry spell (Kohli, 2011). In experiments under controlled conditions, the highest incidence of wheat blast occurred at 30°C with increasing wetness; at 25°C and 40 hours of wetness, disease severity was around 85% (Cardoso et al. 2008). Rice blast is favored at lower temperatures of 21-27°C and 10-14 hours of wetness, and GLS develops best at 25-30°C and extended wetness duration (Suzuki 1975; Uddin et al. 2003a; Tosa et al. 2004). Conversely, dry conditions have a negative effect on *M. oryzae* diseases. For instance, Uddin (2003) show

that air drying ryegrass after spray inoculation with *M. oryzae* inhibited the development of gray leaf spot symptoms. As mentioned earlier, some forms of MoL are highly virulent on non-primary host plants at high temperatures but are host-specific at low temperatures (Tosa et al. 2004). Based on these studies, one can conclude that temperature and wetness duration play an important role in host specificity and the development of *M. oryzae* diseases.

For wheat spike pathogens such as blast and Fusarium head blight (FHB), the latter caused by *Fusarium graminearum* and other species environmental conditions and genetic resistance affect initial infection and spread within the spikes. Extensive research has been conducted on the epidemiology of FHB, and the experimental approaches in MoL research were based on techniques used for both FHB and screening techniques for MoT-incited blast. In the FHB-wheat pathosystem, point inoculations (Anderson et al. 2015), which involves injecting spores inside of one glume on a spike, are commonly used to screen cultivars for resistance to spread of the pathogen within the spike (Type II resistance), which quantitatively measures resistance to colonization (Miedaner et al. 2003). On the other hand, spray inoculation is used to screen for resistance to initial infection (Type I resistance) (Engle 2003). Given that the colonization of *M. oryzae* within wheat spikes is currently poorly understood, point inoculations can also serve as an approach for studying factors that affect the progress of visual disease symptoms from one spikelet to another and over time. The inoculation techniques used in FHB research can also be used to characterize types of cultivar resistance to wheat blast, another major knowledge gap in the biology of this disease. It is also important to assess the range of wheat growth stages of

susceptibility to MoT and MoL, both to fine-tune inoculation protocols for future wheat blast studies and to adjust fungicide application timing for disease management in the field.

The amount of inoculum in a field has a significant impact on the incidence and severity of wheat blast. For instance, Gomes et al (2019) found that spray inoculating only 5 percent of the field of a blast-susceptible wheat cultivar resulted in approximately 65 percent spike blast incidence (i.e., 65% of the spikes with symptoms) at 50 days after inoculation, and more than 90 percent incidence resulted from an initial inoculation of only 30 percent of a field. In all cases, the temporal change in disease intensity was best described with the logistic growth model, but model parameters varied among cultivars and levels of primary inoculum. Also alluding to the importance of in-field inoculum for the development of wheat blast, Farman et al (2017) reported based on an empirical model that conditions in the Princeton, Kentucky, area where the solitary blast-affected spike was found were more conducive to the build-up of MoL conidia during wheat anthesis in 2011, the year of the find, than in previous years.

MANAGEMENT STRATEGIES FOR WHEAT BLAST

Wheat blast is currently being managed through a variety of strategies, including cultural practices, fungicide application, and genetic resistance. In regions of South America where wheat blast is endemic, some communities use planting date as a form of avoidance for cultural management of wheat blast (de Oliveira Coelho et al. 2016). In some years and regions, wheat planted earlier in the season is more prone to blast because

the beginning of the season is a wetter, more conducive environment for MoT infection and blast development (Mehta et al. 1992). Wheat growers in Santa Cruz, Bolivia, thus plant spring wheat seeds in mid-May to mid-June so that spike emergence coincides with hot, dry conditions that are less conducive to infection by MoT (*personal communication, CAICO).*

Chemical sprays were one of the first strategies attempted to manage wheat blast. However, identifying the most effective active ingredients and mixtures of the same, the appropriate application timing, and number of applications has been challenging due in part to a lack of basic understanding of the biology of the pathogen and epidemiology of the disease and the evolution of resistance to some fungicides in the pathogen population. Fungicide applications made after visual symptom development are usually less effective than those made before disease onset. Wheat fields that are already symptomatic with blast lesions or bleaching at the time of fungicide application only have a marginal decrease in final severity (Maciel et al. 2014; Pagani et al. 2014). Foliar fungicides that were used in the 1990s for effectively controlling rice blast, including probenazole and tricyclazole, provided good protection against leaf blast but were ineffective against spike blast (Urashima et al. 1994). Spike protection was successful when strobilurins (quinone-outside inhibitor, QoIs) were used in the early 2000's, but widespread resistance to QoIs was observed in central and southern Brazil (Castroagudin et al. 2015). Interestingly, in 2000, several MoL isolates exhibited resistance to strobilurins in Kentucky ryegrass fields (Vincelli and Dixon 2002).

In 2006, one-hundred South American wheat cultivars were screened for partial resistance to spike blast using endemic MoT isolates, with disease severity (average percent of the spike area [equivalent to percent of spikelets) with symptoms) ranging from 10 to 86%. Cultivars were categorized as having moderately resistant reactions if they exhibited less than 25 percent severity, and susceptible if they developed 50 percent or higher severity (Prestes et al. 2007). US hard red winter wheats have also been screened for resistance against MoT, expressing a similar continuum of reactions (Cruz et al. 2012). Higher levels of resistance were found in synthetic wheat, and greater susceptibility in tetraploid wheat (Cruz et al. 2012; Chuma et al. 2010). Similar to what was observed by Correa-Victoria (1993) when repeatedly screening rice genotypes for resistance to blast using different isolates of the pathogen, when South American wheat cultivars that initially exhibited moderate levels of resistance to blast were screened again several years later, they exhibited a more susceptible-type response when inoculated with contemporary and more aggressive isolates of the pathogen (Igarashi et al. 1990).

Screening wheat cultivars in naturally infected fields led to the identification of natural sources of resistance, and several genes have been identified that confer reduction in disease severity (Rios et al. 2016; Ferreira et al. 2018; Cruz et al. 2016). Quantitative traits loci (QTLs) conferring resistance to leaf and spike blast have been identified in seedlings (5 QTLs) and spikes (4 QTLs), but the seedling and heading QTLs did not co-locate, even though the leaf and spike reactions were positively correlated (Goddard et al. 2020). This led the authors to hypothesize that resistance at different growth stages was controlled by different genes. Rios et al. (2016) found that an anthesis fungicide application

alone (13.3% epoxiconazole + 5% pyraclostrobin) reduced blast severity by 77 and 95% relative to a susceptible untreated check (in years one and two, respectively), genetic resistance alone reduced severity by 44% in year one and 64% in year two, whereas the combination of the fungicide and genetic resistance reduced final spike blast severity by more than 90% and the temporal rate of disease progress by 75%.

One of the most promising sources of quantitative resistance to wheat blast is the 2NS translocation from *Aegilops ventricosa,* which is well known for conferring resistance to root-knot and cyst nematodes, powdery mildew, and some races of wheat rusts (Cruz et al. 2016; Ferreira et al. 2018). When near-isogenic lines with and without the 2NS translocation were planted in MoT infested fields, there was significant quantitative resistance to spike blast but not to leaf blast in lines with 2NS (Cruz et al. 2016). However, the effectiveness of 2NS seemed to be influenced by the genetic background of the lines in which it is found, isolate of the pathogen used for inoculation, and environmental conditions. As MoT continues to mutate and evolve, more virulent strains have reduced the effectiveness of the 2NS translocation, and other possible resistance genes are being screened for both under controlled and field conditions (Islam et al. 2020).

Other novel approaches that have had some success in minimizing wheat blast include: applying macrolide antibiotics which reduce appressoria formation and mycelial growth (Chakraborty et al. 2020); foliar application of silicon gas which helps to mitigate biotic and abiotic stresses (Perez 2014); and calcium and magnesium silicate applied to soil (Pagani et al. 2014). Given the speed with which MoT can evolve new genes capable of overcoming the defense strategies of wheat and confer resistance to fungicides, it is likely

that a combination of strategies, including deployment of different quantitative resistance genes and a range of chemical modes of action, will be necessary to manage wheat blast.

TEMPORAL AND SPATIAL SPREAD OF DISEASE

Wheat blast intensity increases over space and time during epidemics, and it is important to quantify and model the disease dynamics in these dimensions under field conditions in order to develop precise management guidelines such as timing of fungicide application, tillage, and crop rotation (Ceresini et al. 2018). Disease progress in space and time is a function of interactions between the host plant, the pathogen, and the environment (Madden et al. 2007). This process can be modelled under field conditions to address questions such as whether wheat blast is a monocyclic (primary infections only from local or more distantly-produced inoculum) or a polycyclic (primary and subsequent secondary infections from inoculum produced during the epidemic) disease (Gongora-Canul et al. 2020), and whether in-field crop residue or neighboring grassy weeds act as primary sources of inoculum for disease development. For instance, a monocyclic epidemic may be better described by the monomolecular model, whereas the exponential, logistic, or Gompertz models may be more appropriate for describing the temporal progress of a polycyclic epidemic (Madden et al. 2007)

The best-fit population model would provide insights into the relative importance of primary and secondary inoculum and infection for disease development. Models can also be used to compare epidemics between locations, growing seasons, cultivars, and

management practices (Madden et al. 2007; Waggoner 1986), all of which are important for developing and implementing strategies for minimizing grain yield and quality losses.

While infected seed and infested crop residue have been observed in fields prior to wheat blast development, the major sources of wheat blast inoculum have not been unequivocally identified. The patterns of disease development within a field can offer clues as to the sources of inoculum and methods of inoculum spread (Gigot et al. 2017; Madden et al. 2007). Disease gradients and clustering of disease response can indicate inoculum sources adjacent to or within a field, while a uniform disease response may suggest that the source of the pathogen is external to the field. On the other hand, heterogeneity, may indicate that there is an in-field source of inoculum, which would be important to identify to make informed decisions for integrated disease management (Gigot et al. 2017). If disease spreads in an anisotropic pattern, prevailing winds may play significant roles in the spread of the pathogen within the field, and a microclimate within the field may intensify disease due to factors such as increased humidity around puddles or windbreaks. While some studies have indicated that blast may progress from sporulating leaves to spikes (Cruz et al. 2015), very little is known about the spatiotemporal development of wheat blast at the spatial scale of a field.

DISEASE FORECASTING MODEL

Forecasting models are crucial for sporadic diseases that can devastate the majority of a crop in one season. Such models can be used to help predict the location, time, and

severity of endemic of *M. oryzae* diseases, as well as identify regions that are at risk for an incursion and establishment of virulent *M. oryzae* pathotypes (Cruz et al. 2016; Cruz and Valent 2017). For rice blast, linear regression models were developed using predictors that included high relative humidity duration, the number of days with high levels of precipitation, ambient temperature, planting date, and the amount of nitrogen in soil amendments (Calvero, 1996; Greer and Webster 2001). Gray leaf spot predictive models consider temperature, leaf wetness duration, and their interaction (Harmon and Latin 2003; Uddin et al. 2003a), whereas for wheat blast, Cardoso et al (2008) develop a chart to predict disease intensity using temperature and spike wetness duration as predictors. Based on results from this and studies of the effects of temperature, wetness, and precipitation on the development of *M. oryzae* diseases, Cruz et al. (2016) developed weather-based infection models to identify areas in the US with conditions suitable for the establishment and survival of MoT, and outbreaks of wheat blast.

According to the US climate suitability model which identified regions where wheat blast may be introduced and become established (Cruz et al. 2016), 25% of US wheat-growing areas would be at high risk for epidemics of wheat blast caused by MoT, and most of these are in the hottest winter wheat-producing regions, generally found in the southern states. MoL produced by GLS, however, is more intense around the central states which are slightly cooler than the southern wheat production zones (Harmon and Latin 2003). The single blast-affected spike in the US was found in Kentucky in a region where the predicted danger zone for MoT establishment (Cruz et al. 2016) overlaps with areas were GLS frequently occurs (Farman et al. 2012; Lipps 1998). To create forecasting

models to predict potential wheat blast epidemics in the US, it is important to capture the effects of basic environmental factors such as temperature and relative humidity for MoL-incited spike blast on North American wheat cultivars. These new data can help expand other environment-based models so that a forecast system can ultimately be developed to identify conditions, regions, and times where growers should scout their fields to look for blast-affected spikes. Since there are other diseases and abiotic factors that cause bleached spikes similar to wheat blast, it is imperative that US wheat growers are educated about what to look for and distinguish wheat blast from other causes of bleaching. Predictive models can be useful educational tools, in addition to being used to help guide critical management decisions.

OBJECTIVES

MoL and environment. The possibility of MoL-incited wheat blast becoming more frequent in the U.S. served as the impetus for this research, which was part of a larger project to investigate the risk posed by MoL to U.S. wheat. The primary goal was to identify host, pathogen, and environmental risk factors associated with MoL infection and wheat blast development.

The specific objectives of this research were to **(i)** quantify the effects of temperature and initial high relative humidity duration on MoL infection and spread within winter wheat spikes; **(ii)** model the temporal change in wheat blast intensity as influenced by temperature and RH duration; **(iii)** determine whether inoculum density and crop growth stage at time of inoculation affected the development of spike blast on different wheat cultivars; and **(iv)** quantify the temporal dynamics of wheat spike blast as influenced by inoculum density and cultivar resistance.

MoT and epidemics. To address key knowledge gaps in the epidemiology of wheat blast, research was conducted to monitor, model, and compare naturally occurring wheat spike blast epidemics in Bolivia during a natural epidemic.

The specific objectives were to: **(v)** quantify the temporal progress of spike blast under different growing conditions; **(vi)** estimate time to specific spike blast severity thresholds as influenced by local conditions; **(vii)** determine the effect of leaf blast severity on spike blast epidemics; **(viii)** characterize the spatial pattern of wheat blast measured as spike severity, spike incidence, and leaf severity, and determine if there is

significant clustering or aggregation; **(ix)** determine if there are temporal trends of aggregation; and **(x)** ascertain if there are different trends in aggregation among the three disease response variables.

This dissertation is organized into an introductory chapter and four research chapters. Objectives i and ii are addressed in Chapter 2 (*Quantifying the effects of temperature and relative humidity on the development of wheat blast caused by the Lolium pathotype of Magnaporthe oryzae*); Objectives iii and iv are addressed in Chapter 3 (*Quantifying the impact of wheat growth stage, inoculum concentration, and cultivar susceptibility on the development of wheat blast caused by Magnaporthe oryzae Lolium pathotypes*); Objectives v through vii are addressed in Chapter 4 (*Comparing the temporal development of wheat spike blast epidemics in a region of Bolivia where disease is endemic*); Objectives viii and ix are addressed in Chapter 5 (*Spatial aggregation of wheat blast developing in Bolivia during a natural epidemic*).

REFERENCES

Anderson, W. K. 2010. Closing the gap between actual and potential yield of rainfed wheat. The impacts of environment, management and cultivar. Field Crops Research 116:14-22.

Andersen, K. F., Madden, L. V., and Paul, P. A. 2015. Fusarium head blight development and deoxynivalenol accumulation in wheat as influenced by post-anthesis moisture patterns. Phytopathology 105:210-219.

Aucique Perez, C. E., Rodrigues, F. Á., Moreira, W. R., and DaMatta, F. M. 2014. Leaf gas exchange and chlorophyll a fluorescence in wheat plants supplied with silicon and infected with *Pyricularia oryzae*. Phytopathology 104:143-149.

Baker, C. K., and Gallagher, J. N. 1983. The development of winter wheat in the field. The control of primordium initiation rate by temperature and photoperiod. J. of Agric. Sci. 101:337-344.

Bishnoi, S. K., Kumar, S., and Singh, G. P. 2021. Wheat blast readiness of the Indian wheat sector. Current Science 120:262.

Brondani, C., Vianello, R. P., Garrido, L., and Elias, F. M. 2000. Development of microsatellite markers for the genetic analysis of *Magnaporthe grisea*. Gen. and Mol. Biol. 23:753-762.

Calvero Jr., S. B., Coakley, S. M., and Teng, P. S. 1996. Development of empirical forecasting models for rice blast based on weather factors. Plant Pathol. 4:667-678.

Cardoso, C. A. de A., Reis, E. M., and Moreira, E. N. 2008. Development of a warning system for wheat blast caused by *Pyricularia grisea*. Summa Phytopathol. 34:216-221.

Castroagudín, V. L., Ceresini, P. C., Oliveira, S. C., Reges, J. A., Maciel, J. L., Bonato, A. L., Dorigan, A. F., and McDonald, B. A. 2015. Resistance to QoI Fungicides Is Widespread in Brazilian Populations of the Wheat Blast Pathogen *Magnaporthe oryzae*. Phytopathol. 105:3, 284-294

Ceresini, P. C., Castroagudiin, V. L., Rodrigues, F. A., Rios, J. A., Aucique-P´erez, C. E., Moreira, S. I., Alves, E., Croll, D., and Maciel, J. L. 2018. Wheat blast: past, present, and future. Annu. Rev. Phytopathol. 56:427-456.

Ceresini, P. C., Castroagudiin, V. L., Rodrigues, F. A., Rios, J. A., Aucique-P´erez, C. E., Moreira, S. I., Croll, D., Alves, E., Carvalho, G., Maciel, J. L., and McDonald, B. A. 2019. Wheat blast: from its origins in South America to its emergence as a global threat. Mol. Plant Pathol. 20:155-172.

Chakraborty, M., Mahmud, N. U., Muzahid, A. N. M., Fajle Rabby, S. M., and Islam, T. 2020. Oligomycins inhibit *Magnaporthe oryzae* Triticum and suppress wheat blast disease. PLoS ONE. Online publication. doi:10.1371/journal.pone.0233665.

Chuma, I., Zhan, S., Asano, S., Nga, N.T., Vy, T. T., Shirai, M., Ibaragi, K., and Tosa, Y. 2010. PWT1, an Avirulence Gene of *Magnaporthe oryzae* Tightly Linked to the rDNA Locus, Is Recognized by Two Staple Crops, Common Wheat and Barley. Phytopathol. 100:436-443.

Correa-Victoria, F. J., and Zeigler, R. S. 1993. Pathogenic variability in *Pyricularia grisea* at a rice blast "hot spot" breeding site in eastern Colombia. Plant Dis. 77:1029-1035.

Couch, B. C., Fudal, I., Lebrun, M., Tharreau, D., Valent, B., vanKim, P.,Notteghem, J. L., and Kohn, L. M. 2005. Origins of host-specific populations of the blast pathogen *Magnaporthe oryzae* in crop domestication with subsequent expansion of pandemic clones on rice and weeds of rice. Genetics 170:613-630.

Cruppe G. 2020. Novel sources of wheat head blast resistance in modern breeding lines and wheat wild relatives. Plant dis. 104:35-43.

Cruz, C. D., Bockus, W. W., Stack, J. P., Tang, X., Valent, B., Pedley, K. F., and Peterson, G. L. 2012. Preliminary assessment of resistance among U.S. wheat cultivars to the Triticum pathotypes of *Magnaporthe oryzae*. Plant Dis. 96:1501-1505.

Cruz, C. D., Kiyuna, J., Bockus, W. W., Todd, T. C., Stack, J. P., and Valent, B. 2015. *Magnaporthe oryzae* conidia on basal wheat leaves as a potential source of wheat blast inoculum. Plant Pathol. 64:1491-1498.

Cruz, C. D., Magarey, R. D., Christie, D. N., Fowler, G. A., Fernandes, J. M., Bockus, W. W., Valent, B., and Stack, J. P. 2016. Climate suitability for *Magnaporthe oryzae* Triticum pathotype in the United States. Plant Dis. 100:1979-1987.

Cruz, C. D., and Valent, B. 2017. Wheat blast disease: danger on the move. Trop. Plant Pathol. 42:210-222.

Cruz, M. F. A., Prestes, A. M., Maciel, J. L. N., and Scheeren, P. L. 2010. Partial resistance to blast on common and synthetic wheat genotypes in seedling and in adult plant growth stages. Trop. Plant Pathol. 35:024-031.

Danelli, A. L. D., Fernandes, J. M. C., Maciel, J. L. N., Boaretto, C., and Forcelini, C. A. 2019. Monitoring *Pyricularia* spp. airborne inoculum in Passo Fundo, Rio Grande do Sul – Brazil. Summa Phytopathol. 45:361-367.

de Oliveira Coelho, M. A., Torres, G. A. M., Cecon, P. R., and Santana, F. M. 2016. Sowing date reduces the incidence of wheat blast disease. Pesquisa Agropecuaria Brasileira 51:631-637.

Duveiller, E., Hodson, D., and von Tiedemann, A. 2010. Wheat blast caused by *Maganaporthe oryzae*: a reality and new challenge for wheat research. The 8th International Wheat Conference. St. Petersburg, Russia. Vavilov Research Institute of Plant Industry.

Economic Research Service (ERS), U.S. Department of Agriculture (USDA). Wheat data report – All years. Assessed May 2021. Available online. https://www.ers.usda.gov/data-products/wheat-data/.

Engle, J. S., Madden, L. V., and Lipps, P. E. 2003. Evaluation of inoculation methods to determine resistance reactions of wheat to *Fusarium graminearum*. Plant Disease, 87:1530-1535.

FAO. FAOSTAT. Wheat crop production. Assessed May 2021. Available online. http://www.fao.org/faostat/en/#search/wheat.

Farman, M., Peterson, G., Chen, L., Starnes, J., Valent, B., Bachi, P., Murdock, L., Hershman, D., Pedley, K., Fernandes, J. M., and Bavaresco, J. 2017. The Lolium pathotype of *Magnaporthe oryzae* recovered from a single blasted wheat plant in the United States. Plant Dis. 101:684-692.

Ferreira, J. R., Vancini, C., Deuner, C. C., Torres, G. A. M., Consoli, L., Seixas, C. D. S. 2018. Absence of 2NS/2AS in wheat resistance sources to *Magnaporthe oryzae* in Brazil. Boletim de Pesquisa e Desenvolvimento. Online publication. https://www.embrapa.br/busca-de-publicacoes/-/publicacao/1095170/absence-of-2ns2as-in-wheat-resistance-sources-to-magnaporthe-oryzae-in-brazil.

Gigot, C., Turechek, W., and McRoberts, N. 2017. Analysis of the spatial pattern of strawberry angular leaf spot in California nursery production. Phytopathology 107:1243-1255.

Goddard, R., Steed, A., Chinoy, C., Ferreira, J. R., Scheeren, P. L., Maciel, J. L. N., and Nicholson, P. 2020. Dissecting the genetic basis of wheat blast resistance in the Brazilian wheat cultivar BR 18-terena. BMC Plant Biol. 20:1-15.

Gomes, D. P. 2012. Incidêcia de *Pyricularia grisea* em genótipos de trigo em função da quantidade de inóculo inicial no campo: availaçao de danos e métodos de detecção nas sementes. Viçosa Minas Gerais, Brasil.

Gomes, D. P., Rocha, V. S., Pereira, O. L., and De Souza, M. A. 2017. Damage of wheat blast on the productivity and quality of seeds as a function of the initial inoculum in the field. [Danos da brusone do trigo na produtividade e na qualidade das sementes em função do inóculo inicial no campo] Journal of Seed Science 39:66-74.

Gomes, D. P., Rocha, V. S., Rocha, J., de Souza, M. A., and Pereira, O. L. 2019. Temporal progression of wheat blast as a function of primary inoculum, fungicide application and genotype resistance. [Progresso temporal da brusone do trigo em função do inóculo primário, da aplicação de fungicida e da resistência dos genótipos] Summa Phytopathol. 45:50-58.

Gongora-Canul, C., Salgado, J. D., Singh, D., Cruz, A. P., Cotrozzi, L., Couture, J., Rivadeneira, M. G., Cruppe, G., Valent, B., Todd, T., Poland, J., and Cruz, C. D. 2020. Temporal dynamics of wheat blast epidemics and disease measurements using multispectral imagery. Phytopathology 110:393-405.

Goulart, A. C. P., and Paiva F. A. 1992. Incidência da brusone (*Pyricularia oryzae*) em diferentes cultivares de trigo (*Triticum aestivum*) em condições de campo. Fitopatol. Bras. 17:321-325.

Goulart, A. C. P., Sousa, P. G., and Urashima, A. S. 2007. Danos em trigo causados pela infecção de *Pyricularia grisea*. Summa Phytopathol. 33:358-363.

Greer, C. A., and Webster, R. K. 2001. Occurrence, distribution, epidemiology, cultivar reaction, and management of rice blast disease in California. Plant Dis. 85:1096-1102.

Harmon, P. F., and Latin, R. 2003. Gray leaf spot of perennial ryegrass. Plant Health Progress. Online publication. doi.org/10.1094/PHP-2003-1223-01-DG.

Igarashi, S. 1990. Update on wheat blast (*Pyricularia oryzae*) in Brazil. Wheat for the nontraditional warm areas: a proceedings of the international conference. Foz do Igaçu, Brazil. 480-483.

Igarashi, S., Utiamada, C. M., Igarashi, L. C., Kazuma, A. H., and Lopes, R. S. 1986. *Pyricularia* em trigo, ocorrência de *Pyricularia* sp. no estado do Paraná. Fitopatol. Bras. 11:351-352.

Inoue, Y., Vy, T. T., Yoshida, K., Asano, H., Mitsuoka, C., Asuke, S., Anh, V., Cumagun, C. J., Chuma, I., Terauchi, R., Kato, K., Mitchell, T., Valent, B., Farman, M., and Tosa, Y. 2017. Evolution of the wheat blast fungus through functional losses ni a host specificity determinant. Science 357:80-83.

Islam, M.T., Croll, D., Gladieux, P., Soanes, D.M., Persoons, A., and Bhattacharjee, P. 2016. Emergence of wheat blast in Bangladesh was caused by a South American lineage of *Magnaporthe oryzae*. BMC Biology, 14. Online publication. https://bmcbiol.biomedcentral.com/articles/10.1186/s12915-016-0309-7.

Islam, M. T., Gubta, D. R., Hossain, A., Roy, K. K., He, X., Kabir, M. R., Singh, P. K., Khan, A. R., Rahman, M., and Wang, G. L. 2020. Wheat blast: a new threat to food security. Phytopathol. Research 2:28. Online publication. https://doi.org/10.1186/s42483-020-00067-6.

Kohli, M. M., Mehta, Y. R., Guzman, E., Viedma, L., and Cubilla, L. E. 2011. *Pyricularia* blast - a threat to wheat cultivation. Czech J. Genet. Plant Breed. 47:S130-S134.

Maciel, J. L. N., Ceresini, P. C., Castroagudin, V. L., Zala, M., Kema, G. H. J., and McDonald, B. A. 2014. Population structure and pathotype diversity of the wheat blast pathogen *Magnaporthe oryzae* 25 years after its emergence in Brazil. Phytopathology 104: 95-107.

Madden, L. V., Hughes, G., and van den Bosch, F. 2007. The Study of Plant Disease Epidemics. American Phytopathological Society, St. Paul, MN.

Malaker, P. K., Barma, N. C. D., Tiwari, T. P., Collis, W. J., Duveiller, E., Singh, P. K., Joshi, A. K., Singh, R. P., Braun, H. J., Peterson, G. L., Pedley, K. F., Farman, M. L., and Valent, B. 2016. First Report of Wheat Blast Caused by *Magnaporthe oryzae* Pathotype Triticum in Bangladesh. Plant Disease 100:2330-2330.

Mehta, Y. R., Riede, C. R., Campos, L. A. C., and Kohli, M. M. 1992. Integrated management of major wheat diseases in brazil: An example for the southern cone region of Latin America. Crop Protection, 11: 517-524.

Miedaner, T., Schneider, B., and Geiger, H. H. 2003. Deoxynivalenol (DON) Content and Fusarium Head Blight Resistance in Segregating Populations of Winter Rye and Winter Wheat. Crop Breeding, Gen. & Cytology 43:519-526.

Mottaleb, K. A., Singh, P. K., Sonder, K., Kruseman, G., and Erenstein, O. 2019. Averting wheat blast by implementing a 'wheat holiday': In search of alternative crops in West Bengal, India. PLoS ONE. Online publication. doi:10.1371/journal.pone.0211410.

Murakami, J., Tosa, Y., Kataoka, T., Tomita, R., Kawasaki, J., Chuma, I., and Mayama, S. 2000. Analysis of host species specificity of magnaporthe grisea toward wheat using a genetic cross between isolates from wheat and foxtail millet. Phytopathology 90: 1060-1067.

NC State Extension. 2018. Gray leaf spot on the rise in North Carolina. Assessed May 2021. Available online. https://turfpathology.ces.ncsu.edu/2018/10/gray-leaf-spot-on-the-rise-in-north-carolina/.

Pagani, A. P. S., Dianese, A. C., and Café-Filho, A. C. 2014. Management of wheat blast with synthetic fungicides, partial resistance and silicate and phosphite minerals. Phytoparasitica 42: 609-617.

Pieck, M. L., Ruck, A., Farman, M. L., Peterson, G. L., Stack, J. P., Valent, B., and Pedley, K. F. 2017. Genomics-Based Marker Discovery and Diagnostic Assay Development for Wheat Blast. Plant Dis. 101:103-109.

Prabhu, A. S., Filippi, M. C., and Castro, N. 1992. Pathogenic variation among isolates of *Pyricularia oryzae* affecting rice, wheat, and grasses in Brazil. Int. J. Pest Manag. 38:367-371.

Prestes, A.M., Arendt, P.F., Fernandes, J.M.C., and Scheeren, P.L. 2007. Resistance to Magnaporthe grisea among Brazilian wheat genotypes. Buck H.T., Nisi J.E., Salomón N. (eds) Wheat Production in Stressed Environments. Developments in Plant Breeding, vol 12. Springer, Dordrecht.

Rios, J. A., Rios, V. S., Paul, P. A., Souza, M. A., Araujo, L., and Rodrigues, F. A. 2016. Fungicide and cultivar effects on the development and temporal progress of wheat blast under field conditions. Crop Prot. 89:152-160.

Sadat, A., and Choi, J. 2017. Wheat blast: A new fungal inhabitant to Bangladesh threatening world wheat production. Plant Pathol. J. 33:103-108.

Shafer, M., Ojima, D., Antle, J. M., Kluck, D., McPherson, R. A., Peterson, S., Scanlon, B., and Sherman, K. 2014. Great Plains. Climate change impacts in the United States: the third national climate assessment. U. S. Global Change Research Program, Washington, D. C.

Silva, G. B., and Prabhu, A. S. 2005. Quantificação de conídios de *Pyricularia grisea* no plantio direto e convencional de arroz de terras altas. Fitopatologia Brasileira, Brasília 30:569-573.

Suzuki, H. 1975. Meteorological factors in the epidemiology of rice blast. Annual Review of Phytopathology 13:239-256.

Surovy, M.Z., Mahmud, N.U., Bhattacharjee, P., Hossain, M.S., Mehebub, M.S., Rahman, M., Majumdar, B. C., Gupta, D. R., and Islam, T. 2020. Modulation of nutritional and biochemical properties of wheat grains infected by blast fungus *Magnaporthe oryzae* Triticum pathotype. Frontiers in Microbiol. 11:1174.

Tembo, B., Mulenga, R. M., Sichilima, S., M'siska, K. K., Mwale, M., Chikoti, P. C., Singh, P. K., He, X., Pedley, K. F., Peterson, G. L., Singh, R. P., and Braun, H. J. 2020. Detection and characterization of fungus (*Magnaporthe oryzae* pathotype Triticum) causing wheat blast disease on rain-fed grown wheat (*Triticum aestivum* L.) in Zambia. PLoS ONE 15(9): e0238724. Online publication. doi.org/10.1371/journal.pone.0238724

Tosa, Y., Hirata, K., Tamba, H., Nakagawa, S., Chuma, I., Isobe, C., Osue, J., Urashima, A. S., Don, L. D., Kusaba, M., Nakayashiki, H., Tanaka, A., Tani, T., Mori, N., and Mayama, S. 2004. Genetic constitution and pathogenicity of Lolium isolates of *Magnaporthe oryzae* in comparison with host species specific pathotypes of the blast fungus. Phytopathology 94:454-462.

Uddin, W., Serlemitsos, K., and Viji, G. 2003a. A temperature and leaf wetness duration-based model for prediction of gray leaf spot of perennial ryegrass turf. Phytopathology 93:336-343.

Uddin, W., Viji, G., and Vincelli, P. 2003b. Gray leaf spot (blast) of perennial ryegrass turf: an emerging problem for the turfgrass industry. Plant Dis. 87:880-889.

Urashima, A. S., Igarashi, S., and Kato, H. 1993. Host range, mating type, and fertility of *Pyricularia grisea* from wheat in Brazil. Plant Dis. 77:1211-1216.

Urashima, A. S., Lavorent, N. A., Goulart, A. C. P., and Mehta, Y. R. 2004. Resistance spectra of wheat cultivars and virulence diversity of Magnaporthe grisea isolates in Brazil. Fitopatologia Brasileira 29:511-518.

Urashima, A. S., Grosso, C. R. F., Stabili, A., Freitas, E. G., Silva, C. P., Netto, D. C. S., Franco, I., and Merola Bottan, J. H. 2009. Effect of Magnaporthe grisea on seed germination, yield, and quality of wheat. Wang, G. W., and Valent, B. (eds) Advances in genetics, genomics and control of rice blast disease. Springer, Netherlands, pp 267-277.

Valent, B., Farman, M., Tosa, Y., Begerow, D., Fournier, E., Gladieux, P., Islam, M. T., Kamoun, S., Kemler, M., Kohn, L. M., Lebrun, M.-H., Stajich, J. E., Talbot, N. J., Terauchi, R., Tharreau, R., and Zhang, N. 2019. *Pyricularia* graminis-tritici is not the correct species name for the wheat blast fungus: response to Ceresini et al. (MPP 20:2). Mol. Plant Pathol. 20:173-179.

Viji, G., Wu, B., Kang, S., Uddin, W., and Huff, D. R. 2001. *Pyricularia grisea* causing gray leaf spot of perennial ryegrass turf: Population structure and host specificity. Plant Disease 85: 817-826.

Villari, C., Mahaffee, W. F., Mitchell, T. K., Pedley, K. F., Pieck, M. L., and Peduto Hand, F. 2017. Early detection of airborne inoculum of *Magnaporthe oryzae* in turfgrass fields using a quantitative LAMP assay. Plant Disease, 101:170-177.

Vincelli, P., and Dixon, E. 2002. Resistance to QoI (strobilurin-like) fungicides in isolates of *Pyricularia grisea* from perennial ryegrass. Plant Dis. 86:235-240.

Waggoner, P. E. 1986. Progress curves of foliar diseases: Their interpretation and use. Plant Disease Epidemiology. Vol. 1, Population Dynamics and Management. Leonard, K. J. and Fry, W. (eds) Macmillan, New York, pp 3-37.

Wilson, R. A., and Talbot, N. J. 2009. Under pressure: investigating the biology of plant infection by *Magnaporthe oryzae*. Nat Rev Microbiol. 7:185-95.

Yasuhara-Bell, J., Pedley, K. F., Farman, M., Valent, B., and Stack, J. P. 2018. Specific detection of the wheat blast pathogen (*Magnaporthe oryzae* Triticum) by loop-mediated isothermal amplification. Plant Dis. 102: 2550-2559.

Yesmin, N., Jenny, F., Abdullah, H. M., Hossain, M. M., Kader, M. A., Solomon, P. S., and Bhuiyan, M. A. H. B. 2020. A review on South Asian wheat blast: The present status and future perspective. Plant Pathol. 69:1618-1629.

Yoshida, K., Saunders, D.G.O., Mitsuoka, C., Natsume, S., Kosugi, S., Saitoh, H., Inoue, Y., Chuma, Y., Tosa, Y., Cano, L. M., Kamoun, S., and Terauchi, R. 2016. Host specialization of the blast fungus *Magnaporthe oryzae* is associated with dynamic gain and loss of genes linked to transposable elements. BMC Genomics 17:1.

Chapter 2.
Quantifying the effects of Temperature and Relative Humidity on the Development of Wheat Blast incited by the Lolium Pathotype of *Magnapothe oryzae*

ABSTRACT

The *Triticum* pathotype of *Magnaporthe oryzae* (MoT) that causes wheat blast has not yet been reported in the U.S., but the closely related *M. oryzae* Lolium pathotype (MoL), also capable of inciting blast, is found in several wheat growing regions. Since the epidemiology of MoL-incited wheat blast is unknown, it is difficult to project where and under what conditions this pathogen may be of importance. To quantify conditions favorable for MoL infection and temporal development of wheat blast, separate cohorts of wheat spikes were spray or point inoculated at anthesis and immediately subjected to different combinations of temperature (TEMP; 20, 25, and 30^{o}C) and 100% relative humidity (RH) duration (0, 3, 6, 12, 24, and 48 h). Blast developed under all tested conditions, with both incidence (INC) and severity (SEV) increasing over time. The effects of TEMP on angular-transformed INC and SEV (arcINC and arcSEV) were significant ($P < 0.05$) in most cases, with the magnitude of the TEMP effect influenced by RH duration when spikes were spray-inoculated. Between 12 and 21 days after inoculation (DAI), there were significant, positive linear relationships between hours of high RH and arcINC and arcSEV at 25 and 30^{o}C, but not at 20^{o}C. The estimated rates of increase in transformed

INC or SEV per hour increase in high RH duration were significantly higher at 30°C than at 25°C at 12-14 DAI, but not at 19-21 DAI. The highest estimated temporal rates of increase in INC and SEV and the shortest estimated incubation periods (5 to 8 days) occurred at 25 and 30°C, with 24 and 48 h of high RH immediately after inoculation. These results will contribute to ongoing efforts to better understand the epidemiology of wheat blast caused by MoL as well as MoT.

INTRODUCTION

Magnaporthe oryzae is an ascomycetous fungal pathogen that causes diseases on more than 50 graminaceous plant species worldwide, including economically important crops such as wheat, rice, millet, barely, and ryegrass (Tosa et al. 2004). The taxonomy of this pathogen has been the subject of debate for years (Castroagudin et al. 2016; Ceresini et al. 2018, 2019; Cruz and Valent 2017; Gladieux et al. 2018; Valent et al. 2019), but one very commonly used and generally accepted classification is by pathotype (Cruz and Valent 2017). A pathotype is a subspecific designation that is based on host specialization or adaptation (Ceresini et al. 2018; Cruz and Valent 2017; Valent et al. 2019). We follow this naming convention here. One of the most concerning diseases caused by the Triticum pathotype of *M. oryzae* (MoT) is wheat blast. This disease is characterized by partial or complete bleaching and discoloration of spikes with shriveled, light-weight kernels (Goulart et al. 2007), and in some cases, leaves with oblong lesions with dark edges and light-gray centers (Saharan et al. 2017). Wheat blast is endemic in several wheat growing regions of South America (Kohli et al. 2011) and recently emerged as a threat to wheat

production in South Asia (Cruz and Valent 2017; Sadat and Choi 2017; Saharan et al. 2017). While MoT has not yet been reported in the U.S., there are several native pathotypes of *M. oryzae* that cause diseases on other crops. For instance, the Lolium pathotype (MoL) is the causal agent of gray leaf spot (GLS), a major disease of turf grasses such as tall fescue (*Festuca arundinacea*) and perennial ryegrass (*Lolium perenne*) (Farman et al. 2017; Harmon and Latin 2003; Milazzo et al. 2018), and the Oryzae pathotype (MoO) is the causal agent of rice blast, another economically important disease of global significance (Greer and Webster 2001).

Several studies have been conducted in an effort to determine the host range and phylogenetic relatedness of *M. oryzae* populations from different host species (Ceresini et al. 2018, 2019; Couch et al. 2005; Urashima et al. 1993). Some subgroups or isolates have fairly wide, overlapping host ranges, including crops and weeds that sometimes grow in close proximity to each other, while other subgroups are more host specific (Ceresini et al. 2018,2019; Urashima et al. 1993). For instance, based on greenhouse experiments with seedlings, Urashima et al. (1993) reported that several isolates of the blast pathogen from rice (referred to as *Pyricularia grisea*) caused foliar symptoms on wheat, whereas isolates from wheat did not produce symptoms on any of the rice cultivars tested, but induced typical, sporulating lesions on leaves of perennial ryegrass, tall fescue, and finger miller (*Eleusine coracana*). This led them to hypothesize, following compatibility crosses, that wheat isolates were different from rice isolates, but similar to those from finger millet. This hypothesis was supported by results from recent phylogenetic studies showing that wheat-infecting isolates were more closely related to turf grass-infecting isolates than to rice-

infecting isolates (Castroagudin et al. 2016; Ceresini et al. 2018, 2019; Farman et al. 2017; Gladieux et al. 2018). Some researchers believe that MoT evolved from MoL in Brazil "*through functional losses of a host specificity determinant*" (Inoue et al. 2017). They theorized that MoL isolates carrying the *PWT3* and *PWT4* avirulence genes (which made them avirulent on wheat cultivars carrying the *Rwt3* and *Rwt4* resistance genes) infected highly susceptible *rwt3* cultivars that were widely grown during the first wheat blast outbreaks (Inoue et al. 2017). Once MoL became established on susceptible wheat, specialization occurred following mutation and the loss of function of *PWT3*, eventually leading to the evolution of the MoT pathotype.

In 2011, a single wheat spike was found in Kentucky exhibiting typical signs and symptoms of wheat blast. Subsequent genetic analysis of the fungus isolated from that spike suggested that MoL was the likely causal agent. This was based on the fact that the genome sequence of that isolate was more similar to native U.S. MoL than to South American MoT pathotypes of *M. oryzae* (Farman et al. 2017). This was the first, and to date the only, observed case of naturally occurring wheat blast under field conditions in the U.S. However, the fact that several local isolates of MoL collected years before the Kentucky find were capable of causing blast on U.S. wheats under controlled conditions led some researchers to speculate that previous occurrences of blast may have been misdiagnosed as Fusarium head blight, a disease of similar symptomatology (Farman et al. 2017). Other growth chamber and field studies showed that most U.S. hard red winter wheats, particularly cultivars without the 2NS translocation from *Aegilops ventricosa*, were susceptible to South American MoT (Cruz et al. 2012, 2016), and that several U.S. soft red

winter wheats were susceptible to both MoT and MoL (Mills et al. 2015). These results indicate that the U.S. wheat crop is at risk for infection both from an incursion of MoT as well as from native MoL isolates. The latter is of concern particularly in areas where wheat production overlaps with the occurrence of GLS on perennial ryegrass. However, the fact that winter wheat is harvested between late spring and early summer, well before GLS typically develops (Uddin et al. 2003b) and MoL inoculum builds up, may in part explain why natural MoL infections are not more frequent (Farman et al. 2017).

The possibility of MoL-incited wheat blast becoming more frequent in the U.S. served the impetus for this research, which was part of a larger project to investigate the risk posed by MoL to U.S. wheat. The primary goal was to identify host, pathogen, and environmental risk factors associated with MoL infection and wheat blast development. The specific objectives of our research were to 1) quantify the effects of temperature and initial high relative humidity duration on MoL infection and spread within winter wheat spikes and 2) model the temporal change in wheat blast intensity as influenced by temperature and RH duration. To accomplish these objectives, two methods of inoculation (Anderson et al. 2015) were employed, inoculated spikes were exposed to different temperature and RH regimes, and growth models were fitted to the resulting spike blast incidence and severity data. Mean blast incidence and severity, progress curves, and estimated regression parameters were used to compare blast dynamics among the tested temperature-RH regimes. Findings from this study will be of value for developing models to project where and when blast could develop in the U.S. as a result of infection by native MoL.

MATERIALS AND METHODS

Preparation and maintenance of plants. Three experiments were conducted between 2015 and 2017 in walk-in growth chambers (Conviron BDW40, Winnipeg, Manitoba, Canada) in The Ohio State University Plant Pathology phytotron facility, Wooster, Ohio. Fungicide-treated seeds of the highly MoL-susceptible hard red winter wheat cultivar 'Everest' and an MoL- and MoT-susceptible soft red winter wheat cultivar (Mills et al. 2015) were sown in plastic trays. Once seeds germinated, they were vernalized in a cold room at 3°C, with fluorescent grow lights set to run 16 h on and 8 h off for approximately 10 weeks. After vernalization, trays were placed in Conviron growth chambers for a week, with a temperature progression program that ramped up from 6 to 16°C during each 24-h period, mimicking the natural spring temperature cycle of Wooster, Ohio. Chambers were programmed with a fixed photoperiod of 16 h of light and 8 h of darkness, and relative humidity was maintained between 75 and 95% (mean of approximately 80%).

After the first week in the growth chambers, individual tillers were transplanted to cone-tainers (Stuewe and Sons, Inc. Corvallis, OR) filled with autoclaved, unamended silt loam soil. In each experiment, there were three growth chambers, each containing three carts on which four cone-tainer trays with 98 cones were placed. Minimum and maximum daily temperatures were programmed to increase by 2°C per week from week 2 to week 5 (week 2: 8 and 18°; week 3: 10 and 20°; week 4: 12 and 22°; week 5: 14 and 24°). Once the growth chambers reached the week 5 temperature regime, the temperature cycle was maintained until plants reached the Feekes 10.5 (full head emergence) growth stage, after

which the specific temperature treatments were assigned. The daily and weekly temperature cycles helped to promote uniform and synchronized plant development. Built-in sensors monitored and logged temperature, relative humidity, and light settings.

Plants were checked daily, watered as needed, and fertilized once a week with a nutrient solution. Powdery mildew was controlled as needed with 50% triadimefon (Baleton 50; Bayer CropScience, Research Triangle Park, NC), and 21.4% imidacloprid (Marathon II; OHP Inc., Mainland, PA) was used to control aphids and fungus gnats.

Experimental design, inoculum preparation, and inoculation. The experimental design was a randomized complete block (with three experimental repeats as the blocking factor), with a split-split-plot arrangement of temperature as whole-plot, cultivar as sub-plot, and RH duration as sub-sub-plot. Once plants reached the Feekes 10.5 growth stage, approximately seven weeks after vernalization, each growth chamber was set to a fixed temperature of 20, 25, or 30^{o}C. The 16-h photoperiod and relative humidity of approximately 80% were maintained in all chambers. As spikes reached Feekes 10.5.1 (early anthesis) they were arbitrarily assigned to one of the temperature treatments/growth chambers, point- or spray-inoculated as described by Anderson et al. (2015), and subjected to 0, 3, 6, 12, 24, or 48 h of high RH (> 95%) immediately after inoculation. The intent of the two methods of inoculation was to address specific questions about infection, spread within the spike (colonization), and blast development as influenced by the imposed temperature and RH treatments.

MoL isolate PL2-1 (Farman et al. 2017; Valent et al. 2019), previously collected from *Lolium multiflorum* in Kentucky, was used for inoculation. PL2-1 was reported to be 75% as aggressive as an isolate of MoT from Bolivia (Farman et al. 2017). Prior to conducting the experiment, PL2-1 was used to infect spikes of susceptible cultivar 'Everest' for a cursory assessment of its ability to cause blast and to increase inoculum from diseased tissue. Single spore colonies were grown in Petri plates with autoclaved filter paper (about 1 mm by 1 mm) placed on oatmeal agar (30 g/L quick cook oatmeal; 15 g/L granulated agar; 10 ug/L Carbenicillin). Plates were incubated at room temperature under near-ultraviolet light for a 16-h light, 8-h dark photoperiod. Once sporulation was observed (7 to 14 days after incubation), the filter paper pieces were collected and stored in tubes at -20^{o}C until needed. To produce inoculum for the experiment, a single piece of filter paper was placed in the center of a petri dish of oatmeal agar and incubated for about ten days, after which conidia were harvested with a Rubber Policeman and sterilized water. Spore concentration was estimated using a hemocytometer and diluted using sterilized water to 20,000 spores/mL for spray inoculum and 1,000 spores/mL for point inoculum. A drop of Tween 20 was added to every 50 mL of final spore suspension.

Spray-inoculated spikes were inoculated using a spray bottle, with approximately 2 mL of the spore suspension covering the surface of the spike. For spikes that were point-inoculated, the glume, lemma and palea of the central floret of a spikelet in the middle of the spike were gently pealed back and a drop (10 μL) of the spore suspension was deposited directly into the floret (Anderson et al. 2015). The two types of inoculations were performed separately to minimize cross contamination. Inoculated spikes were then

covered in a clear 0.3 mm plastic bag and secured closed with a tie for 3, 6, 12, 24, or 48 h, depending on the RH treatment. During this period, respiration and water from the spore suspension maintained the surface of spray-inoculated spikes wet, and consequently at high (> 95%) relative humidity, until the bags were removed. To ensure similar wetness and maintain high RH in point-inoculated spikes, approximately 0.5 mL of lab grade water was sprayed inside the plastic bags immediately before they were placed over the spikes. Check spikes (the 0-h high RH treatment) were left uncovered and exposed to the ambient RH (~80%) inside the growth chamber. A piece of flagging tape with a unique identifier (for each spike x treatment-RH x inoculation method combination) was attached to the peduncle of each spike at the time of inoculation so that disease progression of individual spikes could be monitored.

Data collection, organization, and analysis. *Disease assessment.* The first set of spike blast assessments were made between three and seven days after inoculation (DAI) and repeated every three to seven days until approximately Feekes growth stage 11 (milky ripe), when senescence made it difficult to distinguish diseased spikelet from natural bleaching. Percent blast severity was estimated on each spike by counting the number of bleached spikelets, dividing by the total number of spikelets, and multiplying by 100. This is equivalent to incidence at the spikelet scale (Paul et al. 2005). Blast incidence at the level of each experimental unit was estimated from individual-spike severity as the number of diseased spikes, divided by the total number of spikes rated, multiplied by 100. The number of spikes rated per experimental unit varied among treatment combinations and among assessment times for a given combination. This was partly due to the effect of temperature

on crop growth and development, which resulted in some experimental units having a very small number of spikes at the time of the first and last sets of assessments. For instance, cool conditions in experimental units subjected to the 20°C treatment delayed anthesis and crop maturity, and consequently, extended the duration of the blast epidemics. On the other hand, plants exposed to the 30°C treatment matured early and more uniformly, leading to epidemics of shorter duration. To minimize these effects and facilitate comparisons of means among treatments, spikes were pooled over three-day windows at 5-7 days, 12-14 days, 19-21 days, and 26-28 days after inoculation (DAI). Each window was treated as a separate response variable for analysis (i.e., analysis done separately for each time period). Instead of attempting repeated measures analyses of the data, the effect of time on blast development as influenced by temperature and RH was quantified through the fit of growth models (see below). Most spikes subjected to the 30°C treatment senesced before 26-28 DAI, therefore less emphasis is given to this final time period.

Linear mixed model analysis (LMM). The GLIMMIX procedure of SAS (Stroup et al. 2018) was used to fit separate linear mixed models to data from the point- and spray-inoculated experiments to determine the effects of temperature, cultivar, and RH duration on spike blast INC and SEV at 5-7, 12-14, 19-21, and 26-28 days after inoculation (DAI). Year of the experiment, the blocking factor, was treated as a random effect, whereas temperature, cultivar, and RH duration, the whole-, sub-, and sub-sub-plot factors, respectively, were treated as fixed effects in the analyses. Prior to fitting the models, the dependent variables, blast incidence and severity, were arcsine-square root-transformed to stabilize variance.

The model fitted to the data can be written as:

$$y_{ijkl} = \theta + \alpha_i + \beta_j + \tau_k + (\alpha\beta)_{ij} + (\alpha\tau)_{ik} + (\beta\tau)_{jk} + (\alpha\beta\tau)_{ijk} + b_l + d_{il} + w_{ijl} + e_{ijkl},$$

where y_{ijkl} is the response (dependent variable; arcINC, arcSEV) for the *i*-th temperature (TEMP), *j*-th cultivar (CULT), and *k*-th high RH duration (RH) within in the *l*-th block (BLK), θ is the constant (intercept), α_i is the effect of the *i*-th TEMP, β_j is the effect of the *j*-th CULT, τ_k is the effect of the *k*-th RH, $(\alpha\beta)_{ij}$ is the effect of the *i*-th TEMP x *j*-th CULT interaction, $(\alpha\tau)_{ik}$ is the effect of the *i*-th TEMP x *k*-th RH interaction, $(\beta\tau)_{jk}$ is the effect of the *j*-th CULT x *k*-th RH interaction, $(\alpha\beta\tau)_{ijk}$ is the effect of the *i*-th TEMP x *j*-th CULT x *k*-th RH interaction, b_l is the effect of the *l*-th BLK, d_{il} is the effect of the *i*-th TEMP x *l*-th BLK interaction (whole-plot error), w_{ijl} is the effect of *i*-th TRT x *j*-th CULT x *l*-th BLK interaction (sub-plot error), and e_{ijkl} is the residual.

Mean blast incidence and severity on the arcsine-square root-transformed scale (arcINC and acrSEV) were compared among treatments and treatment combinations using *lsmeans* and *lsmestimate* statements in PROC GLIMMIX, with the *cl* option specified to obtain estimates of the 95% confidence intervals around mean differences. For responses with statistically significant interaction effects, the *slicediff* option was used as part of *lsmeans* statements to perform simple-effect hypothesis tests of significance of each factor at each level of the other factors or combination of factors.

Linear and non-linear regression analyses. Based on results from the LMM analyses (Table 2.1.) and graphs of the raw data (Figs. 2.1. and 2.2.), linear mixed model regression analyses were performed on the data from the spray-inoculated experiment to

estimate the rate of change in transformed spike blast incidence and severity per hour increase in high RH duration. The RH effect was generally not statistically significant in the point-inoculation experiment (see Results and Table 2.1.). Separate models were fitted to transformed mean incidence and severity at 5-7 days after inoculation (DAI), averaged across experiments, cultivars, and temperature, whereas separate models were fitted to the means at 20, 25 and 30^{o}C at 12-14 and 19-21 DAI, averaged across experiments and cultivars. In all cases, the GLIMMIX procedure was used for model fitting, with parameter estimated and compared through *estimate* statements.

Results from the primary analyses in Table 2.1. also served as the basis for determining whether to quantify the effects of all temperature x RH treatment combinations on the temporal progress of wheat blast. For the spray-inoculated experiments in which there was evidence of statistically significant temperature x RH interaction effects, separate monomolecular, exponential, logistic, and Gompertz models (Madden et al. 2007) were fitted to the means for each combination, averaged across experiments and cultivars, whereas for the point-inoculated experiments in which the interactions were generally not statistically significant, separate models were fitted to the means for the 20, 25, and 30^{o}C treatments, averaged across experiments, cultivars, and RH. In all case, the NLIN procedure of SAS was used, and model performance was evaluated based on mean square error and coefficient of determination (R^2) from linear regression analysis of relationships between observed and predicted responses.

RESULTS

Effects of temperature and relative humidity on mean wheat blast incidence and severity. Wheat spike blast developed equally well on both cultivars under all of the tested conditions in both spray- and point-inoculated experiments. The first set of bleached, discolored spikelets were observed as early as three days after inoculation (DAI), but both disease incidence and severity (together referred to here as intensity) remained extremely low across all treatments during the first week after inoculation (Fig. 2.1.). For instance, only 22 of the 1,066 (2%) spikes rated between 5 and 7 DAI in the spray-inoculated experiment were symptomatic. Averaged across spikes, treatment factors, and experiments, mean blast incidence and severity at 5-7 DPI were 1.4 and 0.45%, respectively (Fig. 2.1.A and C). The corresponding means were 1.4 and 5.9% in the point inoculated experiment (Fig. 2.1.B and D). These estimates increased substantially with time, reaching overall mean severity of 20% in the spray-inoculated experiment and 34% in the point-inoculated experiment at 19-21 DAI. Variability also increased as the disease progressed, with means ranging from 0 to 100% for both incidence and severity at 12-14 DPI. For instance, the interquartile ranges (IQR) for incidence in the spray inoculated experiment was 28.6, 55.6, and 66.7%, at 12-14, 19-21, and 26-28 DPI, respectively (Fig. 2.1.C). IQRs for incidence at similar time points in the point inoculated experiment were 100%.

Spray inoculation. Since results from linear mixed model analyses showed that the main effect of cultivar and interactions involving cultivar were not statistically significant

in most cases ($P > 0.05$; Table 2.1.), attention was placed on the main and interaction effects of temperature and RH duration, averaged across cultivars. When spikes were spray-inoculated, mean differences between pairs of temperature treatments varied with RH duration and vice versa (statistically significant interactions, Table 2.1.) at 12-14, 19-21, and 26-28 DAI, but not at the early assessment time (5-7 DAI) when disease intensity was very low. Early in the epidemic, temperature had a significant effect on arcsine square root-transformed incidence (arcINC) but not transformed severity (arcSEV), whereas RH significantly affected both responses. Averaged across temperatures, spikes exposed to 48 h of high RH immediately after inoculation had significantly higher mean arcINC and arcSEV at 5-7 DAI than those exposed to 0, 3, 6, 12, or 24 h of high RH (Fig. 2.2.A and B). Subsequent disease development was influenced by the interaction between temperature and RH duration. At 12-14 and 19-21 DAI, the effect of temperature was only significant on spikes initially exposed to 12, 24, and 28 h of high RH, and the effect of RH duration was significant at 25 and 30°C, but not at 20°C. In all cases, means increased as RH duration increased and were higher at 25 and 30°C than at 20°C on spikes initially exposed 24 or 48 h of RH > 95% (Fig. 2.2.C-F).

There were significant, positive linear relationships between RH duration and arcINC and arcSEV at 5-7, 12-14, and 19-21 DAI (Fig. 2.3.). At 5-7 DAI, rates of increase in transformed severity per hour increase in RH > 95% was comparable between incidence (0.011 units/h) and severity (0.012 units/h) (Fig. 2.3.A). However, even at the highest tested RH duration, neither estimated mean incidence nor severity exceeded 0.30% (Fig. 2.3.B). Later in the epidemic, at 12-14 and 19-21 DAI, the rate of increase in transformed

blast intensity per hour increase in RH was influenced by temperature. Slopes were not significantly different from zero at 20°C (not shown in Fig. 2.3.), but at 12-14 and 19-21 DAI, slopes were positive and significantly different from zero at 25 and 30°C. The rates of increase in arcINC and arcSEV per hour increase in high RH were significantly greater ($P < 0.001$) at 30 (0.024/h) than at 25°C (0.015 units/h) at 12-14 DAI, but not at 19-21 DAI (Fig. 2.3.C and E). At 12-14 DAI, the regression line was significantly higher at 30°C than at 25°C at 12, 24 and 28 h of high RH for arcSEV (Fig. 2.3.C), and at 6, 12, 24, and 48 h of high RH for arcINC (Fig. 2.3.E). However, at 19-21 DAI, the difference in heights between the 25 and 30°C regression lines was not statistically significant for arcINC, and was only significant for arcSEV at 24 and 48 h of high RH. A greater number of hours of spike incubation at RH > 95% was required at 25°C than at 30°C for blast to reach a certain intensity at a given time after inoculation (reference lines in Fig. 2.3.D and F). For instance, at 12-14 DAI, an estimated mean severity of 25% was reached with 14.8 h of high RH at 30°C compared to 22.6 h at 25°C (Fig. 2.3.D).

Point inoculation. When spores were deposited directly into the florets of the spikes, the effects of cultivar and interactions involving cultivars were again not statistically significant in the majority of cases (Table 2.1.). The effect of temperature on arcINC and arcSEV at different times after inoculation was highly significant ($P < 0.05$) in most cases, whereas the effects of high RH duration and interaction between temperature and high RH duration were generally not statistically significant ($P > 0.05$; Table 2.1.). Contrary to what was observed in the spray-inoculated experiment, mean differences between pairs of temperature treatments generally were not influenced by RH duration

(non-significant interactions in Table 2.1.). The only exception was at 12-14 DAI where the effects of RH duration and the three-way interaction were statistically significant, but even in this case, the temperature effect was highly significant at all tested levels of RH duration (meaning that the interaction was simply quantitative and not cross-over), contrary to what observed when spikes were spray-inoculated. Transformed mean responses were higher at 30 and 25^{o}C than at 20^{o}C, with all pairwise differences being highly significant at 12-14 and 19-21 DAI, for both incidence and severity (Fig. 2.4.C-F). At 5-7 DAI, the temperature effect was highly significant for arcINC ($P < 0.001$, Table 2.1.), but only marginally significant ($P = 0.079$) for arcSEV. Mean arcINC was significantly greater at 30^{o}C than at 25 or 20^{o}C, but comparable between the latter two temperature treatments (Fig. 2.4.A and B).

Trends in terms of monotonic relationships between spike blast intensity (incidence and severity) and hours of exposure to RH > 95% immediately after inoculation were less clearly defined for point-inoculated spikes (Fig. 2.4.) than those observed for spray-inoculated spikes (Fig. 2.2. and 3). Although means (transformed and observed) were numerically higher for the 24 and 28 h of high RH treatments at 5-7 DAI, trends were fairly flat across high-RH-durations later in the epidemic (Fig. 2.4.). At 12-14 DAI, the timepoint at which the effect of high-RH duration was highly significant (Table 2.1.), there were significant positive relationships between the number of hours of incubation at high RH and arcINC and arcSEV, with a common slope across temperature treatments for both the RH-arcINC and the RH-arcSEV relationships. The rate of change in arcSEV per hour increase in high RH duration was 0.0025 (se = 0.0008) units/h, whereas arcINC increased

at a rate of 0.0055 (se = 0.0015) units/h increase in high RH duration. These rates were considerably lower than those observed for corresponding relationships in the spray-inoculated experiment (Fig. 2.1.C and E). Intercepts for the RH-acrSEV relationship were -0.038 (0.048), 0.259 (se = 0.045), and 0.638 (se = 0.045) for the 20°C, 25°C, and 30°C temperature treatments, respectively. For the RH-arcINC relationship, the corresponding intercepts were -0.054 (se = 0.108), 0.484 (se = 0.103), and 1.108 (se = 0.103). For both relationships, the regression lines were significantly higher ($P < 0.05$) at 30 and 25°C than at 20°C and higher at 30 than at 25°C.

Temperature and relative humidity effects on the temporal dynamics of wheat blast. The magnitude and significance of the main and interaction effects of temperature and high RH duration varied with DAI (Fig. 2.2.-4), providing initial evidence of differential effects of treatment conditions on disease progress. In general, overall mean incidence and severity increased over time under all tested treatment conditions, but based on initial plots of the raw data (not shown), the temporal trend was considerably less well defined at the lowest tested temperature (20°C) and shorter durations of high RH (0-6 h) when compared to the higher temperatures and longer RH durations. Therefore, only disease progress results for the latter set of conditions are emphasized and compared.

Based on the MSE and R^2 values in Table 2.2., the Gompertz model was selected as the most appropriate for describing the temporal dynamics of wheat-blast symptom development in most cases. In both spray- and point-inoculated experiments and for both responses, MSE values were very small, and close to or greater than 90% percent of the variation in observed blast intensity was explained by predicted intensity for the Gompertz

model (R^2 in Table 2.2.). The only exceptions were for the epidemics that developed at 20°C for which the logistic or exponential models provided the best fit. Since it is not appropriate to use rate parameters to directly compare epidemics described by different models (Madden et al 2007), properties of the disease progress curves and time to specific levels of incidence and severity were also used to compare the temporal dynamics of blast among treatments.

Temporal change in spike blast intensity. When spikes were spray-inoculated, blast progress curves were similar for epidemics at 25 and 30°C, but considerably different at 20°C (Fig. 2.5.A and C). At the low temperature, estimated incidence and severity remained lower (< 15%) during the first three weeks after inoculation than at the higher temperatures. Despite the similarities among progress curves at 25 and 30°C (Gompertz model was most appropriate to describe them all), the rate parameters (r_G) varied with temperature and RH duration (Table 2.2.). For instance, for severity, the rate at 30°C with 48 hours of high RH ($r_{G\_30:48}$ = 0.28/day) was significantly greater ($P < 0.05$) than for other temperature-RH-duration conditions ($r_{G\_30:24}$ (0.17/day), $r_{G\_25:24}$ (0.13/day), and $r_{G\_25:48}$ (0.15/day)). The latter three rate parameters were not significantly different from each other. Similar trends were observed for incidence, with $r_{G\_30:48}$ (0.61/day) being significantly greater than $r_{G\_30:24}$ (0.24/day), $r_{G\_25:24}$ (0.17/day), and $r_{G\_25:48}$ (0.28/day). RH duration also affected the rate of increase in incidence at 25°C; $r_{G\_25:48}$ was significantly greater than $r_{G\_25:24}$ (Fig. 2.5.C)

Time to 6, 15, 25, and 50% severity, abbreviated as t_6, t_{15}, t_{25}, and t_{50}, respectively, was estimated as described by Madden et al. (2007) based on the model parameters in Table

2.2. and used as another way of comparing epidemics. In particular, this allowed for comparisons among epidemics described by different growth models. Since the mean number of spikelets per spike was 17 (average cross 3,259 spikes rates in the three experiments), with a single bleached spikelet corresponding to approximately 6% severity, t_6 was considered as a measure of the incubation period – i.e. the estimated mean time to the appearance of one (likely the first) bleached spikelet per spike. This period was within a fairly narrow range (6 to 9 days) at 25 and 30°C with 24 or 48 h of high RH, but took 2.5-4 times longer (24 days) at 20°C, with 48 h of high RH. Correspondingly, t_{15}, t_{25}, and t_{50} were shortest under 30°C and 48 h of high RH, but increased steadily as RH duration and temperature decreased (Table 2.2.). This can be visualized as a shift to the right of the progress curves in Figure 5A. The time taken for 6, 15, 25, and 20% of the spikes to become symptomatic (incidence) followed a similar pattern (Table 2.2. and Fig. 2.5.C).

Temporal spread of infection within spikes. In the point-inoculated experiment, severity rate parameters provide a measure of the mean rate of spread of the pathogen or infection within the spike. In other words, these parameters are indicative, at least in part, of the rate of colonization of the spike. Based on r_G, which was significantly greater at 30°C than at 25°C, colonization was much faster at 30 than at 25°C. The fact that disease severity remained lower throughout the epidemic at 20°C than at 25 or 30°C indicates that spread of the pathogen within the spike was slowest and/or the incubation period was longest at the lowest tested temperature. The time taken for the pathogen to spread and symptoms to become evident on three new spikelets from the point of inoculation/infection (estimated as the difference between t_6 and t_{25}) was 9-10 days at 20°C and 25°C, compared

to 6 days at 30ºC (Table 2.2.). However, even at the highest tested temperature, blast severity did not reach 75% at the time of the last assessment (Fig. 2.5.B).

On the other hand, final spike disease incidence reached and exceeded 90% at all three temperatures (Fig. 2.5.D). Rate parameters for incidence can be interpreted in term of the time taken for additional disease-free spikes to show visual symptoms of blast on at least one spikelet. As was the case with colonization, spikes within a sample developed visual symptoms much faster at 30 and 25ºC, than at 20ºC. For instance, it took 27 days longer for 50% of the point-inoculated spikes to become symptomatic at 20ºC than at 30ºC (Table 2.2.). Close to 100% of the spikes were diseased by 21 DAI at 30ºC, compared to 76% at 25ºC and 18% at 20ºC; it took an additional three weeks for 100% of spikes inoculated at 20ºC to develop typical blast symptoms (Fig. 2.5.D).

DISCUSSION

We demonstrated here as did other researchers (Farman et al. 2017; Tosa et al. 2004; Urashima et al. 1993) that MoL is capable of infecting and causing typical spike blast symptoms on wheat. However, the fact that winter wheat is harvested between late spring and early summer in the U.S., well before gray leaf spot (GLS) typically develops (Uddin et al. 2003b) may in part explain why natural MoL infections are not more frequent (Farman et al. 2017). Farman et al. (2017) hypothesized that temporal separation among the emergence of wheat spikes (Feekes growth state 10.5), GLS development on perennial ryegrass, and peak *M. oryzae* spore production in Kentucky was influenced by weather conditions. They further postulated that climate change will likely lead to conditions

becoming more favorable for *M. oryzae* spore production during wheat heading, increasing the likelihood of future MoL-incited wheat blast epidemics in the U.S. The plasticity of *M. oryzae* in its ability to adapt to new hosts and environmental conditions, and the close relationship between isolates of the pathogen from wheat and perennial ryegrass (Uddin et al. 2003b) further support the likelihood of MoL-incited wheat blast becoming established in the U.S.

Findings from previous cross-infection studies designed specifically to determine whether MoL was capable of infecting wheat did not provide information on the epidemiology of the disease nor were they necessarily indicative of what was likely to occur in the field. For instance, some previous host-range studies demonstrating the ability of isolates of *M. oryzae* from rice or turf grasses to infect wheat were based on inoculations of leaves on seedlings (Tosa et al. 2004; Urashima et al. 1993) instead of spikes, the plant part of greatest importance from the standpoint of grain yield and quality losses due to wheat blast. In addition, some host range studies were conducted using extremely high spore concentrations applied to plants under conditions that were highly conducive for infection (Tosa et al. 2004; Urashima et al. 1993). This makes it difficult to infer what is likely to occur in nature, as fixed, highly conducive, controlled conditions may force infections that likely would not occur in the field. Our study was the first to investigate the effects of different combinations of temperature and high relative humidity duration on spike blast development in the MoL-wheat pathosystem, generating insightful results on temporal disease dynamics.

We observed the highest mean levels of spike blast intensity and the highest temporal rates of increase in incidence and severity at 25 and 30°C, with 24 and 48 h of high (> 95%) relative humidity immediately after inoculation (relative to the situation with 20°C and less than 12 hours of high RH). We then developed models describing relationships between hours of incubation at high RH and blast incidence and severity as well as the temporal dynamics of blast symptom development and spread within spikes as influenced by temperature and RH. While this is all novel for the MoL-wheat pathosystem, our results in terms of temperature and moisture effects were comparable to those reported from studies of MoO on rice, MoL on ryegrass, and MoT on spring wheats in South America. For instance, ideal conditions for rice blast to develop were reported to be temperatures between 25 and 28°C, high relative humidity, and at least four hours of leaf wetness (Suzuki 1975; Greer and Webster 2001). Similarly, based on a controlled-environment study similar to ours, Cardoso et al. (2008) reported that wheat blast was favored by temperatures of 25 and 30°C, with at least 10 h of spike wetness; Uddin et al. (2003a) reported that GLS development on perennial ryegrass was favored by high temperatures (28°C) with at least 24 hours of leaf wetness; and the spread of wheat blast in South America was also found to be associated with a combination of 28°C and high relative humidity (at least 90%) (Alves and Fernandes 2006).

The two inoculation methods used in our experiments and knowledge of the epidemiology of other blast diseases (Suzuki 1975; Uddin et al. 2003b) allowed us to hypothesize about the role of temperature, and moisture in particular, on components of the infection cycle. We observed that duration of high RH was much more important for

blast development when spores were spray-applied to the surface of spikes than deposited inside the florets. Based on work done with rice blast (Suzuki 1975) and GLS (Uddin et al. 2003b), the blast infection process involves spore germination and the formation of appressoria and penetration pegs, all of which require moisture. Assuming that these processes are the same for the MoL-wheat pathosystem, spores deposited directly into the floret of point inoculated spikes bypassed some of the surface-moisture constraints on infection, with spores likely having sufficient moisture inside the florets for infection to occur. On the other hand, spores applied to the surface of spikes and bagged for less than 12 hours likely dried out, arresting germination, appressoria formation, and penetration. This is very consistent with what has been reported for MoO, the rice blast pathotype of *M. oryzae* (Suzuki 1975). Optimum conditions for MoO spore germination and appressoria formation are temperatures between 25 and 28^{o}C and 16 and 25^{o}C, respectively, and the presence of free water (Suzuki 1975). If the surface dries before appressoria are formed, the protoplasm of the spores coagulates and dies, and the extent to which appressoria formation is affected by drying is a function of the duration of wetness before the surface dries (Suzuki 1975).

The effects of moisture duration and temperature on infection would also explain the observed relationships between blast intensity and hours of incubation at > 95% RH. Both transformed incidence and severity for spray inoculation increased as high RH duration increased, but intercepts and, to a lesser extent, slopes for RH-arcINC and RH-arcSEV relationships varied with temperature. These relationships were better defined and more consistent at 25 and 30^{o}C than at 20^{o}C (where disease intensity was much lower). For

our experiments in which applied spores were the only source of inoculum and moisture treatments were only imposed during the first 3 to 48 h after inoculation, an increase in incidence with increasing high RH duration would be equivalent to an increase in the number of spikes initially infected that showed visual symptoms. The same rationale can be used to explain relationships between severity and high RH duration. Spike blast severity as defined in our study is really a measure of incidence at the spikelet level. Therefore, at a fixed time after inoculation, the rate of increase in severity on spray-inoculated spikes per hour increase in high RH duration would have been largely a function of the rate of increase in the mean number of symptomatic spikelets that were initially infected per spike per hour increase in high RH. For reasons discussed above based on work done with MoO on rice (Suzuki 1975), the number of spores that remined viable, germinated, and successfully infected (spikes within a sample and spikelets on spike) likely increased as moisture duration increased, leading to higher incidence and severity. Higher RH-arcSEV regression lines at 30 than at 25ºC, particularly at 24 and 48 h of high RH, could also be explained by the fact that the number of spikelets initially infected and developed symptoms was likely greater at 30 than at 25ºC.

Following initial infection in both the spray- and point-inoculated experiments, blast intensity increased over time at all tested temperatures, particularly when spikes were exposed to 12 or more hours of > 95% RH immediately after inoculation. However, the shape of the disease progress curves over days after inoculation varied among temperature x RH combinations on spray-inoculated spikes and among temperature treatments on spikes that were point-inoculated. Gongora-Canul et al. (2020) and Rios et al. (2016)

observed temporal increases in MoT-incited spike blast intensity under field conditions, with progress curves that varied with in-field inoculum and management practices, respectively. Progress curves are graphical depictions of epidemics that summarize interactions among host, pathogen, and the environment (Madden et al. 2007). Curves of the types (mostly S-shaped, sigmoid) observed in our experiments are often used to describe polycyclic diseases/epidemics, where diseased plants or tissues produce inoculum that are disseminated to new disease-free plants or plant parts where they infect, causing disease intensity to increase over time. However, because of the way our study was conducted and the fact that the growth stage of greatest susceptibility is close to anthesis (Mills, unpublished), spike blast intensity does not fit the classical definition of a polycyclic epidemic. Spores produced during the epidemics were not the drivers of the observed temporal increases in incidence and severity in the growth chambers, since sporulation occurred several days or weeks after symptom development, and consequently after the growth states of greatest host susceptibility (Mills, unpublished). Conditions in the growth chambers were not the most conducive to secondary infection as a result of spore dissemination.

As discussed by Berger et al. (1997) and demonstrated by Paul and Munkvold (2005), new infections and secondary cycles are not the only drivers of temporal disease progress. Lesion expansion is another component of epidemics that may be more important than new infections for temporal disease increase in some situations. This was certainly the case with wheat blast severity in our study. Given that spikes were inoculated once, and in the case of point-inoculation, in a single spikelet, temporal increases in severity were likely

due to spread within the spike, a type of lesion expansion. The rate at which this occurred depended on temperature and high RH duration. These variables affected initial infection as discussed above and subsequent colonization, leading to differences in the severity progress curves over days among treatment combinations. Differences in the rate of lesion expansion would also be a plausible explanation for differences in disease progress between spray- and point-inoculated spikes. In the former case, several spikelets likely became infected initially, leading to spread from multiple points along the spike, compared to the latter where spread within the spike occurred from a single point. This suggests a higher r_G for spray versus point inoculation, which we indeed found for temperatures above 20^{o}C. This resulted in higher mean severity at any given time after inoculation and higher final severity on spray- compared point-inoculated spikes. For incidence, we hypothesize that temporal increases and differences in progress curves among treatments were due to differences in the time it took for inoculated spikes to develop visual symptoms (incubation period). Although spikes were inoculated at about the same growth stage, whether or not they developed visual symptoms and the time it took for that to occur depended on the imposed temperature-RH treatments. This reflects, in part, the distribution of incubation time (Madden et al. 2007) for this disease under these controlled environmental conditions.

The Gompertz growth model best described all the epidemics that developed at 25 and 30^{o}C with high RH duration greater than 12 h. This is consistent with results from a study of the temporal dynamics of wheat spike blast in an area of Bolivia where the disease is endemic (Gongora-Canul et al. 2020). As discussed extensively in classical plant disease epidemiology literature (Berger 1981; Campbell and Madden et al 1990; Madden et al.

2007; Waggoner 1986), this model often provides a better fit than the logistic or other growth models to epidemics with positively skewed progress curves; i.e. epidemics for which most of the area under the curve is to the right of the inflection point. This is often explained in terms of the absolute rate of progress as those epidemics for which the rates approach the point of infection quickly and then decline slowly, in other words, epidemics that develops very rapidly during the first few days or weeks. These trends can be gleaned from the 25 and 30^{o}C disease progress curves, all of which have a relatively short lag phase. Such a rapid early increase in of disease intensity at 25 and 30^{o}C with more than 12 h of high RH duration can again be attributed to higher levels of infection, shorter incubation period, and faster spread within the spike (colonization) under warm, humid conditions compared to cool, dry conditions (20^{o}C and < 12 h of high RH). Under less conducive conditions for disease development, the exponential was the best-fit model. This is consistent with a statement made by Madden et al. (2007) about the exponential model being unrealistic, but a good approximation of more complex models at the start of an epidemic when disease intensity is generally very low.

From our experiments: 1) we showed that like other blast diseases, MoL-incited blast is favored by warm, wet conditions; 2) we developed models for relationships between blast intensity and hours of > 95% RH, generating results useful for understanding the environment conditions driving infection; 3) based on results from point- and spray-inoculation, we formulated hypotheses about the possible role of incubation period and lesion expansion in spike blast epidemics, and 4) we modeled the temporal dynamics of wheat as influenced by temperature and high RH duration, with results suggesting that

MoL-incited spike blast is a polycyclic-type disease at the scale of the spikelet, that under highly favorable conditions, is best described by the Gompertz growth models. Similarities between our results and those from studies conducted in South America where MoT is the causal agent of wheat blast, suggest that the epidemiology of MoL-incited wheat blast may be similar to that of MoT-incited blast. This means that our results could potentially be used to assess disease risk, regardless of which of two pathotypes is causing the infections. However, further research would be needed to formally evaluate the effects of other factors such as MoT and MoL isolates, cultivar resistance, and cyclic temperate and RH regimes on spike blast temporal development. While we anticipate that the absolute value of some of the estimates will likely change under different conditions, trends will likely remain the same, leading to similar conclusions. Our findings are valuable for ongoing efforts to better understand the biology and epidemiology of wheat blast in general, but more specifically, to assess the risk posed by MoL to U.S. wheat and develop strategies for disease control. For instance, inoculation protocols from our study could be useful for characterizing resistance to MoL, and parameters from our models could be used to develop risk assessment models for MoL-incited wheat blast in the U.S. similar to the climate suitability models developed by Cruz et al. (2016) for MoT.

Acknowledgment

This project was supported by Agriculture and Food Research Initiative Competitive Grant no. 2013-68004-20378 from the United States Department National Institute of Food and Agriculture and The Ohio State University Department of Plant Pathology. Salaries and

research support for K. B. Mills, L. V. Madden, and P.A. Paul were provided by state and federal funds to the Ohio Agricultural Research and Development Center.

REFERENCES

Alves, K. J., and Fernandes, J. M. 2006. Influência da temperatura e da umidade relativa do ar na esporulação de Magnaporthe grisea em trigo. Fitopatologia Brasileira 31:579-584.

Anderson, K. F., Madden, L. V., and Paul, P. A. 2015. Fusarium head blight development and deoxynivalenol accumulation in wheat as influenced by post-anthesis moisture patterns. Phytopathology 105:210-219.

Berger R. D. 1981. Comparison of the Gompertz and logistic equations to describe plant disease progress. Phytopathology. 71: 716-719.

Berger, R. D., Bergamin Filho, A., and Amorim, L. 1997. Lesion expansion as an epidemic component. Phytopathology 87:1005-1013.

Campbell, C. L. and Madden, L. V. 1990. Introduction to Plant Disease Epidemiology. John Wiley & Sons, New York.

Cardoso, C. A. de A., Reis, E. M., and Moreira, E. N. 2008. Development of a warning system for wheat blast caused by *Pyricularia grisea*. Summa Phytopathologica 34:216-221.

Castroagudın, V. L., Moreira S. I., Pereira D. A. S., Moreira, S. S., Brunner, P. C., Maciel, J. L. N., Crous, P. W., McDonald, B. A., Alves, E., and Ceresini, P. C. 2016. *Pyricularia graministritici*, a new *Pyricularia* species causing wheat blast. Persoonia 37:199-216.

Ceresini, P. C., Castroagudiin, V. L., Rodrigues, F. A., Rios, J. A., Aucique-Pérez, C. E., Moreira, S. I., Alves, E., Croll, D., and Maciel, J. L. 2018. Wheat blast: Past, Present, and Future. Annu. Rev. Phytopathol. 56:427-456.

Ceresini, P. C., Castroagudiin, V. L., Rodrigues, F. A., Rios, J. A., Aucique-Pérez, C. E., Moreira, S. I., Croll, D., Alves, E., Carvalho, G., Maciel, J. L., and McDonald, B. A. 2019. Wheat blast: from its origins in South America to its emergence as a global threat. Mol. Plant Pathol. 20:155-172.

Couch, B.C., Fudal, I. Lebrun, M., Tharreau, D., Valent, B., Kim, P. V., Notteghem, J. L. and Kohn, L.M. 2005. Origins of host-specific populations of the blast pathogen

Magnaporthe oryzae in crop domestication with subsequent expansion of pandemic clones on rice and weeds of rice. Genetics. 170: 613-630.

Cruz, C. D., Bockus, W. W., Stack, J. P., Tang, X., Valent, B., Pedley K. F., and Peterson, G. L. 2012. Preliminary assessment of resistance among U.S. wheat cultivars to the Triticum pathotypes of *Magnaporthe oryzae*. Plant Dis. 96:1501-1505.

Cruz, C. D., Magarey, R. D., Christie, D. N., Fowler, G. A., Fernandes, J. M., Bockus, W. W., Valent, B., and Stack, J. P. 2016. Climate suitability for *Magnaporthe oryzae* Triticum pathotype in the United States. Plant Dis. 100:1979-1987.

Cruz, C. D. and Valent, B. 2017. Wheat blast disease: danger on the move. Tropical Plant Pathology 42:210-222.

Couch, B. C., Fudal, I., Lebrun, M., Tharreau, D., Valent, B., van Kim, P., Nottéghem, J., and Kohn, L. 2005. Origins of host-specific populations of the blast pathogen *Magnaporthe oryzae* in crop domestication with subsequent expansion of pandemic clones on rice and weeds of rice. Genetics 170:613-630.

Farman, M., Peterson, G., Chen, L., Starnes, J., Valent, B., Bachi, P., Murdock, L., Hershman, D., Pedley, K., Fernandes, J. M., and Bavaresco, J. 2017. The Lolium pathotype of *Magnaporthe oryzae* recovered from a single blasted wheat plant in the United States. Plant Dis. 101:684-692.

Gladieux, P., Condon, B., Ravel, S., Soanes, D., Maciel, J.L.N., Nhani, A., Chen, L., Terauchi, R., Lebrun, M.-H., Tharreau, D., Mitchell, T., Pedley, K.F., Valent, B., Talbot, N. J., Farman, M., and Fournier, E. 2018. Gene flow between divergent cereal- and grass-specific lineages of the rice blast fungus *Magnaporthe oryzae*. mBio, 9: e01219-17. Online publication. https://doi.org/10.1128/mBio.01219-17.

Gongora-Canul, C., Salgado, J. D., Singh, D., Cruz, A. P., Cotrozzi, L., Couture, J., Rivadeneira, M. G., Cruppe, G., Valent, B., Todd, T., Poland, J., and Cruz, C. D. 2020. Temporal dynamics of wheat blast epidemics and disease measurements using multispectral imagery. Phytopathology 110:393-405.

Goulart, A. C. P., Sousa, P. G., Urashima, A. S. 2007. Danos em trigo causados pela infecção de *Pyricularia grisea*. Summa Phytopathologica 33:358-363.

Greer, C. A., and Webster, R. K. 2001. Occurrence, distribution, epidemiology, cultivar reaction, and management of rice blast disease in California. Plant Dis. 85:1096-1102.

Harmon, P. F., and Latin, R. 2003. Gray leaf spot of perennial ryegrass. Plant Health Progress. Online publication. doi:10.1094/PHP-2003-1223-01-DG.

Inoue, Y., Vy, T. T., Yoshida, K., Asano, H., Mitsuoka, C., Asuke, S., Anh, V., Cumagun, C. J., Chuma, I., Terauchi, R., Kato, K., Mitchell T., Valent, B., Farman, M., and Tosa, Y. 2017. Evolution of the wheat blast fungus through functional losses ni a host specificity determinant. Science. 357:80-83.

Kohli, M. M., Mehta, Y. R., Guzman, E., Viedma, L., Cubilla, L. E. 2011. *Pyricularia* blast - a threat to wheat cultivation. Czech J Genet Plant Breed. 47:S130-S134.

Madden, L. V., Hughes, G., and van den Bosch, F. 2007. The Study of Plant Disease Epidemics. American Phytopathological Society, St. Paul, MN.

Milazzo, J., Pordel, A., Ravel, S. and Tharreau, D. 2009. First scientific report of *Pyricularia oryzae* causing gray leaf spot disease on perennial ryegrass (*Lolium perenne*) in France. Plant Dis. 103:1024.

Mills, K. B., Paul, P. A., Madden, L. V., and Peterson, G. L. 2015. Preliminary assessment of differential susceptibility of northern soft red winter wheat cultivars to Lolium and Triticum pathotypes of *Magnaporthe oryzae*. Phytopathology 105:S4.96.

Paul, P. A., El-Allaf, S. M., Lipps, P. E., and Madden, L. V. 2005. Relationships between incidence and severity of Fusarium head blight on winter wheat in Ohio. Phytopathology. 95:1049-1060.

Paul, P. A., and Munkvold, G. P. 2005. Influence of temperature and relative humidity on sporulation of *Cercospora zeae-maydis* and expansion of gray leaf spot lesions on maize leaves. Plant Dis. 89:624-630.

Rios, J. A., Rios, V. S., Paul, P. A., Souza, M. A., Araujo, L., and Rodrigues, F. A. 2016. Fungicide and cultivar effects on the development and temporal progress of wheat blast under field conditions. Crop Protection 89:152-160.

Sadat, A. and Choi, J. 2017. Wheat blast: A new fungal inhabitant to Bangladesh threatening world wheat production. Plant Pathol. 33:103-108.

Saharan, M. S., Bhardwaj, S. C., Chatrath, R., Sharma, P., Choudhary, A. K., and Gupta, R. K. 2017. An overview Journal of Wheat Research 8:1-5

Stroup, W. W. Milliken, G. A., Claassen, E. A., and Wolfinger, R. D. 2018. SAS for Mixed Models: Introduction and Basic Applications. SAS Institute Inc., Cary, NC, USA.

Suzuki, H. 1975. Meteorological factors in the epidemiology of rice blast. Annual Review of Phytopathology 13:239-256.

Tosa, Y., Hirata, K., Tamba, H., Nakagawa, S., Chuma, I., Isobe, C., Osue, J., Urashima, A. S., Don, L. D., Kusaba, M., Nakayashiki, H., Tanaka, A., Tani, T., Mori, N., and Mayama, S. 2004. Genetic constitution and pathogenicity of Lolium isolates of *Magnaporthe oryzae* in comparison with host species-specific pathotypes of the blast fungus. Phytopathology 94:454-462.

Uddin, W., Serlemitsos, K., and Viji, G. 2003. A temperature and leaf wetness duration-based model for prediction of gray leaf spot of perennial ryegrass turf. Phytopathology 93:336-343.

Uddin, W., Viji, G., and Vincelli, P. 2003. Gray leaf spot (blast) of perennial ryegrass turf: an emerging problem for the turfgrass Industry. Plant Dis. 87:880-889.

Urashima, A., S., Igarashi, S., and Kato, H. 1993. Host range, mating type, and fertility of *Pyricularia grisea* from wheat in Brazil. Plant Dis. 77:1211-1216.

Valent, B., Farman, M., Tosa, Y., Begerow, D., Fournier, E., Gladieux, P., Islam, M. T., Kamoun, S., Kemler, M., Kohn, L. M., Lebrun, M-H., Stajich, J. E., Talbot, N. J., Terauchi, R., Tharreau, R., and Zhang, N. 2019. *Pyricularia graminis-tritici* is not the correct species name for the wheat blast fungus: response to Ceresini et al. (MPP 20:2). Mol. Plant Pathol. 20:173-179.

Waggoner, P. E. 1986. Progress curves of foliar diseases: Their interpretation and use. In: Leonard, K. J. and Fry, W. E. (Eds.). Plant Disease Epidemiology. Vol. 1. Population Dynamics and Management. Macmillan Publishing Co., New York NY, USA. pp. 3-37.

Table 2.1. Probability values (significance levels) from linear mixed model analyses of the effects of temperature, cultivar, relative humidity, and their interaction on arcsine-square root-transformed wheat spike blast incidence and severity at different times following inoculation with a spore suspension of an isolate (PL2-1) of the Lolium pathotype of *Magnaporthe oryzae* (MoL)

		Incidence[c]				Severity[c]			
Experiment[a]	Factors[b]	5-7 DAI	12-14 DAI	19-21 DAI	26-28 DAI	5-7 DAI	12-14 DAI	19-21 DAI	26-28 DAI
SPRAY	TEMP	0.041	0.003	0.019	0.002	0.106	0.003	0.001	0.009
	CULT	0.754	0.286	0.049	0.492	0.605	0.715	0.009	0.743
	TEMP*CULT	0.951	0.578	0.499	0.682	0.802	0.542	0.016	0.392
	RH	0.017	<0.001	<0.001	<0.001	0.012	<0.001	<0.001	<0.001
	TEMP*RH	0.351	<0.001	<0.001	0.001	0.250	<0.001	<0.001	<0.001
	CULT*RH	0.923	0.590	0.508	0.455	0.971	0.383	0.929	0.199
	TEMP*CULT*RH	1.000	0.800	0.742	0.217	1.000	0.982	0.382	0.053
POINT	TEMP	<0.001	0.002	0.001	<0.001	0.079	0.001	0.001	0.024
	CULT	0.687	0.576	0.501	0.010	0.683	0.276	0.296	0.157
	TEMP*CULT	0.958	0.523	0.981	0.142	0.867	0.495	0.294	0.501
	RH	0.241	0.001	0.183	0.186	0.389	0.004	0.064	0.086
	TEMP*RH	0.651	0.226	0.102	0.103	0.700	0.314	0.327	0.018
	CULT*RH	0.699	0.648	0.691	0.002	0.655	0.301	0.894	0.005
	TEMP*CULT*RH	0.983	0.005	0.981	0.101	0.854	0.003	0.694	0.094

[a]Two methods of inoculation were used, each treated as a separate experiment. As the name suggests, in the SPRAY inoculated experiment, spikes were sprayed with a spore suspension of MoL. In the POINT inoculated experiment, a drop of the spore suspension was deposited directly inside a floret in the central portion of the spike.

[b]The treatment factors evaluated were temperature (TEMP), hours of high (>95%) relative humidity immediately after inoculation (RH), and cultivar (CULT).

[c]Wheat spike blast incidence (mean proportion of diseased spikes in a sample) and severity (mean proportion of bleached, discolored spikelets per spike) at 5-7, 12-14, 19-21, and 26-28 days after inoculation (DAI).

Table 2.2. Parameters and corresponding statistics from the fit of non-linear forms of growth models to data from controlled environment studies of temporal development of wheat spike blast under different temperature and initial high relative humidity conditions

			Parameters and statistics[d]						Time to *y* blast intensity			
EXP[a]	Response[b]	Conditions[c]	y_o	se(y_o)	Rate	se(r)	MSE	R^2	6	15	25	50
SPRAY	Severity	20°C, 48 h RH > 95%	1.7E-03	7.2E-04	r_E = 0.15	0.011	0.005	0.91	24	30	33	38
		25°C, 24 h RH > 95%	6.6E-05	1.6E-04	r_G = 0.13	0.013	0.008	0.91	9	12	15	20
		25°C, 48 h RH > 95%	4.5E-04	6.1E-04	r_G = 0.15	0.011	0.005	0.96	7	9	11	16
		30°C, 24 h RH > 95%	2.9E-04	6.8E-04	r_G = 0.17	0.021	0.010	0.91	6	9	10	14
		30°C, 48 h RH > 95%	1.5E-06	1.0E-05	r_G = 0.28	0.047	0.016	0.89	6	7	8	11
	Incidence	20°C, 48 h RH > 95%	2.1E-03	1.9E-03	r_L = 0.19	0.028	0.018	0.85	18	23	26	32
		25°C, 24 h RH > 95%	6.9E-06	2.5E-05	r_G = 0.17	0.019	0.010	0.93	8	11	13	17
		25°C, 48 h RH > 95%	7.6E-09	6.2E-08	r_G = 0.28	0.038	0.010	0.93	7	8	9	12
		30°C, 24 h RH > 95%	9.3E-05	3.2E-04	r_G = 0.24	0.034	0.014	0.91	5	7	8	11
		30°C, 48 h RH > 95%	1.1E-47	9.5E-46	r_G = 0.61	0.098	0.007	0.96	6	7	7	8
POINT	Severity	20°C	1.4E-03	9.4E-04	r_E = 0.14	0.016	0.003	0.83	27	33	37	42
		25°C	4.7E-03	3.5E-03	r_G = 0.08	0.007	0.004	0.91	8	13	17	26
		30°C	7.1E-03	5.0E-03	r_G = 0.12	0.010	0.004	0.94	5	8	11	16
	Incidence	20°C	1.9E-02	6.9E-03	r_E = 0.09	0.010	0.014	0.84	13	23	29	36
		25°C	5.0E-04	6.4E-04	r_G = 0.15	0.011	0.005	0.96	7	9	11	16
		30°C	9.2E-06	2.9E-05	r_G = 0.31	0.029	0.005	0.97	5	6	7	9

[a]Two methods of inoculation were used, each treated as a separate experiment. As the name suggests, in the SPRAY inoculated experiment, spikes were sprayed with a spore suspension of an isolate (PL2-1) of the Lolium pathotype of *Magnaporthe oryzae*. In the POINT inoculated experiment, a drop of the spore suspension was deposited directly inside a floret in the central portion of the spike.

continued

Table 2.2. Continued.

[b]Wheat spike blast incidence (mean proportion of diseased spikes in a sample) and severity (mean proportion of bleached, discolored spikelets per spike).

[c]Inoculated spikes were subjected to different temperature and relative humidity treatments; RH represents the number of hours of high (>95%) relative humidity immediately after inoculation.

[d]Estimated y_0 (initial disease intensity) and rate parameters for exponential (r_E), Gompertz (r_G), and logistic (r_L) growth models, and their standard errors (se). MSE = mean square error and R^2 = coefficient of determination for relationship between predicted and observed mean spike blast incidence or severity.

Fig. 2.1. Images of wheat blast development in the growth chamber from spray inoculation (A, B) where disease begins as small dark lesions on multiple glumes, and point inoculation (C, D) where injected spores bypass the glumes to directly infect the rachis and disease spreads from one point vertically down the spike. Black marker was used on the glume above the inoculated glume (C, D) so the point of inoculation would be obvious throughout disease development.

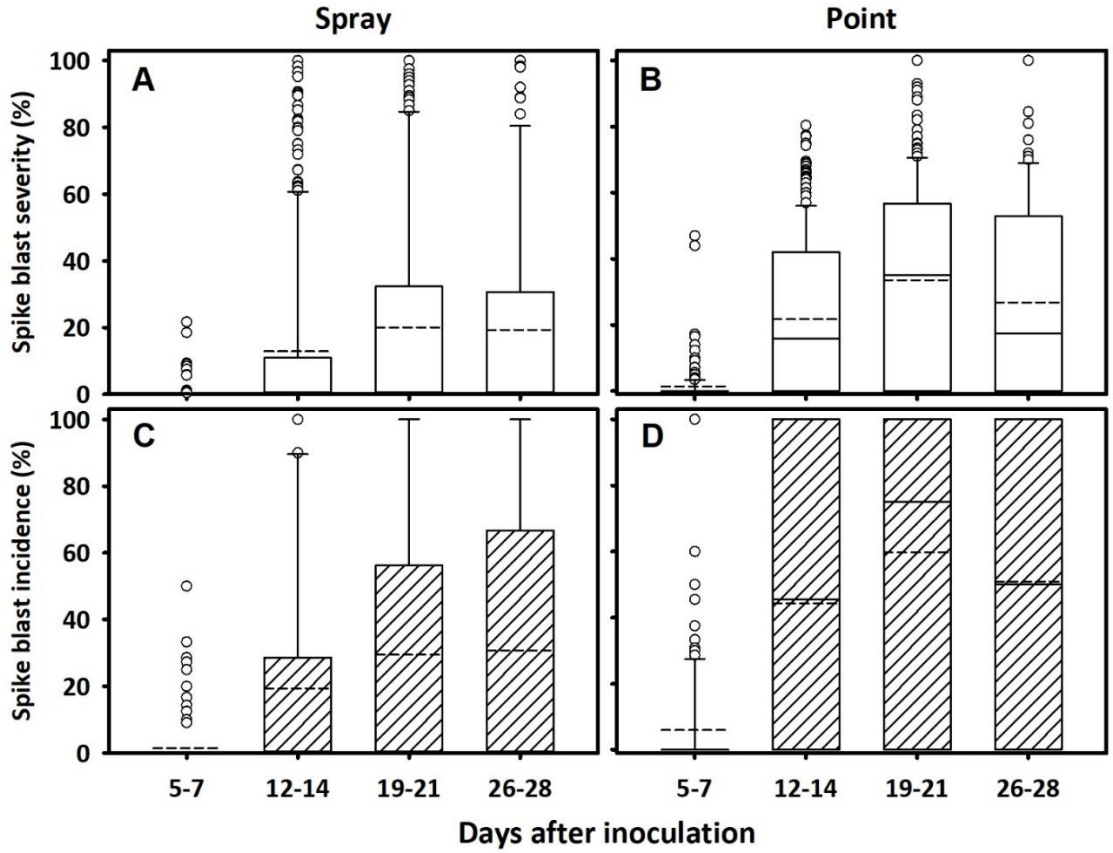

Fig. 2.2. Boxplots showing the distribution of mean wheat spike blast severity (**A** and **B**) and incidence (**C** and **D**) at 5-7, 12-14, 19-21, and 26-28 days after spray (**A** and **C**) or point (**B** and **D**) inoculation with a spore suspension of an isolate (PL2-1) of the Lolium pathotype of *Magnaporthe oryzae*. Broken and solid lines within each box represent means and medians, respectively, while the top and bottom lines of the box represent the 75th and 25th percentiles of the data, respectively. Vertical bars extending beyond the boxes represent the 5th and 95th percentiles, while circles represent outliers.

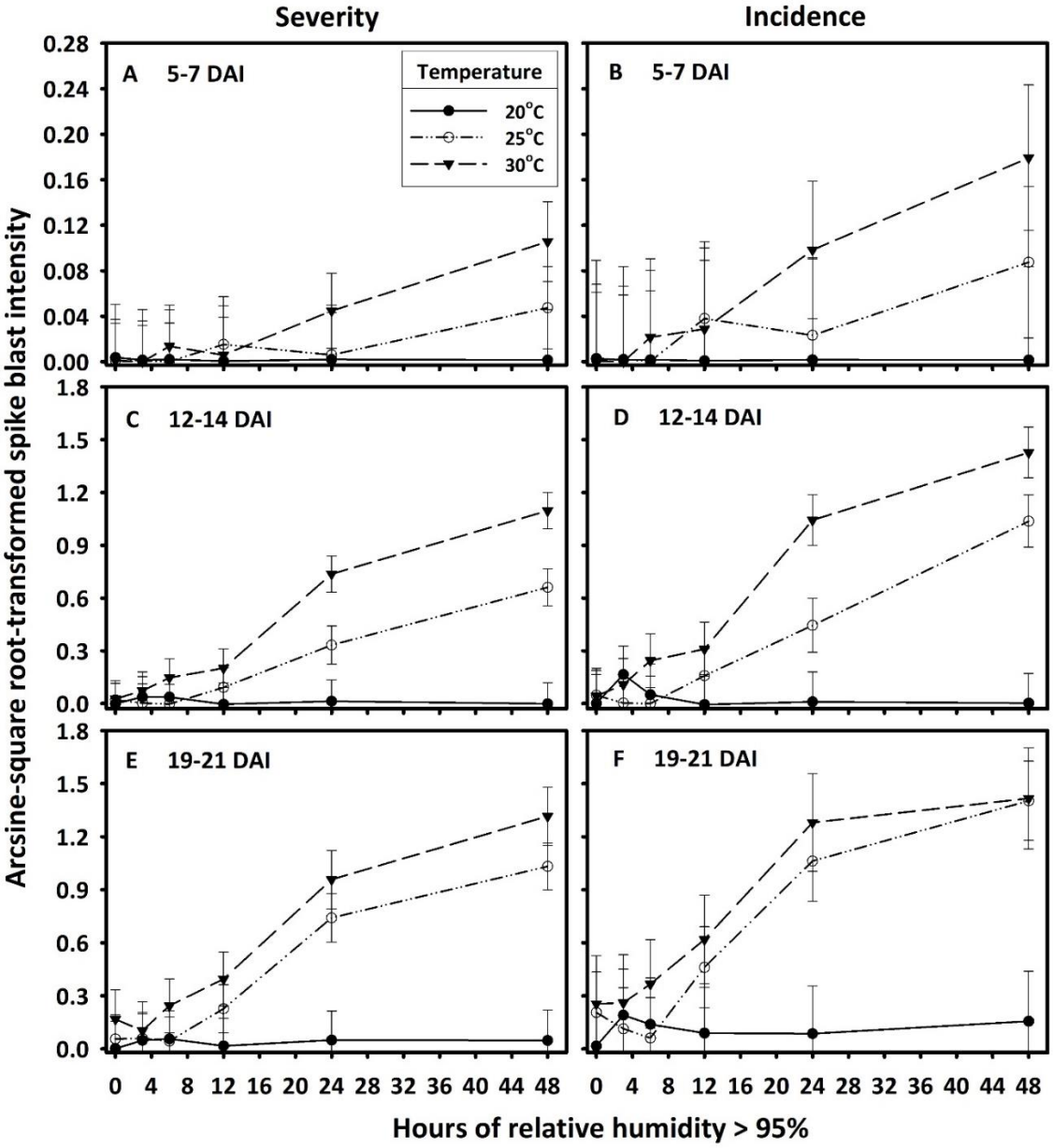

Fig. 2.3. Spray Inoculations: Effects of temperature and the duration of high (>95%) relative humidity immediately after spray inoculation on mean arcsine-square root-transformed spike blast severity (**A**, **C** and **E**) and incidence (**B**, **D**, and **F**) at 5-7 (**A** and **B**), 12-14 (**C** and **D**), and 19-21 (**E** and **F**) days after inoculation with a spore suspension of an isolate (PL2-1) of the Lolium pathotype of *Magnaporthe oryzae*. Points represent least squares means, averaged across wheat spikes, experimental units, cultivars, and replicates. Error bars are 95% confidence intervals around the means. For both responses, the scale on the y-axis was allowed to vary to facilitate visualization and comparison of trends among temperature treatments and assessment times.

Spray Inoculations

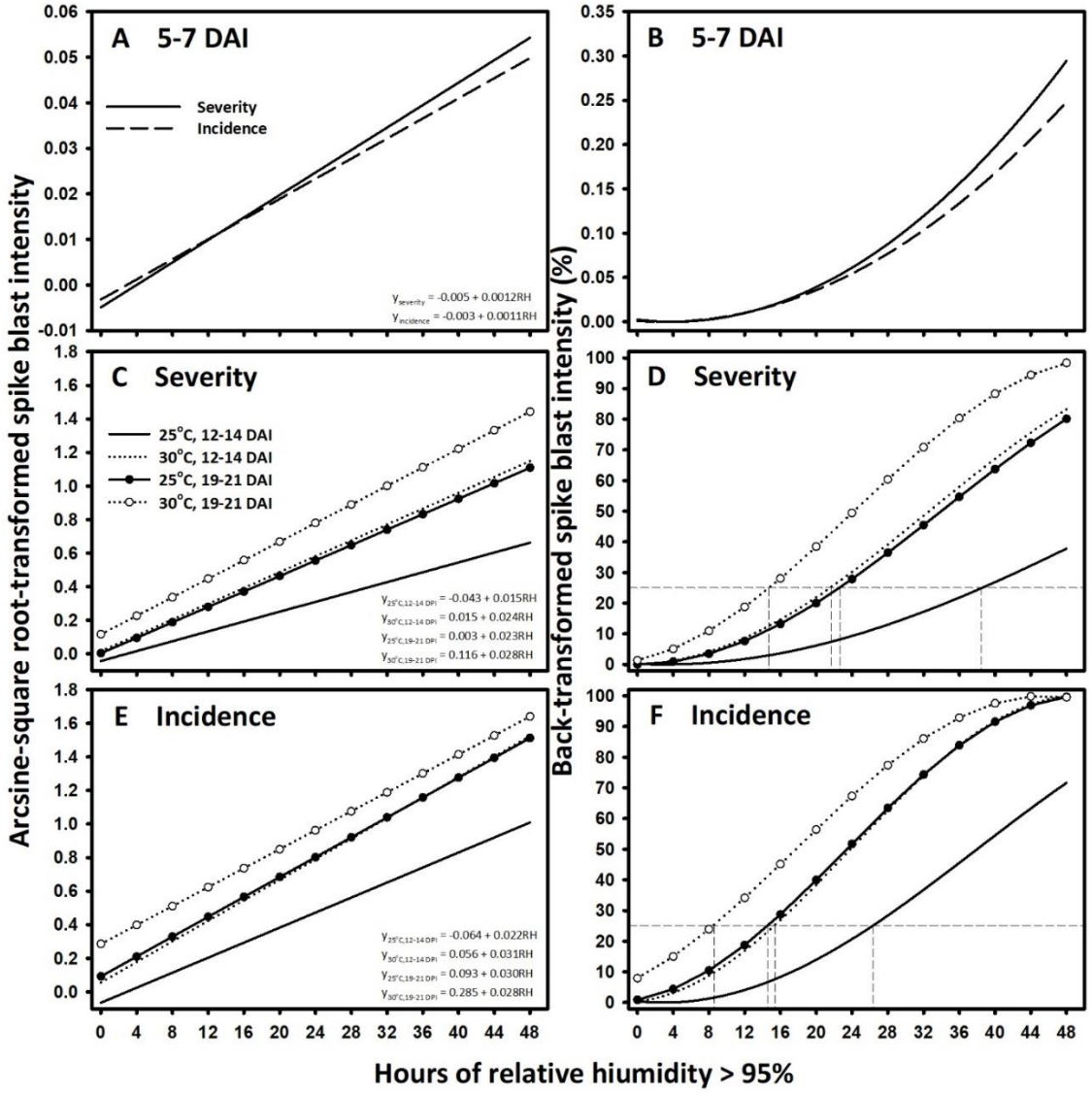

Fig. 2.4. Relationships between hours of exposure to high (> 95%) relative humidity immediately after spray inoculation with a spore suspension of an isolate (PL2-1) of the Lolium pathotype of *Magnaporthe oryzae* and arcsine-square root-transformed (**A, C**, and **E**) and back-transformed (**B**, **D**, and **F**) mean wheat spike blast severity and incidence at 5-7 (**A** and **B**) and 12-14 and 19-21 (**C**-**F**) days after inoculation. Inserts show model equations with intercept and slope parameters that were estimated through linear mixed model regression analyses with hours of high RH. A different scale was used on the y-axis in A and B to facilitate visualization of the trends at the low disease levels.

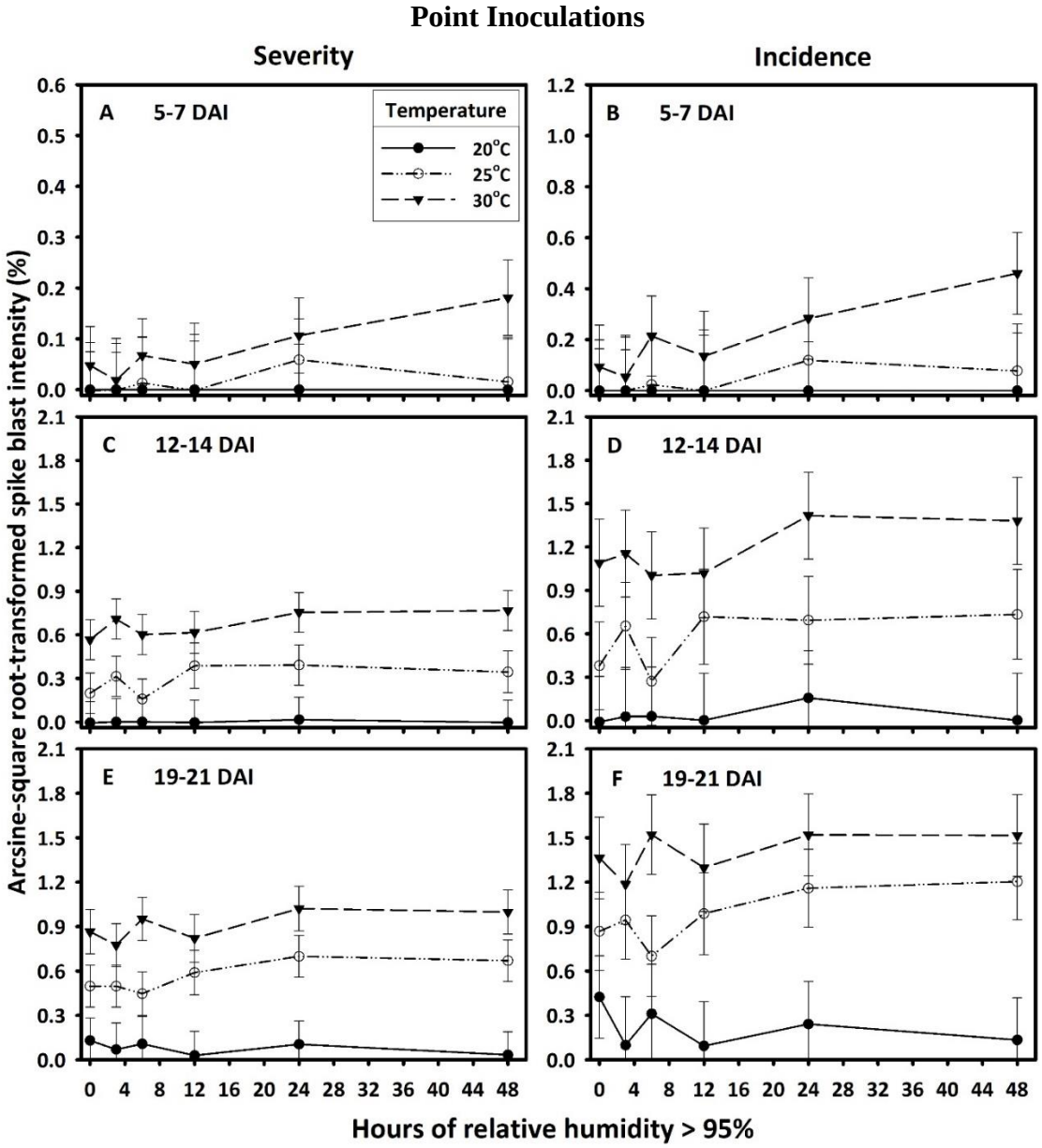

Fig. 2.5. Effects of temperature and the duration of high (>95%) relative humidity immediately after point inoculation on mean arcsine-square root-transformed spike blast severity (**A**, **C** and **E**) and incidence (**B**, **D**, and **F**) at 5-7 (**A** and **B**), 12-14 (**C** and **D**), and 19-21 (**E** and **F**) days after inoculation with a spore suspension of an isolate (PL2-1) of the Lolium pathotype of *Magnaporthe oryzae*. Points represent least squares means, averaged across wheat spikes, experimental units, cultivars, and replicates. Error bars are 95% confidence intervals around the means. For both responses, the scale on the y-axis was allowed to vary to facilitate visualization and comparison of trends among temperature treatments and assessment times.

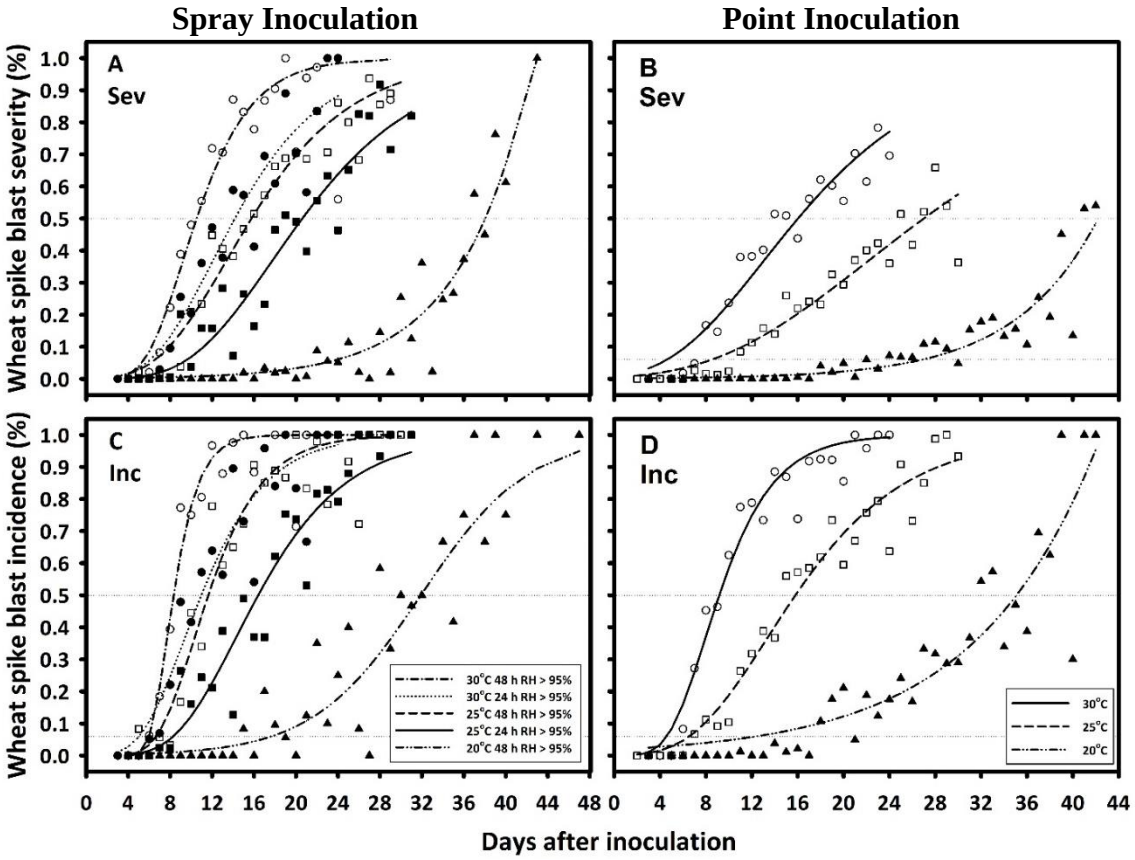

Fig. 2.6. Temporal change in mean wheat spike blast severity (**A** and **B**) and incidence (**C** and **D**) under different temperature and high RH durations (hours of > 95% relative humidity immediately after inoculation) treatments or combinations following spray (**A** and **C**) or point (**B** and **D**) inoculation with spore suspensions of an isolate (PL2-1) of the Lolium pathotype of *Magnaporthe oryzae*. Points represent means averaged across wheat spikes, experimental units, cultivars, and replicates. Lines are predicted responses from non-linear regression fit of growth models to the data for each temperature or temperature x hours of high (> 95%) RH treatment combination. Model parameters are in Table 2.2.

Chapter 3.

Quantifying the impact of Wheat Growth Stage, Inoculum Concentration, and Cultivar Susceptibility on the Development of Wheat Blast Caused by *Magnaporthe oryzae* Lolium Pathotype

ABSTRACT

The spread of wheat blast, caused by the Triticum pathotype of *Magnaporthe oryzae* (MoT), from South America to Asia and Africa has led to increasing concerns about MoT being introduced into the US or native isolates of the Lolium pathotype of the fungus (MoL) jumping from ryegrass to wheat. To better understand the risk posed by MoL to US wheat, this study was designed to quantify the temporal development of MoL-incited WB as influenced by host and pathogen factors. Spikes of a highly susceptible and a moderately susceptible wheat cultivar were inoculated with different MoL spore concentrations (CONC; $2x10^2$, $2x10^3$, $2x10^4$, or $2x10^5$ spores/ml) at growth stages (GS) ranging from Feekes 10.1 to 10.5.4, and temporal changes in blast incidence (INC; proportion of symptomatic spikes) and severity (SEV; average of the proportion of symptomatic spikelets per spike) were compared among treatment factors. There was a statistically significant ($P < 0.05$) interaction effect of cultivar and CONC on INC and SEV at 12-14, 19-21, and 26-28 days after inoculation (DAI), with increasing disease as CONC increased, but with the effect dependent on the cultivars. The highly susceptible cultivar had an average SEV of 31.4% when inoculated with $2x10^3$ spores/ml, whereas it took $2x10^4$

spores/ml for SEV to reach 28.8% on the moderately susceptible cultivar. Growth stage of inoculation did not have an effect on blast. The Gompertz growth model provided a good fit to INC and SEV data. The rate of increase in blast intensity was greater on the highly susceptible cultivar than on the moderately susceptible cultivar, and higher at high than at low inoculum concentrations. Bleaching symptoms began at approximately 5-8 DAI for inoculations with $2x10^5$ spores/ml, compared to 10-20 DAI for inoculations with $2x10^2$ spores/ml. At the highest CONC, INC and SEV increased from 6 to 50% on the highly susceptible cultivar in 3 to 6 days, whereas it took an additional 4 days for blast to reach the same intensity on the moderately susceptible cultivar. These findings are valuable for establishing protocols for testing cultivars or other treatments under controlled conditions, for assessing the risk of MoL-caused wheat blast, and for understanding the rapid increase in disease that is often associated with MoT wheat blast epidemics in commercial fields in South America.

INTRODUCTION

Many economically important graminaceous plant species are susceptible to diseases caused by the ascomycetous fungus *Magnaporthe oryzae*. This pathogen has specialized subpopulations, called pathotypes, that are named for host specialization on crops such as rice (pathotype *Oryzae*), wheat (*Triticum*), perennial ryegrass (*Lolium*), and millets (*Eleusine* and *Setaria*), although isolates of some pathotypes are able to cross-infect a wider range of graminaceous hosts (Ceresini et al. 2018; Cruz and Valent 2017; Tosa et

al. 2004, Valent et al. 2019). Wheat blast, a disease caused by the *Triticum* (MoT) pathotype of *M. oryzae*, was first described in the Brazilian state of Parana in 1985 (Igarashi et al. 1986) and has devastated wheat production in some regions of South America during years with highly conducive conditions for infection and disease development (Urashima et al. 2009, Kohli et al. 2011). Susceptible cultivars have been reported to suffer greater than 90% losses in Bolivia and Brazil (Cruz and Valent 2017, Goulart and Paiva 1992, 2000).

The most characteristic symptoms of wheat blast are partial or complete bleaching of spikes, with spikelets that are either empty or produce small, shriveled kernels (Goulart et al. 2007). Oblong lesions with dark outlines and tan or gray centers may be present on the peduncle or glumes of affected spike (Igarashi et al. 1986). Similar types of lesions may also develop on wheat leaves, but there are fields with high levels of bleaching on the spikes and few, if any, leaf lesions present. Lesions on leaves infected by MoT have been observed to sporulate during the active growing season, including during and after spike emergence (Cruz et al. 2015). Greenhouse and field studies have shown that wheat blast can develop when spikes are artificially inoculated with spores harvested from leaf lesions (Cruz et al. 2015). Results from analyses of the temporal change in naturally developing wheat blast intensity in Bolivia during an El Nino year with disease-favorable conditions showed that spike blast epidemics were best described by logistic models and that, when present, leaf blast could play a role in the development of spike blast (Cruz et al. 2015, Mills et al. 2021).

Although wheat blast was only endemic to South America for thirty years, in 2016 an outbreak occurred in Bangladesh in an estimated 15,000 hectares, with yield losses in affected fields reaching 51% (Islam et al. 2016, Mottaleb et al. 2018). India reported its first wheat blast outbreak in 2017 in the Bengal region bordering Bangladesh, where approximately 1,000 hectares were affected (Malaker et al. 2017). Following the first report in 2016, wheat blast has been observed in Bangladesh in every subsequent wheat growing season, with the number of affected districts increasing from eight to 19 in four years (Islam et al. 2020). Genetic analysis of the South Asian MoT isolate indicated that it was most closely related to a MoT lineage found in Minas Gerais, Brazil, and was likely introduced into Asia through import of contaminated seed (Cruz and Valent 2017, Islam et al. 2016, Sadat and Choi 2016). Unfortunately, wheat blast was also observed in Zambia during the 2017-18 growing season (at incidence ranging from 50 to 100%) and was also confirmed to be caused by MoT (Tembo et al. 2020).

MoT has not yet been reported in the United States (US), but a single wheat spike with characteristic blast symptoms was found in Kentucky in 2011. Subsequent genetic analysis confirmed that the causal agent was an isolate of *Magnaporthe oryzae Lollium* (MoL), which commonly causes gray leaf spot (GLS) on perennial ryegrass (Farman 2017). This suggests that local MoL could pose a threat to US wheat and has led some researchers to speculate that previous occurrences of the disease in US wheat fields may have been confused with Fusarium head blight (FHB), a spike disease of similar symptoms caused by *Fusarium graminearum* and related species. While several studies have tested the susceptibility of US wheats to the MoT pathotype (Cruz et al. 2012) and characterized

conditions favorable for the development of MoT-incited wheat blast (Kohli et al. 2011; Urashima et al. 1993), fewer studies have challenged US wheat varieties with the MoL pathotype (Gary Peterson *unpublished results*; Mills et al. 2015), and less is known about the environmental, host, and pathogen factors that are most conducive to the development of MoL-incited wheat blast.

Based on results from a controlled-environment study of the effect of temperatures and high initial relative humidity durations on the development of MoL-incited wheat blast on US soft red winter wheat (SRWW) cultivars, Mills et al. (2020) showed that optimum conditions for an isolate of MoL to infect and cause wheat blast were congruent with those experienced in US SRWW fields during a typical growing season. This provides further support for the idea that MoL could indeed become a threat to wheat production in the US. Farman et al (2017) hypothesized that in most years, unfavorable weather conditions for MoL inoculum buildup and the temporal separation among wheat heading (Feekes growth state 10.5), GLS development, and peak *M. oryzae* spore production are what prevent natural epidemics of MoL-incited wheat blast from occurring in the US. Since winter wheat is harvested between late spring and early summer, the crop would be out of the field well before GLS typically develops in late July and August (Uddin et al. 2003b), and consequently, before spores of MoL become abundant.

Hypotheses about the temporal separation between wheat development and peak MoL spore production preventing natural epidemics of wheat blast from occurring in commercial fields are based on assumptions that the window of susceptibility to MoL infection is fairly narrow (a single or a few growth stages) and that high inoculum density

at this growth stage is critical for blast development. Similar assumptions are made about the role of inoculum density in the rapid bleaching of spikes commonly observed in wheat blast epidemics in south America, with close to 100 incidence and severity in a very short time (Cruz and Valent 2017). Designed experiments under controlled conditions are needed to evaluate these assumptions to better understand the threat posed by MoL to US wheat and the role of inoculum density in blast epidemics; develop protocols for conducting experiments to study the epidemiology of wheat blast and to screen for resistance; and define growth stages for fungicide application and to generate summary weather variables for modeling the risk of blast epidemics.

Cruz et al (2016) proposed a standardized inoculation protocol for testing wheat cultivars for reaction to blast caused by MoT in biosafety containment. The approach consisted of spray-applying a spore suspension containing 2×10^4 spores/ml to spikes between full head emergence (Feekes 10.5) and early anthesis (Feekes 10.5.1). Similar protocols have been successfully used to screen wheat cultivars for 2NS-mediated resistance to MoT (Cruz et al. 2016) and to determine optimum temperature and RH conditions for the development of MoL-incited blast under controlled conditions (Mills et al. 2020), and to evaluate the impact of wheat blast on components of wheat physiology and grain yield (Rios et al. 2017) and the effect of fungicide and cultivar resistance on the temporal progress of the disease under field conditions (Rios et al. 2016). However, with the application of a single spore concentration at a specific growth stage, none of these studies were designed to determine the influence of infection timing/growth stage,

inoculum density, and their interaction on the development of wheat blast caused by MoL (or MoT) on wheat cultivars with different levels of resistance to blast.

The purpose of this study was to test US wheats with a wide range of inoculum concentrations applied at different crop growth stages to further identify conducive conditions for potential epidemic of wheat blast caused by MoL to occur. The specific objectives were to 1) determine whether inoculum density and crop growth stage of inoculation affected the development of spike blast on different wheat cultivars and 2) quantify the temporal dynamics of wheat spike blast as influenced by inoculum density and cultivar resistance. To accomplish these objectives, a susceptible hard red winter wheat cultivar and a moderately susceptible soft red winter wheat cultivar were inoculated with spore concentration ranging from 2×10^2 to 2×10^5 spores/ml at growth stages ranging from Feekes 10.1 to 10.5.4 and the resulting spike blast incidence and severity were quantified at regular intervals over a period of 28 days. Mean disease intensity at different times after inoculation were used along with estimated parameters from the fit of population growth models as measures of the effects of the tested treatment factors of MoL-incited wheat blast development.

MATERIALS AND METHODS

Preparation and maintenance of plants. Between 2015 and 2017, three experiments were conducted in temperature- and relative humidity-controlled walk-in growth chambers (Conviron BDW40, Winnipeg, Manitoba, Canada). Two wheat cultivars susceptible to both MoL and MoT (Mills et al. 2015) were used in the experiments, the

highly susceptible hard red winter wheat cultivar ‘Everest’ and a moderately susceptible experimental cultivar referred to as ‘12’. Fungicide-treated seeds of these cultivars were sown in plastic trays and grown in a greenhouse until they germinated. Once the seedlings reached the two-leaf stage, they were vernalized in a cold room at 3°C for approximately ten to twelve weeks. The cold room had fluorescent lights programmed to run at a fixed photoperiod of 16 h of light and 8 h of dark, and wheat was watered periodically to maintain soil dampness. Once vernalization was completed, the trays were placed in the walk-in Conviron growth chambers for a week and subjected to a program that approximated daily spring conditions in Ohio. Daily temperatures were ramped up from 6 to 16°C and back to 6°C, lights were programmed with the same fixed photoperiod of 16 h of light and 8 h of dark, and relative humidity was maintained between 75 and 95%.

Following this first week of transitioning out of vernalization, surviving tillers were planted individually into conetainers (Stuewe and Sons, Inc. Corvallis, OR) with autoclaved, unamended silt loam soil. Two walk-in growth chambers were used, each with three rolling carts, and each cart held three trays of 98 conetainers for a total of 1,764 conetainers. Conetainers were planted with tillers from Cultivars Everest (EVE) or Cultivar 12 (one tiller per cone), watered daily, and fertilized with a liquid nutrient solution once a week. Minimum and maximum daily temperatures were increased weekly for weeks 2 to 5 by 2°C to continue emulating the nature spring temperature progression (week 2: 8 and 18°C, week 3: 10 and 20°C, week 4: 12 and 22°C, week 5: 14 and 24°C). Week 5 temperature cycles were maintained until plants reached the desired growth stages for inoculation. The same fixed photoperiod was used throughout the duration of the

experiments. Prior to inoculation, powdery mildew was treated as necessary with 50% triadimefon (Baleton 50; Bayer CropScience, Research Triangle Park, NC) and aphids and fungus gnats were controlled with 21.4% imidacloprid (Marathon II; OHP Inc., Mainland, PA).

Experimental design, inoculum preparation, and inoculation. The experimental design was a randomized complete block with each experiment used as a blocking factor, and a split-split-split organization with growth stage as the whole-plot factor, cultivar as the sub-plot, and inoculum concentration as the sub-sub-plot. As spikes reached the desired growth stages (Feekes 10.1-10.3, 10.5, 10.5.1, and 10.5.4) they were randomly assigned to one of four inoculation concentration treatment groups ($2x10^2$, $2x10^3$, $2x10^4$, or $2x10^5$ spores/ml). Ideally, 20 plants were assigned to each category (sub-sub-plot experimental unit) as the wheat developed but adjustments were made when insufficient spikes developed, with some experimental units having as few as 10 spikes, but no less than 50 spikes across all three experiments. Inoculated plants were moved to and maintained in a third walk-in growth chamber set at 25°C with a photoperiod of 16 h of light and 8 hours of dark and an average relative humidity of 80% (Mills et al. 2020).

Plants were inoculated with the MoL isolate PL2-1 which was collected in Kentucky from *Lollium multiflorum* (Farman et al. 2017) (Fig. 3.1.). In comparison with a highly virulent MoT isolate collected from Bolivia, isolate PL2-1 was reported to cause approximately 75% of the disease intensity on several US wheat cultivars (Farman et al. 2017, Valent et al. 2019). PL2-1 spores had previously been collected from infected plants of ‘Everest’ (Mills et al. 2020) and grown on oatmeal agar (20 g/L quick cook oatmeal; 15

g/L granulated agar; 10 ug/L Carbenicillin) with autoclaved filter paper (approximately 1 by 1 mm). Highly colonized filter papers were collected and stored in microtubes at -20°C. Fresh MoL colonies were grown by placing a single piece of infested filter paper on a petri dish with oatmeal agar and incubating at room temperature under near-ultraviolet light for a fixed photoperiod of 16 h of light and 8 h of dark. Colonies were harvested between 7 and 10 days after incubation by flooding each petri dish with sterilized water and massaging the mycelium with a rubber Policeman. The resulting suspension was filtered through two layers of cheesecloth to collect the conidia. Spore concentrations were estimated using a hemocytometer, and sterilized water was added to produce a suspension with $2x10^5$ spores/ml. The other experimental spore suspensions ($2x10^4$, $2x10^3$, and $2x10^2$ spores/mL) were made through serial dilutions with sterilized water. Four inoculation spray bottles were each filled with 50 mL of a separate spore suspension along with a drop of Tween 20. Spores were freshly harvested every day that plants were inoculated .

Once a spike reached a desired growth stage, it was assigned to an inoculum concentration treatment and a color-coded piece of flagging tape with a unique identifier was attached to the peduncle of the tiller so that its individual disease progression could be recorded. Spikes at early (Feekes 10.1-10.3) or full head emergence (Feekes 10.5), anthesis (Feekes 10.5.1), or watery ripe (Feekes 10.5.4) growth stages were individually spray inoculated with approximately 2 mL of the assigned spore suspension sufficient to fully cover the spike surface. Each freshly inoculated spike was then covered in a 0.3 mm clear plastic bag with a metal twist tie and placed in a growth chamber maintained at a constant 25°C. Bagged spikes maintained continuous tissue wetness from the spray application as

well as through respiration, with high relative humidity. Bags were removed after 24 hours and spikes remained uncovered in the 25°C chamber. This was previously shown to be highly favorable conditions of temperature and initial high RH for MoL to infect and cause spike blast (Mills et al. 2020). Plants were checked daily, watered regularly to maintain damp soil, and fertilized once a week. No pest management applications occurred after inoculation.

Disease assessments began approximately seven days after inoculation and continued for each spike roughly every three to five days until the spike reached the milky ripe growth stage (Feekes 11, an average of 25 days after inoculation [DAI]) when spikes began to senesce and bleach naturally, and thus became indistinguishable from diseased tissue. The time it took for a spike to reach Feekes 11 ranged from 15 to 42 DAI and was negatively related to the inoculum concentration. At each assessment, the presence and number of glume lesions and bleached spikelets on each spike were recorded. Disease severity was defined for each spike as the number of bleached spikelets divided by the number of spikelets present multiplied by 100, and blast incidence was calculated as the number of spikes in an experimental unit with disease symptoms (at least one bleached spikelet) divided by the number of spikes in that experimental unit multiplied by 100 (Paul et al. 2005).

Statistical analyses and model fitting. *Linear mixed model analysis (LMM)*. The effects of wheat growth stage, cultivar, and inoculation concentration on spike blast intensity were analyzed using the GLIMMX procedure of SAS (Stroup et al. 2018) to fit separate linear mixed models to the incidence and severity data. Since disease assessments

were done at 3-5-day intervals, data were pooled for each experimental unit into three-day windows or bins (5-7, 12-14, 19-21, and 26-28 days after inoculation [DAI]) and analyzed separately to compare treatment factors and combination of factors in each bin. The blocking factor, year, and its interactions with growth stage and cultivar were treated as random effects, whereas growth stage, cultivar, and inoculum concentration (whole-, sub-, and sub-sub plots respectively) were fixed effects in the models. The variance-stabilizing arcsine-square root transformation was used on the dependent variables, blast incidence and severity. The model fit to the data can be written as:

$$y_{ijkl} = \theta + \alpha_i + \beta_j + \tau_k + (\alpha\beta)_{ij} + (\alpha\tau)_{ik} + (\beta\tau)_{jk} + (\alpha\beta\tau)_{ijk} + b_l + d_{il} + w_{ijl} + e_{ijkl}, \quad (1)$$

where y_{ijkl} is the response (dependent variable; arcINC, arcSEV) for the *i*-th growth stage (GSTAGE), *j*-th cultivar (CULT), and *k*-th inoculum concentration (CONC) within in the *l*-th block (BLK), θ is the constant (intercept), α_i is the effect of the *i*-th GSTAGE, β_j is the effect of the *j*-th CULT, τ_k is the effect of the *k*-th CONC, $(\alpha\beta)_{ij}$ is the effect of the *i*-th GSTAGE x *j*-th CULT interaction, $(\alpha\tau)_{ik}$ is the effect of the *i*-th GSTAGE x *k*-th CONC interaction, $(\beta\tau)_{jk}$ is the effect of the *j*-th CULT x *k*-th CONC interaction, $(\alpha\beta\tau)_{ijk}$ is the effect of the *i*-th GSTAGE x *j*-th CULT x *k*-th CONC interaction, b_l is the effect of the *l*-th BLK (i.e., year), d_{il} is the effect of the *i*-th GSTAGE x *l*-th BLK interaction (whole-plot error), w_{ijl} is the effect of *i*-th GSTAGE x *j*-th CULT x *l*-th BLK interaction (sub-plot error), and e_{ijkl} is the residual. A similar model and approach were used to identify

temperature and high relative humidity conditions for wheat spike blast development (Mills et al. 2020).

The *lsmeans* and *lsmestimate* statements in PROC GLIMMIX was used to compare mean arcsine-square root-transformed incidence (arcINC) and severity (arcSEV) between treatments and treatment combinations. Simple effect hypothesis tests for treatment factors with statistically significant interaction effects on arcINC or arcSEV were obtained through the *slicediff* option in the *lsmeans* statements (Stroup et al. 2018). These simple-effects hypothesis tests were used to determine the significance (effect) of one factor at each level of another factor or combinations of factors. Results from the LMM were used to identify which factor(s) contributed significantly to arcINC and arcSEV and inform which factors should be included in the regression analyses described below (Table 3.1.).

Linear regression analysis. Since results from the LMM analyses showed that the effects of CULT, CONC, and their interaction (CULT x CONC) were statistically significant ($P < 0.05$) across many of the assessment windows (see Results), linear mixed model regression analyses were performed to quantify relationships between spike blast intensity and CONC as influenced by CULT at 12-14, 19-21, and 26-28 DAI. The models fitted to the data were similar to that shown in eq 1, with arcINC or arcSEV as the dependent variable, but with CONC as a continuous covariate and CULT as the only categorical fixed effect. In addition, the regression models were not fitted to data from the 5-7 DAI bin because mean spike blast INC and SEV were too low, and the range of values too narrow to adequately quantify their relationships with CONC. Approximately 99.6% of the 1295 spikes rated at 5-7 days DAI had severity < 1%. The GLIMMIX procedure in

SAS was used for model fitting and to test whether common-slope or unequal slope models were appropriate for each combination of factors (Stroup et al. 2018). *Estimate* statements were used to calculate the intercepts and slopes for cultivars EVE and 12 for each disease response at each assessment time and to compare these parameters between the cultivars, and to compare means at fixed levels of the covariate.

Non-linear regression analysis. The results from the analyses on significant effects also informed which combinations of factors should be used to evaluate the temporal change in wheat blast incidence and severity. Again, since the CONC x CULT interaction had a highly significant effect on spike blast incidence and severity (on arcsine square-root-transformed scale) at all tested assessment times, monomolecular, exponential, logistic, and Gompertz growth models were individually fitted to data for each CONC x CULT combination (Madden et al. 2007). Each CONC x CULT combination was considered a separate dataset (group) for analysis. All models were fitted to the untransformed mean spike blast severity and incidence data (as proportions) across experiments and growth stages using the NLIN procedure in SAS. The best fit models were then determined based on mean square errors and coefficients of determination (R^2). Models with the lowest MSE and the highest R^2 were selected for subsequent comparisons of epidemics. Model parameters and their standard errors were estimated in PROC NLIN, and t-tests were used to test the null hypothesis of no difference in parameter estimates between pairs of epidemics described by the same model (Madden et al 2007). The parameters were also used to estimate of length of time it took for each epidemic to reach specific levels of blast intensity that are potentially biologically or commercially relevant

(6, 15, 2, and 50%) by substituting the disease level of interest in the model equation and then solving for time as described by Madden et al. (2007).

RESULTS

Wheat blast development - exploratory analysis. Symptoms of wheat blast began as small, dark lesions on the spike glumes around day 5 after inoculation (DAI) for both cultivars (Fig. 3.1). Bleached spikelets were visible on day 5 for Cultivar EVE and day 7 for Cultivar 12. Blast developed at each level of CONC ($2x10^2$, $2x10^3$, $2x10^4$, $2x10^5$) following inoculation at all tested GSTAGE, but intensity was very low at 5-7 days DAI (Fig. 3.2.), with a mean severity and incidence of 1.8 and 6.2%, respectively for Cultivar EVE, and 0.02 and 0.3%, respectively for Cultivar 12. Since BIN 5-7 had very low levels of disease, with the majority of the observations within a very narrow range, data from this BIN was excluded from most of the analyses described below. There was a total of 9,338 disease observations from assessments of 701 spikes. The BINs (12-14, 19-21, 26-28 DAI) included 3,266 of the 9,338observations (35%) that were used in the LMM analyses of variance. The proportion of blast-affected spikelets and spikes increased substantially over time, reaching a final mean severity and incidence of 62 and 84%, respectively, for Cultivar EVE, and 46 and 68%, respectively, for Cultivar 12 (Fig. 3.2.).

The density plots in Fig. 3.2. show the wide range of disease responses, reflecting the extreme differences to the different levels of CONC. Responses were very low at $2x10^2$ spores/ml and very high at $2x10^5$ spores/ml, giving a bimodal distribution. The interquartile

ranges (IQRs) reflected this bimodal pattern; the IQRs for incidence was from 0 to 100% for every BIN and both cultivars. The means and standard errors for each BIN by CULT and CONC are shown in Fig. 3.3. The general pattern was increasing blast intensity with increasing CONC, with the greatest separations in mean incidence and severity between the two cultivars at $2x10^3$ and greater spores/ml at 12-14 and 19-21 DAI (Fig. 3.3.A, B, D, and E). Whereas at the latest assessment time, 26-28 DAI, separations in mean severity between the two cultivars were comparable across all tested CONC (Fig. 3.3.C). For incidence, the greatest separation was at the two lowest concentrations at this late assessment time. Incidence approached or reached 100% at the highest concentration tested at this time, making it difficult to detect a cultivar effect. In previous studies, cultivar EVE was used as a highly susceptible check when screening hard winter wheat for resistance to MoT (Cruz et al. 2012) and Cultivar 12 was identified as moderately susceptible to blast when screened with MoL (Mills, unpublished data), and these data further supported the distinction that EVE is highly susceptible and 12 is moderately susceptible. This susceptibility characterization allowed us to quantify and model the effect of cultivar resistance on the temporal development of spike blast as influenced by inoculum concentration in two different wheat market classes (see below).

Effect of cultivar, inoculum density, and growth state of inoculation. *Linear mixed model analyses.* The main effect of GSTAGE and two- and three-way interactions involving GSTAGE were not statistically significant in most cases ($P > 0.05$, Table 3.1.). The only exceptions were for the main effect of GSTAGE on arcINC at 12-14 DAI and the CONC x GSTAGE interaction effect on arcINC at 26-28 DAI ($P < 0.05$). At earliest time,

12-14 DAI, mean arcINC was significantly greater when spikes were inoculated at the Feekes 10.1-10.3 that and the other three growth stages. Similarly, the effect of GSTAGE on arcSEV at 12-14 DAI was marginally significant ($P < 0.08$, Table 3.1.), with inoculation at Feekes 10.1-10.3 resulting in significantly higher means than inoculations at the Feekes 10.5.1 or 10.5.4 growth stages. At 26-28 DAI, the effect of GSTAGE on arcINC was only statistically significant when spike were inoculated with 2×10^3 spores/ml, whereas the effect of CONC was statistically significant at all tested growth stages of inoculation.

Results from LMM analyses showed that at 12-14, 19-21, and 26-28 DAI the main effect of inoculum concentration (CONC) and its interaction with CULT (CULT x CONC) were statistically significant ($P < 0.05$; Table 3.1) for both arcsine-square root-transformed severity (arcSEV) and incidence (arcINC). The only exception was for arcSEV at 26-28 DAI where the CULT x CONC interaction effect was not significant ($P = 0.51$). Significant CULT x CONC interactions meant that the effect of CULT on the responses depended on CONC and vice versa, consequently, less emphasis place was on the two main effects.

Contrasts (estimated differences) of least squares means on the arcsine-square root transform scale between cultivars at each level of CONC are shown in Table 3.2. At 12-14 DAI, mean arcINC and arcSEV were significantly different ($P < 0.05$) between EVE and Cultivar 12 at the three highest levels on CONC ($2x10^3$, $2x10^4$, $2x10^5$ spores/ml). At 19-21 DAI, this pattern held for mean arcSEV, but was only significant at CONC $2x10^4$ for mean arcINC. At 26-28 DAI, the only significant difference between the cultivars was observed for arcINC when spikes were inoculated with $2x10^3$ spores/ml. For both cultivars, arcINC and arcSEV increased as CONC increased at 12-14, 19-21, and 26-28

DAI, with pairwise differences in means between pairs of CONCs being statistically significant in most cases ($P < 0.05$).

Linear mixed model regression analyses. Separate linear mixed models were fit to the data for each disease assessment time BIN with CONC as a continuous variable and CULT as a categorical fixed effect, and the resulting coefficients were compared between cultivars (Table 3.3). Common-slope models were fit to all the transformed severity data, except for 12-14 DAI in which an unequal slopes model was fitted because . For each combination of BIN and CULT, slopes were positive and significantly different from zero for both arcSEV and arcINC response variables. For the unequal slope models fitted to arcSEV at 12-14 DAI, the rate of increase in arcSEV per unit increase in CONC for Cultivar EVE was over twice the rate for Cultivar 12 (2.89×10^{-3} versus 1.37×10^{-3}). The difference was statistically significant ($P = 0.002$). The arcSEV/CONC regression line was significantly higher for cultivar EVE than Cultivar 12 ($P < 0.05$, Table 3.3). For the common slope models (arcSEV at 19-21 DAI), this difference in intercepts is equivalent a significant difference in height of the regression lines at all levels of inoculum within the range of concentrations tested here. For the unequal slope models (arcSEV at 12-14 DAI), the regression line was also significantly higher for EVE than Cultivar 12 at all tested inoculum concentrations. For all other relationships, the intercepts were not significantly different between the cultivars ($P > 0.05$, Table 3.3).

Non-linear regression analyses – temporal change in spike blast intensity. The MSE and R^2 statistics for the fit of the non-linear forms of the exponential, logistic, Gompertz, and monomolecular models to the disease progress data are given in Table 3.4.

Separate model fits were done for each cultivar and level of CONC. Disease levels were relatively lower and more variable, with a high proportion of zeros, at the $2x10^2$ ml/spore concentration than at higher concentrations, and as such, resulted in all tested growth models fitting the data equally poorly for this low CONC (Figs. 3.4 and 3.5). This was particularly true for models fitted to data for the moderately resistant Cultivar 12 (Table 3.4., Fig. 3.4E, and Fig. 3.5E). For cultivar EVE at all higher concentrations, and to a lesser extent for Cultivar 12, the Gompertz and monomolecular models provided good fits to the data, and better fits than the logistic and exponential models. Further analyses were done using the Gompertz (Madden et al. 2007).

By choosing the same model for all combinations of factors, we were able to compare the rate parameters for spike blast symptom increase over time between levels of CULT and CONC (Figs. 3.4, 3.5). The estimates rates of increase (r_G), intercepts (y_0), and SEs are listed in Table 3.5., and pairwise comparison of the rates between Cultivars EVE and 12 at each level of inoculum concentration are shown in Table 3.6. At all inoculum concentrations greater than $2x10^2$ spores/ml, the temporal rate of change in spike blast intensity was significantly different ($P < 0.001$) between the cultivars, with r_G estimates for EVE being between 1.63 and 2.67 times the estimates for Cultivar 12 for both incidence and severity. Additionally, for both cultivars, rates were compared between highest tested inoculum concentration ($2x10^5$ spore/ml) and each of the other three concentrations using paired t-tests (Table 7). In most cases, r_G estimates were significantly higher ($P < 0.01$) on spikes inoculated with for $2x10^5$ spores/ml than on those inoculated with lower concentrations for both incidence and severity (Table 7). The only exception was for the

comparison of the rates for incidence on Cultivar 12 between the $2x10^4$ and $2x10^5$ spores/ml inoculum concentrations.

Predicted spike disease incidence and severity versus assessment time based on the fits of the Gompertz model are shown in Fig. 3.6. These show the increasing disease intensity at a given time with increasing CONC and the shortening of the time to reach certain pre-determined threshold intensities as CONC increased. To better characterize the differences in temporal development of blast among epidemics resulting from the different CULT x CONC combinations, time to 6, 15, 25, and 50% blast incidence and severity, referred to as t_6, t_{15}, t_{25}, and t_{50}, respectively, specifically were estimated. This was done by substituting the blast threshold and the parameters in Table 3.5 into the Gompertz model equation (eq 4.20 in Madden et al. [2017]) and solving for time (t_S) (Madden et al. 2007). Thus, these calculations simultaneously utilize both the y_0 and r_G results. Since the average number of spikelets per spike was 17.3 across the 9,339 spikes (from all three experimental repetitions) in this study, one bleached spikelet would be approximately 6% severity. Therefore, time to 6% severity (t_6) was used as a good approximation of the mean incubation period, the time between inoculation and symptom development. As expected, spike blast symptoms appeared faster on the susceptible cultivar EVE then on moderately susceptible Cultivar 12, and faster for the highest CONC than for lower inoculum concentrations (Table 3.4). For instance, depending on the inoculum concentrations, the incubation period (t_6) was from 1 to 6 days shorter for EVE than for Cultivar 12. The difference in t_S values between the two cultivars increased as the disease progressed (i.e., for values of t_{15} and higher). As inoculum concentration increased, the range of days

between 6% to 50% blast intensity decreased for both cultivars (Table 3.5.). It took 2.3 times longer for severity on EVE to reach 6% when spikes were inoculated with $2x10^2$ spores/ml (14 days) than with $2x10^5$ spores/ml (6 days), and disease incidence took an average of 1.7 times longer to reach 6% with the lowest concentration compared to higher concentrations (6 and 10 days, respectively) for this cultivar. This difference was amplified in EVE for higher levels of disease, with both incidence and severity taking 3 times longer to reach 50% for spike inoculated with $2x10^2$ spores/ml compared to those inoculated with $2x10^5$ spores/ml (Table 3.5). Cultivar 12 held a similar pattern for disease incidence, where the size of the difference in t_s between the highest and lowest spore concentrations was larger at higher levels of disease. However, for spike severity, the ratio was more consistent, and it took approximately 2.5 times longer for spikes inoculated at $2x10^2$ spores/ml vs $2x10^5$ spores/ml to reach each of the disease severity thresholds.

At the highest inoculum concentration ($2x10^5$ spores/ml), the difference between t_6 and t_{50} was only 3 days for incidence and 6 days for severity for EVE, and about 5 and 11 days, respectively, for the less susceptible Cultivar 12. For disease incidence and severity on cultivar EVE, the difference between t_6 and t_{50} at the lowest tested inoculum concentration ($2x10^2$ spores/ml) was 16 and 22 days, respectively, and for Cultivar 12, it was 27 and 22 days.

DISCUSSION

As previous studies have established, a US *Lolium* isolate of *Magnaporthe oryzae* (MoL) was capable of causing typical wheat blast symptoms and severe disease development on US wheat (Mills et al. 2020; Farman et al. 2017; Tosa et al. 2004; Urashima et al. 1993). We further demonstrated that the growth stage at the time of inoculation between Feeke's 10.1 and 10.5.1 generally did not affect symptom development and disease intensity. Since proper timing of fungicide sprays to control wheat blast is a critical part of a successful management program (Cruz and Valent 2017), it was important to determine at which growth stage(s), if any, wheat spikes are most susceptible to infection by MoL (and MoT). There has been much research on the disease cycle and epidemiology of Fusarium head blight (FHB), caused by *Fusarium gramineaum* and other species, another disease of the spike with infection from by air and rain-dispersed spores (Schmale III and Bergstrom 2003). The timing of fungicides to manage FHB is based on when the spikes are most susceptible to infection, so that fungicides are applied when they are likely to be most effective (Dong 2020). The highest levels of FHB usually occur with infection during anthesis when spores land on anthers that are extruded from florets (Feekes 10.5.1) (Schmale III and Bergstrom 2003). Although wheat is still susceptible to infection by up to two weeks following anthesis, typical bleaching and discoloration of spikelets only occur when spikes are infected during and the first 7 days after anthesis (Pugh et al. 1933; Sutton 1982). Fungicide sprays applied between Feekes 10.5.1 and 10.5.4 are generally most effective to suppress FHB (Paul et al. 2018, 2019).

Additionally, cultivars that are more susceptible to FHB have been observed to have a longer window of susceptibility than less susceptible cultivars (Cowger et al. 2020). To our knowledge, no such information is available on the growth stage(s) of greatest susceptivity of wheat to MoL or the optimum growth stage for the timing of fungicides for disease control.

Our results showed that wheat was equally susceptible to MoL infection when inoculated with spores from early spike emergence (Feekes 10.1) through watery ripe (Feekes 10.5.4). Infection at any of these stages resulted in the development of similar final levels of spike blast intensity based on the mixed model analysis. However, for both Cultivars EVE and 12, spikes that were infected earlier often did not develop any kernels in the bleached spikelets, whereas spikes infected at later growth stages had under-developed kernels above the point of infection and larger-than-normal kernels below the point of infection. This observation about kernel development for earlier versus later infections of wheat spikes was also observed in MoT infected wheat in South America (Goulart et al. 1992). This study did not quantify the yields that resulted from early versus late infections, for which growth stage at time of infection may have a significant effect. The only evidence of an effect of growth stage at the time on infection on spike blast development in our work was seen at 12-14 days after inoculation when mean incidence and severity (both on the transformed scale) tended to be greater (at $P < 0.10$) when spikes were inoculated at the Feekes 10.1-10.3 than at the other three growth stages. The lack of significant interactions between cultivar and growth stage suggests that the window of susceptibility to infection is not cultivar-dependent. However, the future studies will need

to investigate a larger number of cultivars, resistance classes, and market types to draw broader conclusions about infection efficacy at different growth stages, as well as to determine yield effects of infection at different growth stages. Results suggest that wheat spikes would need protection from MoL spores during a wide time window and provides some explanation as to why multiple pre- and post-anthesis fungicide applications are commonly needed to control MoT wheat blast in South America under highly favorable weather conditions (Cruz et al. 2019).

We clearly showed that MoL inoculum density at the time of infection had a significant effect on wheat spike blast onset and temporal development, with a general monotonic increase in disease with increase in inoculum. If we can consider MoL as a model system to study MoT, or at least interpret MoT results based on our MoL findings, the decreasing incubation period and time to specific levels of disease with increasing inoculum density of MoL in this study suggests that inoculum density may be an important factor in the rapid bleaching and discoloration of spikes commonly associated with MoT wheat blast epidemics in South America and elsewhere. Although research has not confirmed all of the possible sources of MoT inoculum for spike infection in naturally occurring blast epidemics, there is increasing evidence that inoculum from leaf lesions during early stages of wheat development (emergence and tillering) may contribute to spike blast (Cruz et al. 2017). Lesions on low-canopy leaves have been observed to sporulate around the time of anthesis and can produce large numbers of spores under controlled conditions (Cruz et al. 2017). Concentrations of inoculum from within-field lesions are easier to quantify than air-borne spores since it is challenging to differentiate among the

different pathotypes of *Magnaporthe* that are commonly present around wheat fields (Danelli et al. 2019). However, recent technological advances using quantitative loop-mediated isothermal amplification (qLAMP) have made it possible to successfully quantify MoL in perennial ryegrass fields up to 12 days before gray leaf spot symptoms appeared with as few as 10 spores in the trap (Villari et al. 2017). As the spore-trap qLAMP systems become more reliable in naturally infested perennial ryegrass fields, they may become an essential tool in management plans for both gray leaf spot and MoL wheat blast. Our findings on the effect of different spore concentrations on disease intensity, together with our previous results on temperature and high relative humidity durations on infection and fungal colonization of spikes, may contribute to defining risk of disease in the field, which could be used for fungicide application decision making.

Cultivar affected the magnitude of MoL blast intensity on spikes and also the functional relationships between inoculum density and spike blast intensity at different times during the epidemic. The highly susceptible cultivar Everest (EVE) generally had higher levels of severity and incidence than the moderately susceptible Cultivar 12 at the evaluated inoculum concentrations. At the lowest inoculum concentration, there were no significant differences in incidence or severity between the cultivars, reflecting the very low disease intensity at this inoculum concentration. However, for higher inoculum concentrations ($> 2x10^2$ spores/ml), and especially beyond the earliest assessment time when disease was always low, one or both disease variables were significantly higher for EVE than Cultivar 12. Based on results from the LMM regression analyses, the rate on increase in incidence or severity (on the transformed scale) at 12-14, 19-21, and 26-28 DAI

per unit increase in inoculum concentrations was comparable between the cultivars. The difference between the cultivars thus was an overall effect, represented by differences in the intercept; the intercept for Cultivar 12 was 24-51% lower than for EVE. The only exception was for severity at 12-14 DAI where EVE had a significantly higher rate (2.89 x 10^{-3}) of increase in transformed severity per unit increase in inoculum density compared to Cultivar 12 (1.37 x 10^{-3}). These estimated parameters support visual observations of higher disease in EVE than in 12.

Both the Gompertz and monomolecular growth models were good fits to the incidence and severity progress curves for most combinations of cultivar and inoculum density. The goodness of fit with the Gompertz model, based on estimated coefficients of determination (R^2) and residual plots, was somewhat better than the monomolecular, and the fit was better at higher than at lower inoculum densities for both cultivars. For instance, the R^2 for severity on EVE increased from 0.49 to 0.92 when inoculum concentrations increased from $2x10^2$ to $2x10^5$ spores/ml; similar increases occurred with Cultivar 12. This pattern of increasing R^2 was the same when incidence was modelled. In addition, the fit for cultivar EVE was generally better than for Cultivar 12. These finding are consistent with those from controlled-environment studies with the same MoL isolate on SRWW which showed that the Gompertz model best described the fastest blast development which occurred in high temperatures with long durations of high relative humidity, but was not the best fit model for conditions which resulted in slower blast development (Mills et al. 2020). Some Bolivian field studies with naturally occurring MoT-incited wheat blast epidemics also showed that Gompertz models were good fits to temporal blast development

(Mills et al. 2021; Gongora-Canul et al. 2020). Although the Gompertz is generally considered an appropriate model for polycyclic diseases, it may approximate a monomolecular model with a time-varying rate parameter, such as when inoculum density changes with time or the probability of infection from a unit of inoculum changes with time (Madden et al. 2007). The fungal colonization of spikes is also analogous to multiple infections with the disease progress model.

Based on results for t-tests, the Gompertz rate parameter (r_G) was significantly higher for EVE than for Cultivar 12 at all inoculum levels higher than $2x10^2$ spores/ml, suggesting that at low levels of inoculum (where disease intensity is lower), the effect of cultivar resistance on the temporal development of spike blast may not be apparent. Moreover, there was a generally increasing r_G with increasing inoculum, consistent with epidemiological theory that the temporal rate for monocyclic diseases is a direct function of inoculum density (Madden et al. 2007). The r_G at the highest CONC was significantly higher than for all the other concentrations within a cultivar. Interestingly, a shift in r_G was observed in several cases between the two cultivars at successive spore densities, where the r_G at one CONC of the more susceptible cultivar was very similar to the r_G at the next higher CONC for the less susceptible cultivar. For instance, r_G was 0.10/day for EVE at $2x10^3$ and 0.11/day for Cultivar 12 at $2x10^4$. Thus, it took a 10-fold increase in inoculum for disease in the less susceptible cultivar to progress over time at about the same rate as in the more susceptible cultivar. This reflects differences in probability of infection and rate at which spikes are colonized, where more spores are needed with the less susceptible cultivar to approximately equal temporal rate results with the more susceptible cultivar.

This effect is also visible as a shift to the right for Cultivar 12 relative to EVE when disease was plotted against time (Fig. 3.6), which can also be seen by the values of t_S (Table 3.5). For instance, for the same example, the time to 50% disease severity (t_{50}) was 22 days for EVE at a CONC of $2x10^3$ and 22 days for Cultivar 12 at $2x10^4$ spore concentration. . This significant difference for $2x10^5$ suggests that this high concentration level may create too much disease pressure for screening different wheat genotypes and effectively reduce the differences in cultivar x CONC reaction. An inoculum concentration of $2x10^4$ spores/ml is an effective standard for testing wheat germplasm against wheat blast caused by MoL. This value is consistent with the standard of $2x10^4$ spores/ml published in an inoculation protocol for testing wheat cultivars with MoT isolates (Cruz et al. 2016).

This difference in the rate of temporal increase in blast intensity was more obvious when cultivars were compared in terms of the time it took for incidence and severity to reach critical thresholds (t_S), an estimated parameter that is a function of the intercept and rate of the Gompertz model. This term could, in part, could be used to explain or characterize the temporal development of spike blast under field conditions. For instance, wheat blast caused by MoT was initially described as emerging *ex nihilo*, i.e., not being present in a field and then all or most of the spikes in the entire field becoming diseased within a few days (C. D. Cruz, *personal communication*). However, more recent research has shown that foliar lesions are often present before spikes are visibly diseased (Mills et al. 2021, Cruz et al. 2017); observed spore production on these leaf lesions under highly favorable weather conditions for infection could explain the apparent “explosive” nature of spike blast development in natural epidemics. In other less favorable conditions (for

sporulation and infection), new infections and colonization of spikes (from spores produced on wheat leaf lesions or other infected plants in the region) could occur at a slower rate in the field, so that disease progress over many days would be observable (Mills et al. 202x). Results from our controlled-environment study with MoL provide some support for the rapidly increasing epidemics that can occur with high inoculum of MoT. Given the information that wheat is more susceptible to MoT than to MoL, the rate of increase could be even higher for the former. For instance, we showed with MoL in the growth chamber that spike blast severity increases from just visible (6% bleaching) to more than 50% in only six days when highly susceptible EVE was inoculated with $2x10^5$ spores/ml. However, when this same cultivar was inoculated with only $2x10^2$ spores/ml, it took 14 days for the first symptoms to emerge, and an additional three weeks elapsed before disease progressed to 50% severity. Disease progression took about 30% longer for the moderately susceptible Cultivar 12, where blast severity took 10 days to increase from 6 to 50% when inoculated with $2x10^5$ spores/ml, and an additional four weeks for the same increase to occur when it was inoculated with only $2x10^2$ spores/ml. Since spike maturation was less than 40 DAI in our experiment, these results show that high disease intensity (e.g., > 50%) may not be reached with low initial inoculum or under conditions that are less favorable for infection (Mills et al. 2021), especially when a moderately resistant cultivar is grown.

This study was an extension of previous work (Mills et al. 2020) that sought to define environmental conditions that lead to MoL-incited spike blast development. The studies help address the risk of MoL-caused blast epidemics if MoL inoculum were

available at the appropriate times, and also serve as a model system to characterize aspects of the risk of blast in the US where MoT does not yet exist. Between these two studies, the rate of disease progress and disease intensity were found to be highest at temperatures between 25 and 30^{o}C, with high moisture or wetness (high relative humidity) periods at infection of 24 or more hours, high initial inoculum concentrations, and susceptible cultivar. Growth stage of wheat (from early head emergence to early grain fill) did not affect disease development. Empirical models were developed quantifying the effects of these factors on spike blast intensity at fixed times after inoculation and on the rate of increase in spike blast. Findings from these studies will be a value for establishing protocols to study wheat blast and screen cultivars for resistance, and models will be of direct value in risk assessment for MoL and, indirectly, for MoT (since MoT is not yet in the US). Testing the susceptibility of wheat germplasm to both MoT and MoL continues to be an important part of preparing for a possible future occurrence of wheat blast disease epidemics in the US (Cruz and Valent 2016). There are published standardized protocols for testing wheat against MoT (Cruz et al. 2016), and this study and the previous on (Mills et al. 2020) provide results that can be used to define conditions for screening cultivars for resistance to MoL, including spray inoculation with $2x10^{4}$ spores/ml between spike emergence and early grain fill, with at least 24 hours of high relative humidity immediately following inoculation, and constant temperature between 25 and 30^{o}C.

REFERENCES

Ceresini, P. C., Castroagudín, V. L., Rodrigues, F. Á., Rios, J. A., Aucique-Pérez, C. E., Moreira, S. I., Alves, E., Croll, D., and Maciel, J. L. N. 2018. Wheat blast: past, present, and future. Annu. Rev. Phytopathol. 56: 427–456.

Cowger, C., Beccari, G., Dong, Y. 2020. Timing of susceptibility to Fusarium head blight in winter. Wheat Plant Dis. 104:2928-2939.

Cruz, C. D. 2013. Wheat blast: quantitative pathway analyses for the Triticum pathotype of *Magnaporthe oryzae* and phenotypic reaction of U.S. wheat cultivars. Kansas State University.

Cruz, C. D., Bockus, W. W., Stack, J. P., Tang, X., Valent, B., Pedley, K. F., and Peterson, G. L. 2012. Preliminary assessment of resistance among U.S. wheat cultivars to the Triticum pathotypes of *Magnaporthe oryzae*. Plant Dis. 96:1501-1505.

Cruz, C. D., Kiyuna, J., Bockus, W. W., Todd, T. C., Stack, J. P., and Valent, B. 2015. *Magnaporthe oryzae* conidia on basal wheat leaves as a potential source of wheat blast inoculum. Plant Pathol. 64:1491-1498.

Cruz, C. D., Magarey, R. D., Christie, D. N., Fowler, G. A., Fernandes, J. M., Bockus, W. W., Valent, B., and Stack, J. P. 2016. Climate suitability for *Magnaporthe oryzae* Triticum pathotype in the United States. Plant Dis. 100:1979-1987.

Cruz, C. D., and Valent, B. 2017. Wheat blast disease: danger on the move. Trop. Plant Pathol. 42:210-222.

Cruz, C. D., Santana, F. M., Todd, T. C., Maciel, J. L., Kiyuna, J., Baldelomar, D. F., Cruz, A. P., Lau, D., Seixas, C. S., Goulart, A. C., Sussel, A. A., Schipanski, C. A., Chagas, D. F., Coelho, M., Montecelli, T. D., Utiamada, C., Custódio, A. P., Rivadeneira, M. G., Bockus, W. W., and Valent, B. 2019. Multi-environment assessment of fungicide performance for managing wheat head blast (WHB) in Brazil and Bolivia. Trop. Plant Pathol. 44**:**183–191.

Danelli, A. L. D., Fernandes, J. M. C., Maciel, J. L. N., Boaretto, C., and Forcelini, C. A. 2019. Monitoring *Pyricularia* sp. airborne inoculum in Passo Fundo, Rio Grande do Sul – Brazil. Summa Phytopathol. 45:361-367.

Farman, M., Peterson, G., Chen, L., Starnes, J., Valent, B., Bachi, P., Murdock, L., Hershman, D., Pedley, K., Fernandes, J. M., and Bavaresco, J. 2017. The Lolium pathotype of *Magnaporthe oryzae* recovered from a single blasted wheat plant in the United States. Plant Dis. 101:684-692.

Goulart, A. C. P., and Paiva F. A. 1992. Incidência da brusone (*Pyricularia oryzae*) em diferentes cultivares de trigo (*Triticum aestivum*) em condições de campo. Fitopatol. Bras. 17:321-325.

Goulart, A. C. P., Sousa, P. G., and Urashima, A. S. 2007. Danos em trigo causados pela infecção de *Pyricularia grisea*. Summa Phytopathol. 33:358-363.

Igarashi, S., Utiamada, C. M., Igarashi, L. C., Kazuma, A. H., and Lopes, R. S. 1986. *Pyricularia* em trigo, ocorrência de *Pyricularia* sp. no estado do Paraná. Fitopatol. Bras. 11:351-352.

Islam, M.T., Croll, D., Gladieux, P., Soanes, D.M., Persoons, A., and Bhattacharjee, P. 2016. Emergence of wheat blast in Bangladesh was caused by a South American lineage of *Magnaporthe oryzae*. BMC Biology, 14. Online publication. https://bmcbiol.biomedcentral.com/articles/10.1186/s12915-016-0309-7.

Islam, M. T., Gubta, D. R., Hossain, A., Roy, K. K., He, X., Kabir, M. R., Singh, P. K., Khan, A. R., Rahman, M., and Wang, G. L. 2020. Wheat blast: a new threat to food security. Phytopathol. Research 2:28. Online publication. https://doi.org/10.1186/s42483-020-00067-6.

Kohli, M. M., Mehta, Y. R., Guzman, E., Viedma, L., and Cubilla, L. E. 2011. *Pyricularia* blast - a threat to wheat cultivation. Czech J. Genet. Plant Breed. 47:S130-S134.

Madden, L. V., Hughes, G., and van den Bosch, F. 2007. The Study of Plant Disease Epidemics. American Phytopathological Society, St. Paul, MN.

Malaker, P. K., Barma, N. C. D., Tiwari, T. P., Collis, W. J., Duveiller, E., Singh, P. K., Joshi, A. K., Singh, R. P., Braun, H. J., Peterson, G. L., Pedley, K. F., Farman, M. L., and Valent, B. 2016. First Report of Wheat Blast Caused by *Magnaporthe oryzae* pathotype Triticum in Bangladesh. Plant Disease 100:2330-2330.

Mills, K. B., Salgado, J. D., Cruz, C. D., Valent, B., Madden, L. V., and Paul, P. A. 2021. Comparing the temporal development of wheat spike blast epidemics in a region of Bolivia where the disease is endemic. Plant Dis, 105:96-107.

Mills, K. B., Madden, L. V., and Paul, P. A. 2020. Quantifying the effects of temperature and relative humidity on the development of wheat blast caused by the Lolium pathotype of *Magnaporthe oryzae*. Plant Dis. 104:2622-2633.

Mills, K. B., Paul, P. A., Madden, L. V., and Peterson, G. L. 2015. Preliminary assessment of differential susceptibility of northern soft red winter wheat cultivars to Lolium and Triticum pathotypes of *Magnaporthe oryzae*. Phytopathology 105:S4.96.

Mottaleb, K. A., Singh, P. K., Sonder, K., Kruseman, G., and Erenstein, O. 2019. Averting wheat blast by implementing a 'wheat holiday': In search of alternative crops in West Bengal, India. PLoS ONE. Online publication. doi:10.1371/journal.pone.0211410.

Paul, P. A., Bradley, C. A., Madden, L. V., Lana, F. D., Bergstrom, G. C., Dill-Macky, R., Wise, K. A., Esker, P. D., McMullen, M., Grybauskas, A., Kirk, W. W., Milus, E., and Rudin, K. 2018. Effects of pre- and postanthesis applications of demethylation inhibitor fungicides on Fusarium head blight and deoxynivalenol in spring and winter wheat. Plant Dis. 102:2500-2510.

Paul, P. A., El-Allaf, S. M., Lipps, P. E., and Madden, L. V. 2005. Relationships between incidence and severity of Fusarium head blight on winter wheat in Ohio. Phytopathology, 95:1049-1060.

Paul, P. A., Salgado, J. D., Bergstrom, G., Bradley, C. A., Byamukama, E., Byrne, A. M., Chapara, V., Cummings, J. A., Chilvers, M. I., Dill-Macky, R., Friskop, A., Kleczewski, N., Madden, L. V., Nagelkirk, M., Stevens, J., Smith, M., Wegulo, S. N., Wise, K., and Yabwalo, D. 2019. Integrated effects of genetic resistance and prothioconazole + tebuconazole application timing on Fusarium head blight in wheat. Plant Dis. 103: 223-237.

Rios, J. A., Rios, V. S., Paul, P. A., Souza, M. A., Araujo, L., and Rodrigues, F. A. 2016. Fungicide and cultivar effects on the development and temporal progress of wheat blast under field conditions. Crop Prot. 89:152-160.

Rios, J. A., Rios, V. S., Paul, P. A., Souza, M. A., Neto, L. B. M. C., and Rodrigues, F. A. 2017. Effects of blast on components of wheat physiology and grain yield as influenced by fungicide treatment and host resistance. Plant Pathol. 66:877-889.

Sadat, A., and Choi, J. 2017. Wheat blast: A new fungal inhabitant to Bangladesh threatening world wheat production. Plant Pathol. J. 33:103-108.

Schmale III, D. G., and Bergstrom, G. C. 2003 Fusarium head blight in wheat. The Plant Health Intsructor. Online publication. DOI:10.1094/PHI-I-2003-0612-01.

Stroup, W. W., Milliken, G. A., Claassen, E. A., and Wolfinger, R. D. 2018. SAS® for Mixed Models: Introduction and Basic Applications. Cary, NC: SAS Institute Inc.

Tembo, B., Mulenga, R. M., Sichilima, S., M'siska, K. K., Mwale, M., Chikoti, P. C., Singh, P. K., He, X., Pedley, K. F., Peterson, G. L., Singh, R. P., and Braun, H. J. 2020. Detection and characterization of fungus (*Magnaporthe oryzae* pathotype Triticum) causing wheat blast disease on rain-fed grown wheat (*Triticum aestivum* L.) in Zambia. PLoS ONE 15(9): e0238724. Online publication. doi.org/10.1371/journal.pone.0238724

Tosa, Y., Hirata, K., Tamba, H., Nakagawa, S., Chuma, I., Isobe, C., Osue, J., Urashima, A. S., Don, L. D., Kusaba, M., Nakayashiki, H., Tanaka, A., Tani, T., Mori, N., and Mayama, S. 2004. Genetic constitution and pathogenicity of Lolium isolates of *Magnaporthe oryzae* in comparison with host species specific pathotypes of the blast fungus. Phytopathology 94:454-462.

Uddin, W., Viji, G., and Vincelli, P. 2003b. Gray leaf spot (blast) of perennial ryegrass turf: an emerging problem for the turfgrass industry. Plant Dis. 87:880-889.

Urashima, A. S., Igarashi, S., and Kato, H. 1993. Host range, mating type, and fertility of *Pyricularia grisea* from wheat in Brazil. Plant Dis. 77:1211-1216.

Urashima, A. S., Lavorent, N. A., Goulart, A. C. P., and Mehta, Y. R. 2004. Resistance spectra of wheat cultivars and virulence diversity of Magnaporthe grisea isolates in Brazil. Fitopatologia Brasileira 29:511-518.

Urashima, A. S., Grosso, C. R. F., Stabili, A., Freitas, E. G., Silva, C. P., Netto, D. C. S., Franco, I., and Merola Bottan, J. H. 2009. Effect of Magnaporthe grisea on seed germination, yield, and quality of wheat. Wang, G. W., and Valent, B. (eds) Advances in genetics, genomics and control of rice blast disease. Springer, Netherlands, pp 267-277.

Valent, B., Farman, M., Tosa, Y., Begerow, D., Fournier, E., Gladieux, P., Islam, M. T., Kamoun, S., Kemler, M., Kohn, L. M., Lebrun, M.-H., Stajich, J. E., Talbot, N. J., Terauchi, R., Tharreau, R., and Zhang, N. 2019. *Pyricularia* graminis-tritici is not the correct species name for the wheat blast fungus: response to Ceresini et al. (MPP 20:2). Mol. Plant Pathol. 20:173-179.

Villari, C., Mahaffee, W. F., Mitchell, T. K., Pedley, K. F., Pieck, M. L., and Peduto Hand, F. 2017. Early detection of airborne inoculum of *Magnaporthe oryzae* in turfgrass fields using a quantitative LAMP assay. Plant Disease, 101:170-177.

Table 3.1. Probability values from linear mixed model analyses of the effects of wheat growth stage, cultivar type, inoculum concentration, and their interactions on arcsine-square root-transformed wheat spike blast incidence and severity at different times following inoculation with a spore suspension of an isolate (PL2-1) of the Lolium pathotype of *Magnaporthe oryzae*

	Incidence[b]			Severity[b]		
Factors[a]	12-14 DAI	19-21 DAI	26-28 DAI	12-14 DAI	19-21 DAI	26-28 DAI
GSTAGE	0.015	0.449	0.406	0.076	0.572	0.790
CULT	0.028	0.093	0.166	0.006	0.034	0.153
CULT*GSTAGE	0.739	0.799	0.724	0.619	0.883	0.852
CONC	<0.001	<0.001	<0.001	<0.001	<0.001	<0.001
CONC*GSTAGE	0.262	0.120	0.032	0.535	0.576	0.398
CULT*CONC	0.002	0.043	0.001	<0.001	0.016	0.509
CULT*CONC*GSTAGE	0.303	0.648	0.249	0.445	0.962	0.259

[a]The treatment factors evaluated were Feekes growth stage (GSTAGE, Feekes 10.1-3, 10.5, 10.5.1, 10.5.4), spore concentration (CONC, 2e2, 2e3, 2e4, 2e5 spores per mL), and cultivar (CULT).

[b]Wheat spike blast incidence (mean proportion of diseased spikes in a sample) and severity (mean proportion of bleached, discolored spikelets per spike) at 12-14, 19-21, and 26-28 days after inoculation (DAI). Models were fitted to arcsine-square root-transformed incidence and severity data.

Table 3.2. Estimated differences in least square means between cultivars[a] 12 and EVE at each level of inoculum concentration (CONC) of an isolate (PL2-1) of the Lolium pathotype of *Magnaporthe oryzae* and corresponding standard errors (SE), levels of significance (*P* value), and upper and lower limits of the 95% confidence intervals around the estimates

		Severity[b]					Incidence[b]				
DAI[c]	CONC[d]	ESTIMATE[e]	SE	*P* value[f]	Lower	Upper	ESTIMATE	SE	*P* value[f]	Lower	Upper
12-14	2e2	-0.018	-0.055	0.740	-0.130	0.094	-0.023	0.088	0.796	-0.207	0.163
	2e3	-0.268	-0.060	<0.001	-0.391	-0.145	-0.355	0.097	0.002	-0.557	-0.152
	2e4	-0.295	-0.060	<0.001	-0.418	-0.172	-0.037	0.097	0.001	-0.572	-0.167
	2e5	-0.492	-0.060	<0.001	-0.615	-0.369	-0.551	0.097	<0.001	-0.753	-0.349
19-21	2e2	-0.134	0.072	0.104	-0.304	0.036	-0.177	0.120	0.222	-0.526	0.172
	2e3	-0.242	0.072	0.012	-0.412	-0.072	-0.328	0.120	0.059	-0.677	0.022
	2e4	-0.381	0.072	0.001	-0.551	-0.211	-0.466	0.120	0.022	-0.815	-0.117
	2e5	-0.344	0.072	0.002	-0.513	-0.174	-0.292	0.120	0.079	-0.641	0.057
26-28	2e2	-0.252	0.145	0.191	-0.743	0.240	-0.330	0.163	0.139	-0.857	0.198
	2e3	-0.363	0.142	0.100	-0.841	0.145	-0.608	0.159	0.039	-1.155	-0.061
	2e4	-0.350	0.139	0.112	-0.881	0.180	-0.272	0.155	0.200	-0.845	0.301
	2e5	-0.273	0.144	0.167	-0.768	0.222	-0.094	0.162	0.605	-0.626	0.438

[a]Wheat cultivar - Everest (EVE), a hard red winter wheat that is highly susceptible to wheat blast and 12 a soft red winter wheat cultivar that is moderately susceptible to blast.

[b]Wheat blast disease severity (mean proportion of diseased spikelets per spike) and incidence (mean proportion of diseased spikes per sample). Models were fitted to arcsine-square root-transformed incidence and severity data.

[c]Disease assessments were grouped into bins representing days after infection (DAI): 12-14, 19-21, and 26-28 DAI.

[d]Inoculum concentration in spores/ml.

[e]Least square mean difference between cultivars at each level of inoculum concentration.

[f]Least square means were compared using t-tests. *P* values less than 0.05 indicates that least square means are significantly different between 12 and EVE.

Table 3.3. Intercepts, slopes, and their standard errors (SE) from linear mixed model regression analyses of relationships between inoculum concentration of an isolate (PL2-1) of the Lolium pathotype of *Magnaporthe oryzae* and wheat blast incidence and severity for cultivars 12 and Everest at different disease assessment windows in days after infection (DAI)

		12-14 DAI				19-21 DAI				26-28 DAI			
Response[a]	Cultivar[c]	*a*	SE	Slope	SE	*a*	SE	Slope	SE	*a*	SE	Slope	SE
Severity	EVE	0.414	-0.035	2.9E-3	4.0E-4	0.676	-0.054	2.8E-3	3.3E-4	0.899	-0.010	2.6E-03	3.9E-4
	12	0.217	-0.039	1.4E-3	4.3E-4	0.401	-0.054	2.8E-3	3.3E-4	0.612	-0.099	2.6E-03	3.9E-4
	Diff[c]	0.197*	-0.044	1.5E-3*	5.9E-4	0.275*	-0.052	0	0	0.287	-0.136	0	0
Incidence	EVE	0.698	-0.066	3.0E-3	4.7E-4	0.979	-0.083	3.2E-3	4.4E-4	1.220	-0.115	2.4E-03	5.0E-4
	12	0.341	-0.071	3.0E-3	4.7E-4	0.663	-0.083	3.2E-3	4.4E-4	0.931	-0.110	2.4E-03	5.0E-4
	Diff	0.357	-0.074	0	0	0.316	-0.104	0	0	0.289	-0.160	0	0

[a]Wheat blast disease severity (mean proportion of diseased spikelets per spike) and incidence (mean proportion of diseased spikes per sample). Models were fitted to arcsine-square root-transformed incidence and severity data.

[b]Wheat cultivar - Everest (EVE), and hard red winter wheat that is highly susceptible to wheat blast and 12 a soft red winter wheat cultivar that is moderately susceptible to blast.

[c]Difference in linear equation coefficient estimates between cultivars.

*Parameter differences that are statistically significant ($P < 0.05$)

Table 3.4. Mean square error (MSE) and coefficient of determination (R^2) from linear regression analyses of relationships between observed and predicted wheat blast intensity from the fit of nonlinear forms of exponential, logistic, Gompertz, and monomolecular growth models to data from controlled environment studies of the temporal change of wheat blast severity and incidence as influenced by cultivar and inoculum concentration of an isolate (PL2-1) of the Lolium pathotype of *Magnaporthe oryzae*

			Exponential		Logistic		Gompertz		Monomolecular	
Response[a]	Cultivar[b]	CONC[c]	MSE[d]	R^2	MSE	R^2	MSE	R^2	MSE	R^2
Severity	EVE	2e2	0.022	0.44	0.021	0.46	0.021	0.49	0.021	0.47
		2e3	0.015	0.80	0.011	0.85	0.010	0.87	0.012	0.84
		2e4	0.034	0.71	0.011	0.91	0.009	0.92	0.011	0.91
		2e5	0.046	0.57	0.010	0.90	0.009	0.92	0.010	0.91
	12	2e2	0.017	0.28	0.017	0.28	0.017	0.29	0.017	0.26
		2e3	0.036	0.34	0.034	0.39	0.032	0.42	0.031	0.44
		2e4	0.043	0.61	0.034	0.68	0.033	0.69	0.036	0.67
		2e5	0.048	0.59	0.034	0.71	0.033	0.72	0.035	0.70
Incidence	EVE	2e2	0.042	0.49	0.037	0.56	0.035	0.58	0.036	0.57
		2e3	0.032	0.73	0.017	0.86	0.017	0.86	0.019	0.84
		2e4	0.055	0.53	0.006	0.95	0.005	0.96	0.008	0.93
		2e5	0.053	0.42	0.008	0.92	0.007	0.92	0.008	0.91
	12	2e2	0.046	0.29	0.045	0.30	0.045	0.30	0.048	0.27
		2e3	0.074	0.39	0.068	0.45	0.066	0.46	0.067	0.45
		2e4	0.061	0.54	0.044	0.66	0.043	0.67	0.044	0.66
		2e5	0.056	0.55	0.023	0.82	0.022	0.83	0.027	0.78

[a]Wheat blast severity (mean proportion of diseased spikelets per spike) and incidence (mean proportion of diseased spikes per sample).
[b]Wheat cultivar - Everest (EVE), a hard red winter wheat that is highly susceptible to wheat blast and 12 a soft red winter wheat cultivar that is moderately susceptible to blast.
[c]Inoculum concentration in spores/ml.
[d]Mean Square Error (MSE) is an absolute measure of the distance between the observed data and model predicted data, and the R^2 value is the coefficient of determination from linear regression analysis of relationships between predicted and the observed responses.

Table 3.5. Estimated parameters and corresponding statistics from the fit of the Gompertz population growth model to data from controlled environment studies of temporal development of wheat spike blast as influenced by cultivar and spore inoculum concentration of an isolate (PL2-1) of the Lolium pathotype of *Magnaporthe oryzae*

			Parameters and fit statistics[d]						Time to blast intensity (days)[e]			
Response[a]	Cultivar[b]	CONC[c]	y_o	se(y_o)	Rate (r_G)	se(r_G)	MSE	R^2	6%	15%	25%	50%
Severity	EVE	2e2	1.29E-03	2.30E-03	0.063	0.011	0.021	0.49	14	20	25	36
		2e3	1.58E-03	1.42E-03	0.101	0.007	0.010	0.87	8	12	15	22
		2e4	7.30E-05	1.19E-04	0.177	0.012	0.009	0.92	7	9	11	15
		2e5	6.24E-06	1.60E-05	0.246	0.019	0.010	0.91	6	7	9	12
	12	2e2	3.97E-04	1.22E-03	0.051	0.014	0.017	0.29	20	28	34	47
		2e3	8.10E-03	1.06E-02	0.056	0.011	0.032	0.42	10	17	22	34
		2e4	7.80E-04	1.70E-03	0.108	0.015	0.033	0.69	9	12	15	22
		2e5	3.04E-04	8.23E-04	0.136	0.018	0.033	0.72	8	11	13	18
Incidence	EVE	2e2	1.42E-03	2.53E-03	0.087	0.012	0.035	0.58	10	14	18	26
		2e3	4.04E-04	6.49E-04	0.163	0.014	0.017	0.86	6	9	11	15
		2e4	2.01E-19	2.30E-18	0.402	0.026	0.005	0.96	7	8	9	10
		2e5	3.44E-31	1.05E-29	0.550	0.053	0.007	0.92	6	7	7	8
	12	2e2	6.07E-04	2.04E-03	0.065	0.017	0.045	0.30	15	21	26	37
		2e3	4.75E-03	9.52E-03	0.088	0.017	0.066	0.46	7	12	15	23
		2e4	1.65E-03	3.83E-03	0.150	0.023	0.043	0.67	5	8	10	15
		2e5	4.71E-09	4.33E-08	0.263	0.037	0.022	0.83	7	9	10	13

[a]Wheat blast severity (mean proportion of diseased spikelets per spike) and incidence (mean proportion of diseased spikes per sample)
[b]Wheat cultivar - Everest (EVE), a hard red winter wheat that is highly susceptible to wheat blast and 12 a soft red winter wheat cultivar that is moderately susceptible to blast.
[c]Inoculum concentration in spores/ml.

continued

Table 3.5. Continued.

[d]Parameters for the Gompertz models including the intercept (y_o), Rate (r_G), and their standard errors; as well as the fit statistics from linear regression analyses of relationships between actual to predicted responses, with smaller mean square errors (MSE) and larger R^2 (the coefficient of determination) values indicating better fit.

[e] The estimated number of days after inoculation it took for severity or incidence to reach specific levels (6, 15, 25, and 50%) for cultivar x inoculum concentrations combination.

Table 3.6. T-statistics and levels of significance (*P* value) for comparison the Gompertz rate parameter between cultivars EVE and 12 at different inoculum concentrations of an isolate (PL2-1) of the Lolium pathotype of *Magnaporthe oryzae*

Response[a]	CONC[b]	df	*t*-value	p-value[c]
Severity	2e2	134	1.33	0.186
	2e3	131	5.28	<0.001
	2e4	129	7.59	<0.001
	2e5	121	25.73	<0.001
Incidence	2e2	134	1.84	0.068
	2e3	131	7.33	<0.001
	2e4	129	21.03	<0.001
	2e5	121	5.42	<0.001

[a]Wheat blast severity (mean proportion of diseased spikelets per spike) and incidence (mean proportion of diseased spikes per sample).

[b]Inoculum concentration in spores/ml.

[c]*P* value < 0.05 indicate that rate parameters are significantly different between cultivars.

Table 3.7. T-statistics and levels of significance (*P* value) for comparisons of Gompertz rate parameters for incidence and severity between the highest tested inoculum concentration of an isolate (PL2-1) of the Lolium pathotype of *Magnaporthe oryzae* and three lower inoculum concentrations (2e2, 2e3, and 2e4 spores/ml) for two cultivars

Response[a]	Cultivar[b]	CONC	df	*t*-value	p-value[c]
Severity	EVE	2e2	137	12.04	<0.001
		2e3	136	8.46	<0.001
		2e4	136	4.79	<0.001
	12	2e2	116	7.41	<0.001
		2e3	114	5.54	<0.001
		2e4	112	2.64	0.009
Incidence	EVE	2e2	137	8.98	<0.001
		2e3	136	7.57	<0.001
		2e4	136	3.21	<0.001
	12	2e2	116	6.04	<0.001
		2e3	114	5.35	<0.001
		2e4	112	3.89	<0.001

[a]Wheat blast disease severity (mean proportion of diseased spikelets per spike) and incidence (mean proportion of diseased spikes per sample).

[b]Wheat cultivar - Everest (EVE), a hard red winter wheat that is highly susceptible to wheat blast and 12 a soft red winter wheat cultivar that is moderately susceptible to blast.

[c]*P* value < 0.05 indicate that rate parameters are significantly different between the pairs of inoculum concentrations being compared.

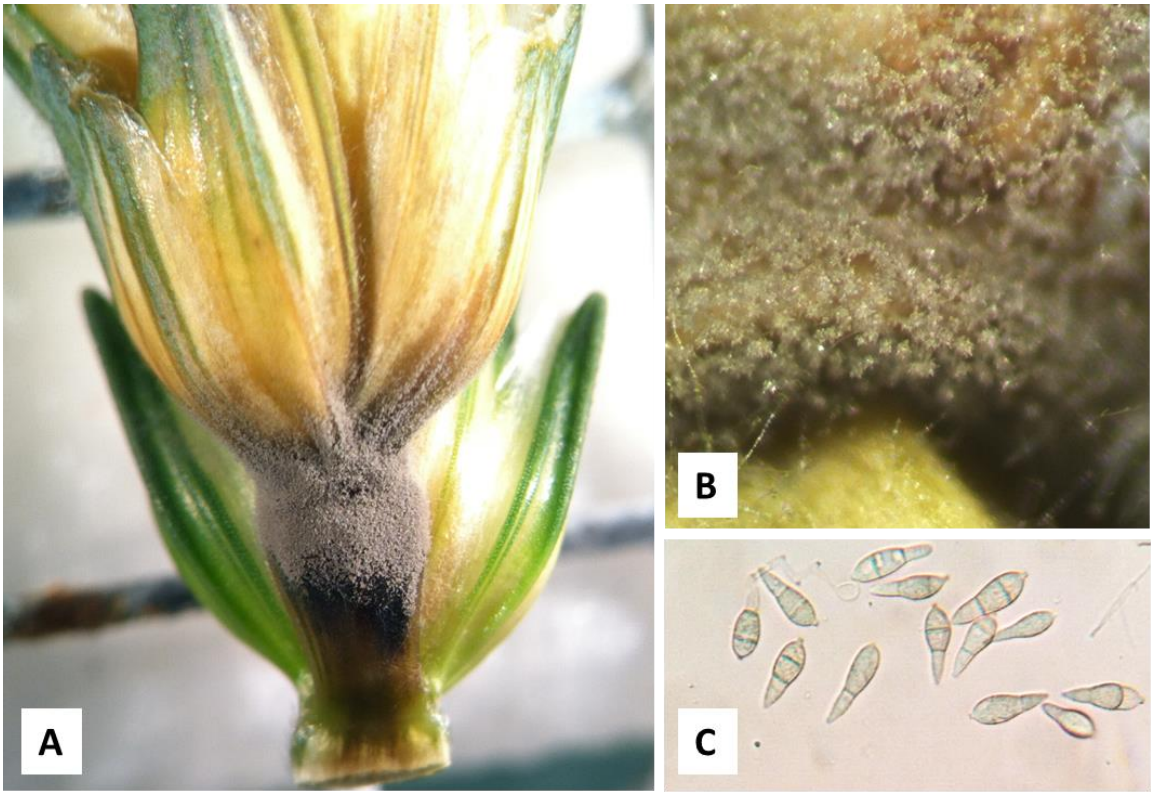

Fig. 3.1. Signs and symptoms of wheat blast caused by MoL on the highly susceptible cultivar Everest. **A –** A symptomatic spikelet and rachis displaying the typical bleached spikelet above the dark point of infection in the rachis, and signs of sporulating lesion; **B** – Close up of the same sporulating lesion in (A), with visible conidiophores; **C** – MoL conidia collected from the lesion in (B) and viewed under 100x magnification.

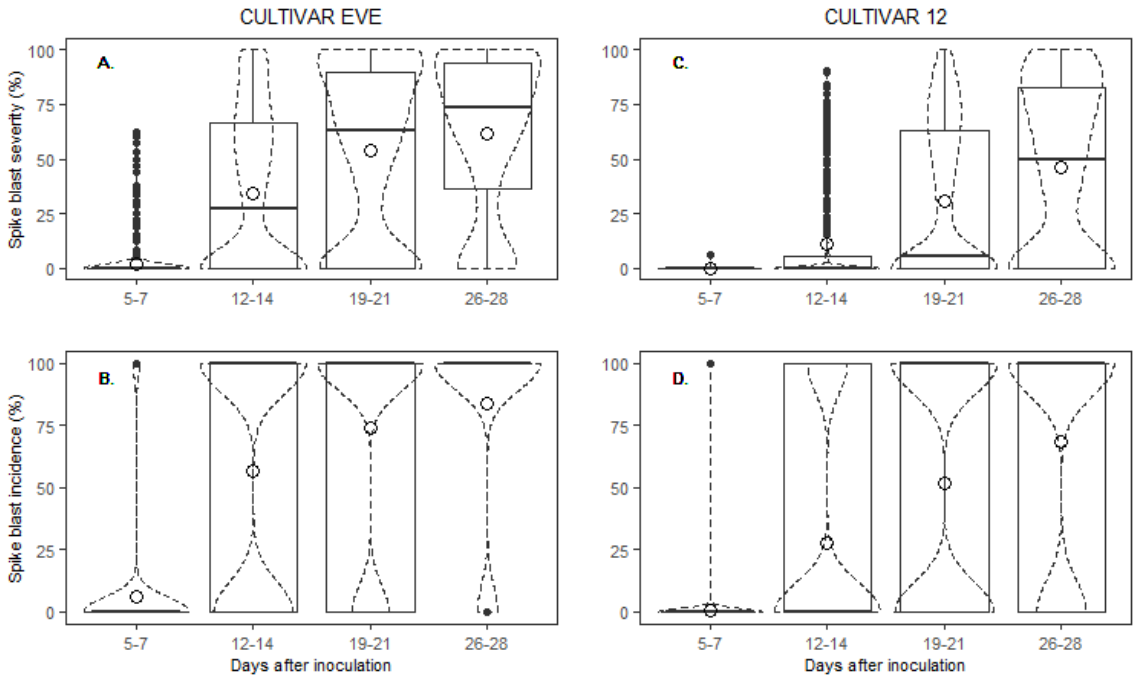

Fig. 3.2. Boxplots showing the distribution of mean wheat spike blast severity (**A** and **C**) and incidence (**B** and **D**) for cultivars Everest (EVE, a hard red winter wheat that is highly susceptible to wheat blast) and 12 (a soft red winter wheat cultivar that is moderately susceptible to blast) across inoculum concentrations, replications, and experiments at 5-7, 12-14, 19-21, and 26-28 days after spray inoculation with spore suspensions of an isolate (PL2-1) of the Lolium pathotype of *Magnaporthe oryzae*. Theses boxplots display a mirrored density to better present the proportion of values around disease levels of 0 and 1. The empty circle and solid lines within each box represent means and medians, respectively. Vertical bars extending beyond the boxes represent the 5th and 95th percentiles, while filled circles represent outliers. The dashed line displays the distribution of response. These data are strongly bimodal due to the differences in responses to the inoculum concentrations (2e2, 2e3, 2e4, and 2e5 spores/ml) that are consolidated in each bar.

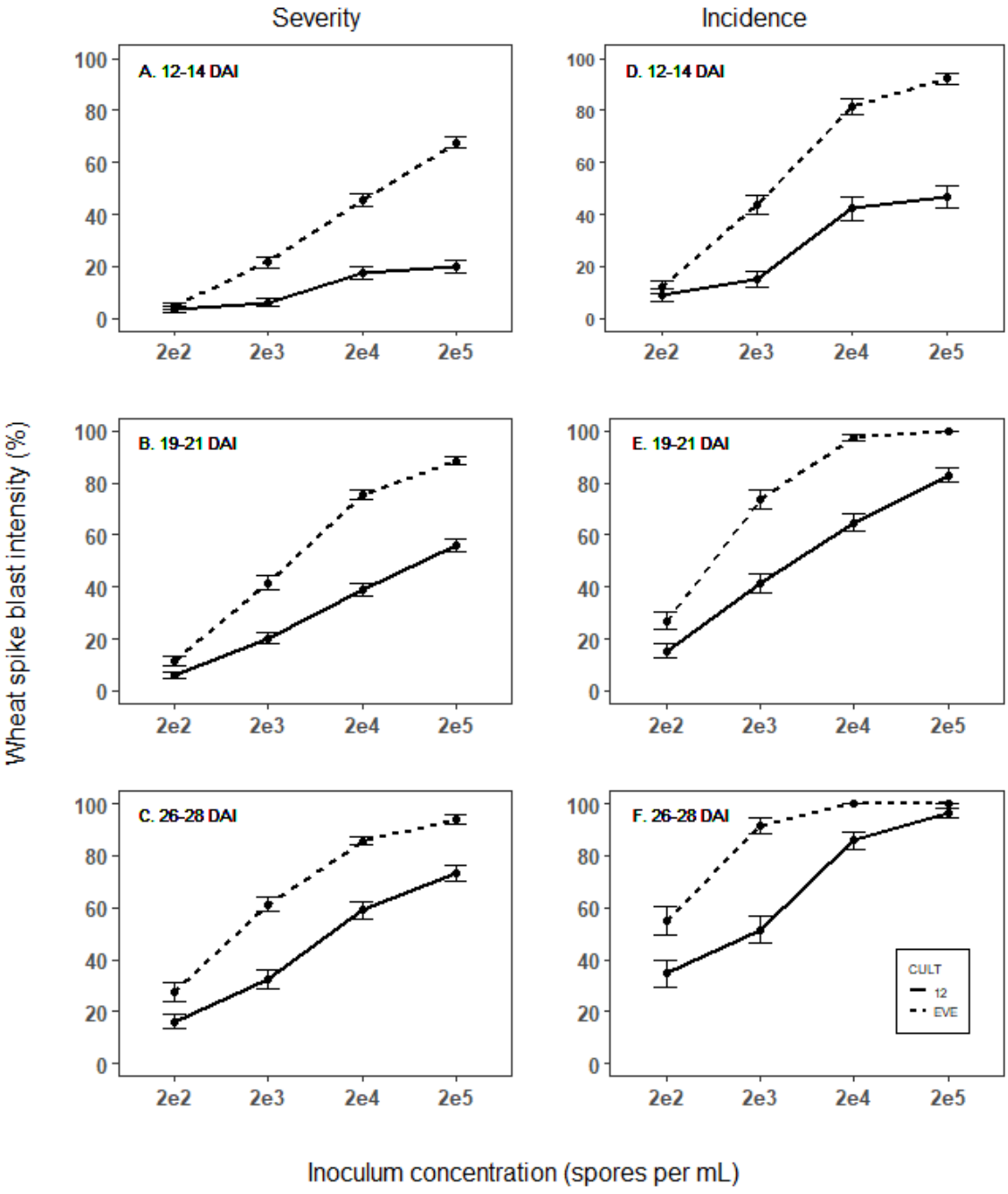

Fig. 3.3. Mean wheat blast severity (**A, B,** and **C**) and incidence (**D, E,** and **F**) at 12-14 (**A** and **D**), 19-21 (**B** and **E**), and 26-28 days (**C** and **F**) after inoculation (DAI) of cultivars Everest (EVE, a hard red winter wheat that is highly susceptible to wheat blast) and 12 (a soft red winter wheat cultivar that is moderately susceptible to blast) with an isolate (PL2-1) of the Lolium pathotype of *Magnaporthe oryzae*. Points are means across wheat spikes, experimental units, and growth stages. Error bars standard error of the mean.

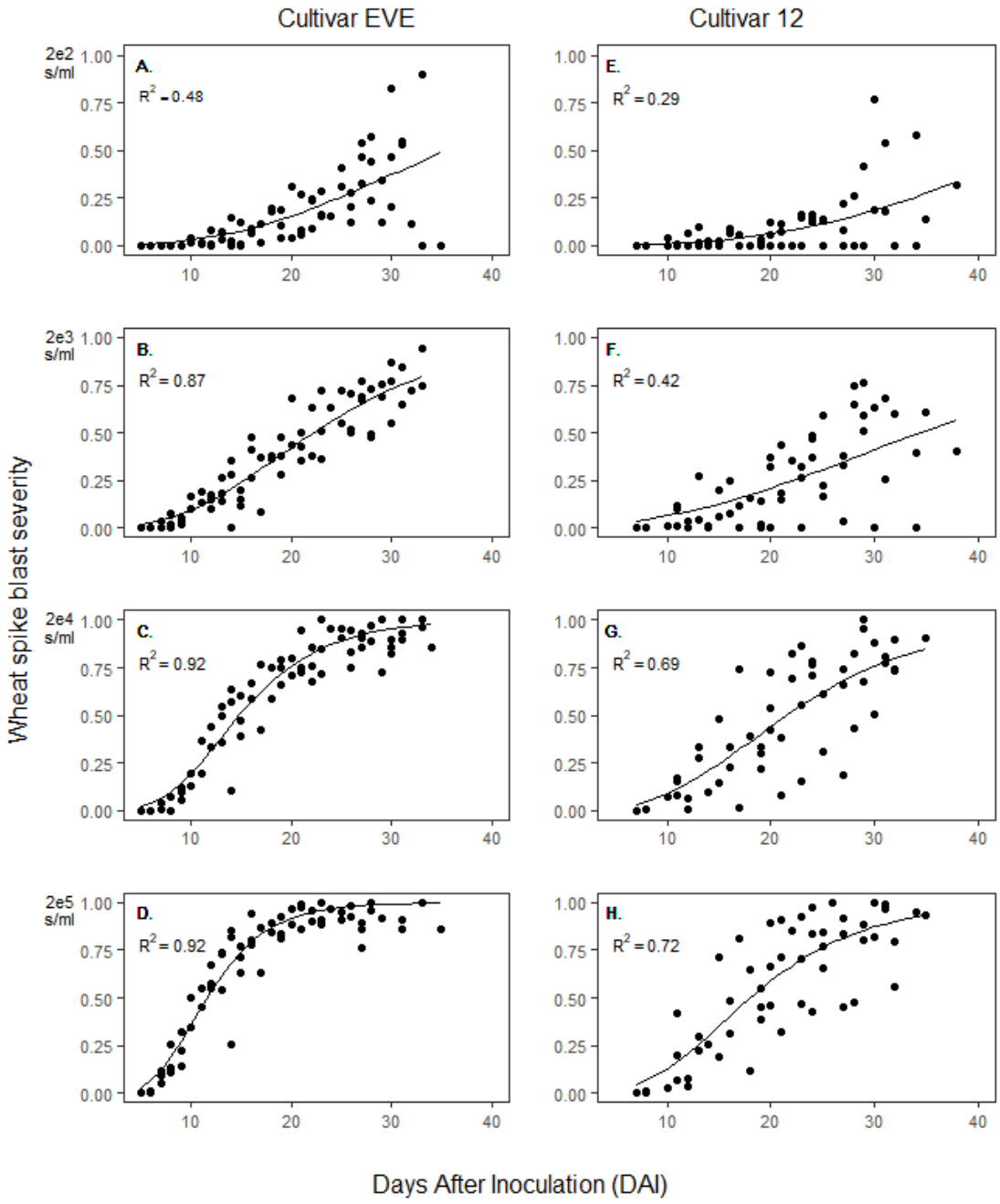

Fig. 3.4. Temporal change in mean wheat spike blast severity for **A, B, C,** and **D**, wheat cultivars Everest (EVE, a hard red winter wheat that is highly susceptible to wheat blast) and **E, F, G** and **H**, 12 (a soft red winter wheat cultivar that is moderately susceptible to blast) inoculated with 2e2 (**A** and **E**), 2e3 (**B** and **F**), 2e4 (**C** and **G**), or 2e5 (**D** and **H**) spores/ml of an isolate (PL2-1) of the Lolium pathotype of *Magnaporthe oryzae*.

continued

Fig. 3.4. Continued.

Lines are predicted severity from the non-linear fit of the Gompertz growth models to the data for each combination of cultivar and inoculum concentration. Points are means across years, experimental units, growth stages, and spikes for each DAI. R^2 (coefficient of determination) from linear regression analysis of relationships between predicted and observed severity. Higher R^2 values indicate a close fit between the predicted and observed data severity.

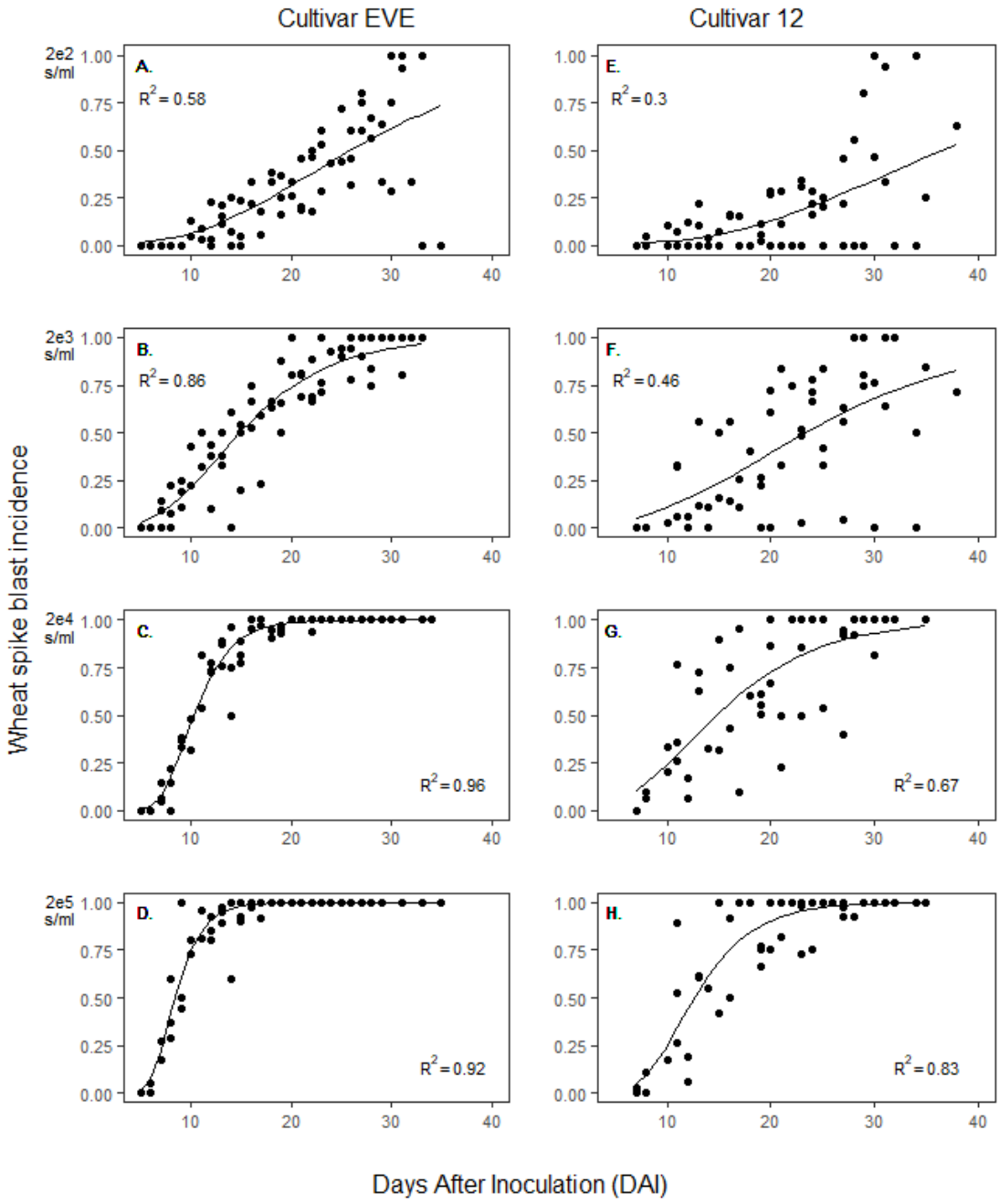

Fig. 3.5. Temporal change in mean wheat spike blast incidence for **A, B, C,** and **D**, wheat cultivars Everest (EVE, a hard red winter wheat that is highly susceptible to wheat blast) and **E, F, G** and **H**, 12 (a soft red winter wheat cultivar that is moderately susceptible to blast) inoculated with 2e2 (**A** and **E**), 2e3 (**B** and **F**), 2e4 (**C** and **G**), or 2e5 (**D** and **H**) spores/ml of an isolate (PL2-1) of the Lolium pathotype of *Magnaporthe oryzae*.

continued

Fig. 3.5.Continued.

Lines are predicted incidence from the non-linear fit of the Gompertz growth models to the data for each combination of cultivar and inoculum concentration. Points are means across years, experimental units, growth stages, and spikes for each DAI. R^2 (coefficient of determination) from linear regression analysis of relationships between predicted and observed incidence. Higher R^2 values indicate a close fit between the predicted and observed data incidence.

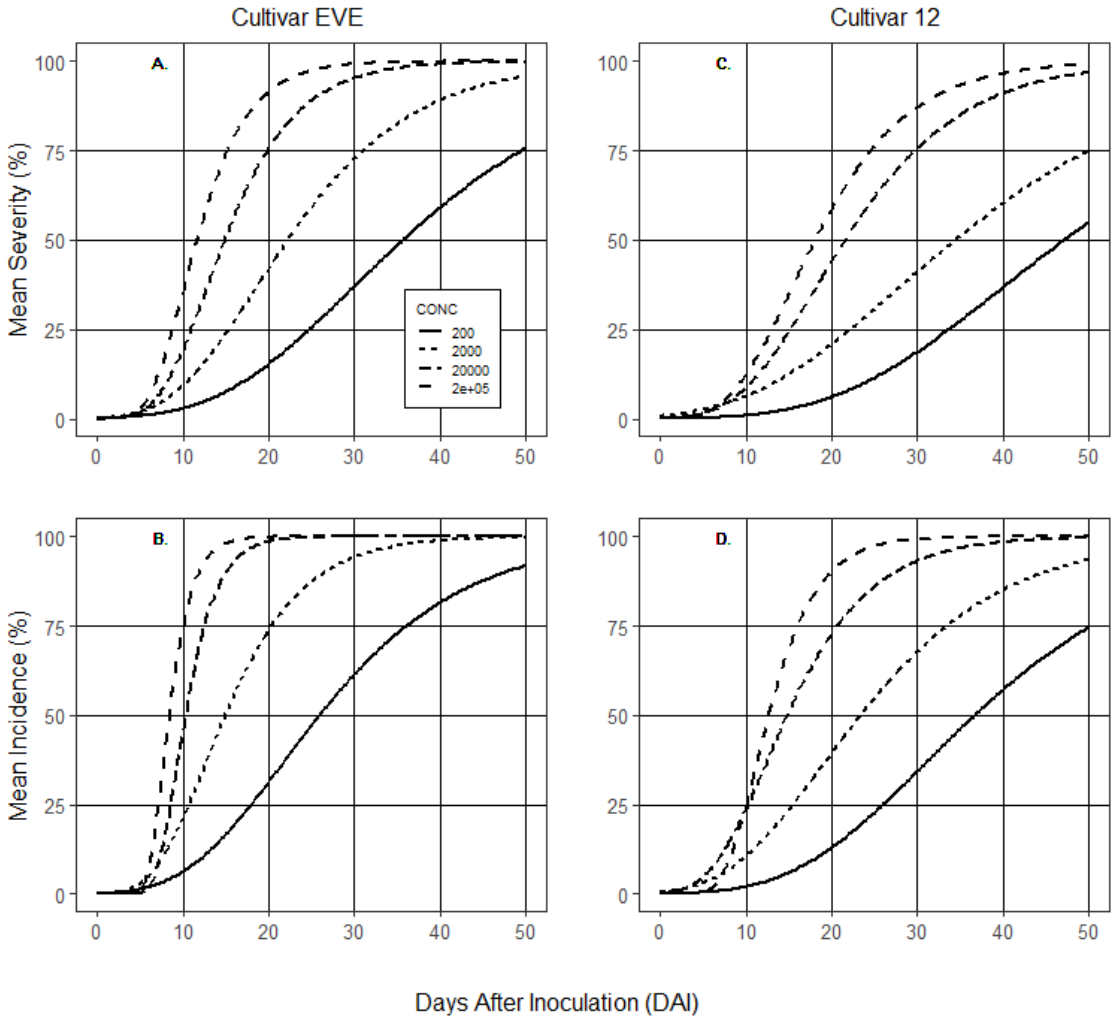

Fig. 3.6. Disease progress curves for **A** and **C**, wheat spike blast severity and **B** and **D**, incidence for wheat cultivars Everest (**A** and **B**) and 12 (**C** and **D**). Plotted lines are predicted values from fit of the non-linear form of the Gompertz model to each combination of cultivar and initial inoculum concentration (2e2, 2e3, 2e4 and 2e5 spores/ml) of an isolate (PL2-1) of the Lolium pathotype of *Magnaporthe oryzae*.

Chapter 4.
Comparing the Temporal Development of Wheat Spike Blast Epidemics in a Region of Bolivia where the Disease is Endemic

ABSTRACT

Epidemics of wheat blast, caused the Triticum pathotype of *Magnaporthe oryzae*, were studied in the Santa Cruz del la Sierra region of Bolivia to quantify and compare the temporal dynamics of the disease under different growing conditions. Six plots of a susceptible wheat cultivar were planted at Cuatro Cañadas (CC), Okinawa1 (OK1) and Okinawa2 (OK2) in 2015. Spike blast incidence (INC) and severity (SEV) and leaf blast severity (LEAF) were quantified in each plot at regular intervals on a 10 x 10 grid (n = 100 clusters of spikes), beginning at head emergence (Feekes growth stage 10.5), for a total of 9 assessments at CC, 6 at OK1, and 6 at OK2. Spike blast increased over time for as many as 20-30 days before approaching a mean INC of 100%, and a mean SEV of 60 to 75%. The logistic model was the most appropriate for describing the temporal dynamics of spike blast. The highest absolute rates of disease increase occurred earliest at OK1 and latest at OK2, and in all cases, coincided with major rain events. Estimated y_0 values (initial blast intensity) were significantly ($P < 0.05$) higher at OK1 than at CC or OK2, whereas r_L values (the logistic rate parameter) were significantly higher at OK2 than at CC or OK1. It took

about 10 fewer days for SEV to reach 10, 15, or 20% at OK1 compared to OK2 and CC. Based on survival analyses, the survivor functions for time to 10, 15 and 20% SEV (t_s) were significantly different between OK1 and the other locations, with the probabilities of SEV reaching the thresholds being highest at OK1. LEAF at 21 days after Feekes 10.5 had a significant effect on t_s at OK1. For every 5% increase in LEAF, the chance of SEV reaching the thresholds by day 21 increased by 30 to 55%.

INTRODUCTION

Wheat blast, caused by the Triticum pathotype of the fungus *Magnaporthe oryzae* (MoT), is a disease that affects leaves, spikes and other aboveground parts of the wheat plant (Urashima 2010). MoT can infect leaves throughout the growing season, causing oblong lesions with dark edges and centers that are light gray during sporulation and straw-colored thereafter (Cruz and Valent 2017; Gongora-Canul et al. 2020; Igarashi 1990; Igarashi et al. 1986; Lima 2004). However, damage to the spike is often more conspicuous, extensive, and of greater concern from a yield loss standpoint (Cruz and Valent 2017; Kohli et al. 2011). Under favorable conditions for infection and disease development (25 to 30^{o}C with 24 to 48 h of leaf wetness or high relative humidity [Cardoso et al. 2008; Mills et al. 2020]), spike blast symptoms become apparent on emerging spikes (Cruz and Valent 2017; Urashima 2010). Once the pathogen damages the rachis it restricts water and nutrient transport to the developing grain (Prabhu et al. 1992; Torres et al. 2009), grain fill is reduced, and spikes become bleached with shriveled, light-weight kernels (Goulart et al.

2007). An entire field may become diseased in a relatively short time, with 100% incidence and severity, leading to complete yield loss (Cruz and Valent 2017; Kohli et al. 2011).

Wheat blast emerged in the state of Parana, Brazil, in 1985 (Prabhu et al. 1992), and quickly spread to other wheat-production regions of South America (Ceresini et al. 2018, 2019). The first major outbreak in Bolivia was reported in 1996, with an estimated yield loss of almost 80% (Barea and Toledo 1996), then in 2002, Paraguay lost more than 70% of its early-planted wheat crop to blast (Kohli et al. 2011; Martinez et al. 2019), followed in 2007 by the first report of the disease in Argentina (Cabrera and Gutiérrez 2007). Until recently, wheat blast was limited to regions of South America, but in February 2016, an outbreak occurred in Bangladesh (Malaker et al. 2016). The disease now poses a threat to wheat production in other countries in Asia such as China, Pakistan, and India (Cruz and Valent 2017), and there are growing concerns about its potential to impact the global wheat market if it continues to spread. In the United States, blast may threaten wheat production through the incursion of MoT isolates from South America or infections caused by native isolates of the Lolium pathotype (MoL) of the fungus (Mills et al. 2020). The possibility of the latter occurring is supported by the fact that a blast-affected spike was observed in Kentucky in 2011 and subsequent characterization of the causal agent showed that it was more closely related to local MoL than to South American MoT isolates of the pathogen (Farman et al. 2017).

Studies have been conducted to evaluate management strategies for wheat blast based largely on fungicide application and cultivar resistance (Cruz et al. 2010, 2012; Rios et al. 2016), but research into the epidemiology of this disease is still in its infancy (Cruz

et al. 2016; Gongora-Canul et al. 2020; Mills et al. 2020). For instance, there is an incomplete understanding of how the disease develops and spreads in time and space through naturally infected fields. Growers and researchers have described, in some instances, a sudden, uniform, and synchronized bleaching of spikes across entire fields, without observing prior disease symptoms (Cruz et al. 2015). In Bangladesh, blast was portrayed as emerging *ex nihilo,* then quickly spreading across five districts in less than two weeks (Sadat and Choi 2017). However, despite suggestions of "spontaneous" bleaching, there is increasing evidence, based on the presence of the pathogen on basal leaves, that the disease may be spreading from local in-field inoculum sources (Cruz et al. 2015; Gongora-Canul et al. 2020; Rios et al. 2013). Basal leaf lesions have been observed to sporulate during spike emergence, but it is unknown whether these are important sources of inoculum for the spike blast phase of the disease or if infected crop residue plays a major role in disease development (Cruz et al. 2015).

Studies of spatial and temporal progress are important for understanding disease dynamics under field conditions and are invaluable for developing management guidelines such as fungicide application, tillage, and crop rotation. Disease progress in space and time is a function of interactions among the host plant, the pathogen, and the environment (Madden et al. 2007). This process can be modeled under natural field conditions to address questions such as whether wheat blast is a monocyclic or a polycyclic disease (Gongora-Canul et al. 2020) and whether in-field crop residue or neighboring grassy weeds serve of primary sources of inoculum for disease development. For instance, a monocyclic epidemic may be better described by the monomolecular model, while the exponential,

logistic, or Gompertz models may be more appropriate for describing the temporal progress of a polycyclic epidemic (Madden et al. 2007). The best-fit population growth model would provide insights into the relative importance of primary and secondary inoculum and infection for disease development. Models can also be used to compare epidemics among locations, growing seasons, cultivars, and management practices (Madden et al. 2007; Waggoner 1986), all of which are important for developing and implementing strategies for minimizing grain yield and quality losses.

To address key knowledge gaps in the epidemiology of wheat blast, the current investigation was conducted to monitor, model, and compare naturally occurring wheat spike blast epidemics in Bolivia. The specific objectives were to: 1) quantify the temporal progress of spike blast under different growing conditions, 2) estimate time to specific spike blast severity thresholds as influenced by local conditions, and 3) determine the effect of leaf blast severity on spike blast epidemics. To accomplish these objectives, field plots were established in three distinct humidity zones in the Santa Cruz de la Sierra region of the country where the disease is endemic, and incidence and severity data were collected at regular intervals between disease onset and crop senescence. Models were then fitted to quantify and compare the temporal rate of change in spike blast intensity among the locations, and parameters from the best-fit models were used to estimate the time it took for blast severity to reach pre-determined thresholds as influenced by field location and leaf blast severity based on time-to-event (survival) analysis.

MATERIALS AND METHODS

Field plot establishment and management. Three experiments were conducted in commercial wheat fields in the agricultural region north of Santa Cruz de la Sierra, Bolivia, during the fall and winter of 2015. Plots were established at Okinawa 1 (OK1; S 17°14.55, W 62°53.35); Okinawa 2 (OK2; S 17°20.41, W 62°52.60) and Cuatro Cañadas (CC; S 17°26.48, W 62°35.91) (Fig. 4.1.). The Okinawa locations were selected for this study because they had high levels of wheat blast in 2013, an abnormally warm growing season (C. D. Cruz, *personal communication*). Cuatro Cañadas was chosen as the third location because it was reported to be in a dryer, less humid region compared to the Okinawa locations (Barea and Aguanta 2012). The year this study was conducted was predicted to experience a very strong El Niño-Southern Oscillation event, which suggested that conditions would have been highly conducive for wheat blast (Kohli et al. 2011). According Kohli et al (2011), an El Niño year in parts of South America where wheat blast is endemic is characterized by frequent rainfall and temperatures between 18 and 25^{o}C during anthesis, followed by warm, humid days. The anticipated weather event did occur, and high levels of wheat blast developed throughout the Santa Cruz de la Sierra region.

To maximize the chance of natural infection, fields were planted at earlier dates than those typically chosen in commercial production fields. Plots were planted on 15 April at OK1, 20 April at OK2, and 8 May at CC. A highly susceptible wheat cultivar, Atlax (CAICO, Santa Cruz de la Sierra, Bolivia), was planted at a seeding rate of 80 seeds/m and a row spacing of 20 cm. Six 27 x 27-m plots were planted at each location, with a 2-m

border of sorghum separating adjacent plots. At both OK1 and OK2, a single row of plots was planted from east to west, whereas at CC, two rows, each with three plots, were planted. Plots were managed by collaborators from the ANAPO (Asociación de Productores de Oleaginosas y Trigo - ANAPO) Agriculture Cooperative in accordance with recommended agronomic practices for wheat cultivation in Bolivia (ANAPO 2015). Temperature and relative humidity were recorded hourly using sensors and weatherproof data loggers (HOBO Pro-V2, Onset, Cape Cod, MA) deployed at spike height (approximately 1 m above the soil surface) in the center of one plot at each location. Rainfall data were recorded on Vantage Pro2 weather stations (Davis Instruments, Hayward, CA) located approximately 100, 300, and 3,000 m from the plots at OK1, CC and OK2, respectively.

Disease quantification. A two-stage cluster sampling approach was used to quantify wheat blast intensity. At each location, each plot was marked to create a 10 x 10 grid, and blast assessments were made at each of the one hundred intersection nodes (sampling sites) of the grid. The distance between adjacent nodes was approximately 2.55 m. Spike emergence was asynchronous and occurred over the course of about ten days, with some secondary tillers heading as grain fill occurred on primary tillers. To minimize possible effects of such a wide heading window, spikes in the primary group of tillers were rated for blast. At each sampling site (i.e., node of the field lattice), blast severity (SEV) was estimated on individual spikes (n = 5 to 30; a cluster) as the proportion of spikelets with visual symptoms. Incidence (INC) was quantified as the proportion of diseased spikes at each node (number of spikes with blast symptoms divided by the total number of spikes

in the sample). The severity of leaf blast (LEAF; based on symptom characteristics) was also estimated at each node by examining the flag leaves of four sets of five primary tillers and estimating the mean proportion of leaf area diseased. LEAF was also rated at each internode (approximately halfway between adjacent nodes) at OK1 and OK2, for an additional 81 leaf severity ratings per plot.

Spike severity ratings began at approximately full head emergence (Feekes growth stage 10.5, Large 1954) at each location (9 June at OK1; 18 June at OK2; 10 July at CC) and repeated every 3-4 days until primary tillers reached the soft dough growth stage, Feekes GS 11.2 (29 June in OK1; 13 July in OK2; 7 August in CC). A final disease assessment was made at soft dough as this was the growth stage after which it became difficult to differentiate between diseased and naturally senescent spikes. The length of time from spike emergence to senescence, and consequently, the number of assessments, varied among locations. LEAF ratings were initiated before Feekes 10.5 at OK2 and CC, when most of the fields were at the Feekes 9 growth stage. At OK1, the first set of LEAF ratings were made when the majority of the field was at Feekes 10.5.1. Due to weather and time constraints, two of the six plots were not rated at CC, and plots at OK2 were not rated between June 28 to July 9. Additionally, the final disease assessment at OK2 was made on only 2 of the 6 plots. Consequently, a total of approximately 3,600 assessments were made at CC (4 plots x sampling 100 sites x 9 assessment per sampling site), compared to 3,000 at OK1 (6 plots x 100 sites x 5 assessments per site) and 3,100 at OK2 (2-6 plots x 100 sites x 1-6 assessments per site).

Data analysis. *Temporal development of spike blast.* For spike blast incidence (INC) and severity (SEV), means at each assessment time, averaged across sampling nodes and plots, were estimated and used to model the temporal dynamics of spike blast. Since a few of the early assessments were made before heading was widespread, nodes with fewer than 15 spikes were not included in the final datasets because of low precision of means with such a small number of observations (Madden et al. 2007). Separate monomolecular, exponential, logistic, and Gompertz population growth models (Madden et al. 2007), in their nonlinear forms, were fitted to the means of the distributions of INC and SEV at each assessment time using the MODEL procedures of SAS. Diagnostic plots generated through the *plots* option in PROC MODEL were used along with fit statistics such as mean squared error (MSE) and R^2 as measures of model performance. Prior to selecting the final model to estimate parameters and compare epidemics, a series of preliminary model-fitting steps were run to check and correct for heteroscedasticity and serial correlation of residuals (see Madden and Hughes for details [1995]). White's (White 1980) and the modified Breusch-Pagan (Breusch and Pagan 1979) tests of heteroscedasticity, and the Durbin-Watson (Durbin and Watson 1950) and Godfrey Lagrange multiplier (Godfrey 1978a, 1978b) tests for residual autocorrelation were run through the *fit* statement in PROC MODEL to test the null hypotheses of homoscedasticity and uncorrelated residuals, respectively. For situations in which the null hypothesis of homoscedasticity was rejected (Table 4.1.), models were refitted using weights as recommended by Madden and Hughes (1995) and Madden et al. (2007) to correct for heteroscedasticity.

Weights was defined as:

$$W_i = \frac{1}{INC(1 - INC)} \tag{1a}$$

for incidence and

$$W_s = \frac{1}{SEV(1 - SEV)} \tag{1b}$$

for severity.

Since disease progress was quantified as a time series, incidence and severity values at a certain time were assumed to be correlated with prior values, i.e., recurring assessments were not biologically independent from each other (Madden and Hughes 1995). This may translate into correlation of residuals. Lack of independence, and consequently, high autocorrelation of residuals, may lead to artificially low standard errors of parameter estimates, which in turn may lead to erroneous conclusions when comparing epidemics (Madden and Hughes 1995), a primary focus of the current investigation. To correct for autocorrelation, models for which the null hypothesis of no serial correlation was rejected (Table 4.1.) were refitted with a first-order autoregressive [AR(1)] error term using the %AR macro in PROC MODEL. Autocorrelation and partial autocorrelation function plots (plots of the correlation coefficients and partial correlation coefficients, respectively, versus time lags) were used as a guide for defining the number of AR terms to include in the model.

Based on the statistics in Table 4.2., residual and raw data plots, and statistics from linear regression analyses of relationships between predicted and observed blast intensity, the logistic model was chosen as the most appropriate for describing the dynamics of wheat

spike blast at all locations. Although the exponential model fit the data just as well as the logistic model in most cases (Table 4.2.), the latter was chosen over the former because it is more biologically meaningful. Unlike the logistic model, the exponential model does not have term for healthy individuals or tissues, meaning that it assumes that healthy spike tissue is at a maximum throughout an epidemic, i.e., the rate of disease progress is not slowed down by the depletion of healthy individuals or tissues (Madden et al. 2007). This is unrealistic for making any predictions when disease is not low, particularly in our case where a finite number of spikes of a fixed size was rated. The nonlinear forms of this model can be written as:

$$y = \frac{1}{1 + \left(\frac{1 - y_0}{y_0}\right) e^{(-r_L t)}} \quad (2)$$

where y is disease intensity (INC or SEV; as a proportion), r_L is the rate parameter (per day), t is time in days after Feekes 10.5, and y_0 is disease intensity at the start of the epidemic. Estimated model parameters and predicted mean blast intensity, averaged across sample nodes and plots, were used along with their standard errors to compare epidemics among the three locations using Welch's independent-sample *t*-tests (Madden et al. 2007; Derrick et al. 2016; Welch 1947). This is a modification of the Student *t*-test that is robust to unequal variability among estimates from the three locations that likely resulted from differences in growing conditions and sample sizes. Since crop growth and development varied among locations, predicted mean incidence and severity at 21 days after full head emergence were compared instead of final incidence and severity at any one calendar date.

Time-to-event analysis. For some pathosystems, there are certain critical levels of disease at or above which yield and quality losses may occur (Madden et al. 2007), and at which management or grain marketing decisions are made. One approach for using models of disease dynamics to help guide decision-making is to estimate the time it takes for disease intensity to reach predetermined thresholds and compare the results among experimental factors, locations, or growing seasons (Madden et al. 2007). Separate logistic models were fitted to mean spike blast data from each sample node, and the resulting parameters were used to estimate the time (in days) it took for blast severity to reach thresholds of 10, 15, and 20% at each node at each location (Fig. 4.4.) by solving equation 2 for time, *t*. The equation can be written as:

$$t_S = \frac{ln\left(\frac{1-y_S}{y_S}\right) - ln\left(\frac{1-y_0}{y_0}\right)}{-r_L} \quad (3)$$

where t_S is time in days from Feekes 10.5 to 10, 15, or 20% severity (t_{10}, t_{15}, or t_{20}, respectively), y_S is the specific severity threshold (y_{10}, y_{15} or y_{20}), and y_0 and r_L are parameters for the logistic models as defined above. These thresholds were loosely based on the work of Rios et al. (2016), which showed that 10, 15, and 20% spike blast severity at 14 days after inoculation (anthesis) were associated with grain yield reductions of approximately 35, 52, and 88%, respectively.

The t_S data were right censored because the disease levels of interest were not always reached by the end of the observation period. To account for this situation, a survival analysis was performed for the t_S data (Nesi et al. 2013; Ojiambo and Scherm 2005; Scherm and Ojiambo 2004). Using each node as a separate observation, the

probability of severity not reaching ("surviving") y_{10}, y_{15} or y_{20} by 21 data after Feekes 10.5 was estimated for the population of nodes at each location. Based on the estimated t_S values, rounded to the nearest day, each observation was assigned a code of 1 if y_S was reached by day 21 after heading (considered here as the event of interest) and 0 otherwise (considered as censored). In other words, observations with $t_S > 21$ were considered censored at 21 days after heading (Table 3.3). Time-to-event (also known as survival) analysis was then performed with the LIFETEST procedure of SAS, through which the Kaplan-Meier method (Kaplan and Meier 1958) was used to estimate survivor functions and the Life-Table method was used to construct survival curves for each y_S at each location (Allison 2010). Survival curves are plots of the probability of "surviving" a specific disease threshold for at least 21 days after heading. To determine the effect of location on time to 10, 15, or 20% spike blast severity, the null hypothesis of no difference in survival curves (survivor functions) among locations was tested using the log-rank test in PROC LIFETEST (Allison 2010; Bland and Altman 2004; Goel et al. 2010).

Leaf blast effect on spike blast survivor function. The association between leaf and spike blast is still largely unknown, but the fact that lesions on leaves are capable of producing copious amounts of spores has led some researchers to hypothesize that leaf blast is a potential source of inoculum for the development of spike blast (Cruz et al. 2015; Gongora-Canul et al., 2019). Here we expanded the time-to-event analysis to determine whether leaf blast severity at approximately 21 days after Feekes 10.5 (20 days after at OK1, 21 days after at CC, and 23 days after at OK2) had an effect on the probability of spike blast reaching 10, 15, or 20% severity by 21 days after heading. Repeating the

analyses described above, we included leaf blast severity (LEAF) as a categorical fixed effect with three level (LEAF < 25%, 25 ≤ LEAF < 50%, and 50% ≤ LEAF), estimated and plotted survivor functions for reach location x LEAF category combination, and tested the null hypothesis of no difference in survivor functions between pairs of location x LEAF combinations. Then based on the results, we used the TEST statement in PROC LIFETEST to estimate the direction and significance of the association between LEAF as a continuous covariate and time-to-event (SEV reaching 10, 15, or 20% by 21 days after heading) at each location.

Quantifying the magnitude of location and leaf blast severity effects. The analyses described in the previous two paragraphs provide estimates of the significance of location and leaf blast effects of spike blast survivor function, but for reasons outlined in Allison (2010), they are not the best approaches for quantifying the magnitude of these effects. In addition, none of the commonly-used survival (lifetime) distributions, required for valid implementation of parametric Accelerated Failure Time (AFT) regression analyses in PROC LIFEREG, appeared to be appropriate for our data set. We therefore fitted semiparametric Cox regression models (Allison 2010) to the survival data, with location and LEAF as categorical and continuous covariates, respectively. However, since the proportional hazards assumption was not met (i.e., the "failure rate" depended on time or a time-varying covariate), instead of employing the commonly used Cox proportional hazards modeling approach, we fitted nonproportional hazard models using the PHREG procedure in SAS, with time-dependent covariates included in the models. We modeled the effect of location (recoded as 1 for CC, 2 for OK1 and 3 for OK2) on time to 10, 15

and 20% (y_{10}, y_{15} and y_{20}) spike blast severity (SEV), with location x time (t_s) interaction terms included in the models as the time-dependent covariates. *Class*, *contrast* and *estimate* statements in PROC PHREG were then used for hypothesis testing and to compare locations based on hazard ratios.

Similarly, the effect of leaf blast severity (LEAF) was modeled using PROC PHREG, with LEAF x t_s interaction terms included in the models as time-dependent covariates to account for the fact that proportional hazard assumption was violated. Rates of increase in the likelihood of SEV reaching the specific thresholds (hazard ratio) for every 5% increase in LEAF were then estimated from the model parameters along with their 95% confidence intervals. The effect of LEAF was only quantified at Okinawa 1, since results from the LIFETEST procedure indicated that leaf blast severity did not have an effect on the survivor functions at Cuatro Cañadas and only affected the function at Okinawa 2 when the probability of SEV reaching 15% was estimated.

RESULTS

Growing conditions and crop and wheat blast development. Growing conditions and crop development varied among the locations. Mean temperature and relative humidity (RH) were 20-21^{o}C and 89%, respectively, at OK1 and OK2, compared to 22.4^{o}C and 82% RH at CC. At CC, a single major rainfall event of 70 mm occurred during the first week of heading (Fig. 4.2.A), whereas at OK1, it rained on four of the seven days, for a total of 64 mm (Fig. 4.2.B). Barring a single rainfall event of 1.60 mm, it was rain-free during the first week and a half after initial heading at OK2, after which it rained

on six of the next eight days, for a total of 126 mm (Fig. 4.2.C). Spike emergence (Feekes 10.5) was earliest and most synchronized at OK1 and latest and most asynchronized at CC. The first set of fully emerged spikes were observed at 56 days after planting (DAP) at OK1, 59 DAP at OK2, and 63 DAP at CC. At approximately 60 DAP, 80% (481) of the 600 sampling sites (nodes on the grid) at OK1 had 10 to 20 tillers at the Feekes 10.5 growth stage, 80% of the nodes at OK2 had fewer than six tillers at Feekes 10.5, and 94% (377) of the 400 nodes at CC had no tillers at Feekes 10.5. At 70 DAP, 15 or more spikes were rated at 68% of the nodes at OK1, 37% at OK2, and 9% at CC.

The first set of spike blast symptoms were observed shortly after spikes emerged at all locations, but initial incidence (INC) and severity (SEV) were low during the first week and varied considerably among the three locations (Fig. 4.3.). For instance, at 6-7 days after Feekes 10.5, 77, 47, and 11% of the nodes were blast-free at CC, OK2 and OK1, respectively. The distribution of mean blast intensity also varied among assessment times and locations. At approximately three weeks after Feekes 10.5, mean SEV was 57% at OK1, 28% at OK2, and 18% at CC, with 50 percent of the node (sampling site) means between 43 and 71% (an interquartile range [IQR] of 28%), between 9 and 40% (IQR = 29%), and between 12 and 24 (IQR = 12%) at OK1, OK2, and CC, respectively. For INC, the corresponding means and IQRs were 86 and 25%, 99 and 0%, and 53 and 25%. Mean INC and SEV at the time of the last assessment (20, 25 and 28 days after Feekes 10.5 at OK1, OK2, and CC) were 86 and 58% at OK1, 100 and 74% at OK2, and 95 and 71% at CC.

Mean leaf blast severity (LEAF) at approximately three weeks after Feekes 10.5, ranged from 0.6-5 to 98-100%, depending on the location (Fig. 4.3. G, H, and I), with an overall mean of 37% at OK1, 28% at OK2, and 41% at CC. Approximately 44% of the sampling sites at OK1 had mean LEAF < 25%, 27% had means between 25 and 50% (25 ≤ LEAF < 50%), and 29% had mean LEAF > 50%. The corresponding percentages of mean LEAF in the three categories were 57, 27 and 16%, respectively, at OK2, and 42, 17 and 41% at CC.

Temporal development of wheat spike blast. For several of the model-response combinations, there was evidence of serial correlation of residuals and heteroscedasticity, based on the formal statistical tests (Table 4.1.), even though the residual plots did not always accuse these violations (data not shown). With very few exceptions, the two tests for serial correlation and two for heteroscedasticity agreed with each other. The violations tended to be more frequent and consistent across models and locations for severity than for incidence. Models fitted to data from CC had more issues with heteroscedasticity, particularly for severity, than with autocorrelation. For the monomolecular model fitted to incidence and severity data from CC, the null hypotheses of homoscedasticity and uncorrelated residuals were rejected by at least one test ($P < 0.05$, Table 4.1.). Similar trends were observed with the exponential models at OK1, with the null hypotheses being rejected for both incidence and severity; with the Gompertz and logistic models, the hypotheses were rejected for severity but not for incidence. At OK2, autocorrelation was less of a problem than heteroscedasticity; the null hypothesis of homoscedasticity was rejected for all model fits by at least one test. Refitting models with weights and/or with a

first-order autoregressive error term did correct for heteroscedasticity and serial correlation of residuals, respectively, in some but not all cases.

The model parameters and statistics in Table 4.2. are from the fit of models corrected for heteroscedasticity and serial correlation of residuals. While the logistic, exponential, and Gompertz models fit the data reasonably well, the monomolecular model was not a good fit. The mean squared differences in in blast intensity between predicted and observed values (MSE) were among the lowest, and R^2 values were among the highest for the logistic model (Table 4.2.). For instance, for both INC and SEV at CC, the logistic and Gompertz models had the highest and comparable R^2 values (0.97 to 0.98). The same two models had the highest R^2 for SEV at OK1, but for INC, R^2 values were comparable (0.87 to 0.89) among the models. At OK2, the exponential and logistic models had the highest R^2 for SEV, and this statistic was highest with the exponential model for INC. Patterns of the residual plots were comparable among the models (data not shown).

Based on the fit statistics, the logistic model was chosen as the most appropriate for comparing epidemics among the locations. Estimated initial INC and SEV (y_o) and rate parameters (r_L) for both measures of spike blast varied considerably among locations. For both INC and SEV, r_L values (Table 4.2.) were significantly greater ($P < 0.001$) at OK2 than at OK1 and CC, and significantly higher at CC than at OK1 for INC, but not SEV. Opposite trends were observed for y_o, with the estimates being significantly higher at OK1 than at CC and OK2, and greater at CC than at OK2 for SEV, but not for INC. Estimated predicted INC at 21 days after Feekes 10.5 was significantly greater at OK1 (89%) and OK2 (98%) than at CC (55%), whereas for SEV, the estimated predicted value at 21 days

after full head emergence was significantly higher at OK1 (70%) than at CC (16%) and OK2 (8%).

Time-to-event analysis. *Estimated time to 10, 15, and 20% spike blast severity*. The time it took for SEV (t_s) to reach certain thresholds (10, 15, and 20%), estimated using the parameters from the logistic model, varied among locations and among sampling sites within locations. For instance, at OK2, it took an estimated 11 to 25 days for severity to reach 10% (t_{10}), whereas at OK1 and CC, that same level of severity was reached between 1 and 19 days and 6 and 26 days, respectively (Fig. 4.4.). Mean t_{10} was 19, 10, and 22 days at CC, OK1 and OK2, respectively (Fig. 4.4.A, D, and G). The corresponding mean t_{15} and t_{20} values were 21, 12 and 23 days (Fig. 4.4.B, E, and H) and 22, 13, and 23 days (Fig. 4.4.C, F, and I); it took about 10 fewer days for a given threshold to be reached at OK1 compared to OK2 and CC.

Survivor function and estimated survival probability. The probabilities of SEV reaching y_{10}, y_{15}, or y_{20} (10, 15, or 20%) between 1 and 21 days after full head emergence (i.e., 1 – "survival" probability) were estimated and formally compared among locations through survival (time-to-event) analysis. At OK1, the SEV thresholds were reached at more than 98% at the sampling sites by 21 says after Feekes 10.5 (i.e., 1 – survival ≥ 0.98) (Table 4.3.). The probability of reaching the thresholds earlier in the epidemic (for instance, 14 days after Feekes 10.5) was also fairly high (0.55 to 0.85) at OK1 compared to the other two locations (Table 4.3.). The opposite trend was observed at OK2 where a large percentage (83 to 96%) of the observations were censored at 21 days. In other words, probabilities of survival (not reaching the threshold by 21 days after Feekes 10.5) were

between 0.83 and 0.96 (Fig. 4.5.A, C and E), equivalent to probability of reaching y_S between 0.04 (1 – 0.96) and 0.17 (1 – 0.83). Probabilities of reaching y_{10}, y_{15}, or y_{20} by 21 days after full head emergence were intermediate (0.73, 0.46, and 0.28, respectively) at CC (Table 3.3).

Effect of location and leaf blast severity on spike blast survivor function. For all but one pairwise comparison between locations, the survivor functions were significantly different among locations for y_{10}, y_{15}, or y_{20} ($P < 0.05$, Table 4.4.). The effect of LEAF (as a categorical variable) on spike blast time-to-event was statistically significant ($P < 0.05$) at OK1 for all three thresholds, only for y_{15} at OK2, but was not statistically significant for any of the thresholds at CC (Table 4.4. and Fig. 4.5.B, D, and F). The negative signs of the log-rank test statistics in Table 4.4. indicate that as LEAF increased, time to y_{10}, y_{15}, or y_{20} decreased. As showed in Fig. 4.5.B, D, and F, the probabilities of spike blast not reaching y_{10}, y_{15}, or y_{20} were highest (0.25, 0.44, and 0.67, respectively) when LEAF was less than 25% and lowest (0.05, 0.09, 0.18, respectively) what LEAF was greater than 50%. In other words, when LEAF was ≥ 50%, the probability of SEV reaching 20% by 21 days after Feekes 10.5 was 0.82; when LEAF was between 25 and 50% (25 ≤ LEAF < 50%), the probability was 0.62; and when LEAF was < 25%, the probability was only 0.33.

Through Cox nonproportional hazard regression analysis, hazard ratios (HR) were estimated as measures of the magnitude of location and LEAF effects on the likelihood of SEV reaching 10, 15, or 20% (y_{10}, y_{15}, or y_{20}) by 21 days after Feekes 10.5. An HR value of 1 means that the event (y_{10}, y_{15}, or y_{20} being reached) is equally likely between the groups being compared; HR > 1 means that the event is less likely in the reference group that in

the group being compared; and HR < 1 means the opposite. For comparisons between pairs of locations, the tested null hypothesis was HR = 1. Using OK1 as the reference, the HRs were all less than 1, and considerably so for comparisons between OK1 and CC. This meant that the probabilities of SEV reaching the thresholds were higher for OK1 than CC. For instance, the chance of SEV reaching 10, 15, or 20% by day 21 after heading was more than 100 times greater at OK1 than at CC. The chance of SEV reaching 10 and 15% was more than 26 and 7 times greater at OK1 than at OK2. Contrast between OK1 and OK2 for y_{20} was not statistically significant ($P > 0.05$). For LEAF as a continuous covariate, for every 5% increase in severity, the likelihood of SEV reaching 10, 15, and 20% by 21 days after Feekes 10.5 increased by 31, 43, and 55%, respectively (HRs of 1.31, 1.43, and 1.55; Fig. 4.6.).

DISCUSSION

In this study, we successfully quantified the temporal development of wheat spike blast at three field locations in the Santa Cruz de la Serra region of Bolivia where the disease is endemic, in a year (2015) during which a strong El Niño-Southern Oscillation events led to conditions being conducive (rainfall and temperatures between 18 and 25ºC during anthesis, followed by warm, humid days) for disease development (Cardoso et al. 2008; Kohli et al. 2011). Although less favorable weather in 2016 prevented the experiments from being repeated for a second growing season, the fact that plots were planted on different dates and growing conditions varied among the locations in the first season meant that the crop, and consequently, the epidemics, developed under different

conditions at the three locations, allowing us to make acceptable comparisons. In all three fields, disease intensity increased over time for as many as 25-30 days before reaching or approaching 100% mean incidence, and in all cases, without reaching mean severity of 100% at the time of the final assessment. The results of the temporal increase in spike blast intensity are consistent with those reported by Gomes et al. (2019), Gongora-Canul et al. (2020) and Rios et al. (2016). Of the population growth models fitted to the data, the exponential and logistic were the most appropriate for describing the temporal change in incidence and severity. However, from a biological standpoint, as discussed by Madden et al. (2007), given that the same cohort of wheat spikes of a fixed size was rated at each time, it is unrealistic to expect spike blast to increase indefinitely over time as suggest by the exponential model. So, although the simplified exponential representation of spike blast temporal dynamics would likely be appropriate for situations in which blast intensity is relatively low (Madden et al. 2017), we opted to focus our attention on the more biologically relevant logistic model (of equally good fit). This model describes epidemics that increase over time and then "levels off" as healthy individuals and host tissues become limiting. The exponential model is a special case of the logistic model.

The fact that the logistic model was generally the most appropriate for describing wheat spike blast epidemics at all three locations and that it provided very good fit to both incidence and severity data, allowed us to make several interpretations about spike blast epidemiology. For instance, the fit of this model is consistent with a polycyclic-like disease. This would suggest that primary infections from resident inoculum within or outside the fields, the production and spread of inoculum during the season, and secondary

infection of healthy spikes drive epidemics. However, the logistic shape of the disease progress curves is also consistent with a monocyclic disease in which the rate parameter (r_M) increases over time (Madden et al. 2007). This occurs when either the primary (and only) inoculum for spike infection increase monotonically over time or the efficiency with which this inoculum causes infection increases over time (for instance, due to increasing favorability of the environment for dispersal or infection). If overwintering structures were the main source of inoculum and r_M were constant, the monomolecular model would have probably provided a better fit than was observed in the study. The spike blast incidence progress curves support the idea of a monocyclic epidemic with increasing r_M, because there would have been insufficient time for infected spikes to produce inoculum that would infect other spikes (on primary tillers) in the epidemic. One may argue that the asynchronous heading observed in this study - a common characteristic of the wheat crop that results largely from secondary tiller development after primary tillers are produced – and infection of the later-produced secondary spikes could have contributed to the temporal change in incidence. However, this was unlikely to occur over the entire duration of the epidemic (20+ days after Feekes 10.5), as was the case here.

We can refer to spike blast as a "polycyclic-like" disease because we do not have data showing that spores spreading from diseased to healthy spikes were the primary drivers of the epidemic, a necessary condition stipulated in the classical definition of a polycyclic disease (Madden et al. 2007). Throughout the epidemic, spores infecting the spikes could have come from overwintering and external sources or from sporulating leaves as hypothesized by Cruz et al. (2015), Gongora-Canul (2020), and Cruppe (2020).

The shape of the spike blast progress curves could directly reflect the temporal development of disease on the leaves, with spores dispersing from the sporulating leaf lesions to the spike. This is fully consistent with a monocyclic process for spike disease incidence (and possibly severity) with increasing r_M. The logistic (or any polycyclic) population growth of leaf blast severity would mean that inoculum was increasing over time, infecting spikes (even at fixed infection efficacy of inoculum), and leading to increasing r_M. This was a motivation for characterizing spike blast epidemics with a survival analysis that accounted for leaf disease severity. Moreover, for spike blast severity (equivalent to incidence of diseased *spikelets*), a temporal increase in the mean proportion of diseased spikelets per spike could have resulted from spread of the fungus within the spike (colonization), even if new infections of spikelets from spores produced on other spikes did not occur. Working in a closed system in which applied spores was the only source of inoculum, Mills et al. (2020) clearly showed through point-inoculations (Andersen et al. 2015) of wheat spikes with an isolate of the Lolium pathotype of *M. oryzae* (MoL) that severity increased in over time in a manner consistent with a polycyclic disease.

Although the logistic model was considered appropriate for describing epidemics at all three locations, model parameters differed, causing the curves to shift among locations. That is, the period with highest absolute rate of disease increase, *dy/dt*, occurred much later for spike severity at OK2 (such that y was not close to the maximum by the last assessment time) and earliest at OK1. This reflects the fact that OK2 had the highest r_L and lowest y_0, and OK1 had the highest y_0 and lowest r_L for spike severity. CC was intermediate. The same trends in the parameter estimates were found for spike incidence,

although overall incidence was much higher than severity, which is a well-known phenomenon (Paul et al. 2005). Differences among the locations were likely due to differences in weather conditions, crop development, and inoculum abundance and infection efficiency. Summaries for temperature and RH were very similar for OK1 and OK2, but the amounts, frequency, and distribution of rainfall differed considerable between the two locations. At OK1, it rained on four of the first seven days after initial heading, for a total precipitation of 64 mm, whereas at OK2, it remained rain-free during the first 11 days after initial heading, and then rained on six of the next eight days, for a total of 126 mm. At both locations, the rain events occurred during the week before the highest absolute rate of disease increase (the inflection point) occurred, thus explaining why incidence and severity peaked much later at OK2 than at OK1.

Differences in inoculum density, due in part to inoculum produced on leaves, and to a lesser extent, heading synchrony could have also been the reasons for differences in spike blast development between OK1 and OK2. For instance, during the early stages of crop development (before heading), foci of naturally-infected tillers with sporulating lesions were observed in both fields. However, these inoculum foci were larger and more abundant at OK1, the location with the highest mean leaf blast severity, than at OK2 (J. D. Salgado, *personal communication*). Higher levels of in-field inoculum combined with rainfall during heading were likely the reasons for higher y_0 at OK1 compared to OK2. Higher y_0 coupled with more synchronized heading and the absence of later-season rainfall could have resulted in lower r_L at OK1 than at OK2. With the very low y_0 at OK2, predicted disease severity only reached 0.75 by the last assessment (26 days after heading), even with

the very high r_L. A similar set of arguments could be used to explain differences in parameter estimates, and consequently, spike blast progress between OK1 and CC and OK2 and CC. For instance, as was the case at OK1, it also rained during the first week of heading at CC, but only in a single event totaling 70 mm. This would have stimulated inoculum production, and consequently, higher initial blast intensity (y_0) at CC than at OK2, where it did not rain during early heading. However, frequent and abundant late-season rainfall coupled with synchronized heading and an abundance of healthy spike at OK2 (due to significantly lower y_0 and retarded disease progress during the first 3 weeks after heading) would have resulted in the highest absolute rate of increase in spike blast severity occurring much later at OK2 than at CC, where it did not rain late in the season.

By definition, y_0 and r_L both influenced time to 10, 15 and 20% severity (t_S; equation 3), but sometimes differences in y_0 could override large differences in r_L between epidemics in the prediction of times to different severity thresholds. In the long run, epidemics characterized by the logistic model are more sensitive to the rate parameter than to y_0 (Madden et al. 2007); however, the orders-of-magnitude differences in y_0 (e.g., 10^{-8} to 10^{-3} for severity) between the locations were large enough to dominate in determining the time it took for spike blast to reach these relatively low levels of severity. Although r_L for severity was significantly lower at OK1 than at OK2, and numerically lower than at CC, the earlier establishment of blast at OK1 (higher y_0) than at OK2 and CC resulted in t_S (time to the 10, 15 and 20% severity thresholds) being about 10-12 days shorter at OK1 than at CC and OK2. When compared to CC, the higher r_L at OK2 did compensate for the fact that y_0 was significantly lower, resulting in the two locations having very similar t_S

values. As discussed above, the observed pre-heading sporulating leaf blast foci likely contributed to earlier spike blast establishment (higher y_0), and consequently, shorter time-to-event at OK1 than at OK2 and CC. Although we were unable to deploy spore traps in our experiments, we did quantify spore density within plots prior to Feekes 10.5 through leaf washes and spore counts (Cruz et al. 2015) and found that 30 to 100 times more spores were present on plants with high leaf blast severity than on plants without leaf blast (Cruz, *unpublished*). Results from the survival analysis corroborated these observations and formally showed an association between leaf blast severity and spike blast survival/failure time at OK1 (i.e. the probability of spike blast "surviving" or reaching each threshold at a given time). The effect of leaf blast severity on spike blast time-to-event was statistically significant at OK1 for all t_S, with the probability of the severity thresholds being reached at any given time increasing as leaf blast severity increased. This is consistent with the high y_0 in OK1. The nonproportional hazard-model analysis may not have had sufficient precision to consistently detect leaf blast severity effects when y_0 was much lower than at OK1.

Wheat blast management in Bolivia and other parts of South America where the disease is endemic are not usually based on knowledge and understanding of disease epidemiology. For instance, there are no deployed disease forecasting or risk assessment tools to help guide fungicide applications or yield loss models from which economic injury levels or damage thresholds can be established. This may in part explain the inconsistency in results among fungicide trials in terms of efficacy (Cruz and Valent 2017; Cruz et al., 2019). Findings from the present study will be useful for developing and improving blast

management guidelines, particularly if coupled with risk assessment and economic analysis models. For instance, in Bolivia, where some fields with 30% or higher wheat blast severity are abandoned (J. Kiyuna, *personal communication*), results from our time-to-event analysis could be used to help guide fungicide application to reduce disease progress and minimize the risk of this decision threshold being reached. This could be tailored to each field based the specific characteristic of the epidemic. For instance, under conditions similar as those prevalent at OK1, with low t_S values (10 or 15% for instance), fields will have to be treated with an effective fungicide early enough to reduce the likelihood of these thresholds being reached through a reduction in r_L. Moreover, given the observed importance of y_0 and leaf blast severity for spike blast development, especially for some epidemics, strategies to reduce initial inoculum and even an early fungicide application to manage leaf blast would be of value for reducing the onset and severity of spike blast. This could lead to critical thresholds being reached after grain-fill is complete as was the case at OK2 and CC, thus reducing the impact of spike blast on grain yield. As Rios et al. (2016) demonstrated, spike blast severity at 10 days after anthesis has a stronger negative effect on grain yield than severity at 21 days after anthesis. Finally, one cannot rule out the possibility of the appropriate decision being to abandon a field in some cases; predictions of t_S would give guidance in this regard, if coupled with an economic analysis.

Acknowledgment

This project was supported by Agriculture and Food Research Initiative Competitive Grant no. 2013-68004-20378 from the United States Department National Institute of Food and

Agriculture and The Ohio State University Department of Plant Pathology. Salaries and research support for K. B. Mills, J. D. Dalgado, L. V. Madden, and P.A. Paul were provided by state and federal funds to the Ohio Agricultural Research and Development Center. The authors wish to thank the support provided by Cooperativa Agropecuaria Integral Colonias Okinawa (CAICO), Centro Tecnológico Agropecuario en Bolivia (CETABOL), and Asociación de Productores de Oleaginosas y Trigo (ANAPO) with the experiments conducted in Bolivia. The authors wish to acknowledge Diego F. Baldelomar, Javier Kiyuna, Maryluz Huainoca, and Juan Vasquez for their help with field activities.

REFERENCES

Allison, P.D. 2010. Survival Analysis Using the SAS System: A Practical Guide, Second Edition. Cary, NC, SAS Institute Inc.

Anapo. Asociación de Productores de Oleaginosas y Trigo. 2015. Recomendaciones Técnicas para el cultivo de trigo. Santa Cruz, Bolivia.

Andersen, K. F., Madden, L. V., and Paul, P. A. 2015. Fusarium head blight development and deoxynivalenol accumulation in wheat as influenced by post-anthesis moisture patterns. Phytopathology 105:210-219.

Barea, G. and Aguanta, G. 2012. Manual de Recomendaciones Técnicas: Cultivo de trigo. Asociación de Productores de Oleaginosas y Trigo ANAPO. Página 14.

Barea G., Toledo J. 1996. Identificación y zonificación de piricularia o bruzone (*Pirycylaria oryzae*) en el cultivo del trigo en el dpto. de Santa Cruz. In: CIAT. Informe Técnico. Proyecto de Investigación Trigo, Santa Cruz, 76–86.

Bland, J. M. and Altman, D. G. 2004. The logrank test. British Med. J. 1:328:1073.

Breusch, T. S., and Pagan, A. R. 1979. A simple test for heteroskedasticity and random coefficient variation. Econometrica 47:1287-1294.

Cabrera, M. and Gutiérrez, S. 2007. Primer registro de *Pyricularia grisea* en cultivos de trigo del NE de Argentina. Depto. Protección Vegetal, Facultad de Ciencias Agrarias, UNNE. Corrientes, Argentina.

Cardoso, C. A. de A., Reis, E. M., and Moreira, E. N. 2008. Development of a warning system for wheat blast caused by *Pyricularia grisea*. Summa Phytopathol. 34:216-221.

Ceresini, P.C., Castroagudín, V.L., Rodrigues, F.Á., Rios, J.A., Aucique-Pérez, C.E., Moreira, S.I., Alves, E., Croll, D. and Maciel, J.L.N. 2018. Wheat blast: past, present, and future. Annu. Rev. Phytopathol. 56: 427–456.

Ceresini, P. C., Castroagudín, V. L., Rodrigues, F. Á., Rios, J. A., Aucique-Pérez, C. E., Moreira, S. I., Croll, D., Alves, E., Carvalho, G., Maciel, J. L. N., and McDonald, B. A. 2019. Wheat blast: from its origins in South America to its emergence as a global threat. Mol. Plant Pathol. 20:155-172.

Cruppe, G. 2019. Wheat blast management through identification of novel sources of genetic resistance and understanding of disease dynamics. Ph.D. Dissertation, Department of Plant Pathology, Kansas State University, Manhattan, KS.

Cruz, C. D. and Valent, B. 2017. Wheat blast disease: danger on the move. Tropical Plant Pathology 42:210-222.

Cruz, C. D., Santana, F., Todd, T. C., Maciel, J., Kiyuna, J., Baldelomar, D., Cruz, A.P., Lau, D., Seixas, C., Goulart, A., Sussel, A., Schipanski, Chagas, D.F., A., Coelho, M., Dellanora, T., Utiamada, C., Custódio, Rivadeneira, M.G., A., Bockus, and Valent, B. 2019. Multi-environment assessment of fungicide performance for managing wheat head blast (WHB) in Brazil and Bolivia. Tropical Plant Pathology 44:183-191.

Cruz, C. D., Bockus, W. W., Stack, J. P., Tang, X., Valent, B., Pedley, K. F., and Peterson, G. L. 2012. Preliminary assessment of resistance among U.S. wheat cultivars to the Triticum pathotype of *Magnaporthe oryzae*. Plant Dis. 96:1501-1505.

Cruz, C. D., Kiyuna, J., Bockus, W. W., Todd, T. C., Stack, J. P., and Valent, B. 2015. *Magnaporthe oryzae* conidia on basal wheat leaves as a potential source of wheat blast inoculum. Plant Pathol. 64:1491-1498.

Cruz. C. D., Peterson. G. L., Bockus, W. W., Kankanala, P., Dubcovsky, J., Jordan, K. W., Akhunov, E., Chumley, F., Baldelomar, F. D., Valent, B. 2016. The 2NS translocation from *Aegilops ventricosa* confers resistance to the *Triticum* Pathotype of *Magnaporthe oryzae*. Crop Sci 56:990–1000.

Cruz, M. F. A., Prestes, A. M., Maciel, J. L .N., Scheeren, P. L. 2010. Partial resistance to blast on common and synthetic wheat genotypes in seedling and in adult plant growth stages. Trop Plant Pathol 35:24–31

Derrick, B., Toher, D., and White, P. 2016. Why Welch's test is Type I error robust. Quantitative Methods for Psychology. 12:30-38.

Durbin, J., and Watson, G. S. 1950. Testing for serial correlation in least squares regression, I. Biometrika. 37:409–428.

Farman, M., Peterson, G., Chen, L., Starnes, J., Valent, B., Bachi, P., Murdock, L., Hershman, D., Pedley, K., Fernandes, J. M., and Bavaresco, J. 2017. The Lolium pathotype of *Magnaporthe oryzae* recovered from a single blasted wheat plant in the United States. Plant Dis. 101:684-692.

Goel M.K., Khanna P., and Kishore J. 2010. Understanding survival analysis: Kaplan-Meier estimate. Int J Ayurveda Res. 1:274-8.

Gomes, D.P.; Rocha, V.S.; Rocha, J.R.A.S.C.; Souza, M.A.; Pereira, O.L. 2019. Progresso temporal da brusone do trigo em função do inóculo primário, da aplicação de fungicida e da resistência dos genótipos. Summa Phytopathol. 45:50-58.

Gongora-Canul, C., Salgado, J. D., Singh, D., Cruz, A. P., Cotrozzi, L., Couture, J., Rivadeneira, M. G., Cruppe, G., Valent, B., Todd, T., Poland, J., and Cruz, C. D. 2020. Temporal dynamics of wheat blast epidemics and disease measurements using multispectral imagery. Phytopathology 110:393-405.

Godfrey, L. G. 1978a. Testing against General Autoregressive and Moving Average Error Models When the Regressors Include Lagged Dependent Variables. Econometrica 46: 1293–1301.

Godfrey, L. G. 1978b. Testing for Higher Order Serial Correlation in Regression Equations When the Regressors Include Lagged Dependent Variables. Econometrica 46: 1303–1310.

Goulart, A. C. P., Sousa, P. G., Urashima, A. S. 2007. Danos em trigo causados pela infecção de *Pyricularia grisea*. Summa Phytopathologica 33:358-363.

Igarashi S. 1990. Update on wheat blast (*Pyricularia oryzae*) in Brazil. In: Saunders DA (ed) Wheat for the nontraditional warm areas: a proceeding of the international conference. Foz do Iguaçu, Brazil, pp 480–483.

Igarashi, S., Utiamada, C. M., Igarashi, L. C., Kazuma, A. H., and Lopes, R. S. 1986. Pyricularia em trigo, ocorrência de Pyricularia sp. no estado do Paraná. Fitopatol. Bras. 11:351-352.

Kaplan, E. L., and Meier, P. 1958. Nonparametric estimation from incomplete observations. J. Amer. Statist. Assoc. 53:457–481.

Kohli, M. M., Mehta, Y. R., Guzman, E., Viedma, L., and Cubilla, L. E. 2011. *Pyricularia* blast - a threat to wheat cultivation. Czech J Genet Plant Breed 47:S130-S134.

Large, E. C. 1954. Growth stages in cereals illustration of the Feekes scale. Plant Pathol. 3:128-129.

Lima, M. 2004. Giverela ou brusone? Orientações para indentificação correta dessas enfermidades em trigo e em cevada. Embrapa Trigo Documentos online, 40. http://www.cnpt.embrapa.br/biblio/do/p_do40.pdf

Madden, L.V., and Hughes, G. 1995. Plant disease incidence: distributions, heterogeneity, and temporal analysis. Annu. Rev. Phytopathol. 33:529-564.

Madden, L. V., Hughes, G., and van den Bosch, F. 2007. The Study of Plant Disease Epidemics. American Phytopathological Society Press, St. Paul, MN.

Malaker, P. K., Barma, N. C. D., Tiwari, T. P., Collis, W. J., Duveiller, E., Singh, P. K., Joshi, A. K., Sigh, R. P., Braun, H. J., Peterson, G. L., Pedley, K. F., Farman, M. L., and Valent, B. 2016. First report of wheat blast caused by *Magnaporthe oryzae* pathotype Triticum in Bangladesh. Plant Dis. 100: 2330.

Martínez, S. I., Sanabria, A., Fleitas, M. C., Consolo, V. F., and Perelló, A. 2019. Wheat blast: Aggressiveness of isolates of *Pyricularia oryzae* and effect on grain quality. Journal of King Saud University - Science 31:150-157.

Mills, K. B., Madden, L. V., and Paul, P. A. 2020. Quantifying the effects of temperature and relative humidity on the development of wheat blast caused by the Lolium pathotype of Magnapothe oryzae. Plant Dis. 104. Online publication. https://doi.org/10.1094/PDIS-12-19-2709-RE.

Nesi, C. N., Shimakura, S. E., Ribeiro Junior, R. J., and De Mio, L. L. 2013 Survival analysis in plant pathology. IDESIA (Chile). 31:017-110.

Ojiambo P. S., and Scherm, H. 2005. Survival analysis of time to abscission of blueberry leaves affected by Septoria leaf spot. Phytopathology 95: 108-113.

Paul, P. A., El-Allaf, S. M., Lipps, P. E., and Madden, L. V. 2005. Relationships between incidence and severity of Fusarium head blight on winter wheat in Ohio. Phytopathology. 95:1049-1060.

Prabhu, A. S.; Filippi, M. C., and Castro, N. 1992. Pathogenic variation among isolates of *Pyricularia oryzae* affecting rice, wheat, and grasses in Brazil. Journal of Tropical Pest Management 38:367-371.

Rios, J. A., Rios, V. S., Paul, P. A., Souza, M. A., Araujo, L., Rodrigues, F. A. 2016. Fungicide and cultivar effects on the development and temporal progress of wheat blast under field conditions. Crop Prot 89:152–160

Rios, A., Debona, D., Duarte, H., and Rodrigues, F. 2013. Development and validation of a standard area diagram set to assess blast severity on wheat leaves. Eur. J. Plant Pathol. 136:603-611.

Sadat, A. and Choi, J. 2017. Wheat blast: A new fungal inhabitant to Bangladesh threatening world wheat production. Plant Pathol. 33:103-108.

Scherm, H. and Ojiambo, P. S. 2004. Applications of survival analysis in botanical epidemiology. Phytopathology 94:1023-1026.

Torres, G., Santana, F., Fernandes, J., and Só E Silva, M. 2009. Doenças da espiga causam perda de rendimento em trigo nos estados do Paraná, São Paulo e Mato Grosso do Sul. Emprapa Trigo. Comunicado Técnico online, 255.
https://www.infoteca.cnptia.embrapa.br/bitstream/doc/821793/1/pco255.pdf

Urashima A. S. 2010. Wheat blast. In: Bockus WW, Bowden RL, Hunger RM, Murray TD, Smiley RW (eds) Compendium of wheat diseases and pests. American Phytopathological Society Press, St. Paul, pp 22–23.

Waggoner, P. E. 1986. Progress curves of foliar diseases: Their interpretation and use. In: Leonard, K. J. and Fry, W. E. (Eds.). Plant Disease Epidemiology. Vol. 1. Population Dynamics and Management. Macmillan Publishing Co., New York NY, USA. pp. 3-37.

Welch, B. L. 1947. The generalization of ‘student’s’ problem when several different population variances are involved. Biometrika 34: 28–35.

White, H. 1980. A heteroskedasticity-consistent covariance matrix estimator and a direct test for Heteroskedasticity. Econometrica 48:817–838.

Table 4.1. Statistics and levels of significance for tests of serial correlation and heteroscedasticity from the fit of population growth models to wheat blast incidence (mean proportion of diseased spikes) and severity (mean proportion of diseased spikelets per spike) data collected from separate fields in Cuatro Cañadas, Okinawa 1, and Okinawa 2, near Santa Cruz de la Sierra, Bolivia in 2015

Location	Response	Model	Serial Correlation[a]					Heteroscedasticity[b]			
			Durbin-Watson			Godfrey		White		Breusch-Pagan	
			d	*P* < DW	*P* > DW	LM	*P*	W	*P*	BP	*P*
Cuatro Cañadas (CC)	Incidence	Exponential	1.34	0.023	0.977	5.38	0.020	8.26	0.142	1.03	0.311
		Monomoecular	0.72	<0.001	0.999	15.62	<0.001	20.85	0.001	2.34	0.127
		Logistic	2.02	0.482	0.518	0.01	0.924	7.15	0.210	0.27	0.602
		Gompertz	1.60	0.115	0.885	1.15	0.284	3.71	0.593	0.53	0.465
	Severity	Exponential	2.03	0.516	0.484	0.03	0.865	13.77	0.017	4.84	0.028
		Monomoecular	0.72	<0.001	0.998	18.46	<0.001	26.10	<0.001	12.26	<0.001
		Logistic	1.93	0.403	0.597	0.04	0.843	12.43	0.029	4.62	0.032
		Gompertz	1.61	0.126	0.874	1.23	0.267	7.35	0.025	3.43	0.064
Okinawa 1 (OK1)	Incidence	Exponential	1.09	0.002	0.999	7.10	0.008	18.80	0.002	6.27	0.012
		Monomoecular	2.05	0.504	0.496	0.03	0.857	3.99	0.551	1.40	0.237
		Logistic	1.44	0.037	0.963	2.36	0.124	7.34	0.197	0.01	0.913
		Gompertz	1.63	0.120	0.880	1.04	0.3076	5.58	0.3497	0.80	0.373
	Severity	Exponential	0.87	<0.001	0.999	11.53	<0.001	15.53	0.008	12.84	0.003
		Monomoecular	1.40	0.023	0.977	3.69	0.055	7.26	0.123	2.26	0.133
		Logistic	0.84	<0.001	0.999	11.36	<0.001	16.53	0.006	14.19	<0.001
		Gompertz	0.84	<0.001	0.999	11.62	0.001	13.34	0.020	11.67	0.001
Okinawa 2 (OK2)	Incidence	Exponential	2.49	0.917	0.084	3.96	0.047	30.48	<0.001	24.35	<0.001
		Monomoecular	1.78	0.262	0.738	0.17	0.679	29.87	<0.001	19.22	<0.001
		Logistic	2.35	0.847	0.153	2.23	0.136	11.74	0.039	0.14	0.710
		Gompertz	1.67	0.216	0.785	4.19	0.041	12.21	0.002	0.53	0.465
	Severity	Exponential	1.90	0.447	0.553	0.02	0.883	15.04	0.005	7.78	0.005
		Monomoecular	1.95	0.422	0.578	0.02	0.883	29.69	<0.001	12.97	<0.001
		Logistic	1.88	0.436	0.564	0.04	0.844	14.76	0.005	7.67	0.006
		Gompertz	2.51	0.915	0.085	3.86	0.049	23.24	<0.001	18.00	<0.001

[a]Durbin-Watson test statistic (*d*): a value of 2 means no autocorrelation was detected in the data, 0 to 2 means positive autocorrelation, and 2 to 4 indicates negative autocorrelation at a specific lag (one in this case); *P* < DW is the significance level for testing positive autocorrelation, whereas *P* > DW is for testing negative autocorrelation. LM is the Godfrey Lagrange multiplier test statistic and *P* = level of significance. Both are tests of the null hypothesis that the residuals are uncorrelated (no serial correlation).

[b]Tests of the null hypothesis of equal (constant) error variance across observations (homoscedasticity): W and BP are the White and modified Breusch-Pagan test statistics, respectively, and *P* = level of significance.

Table 4.2. Estimated parameters and corresponding statistics from non-linear regression fit of population growth models to spike blast incidence (mean proportion of diseased spikes) and severity (mean proportion of diseased spikelets per spike) data collected from Cuatro Cañadas (CC), Okinawa 1 (OK1), and Okinawa 2 (OK2), near Santa Cruz de la Sierra, Bolivia in 2015

Response	Location	Parameters and Statistics[a]					
		y_0	se(y_0)	$r_\bullet$	se($r_\bullet$)	MSE	R^2
		Exponential					
Incidence	Cuatro Cañadas	5.20E-02	1.80E-02	0.102	0.013	0.009	0.93
	Okinawa 1	1.90E-01	3.20E-02	0.079	0.008	0.075	0.88
	Okinawa 2	1.20E-02	2.40E-03	0.191	0.008	0.017	0.99
Severity	Cuatro Cañadas	1.60E-03	5.10E-04	0.213	0.012	0.025	0.95
	Okinawa 1	1.50E-02	4.70E-03	0.190	0.016	0.052	0.88
	Okinawa 2	8.40E-05	6.70E-05	0.349	0.031	0.020	0.94
		Monomolecular					
Incidence	Cuatro Cañadas	-5.93E-01	2.44E-01	0.030	0.005	0.380	0.72
	Okinawa 1	-1.21E-01	4.84E-02	0.080	0.006	0.011	0.87
	Okinawa 2	-2.44E-01	8.87E-02	0.105	0.016	2.556	0.88
Severity	Cuatro Cañadas	-5.35E-01	1.98E-01	0.020	0.003	0.120	0.76
	Okinawa 1	-2.59E-01	7.30E-02	0.047	0.007	0.010	0.78
	Okinawa 2	-1.06E-01	3.94E-02	0.023	0.004	0.016	0.63
		Logistic					
Incidence	Cuatro Cañadas	1.90E-03	8.20E-04	0.307	0.021	0.003	0.98
	Okinawa 1	7.55E-02	2.00E-02	0.220	0.025	0.011	0.87
	Okinawa 2	5.50E-04	3.00E-04	0.540	0.047	0.026	0.99
Severity	Cuatro Cañadas	1.90E-04	6.70E-05	0.331	0.014	0.011	0.98
	Okinawa 1	5.90E-03	1.90E-03	0.285	0.018	0.041	0.90
	Okinawa 2	3.90E-08	8.60E-08	0.695	0.091	0.021	0.93
		Gompertz					
Incidence	Cuatro Cañadas	8.80E-25	1.44E-23	0.220	0.015	0.003	0.98
	Okinawa 1	2.48E-02	1.56E-02	0.153	0.015	0.010	0.89
	Okinawa 2	2.63E-45	1.28E-43	0.348	0.055	0.002	0.99
Severity	Cuatro Cañadas	2.49E-43	5.86E-42	0.194	0.010	0.013	0.97
	Okinawa 1	2.30E-05	3.20E-05	0.151	0.009	0.034	0.92
	Okinawa 2	1.90E-05	6.50E-05	0.113	0.016	0.065	0.80

[a] y_0 = initial level of incidence or severity, se(y_0) = standard error of y_0, $r_\bullet$ = rate parameter for the exponential (r_E), monomolecular (r_M), logistic (r_L), and Gompertz (r_G) models, se($r_\bullet$) = standard error of $r_\bullet$, MSE = estimated mean squared error is the average squared difference between estimated and actual incidence or severity values, and R^2 = percent variability in blast intensity explained by the estimated model over the variability explained by a mean model.

Table 4.3. Summary of the wheat spike blast severity dataset collected from fields in Cuatro Cañadas (CC), Okinawa 1 (OK1), and Okinawa 2 (OK2) near Santa Cruz de la Sierra, Bolivia in 2015 in terms of the total number of samples collected, and samples classified as events or censored

					Survival/Failure[b]		
Severity[a]	Location	Samples	Event	Censored	7	14	21
10%	Cuatro Cañadas	395	318	77	0.99/0.01	0.98/0.02	0.27/0.73
	Okinawa 1	585	585	0	0.83/0.17	0.15/0.85	0.00/1.00
	Okinawa 2	161	28	133	1.00/0.00	0.99/0.01	0.83/0.17
	Total	1141	931	210			
15%	Cuatro Cañadas	395	224	171	1.00/0.00	0.99/0.01	0.54/0.46
	Okinawa 1	593	592	1	0.93/0.07	0.29/0.71	0.00/1.00
	Okinawa 2	161	16	145	1.00/0.00	0.99/0.01	0.90/0.10
	Total	1149	832	317			
20%	Cuatro Cañadas	395	129	266	1.00/0.00	0.99/0.01	0.72/0.28
	Okinawa 1	593	587	6	0.94/0.06	0.45/0.55	0.02/0.98
	Okinawa 2	161	7	154	1.00/0.00	0.99/0.01	0.96/0.04
	Total	1149	723	426			

[b]Mean spike blast severity (mean proportion of diseased spikelets per spike) at 21 days after full head emergence (Feekes 10.5) at and above which a sample (a set of at least 15 spikes per sample site within a field/location) was classified as an event. Samples with mean severity below the cutoff levels at 21 days after Feekes 10.5 were considered censored for time-to-event analysis.

[b]Probabilities of surviving (Survival) and failing to survive (Failure) at 7, 14 and 21 days after Feekes 10.5. In other words, these are the estimated probabilities of not reaching (Survival) or reaching (Failure) 10, 15, or 20% severity at 7, 14, and 21 days after Feekes 10.5.

Table 4.4. Summary statistics from log-rank tests of the null hypotheses of no difference in survivor function between pairs of locations and no effect of leaf blast severity on spike blast survivor function at each location[a]

	Location effect[b]		Leaf blast severity effect[c]				
SEV	Comparison	*P* Value	Location	Test statistic	SE	χ^2	*P* Value
10%	CC vs OK1	<0.001	CC	-0.48	4.39	0.01	0.913
	CC vs OK2	0.048	OK1	-70.44	5.07	193.20	<0.001
	OK1 vs OK2	<0.001	OK2	-2.62	1.12	5.47	0.019
15%	CC vs OK1	<0.001	CC	-0.69	3.68	0.04	0.851
	CC vs OK2	0.452	OK1	-75.44	5.02	225.90	<0.001
	OK1 vs OK2	<0.001	OK2	-0.41	0.84	0.23	0.630
20%	CC vs OK1	<0.001	CC	-0.33	2.79	0.01	0.906
	CC vs OK2	<0.001	OK1	-76.96	4.96	240.50	<0.001
	OK1 vs OK2	<0.001	OK2	-0.53	0.56	0.89	0.345

[a]SEV = mean spike blast severity (mean proportion of diseased spikelets per spike) at 21 days after full head emergence (Feekes 10.5) used as the threshold/event for time-to-event analysis; CC, OK1, and OK2 are Cuatro Cañadas, Okinawa 1, and Okinawa 2, respectively, the three levels of the categorical variable field location.

[b]Pairwise comparison of survivor function and level of significance (*P* value) adjusted for multiple comparison usning the Tukey-Kramer method.

[c]Logrank test statistic, standard error (SE), chi-square value (χ^2), and level of significance (*P* value) from tests of the null hypothesis that leaf blast severity at 21 days after Feekes 10.5 is unrelated to spike blast survival time.

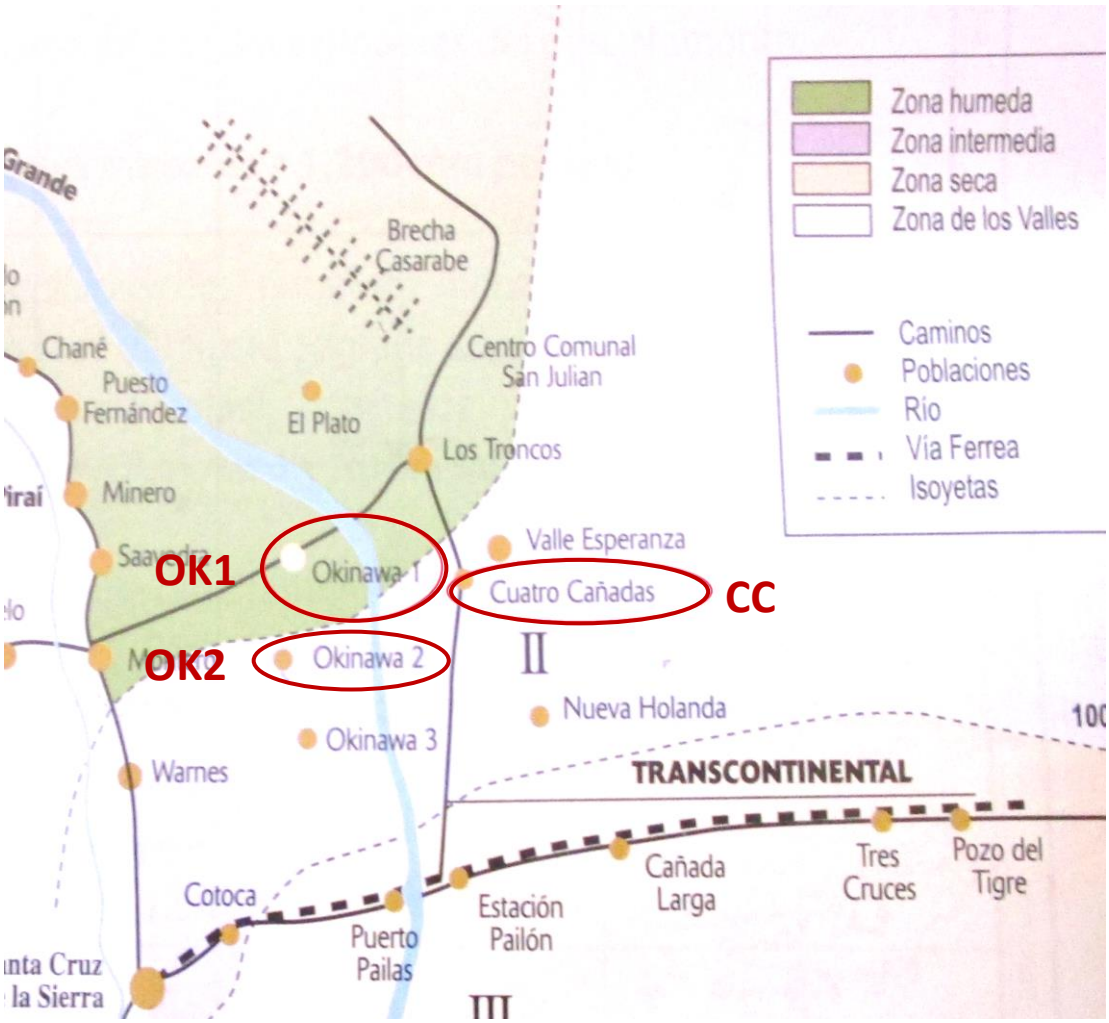

Fig. 4.1. Map of wheat production zones in Santa Cruz de la Sierra, Bolivia, according to rain levels. The three locations for this research were Okinawa 1 (OK1), Okinawa 2 (OK2), and Cuatro Cañadas (CC) (ANAPO publication, 2015).

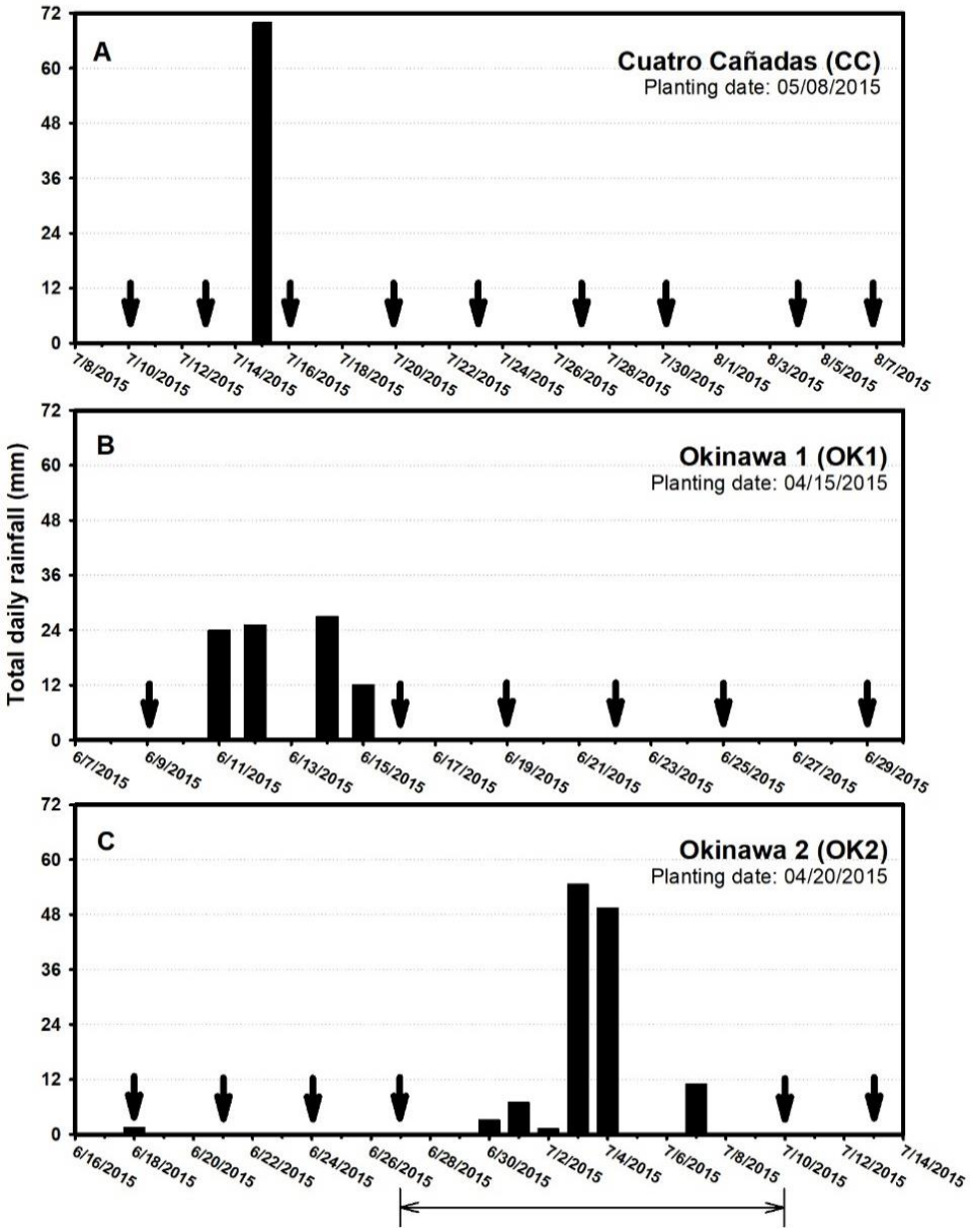

Fig. 4.2. Total daily rainfall between wheat heading (Feekes growth stage 10.5) and final wheat blast assessment in research plots at Cuatro Cañadas (S 17°26.48, W 62°35.91), Okinawa 1 (S 17°14.55, W 62°53.35), and Okinawa 2 (S 17°20.41, W 62°52.60) near Santa Cruz de la Sierra, Bolivia. Arrows indicate disease assessment dates, with the first being at Feekes 10.5. The horizontal bar shows the period during which heavy rainfall and flooding prevented access to plots at Okinawa 2

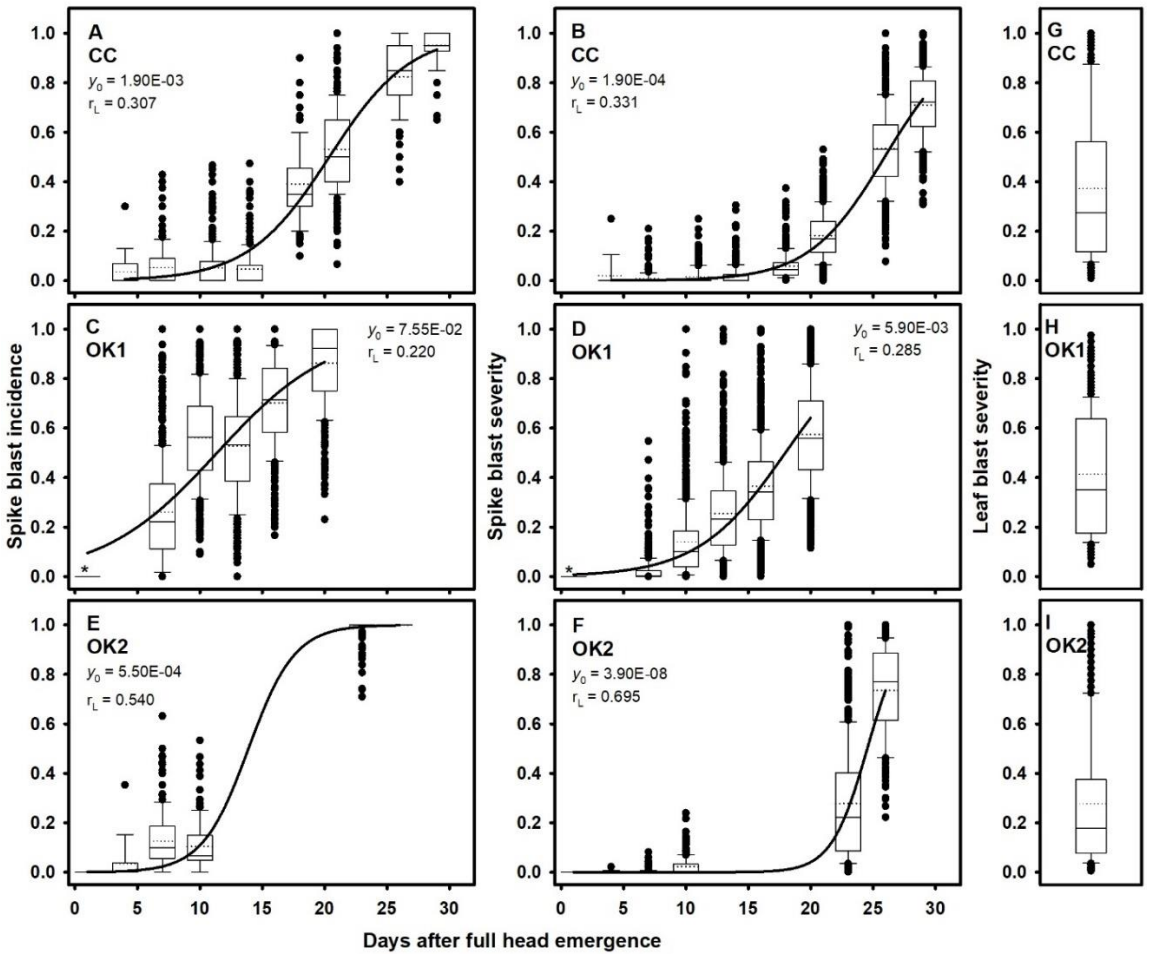

Fig. 4.3. Box plots showing the distribution of, and temporal change in, mean wheat spike blast incidence (**A**, **C**, and **E**, proportion of diseased spike in a sample of at least 15 spikes) and severity (**B**, **D**, and **F,** mean proportion of bleached, discolored spikelets per spike) in naturally infected wheat fields at Cuatro Cañadas (CC; S 17°26.48, W 62°35.91), Okinawa 1 (OK1; S 17°14.55, W 62°53.35), and Okinawa 2 (OK2; S 17°20.41, W 62°52.60) near Santa Cruz de la Sierra, Bolivia. **G**, **H** and **I** show the distribution of mean leaf blast severity on the flag leaf at 21, 20, and 23 days after full head emergence (Feekes growth stage 10.5) at CC, OK1, and OK2, respectively. Broken and solid lines within each box represent means and medians, respectively, while the top and bottom lines of the box represent the 75th and 25th percentiles of the data, respectively. Vertical bars extending above and below the boxes represent the 5th and 95th percentiles, while symbols represent outliers. Progress curves are for estimated predicted incidence and severity from the fit of the logistic population growth models to the means of the distributions at each assessment time following Feekes 10.5. Parameters are in Table 2. *Since the initial level of disease was extremely low at the time of the first assessment at OK1, mean intensity was estimated based on visual inspections of the plots instead or assessments of individual spikes.

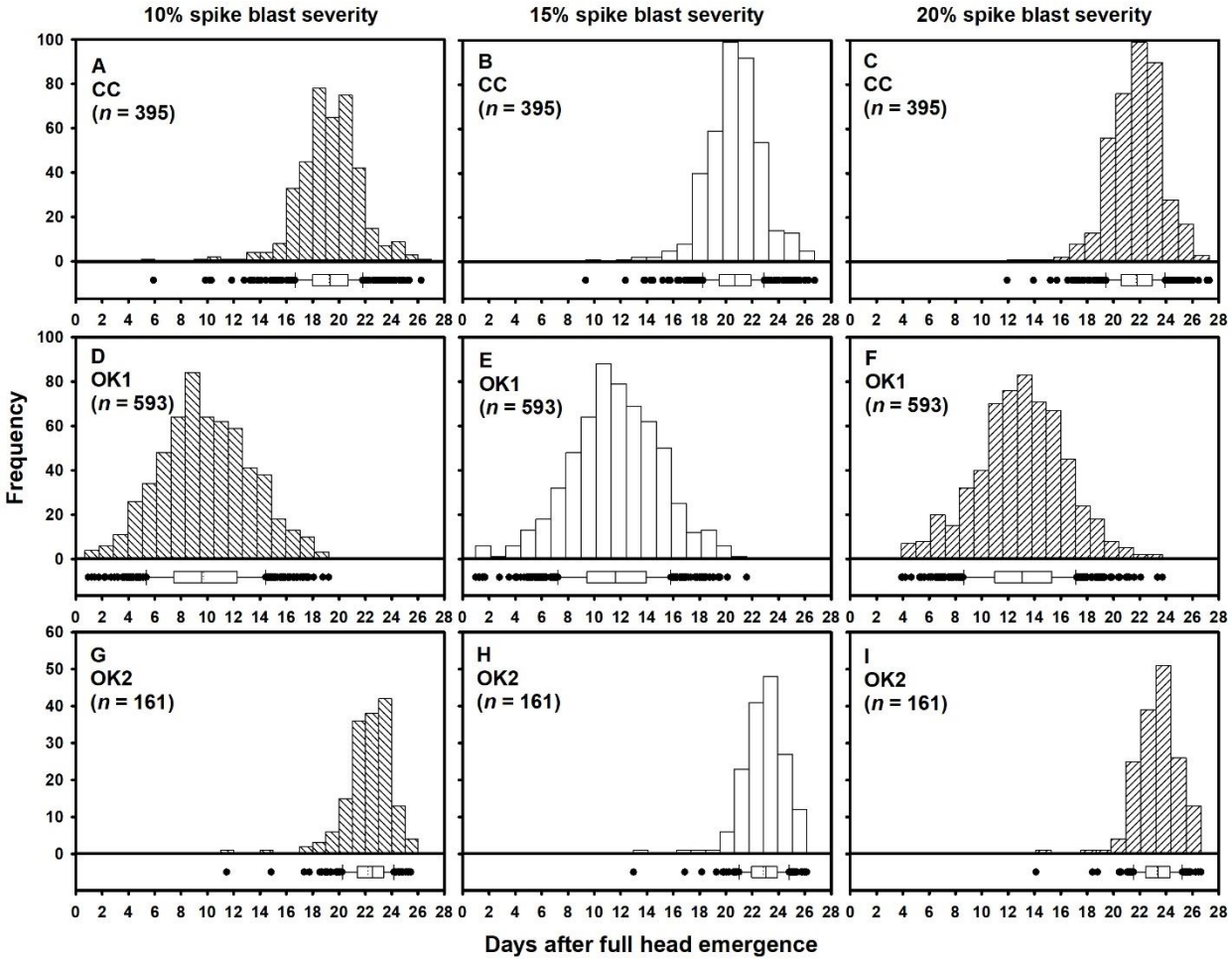

Fig. 4.4. Histograms and box plots showing the distribution of time (days after Feekes growth state 10.5, full head emergence) to at least 10 (**A**, **D**, and **G**), 15 (**B**, **E**, and **H**), and 20% (**C**, **F**, and **I**) wheat blast severity (mean proportion of bleached, discolored spikelets per spike) estimated with equation 3 using parameters from the fit of logistic population growth models to data collected from naturally infected wheat fields at Cuatro Cañadas (CC; S 17°26.48, W 62°35.91), Okinawa 1 (OK1; S 17°14.55, W 62°53.35), and Okinawa 2 (OK2; S 17°20.41, W 62°52.60) near Santa Cruz de la Sierra, Bolivia. Broken and solid lines within each boxplot represent means and medians, respectively, while the left and right edges of the box represent the 25th and 75th percentiles of the data, respectively. Whiskers extending beyond the boxes represent the 5th and 95th percentiles, whereas circles represent outliers.

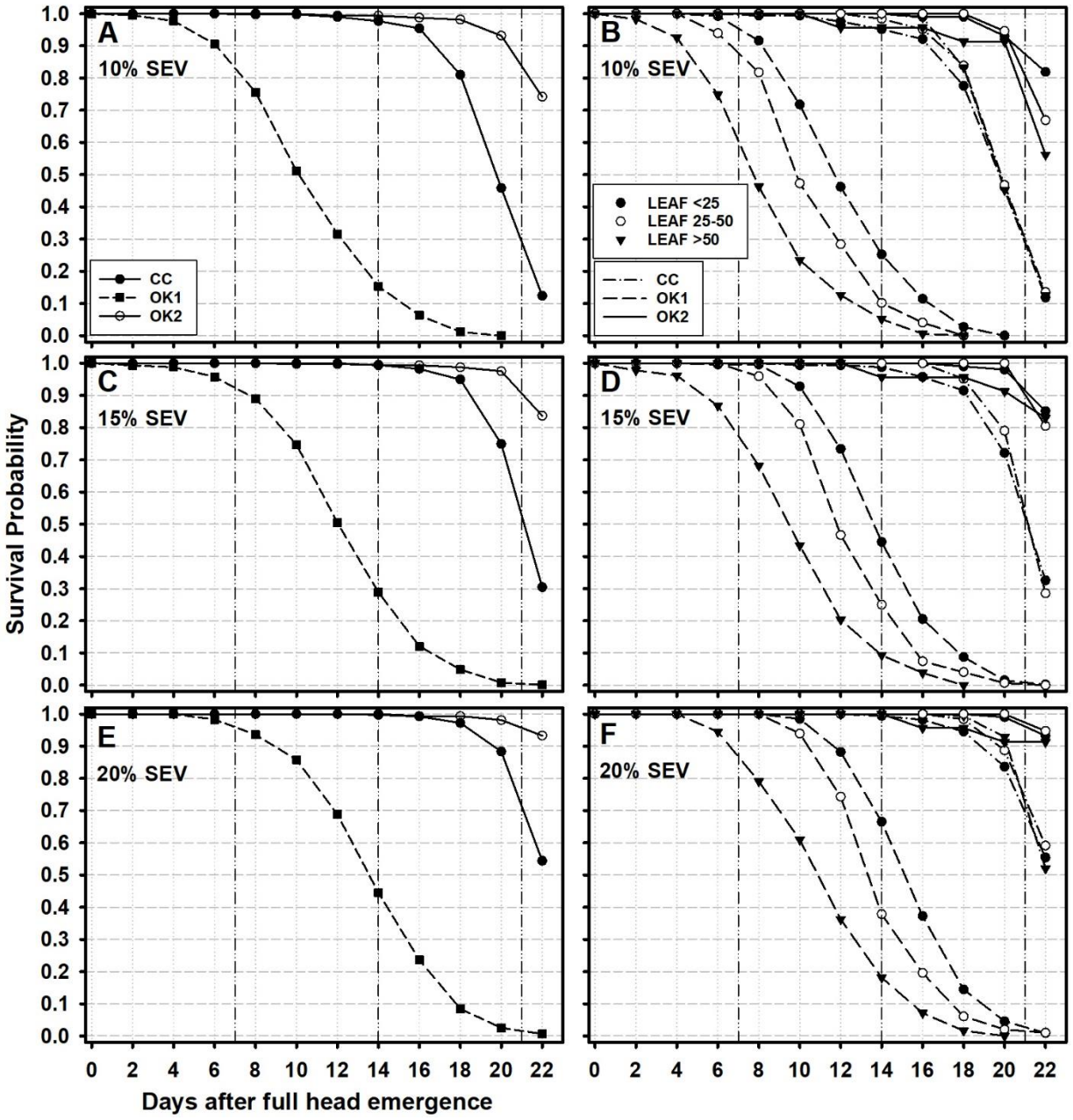

Fig. 4.5. Survival curves for time to at least 10 (**A** and **B**), 15 (**C** and **D**), or 20 (**C** and **D**) percent wheat spike blast severity (SEV, mean proportion of bleached, discolored spikelets por spike) for naturally infected wheat fields in Cuatro Cañadas (CC; S 17°26.48, W 62°35.91), Okinawa 1 (OK1; S 17°14.55, W 62°53.35), and Okinawa 2 OK2; S 17°20.41, W 62°52.60) near Santa Cruz de la Sierra, Bolivia,

continued

Fig. 4.5. Continued.

and for leaf blast severity (LEAF; percent flag leaf area diseased at 21 day after Feekes 10.5) categories (LEAF < 25%, 25 ≤ LEAF < 50%, and 50% ≤ LEAF) at each location. For the purpose of these analyses, an event was considered to have occurred if the specific level of spike blast severity (10, 15, or 20%) was reached or exceeded at 21 days after full head emergence (Feekes 10.5). Lines represent estimated probabilities of the event not occurring; in survival analysis terms, this would be equivalent to the probability of "surviving" the event.

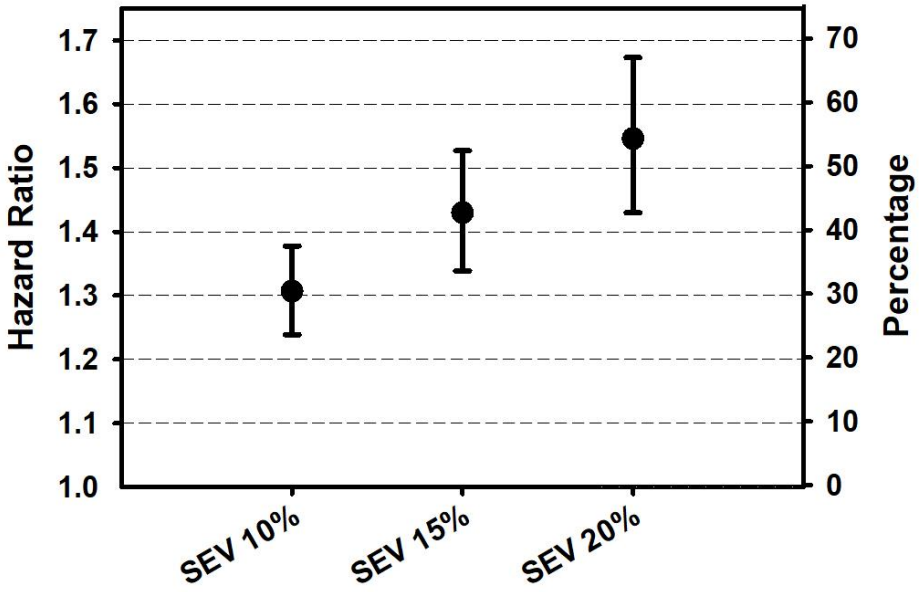

Fig. 4.6. Hazard ratios from Cox nonproportional hazard regression analyses of associations between wheat leaf blast severity (mean percent flag leaf area diseased at 21 days after Feekes 10.5) and time to 10, 15 and 20% spike blast severity (SEV, mean proportion of bleached, discolored spikelets per spike).

Chapter 5:
Spatial Aggregation of Wheat Blast Developing in Bolivia During a Natural Epidemic

ABSTRACT

A spatial pattern analysis of foliar and spike disease intensity was conducted for a natural epidemic of wheat blast (caused by the Triticum pathotype of *Magnaporthe oryzae* [MoT]) which occurred in 2015 in Santa Cruz de la Sierra, Bolivia. The highly susceptible cultivar Atlax was planted in research fields at three locations, Okinawa 1 (OK1 on 15 April), Okinawa 2 (OK2 on 20 April), and Cuatro Cañadas (CC on 8 May), and disease was assessed throughout the epidemics in up to six plots per location. Disease assessments quantified spike blast incidence (INC, the proportion of diseased spikes in a sample), spike blast severity (SEV, the mean proportion of diseased spikelets in a sample), and leaf severity (LEAF, the mean proportion of disease on flag leaves). At each rating time (6 for OK1 and OK2, 9 for CC), Moran's *I* spatial autocorrelation coefficient was calculated for the logit transformation of each disease variable (INC, SEV, LEAF), and significance was determined using the standard normal statistic (*Z*). Significant *I* values indicated that the

disease intensity values in neighboring disease sampling nodes were more likely to be similar than disease values at greater distances. A nonsignificant *I* indicates that the pattern is indistinguishable from random.

The fit of a general linear mixed model indicated that rating time, disease response variable (SEV, INC, LEAF) and location, and their interactions had significant effects on *I.* The least squares means were higher for OK1 (0.31), the earliest planted field, than for OK2 (0.14) and CC (0.07). At the hierarchical scale of location, mean *I* was higher for LEAF (0.25) than for SEV (0.16) and INC (0.10). Interaction means confirmed that CC had the lowest means or equal to the lowest means for all disease measurements (0.04–0.12), and that the highest means were for LEAF at OK1 (0.39) and OK2 (0.25), and SEV at OK1 (0.32). At the earliest-planted location, OK1, 95% of the *I* values were significant, while in OK2, 66% were significant, and in the latest-planted location, CC, only 42% were significant. There was no overall trend in *I* with rating time or level of disease within plots, and the interaction means indicated that rating time had only minor impact on the differences in *I* between disease measurements and locations. Although non-random spatial aggregation was more common in the earlier plantings, final disease levels for INC, SEV, and LEAF were lowest at OK1 (86, 57, 37%) than at OK2 (100, 72, 53%) and CC (95, 71, 87%). Leaf lesions developed before spike emergence and sporulated during the wheat growing season, potentially leading to infections of spikes and secondary infections of leaves, the latter being characterized by increased aggregation of disease.

INTRODUCTION

Wheat production in South America has been deeply affected by epidemics of wheat blast during years with weather conditions conducive for disease development , such as those with high temperatures and high relative humidity when complete yield loss have been reported in some regions (Cruz and Valent 2017, Urashima et al. 2009). In 2016 and 2017, wheat blast emerged in Bangladesh, India, and Zambia (Islam et al. 2020; Mottaleb et al. 2019; Tembo et al. 2020; Yesmin et al. 2020), increasing the threat to global wheat production. The causal agent of this disease is the Triticum pathotype of the fungus *Magnaporthe oryzae* (MoT). *M. oryzae* is a significant fungal pathogen on other crops such as rice, where the Oryzae pathotype causes rice blast, and perennial ryegrass, where the Lollium pathotype causes gray leaf spot (GLS). Both rice blast and GLS are polycyclic diseases where lesions from infected tissues produce ascospores that spread to healthy plants that then become infected and continue spreading the disease throughout the growing season (Chiang and Huang 2005; Suriya Rao et al. 2007; Uddin et al. 2003). There are currently debates about whether wheat blast is also a polycyclic disease, like others caused by *M. oryzae* pathotypes, or if it is a monocyclic disease (when pathogens only produce one cycle of disease in a season) (Cruz and Valent 2017).

Wheat leaves and spikes can both be infected during a wheat blast epidemic, although the disease on the spikes is more economically significant (Igarashi 1990; Kohli et al. 2011; Rios et al. 2013). The emergence of wheat spikes is inherently asynchronous, and depending on the growing conditions, tillering habit of the cultivar, and crop production practices, spike-bearing tillers may develop over the course of several weeks

(Cruz and Valent 2017; Mills et al. 2021; Chapter 4). In addition, at the field level, variations in topography and edaphoclimatic conditions lead to spatial variation in spike emergence. Due to this spatio-temporal variation in crop development, and consequently, favorable growth stages for infection (Chapter 4 of this dissertation), there are multiple times when spikes can become infected in a production field, creating an opportunity for MoT to go through several clonal generations or spores to be blown in from external sources that can infect spikes throughout one season, leading to temporal and spatial variation in spike blast development and intensity.

There is increasing evidence supporting the idea that wheat blast may be a polycyclic epidemic. Blast lesions that develop on leaves can sporulate prior to and during spike emergence, and under laboratory conditions, these foliar spores have been shown to infect wheat spikes (Cruz et al. 2015). Temporal analyses of wheat blast development under both natural and laboratory conditions revealed that disease progress was appropriately described by logistic and Gompertz growth models, which are generally used to describe polycyclic epidemics (Gongora-Canul et al. 2020; Mills et al. 2020 and 2021; Chapters 3 and 4 in this dissertation). Spatial analyses of the pattern and spread of wheat blast during a season are important both for incorporating pattens into models, as well as for understanding the mechanics of disease spread within a field (Madden et al. 1988 and 2007; Ristaino and Gumpertz 2000; Yesmin et al. 2020) and for gaining insight as the source of inoculum for blast development, a major knowledge gap in epidemiology of this disease. Ultimately, understanding the spatio-temporal progress of wheat blast will help elucidate

the epidemiology of the disease and be useful for management of the disease before and during the growing season.

Geo-spatial analyses on the development of rice blast have been conducted at several spatial scales, from within-field to regional levels, and even country-wide in China (Chiang and Huang 2005; Guo et al. 2016; Suriya Rao et al. 2007). Wheat blast disease intensity has been reported at both field and regional levels in South America and South Asia, but no explicit spatial pattern analysis research has been published. In fact, there are very few studies that analyze the spatio-temporal development of wheat blast under natural conditions at the field level (Cruz et al. 2015; Mills et al. 2021; Chapter 3). However, despite the limited research on the spatial progress of wheat blast, there is anecdotal evidence from observations made by wheat farmers and seed companies, as well as my own experience, in Bolivia that wheat blast likely spreads from clusters of plants with severely diseased and sporulating leaves (hotspots) in a field both before and after spikes emerge (CAICO, *personal communication* 2015). There are additional anecdotes that some wheat fields that have no foliar lesions will develop a sudden, synchronous spike blast throughout the field (Cruz and Valent 2017; CAICO *personal communication* 2015; Igarashi et al. 1986), leading to the conclusion that in-field hotspots may not be the only or primary source of inoculum for wheat blast epidemics.

The presence of hotspots would be associated with significant clustering instead of a uniform, synchronized development of diseased plants in fields or plots, which can be quantified with a range of spatial statistics (Chellemi et al. 1987; Cliff and Ord 1970; Moran 1950; Madden et al. 2007; Reynolds et al. 1987). Fields that are intensively mapped, where

locations and disease status of plants are known and recorded, are often evaluated using cross-product statistics such as spatial autocorrelation, spatial semi-variograms, or SADIE (Spatial Analysis by Distance Indices) (Madden et al. 2007; Nicot et al. 1984; Reynolds et al. 1987). Moran's *I* is one version of a spatial autocorrelation coefficient that is especially well-suited for characterizing clustering or aggregation of random variables (Cliff and Ord 1970). Other types of spatial analyses are possible for sparsely sampled fields when disease is measured by incidence (Madden et al. 2007). Spatial analyses have been conducted for both sparsely sampled and intensively sample rice fields with rice blast (Guo et al. 2016; Suriya Rao et al. 2007; Chiang and Huang 2005). Similar studies for wheat blast are crucial to better understand the epidemiology of the disease.

The objectives of this study were to: 1) characterize the spatial pattern of wheat blast measured as spike severity, spike incidence, and leaf severity, and determine if there is significant clustering or aggregation; 2) determine if there are temporal trends of aggregation; and 3) ascertain if there are different trends in aggregation among the three disease response variables.

MATERIALS AND METHODS

Field trial location, plot establishment and management. A natural wheat blast epidemic occurred in Bolivia during the fall and winter of 2015 (Mills et al. 2021). Three field locations with historically different microclimates, two of which previously had wheat blast at high levels in 2013 (C. D. Cruz, *personal communication*), were chosen from the

agricultural region north of Santa Cruz de la Sierra, Bolivia. These locations were Okinawa 1 (OK1; S 17°14.55, W 62°53.35), Okinawa 2 (OK2; S 17°20.41, W 62°52.60), and Cuatro Cañadas (CC; S 17°26.48, W 62°35.91). CC was characterized as being dryer and less humid than OK1 and OK2 (Barea and Aguanta 2012). A strong El Niño-Southern Oscillation event, similar to one in 2013 which was associated with devastating levels of wheat blast (Cruz and Valent 2016), was anticipated to hit this region in Bolivia during the 2015 growing season, potentially creating highly favorable conditions for natural wheat blast development (Kohli et al. 2011). Hourly temperature and relative humidity, recorded using weatherproof data loggers (HOBO Pro-V2, Onset, Cape Cod, MA) attached to a stake at the approximate height of a wheat spike in the center of the plots at each location, were compared with the measurements from the Santa Cruz International Airport weather station. Due to the intensity of the weather conditions associated with El Niño, the expected environmental variation among the locations was not very pronounced during this growing season, and some of the storm events restricted field sampling.

Wheat planted early in the season Santa Cruz de la Sierra region of Bolivia has been observed to be more severely affected by blast infections (de Oliveira Coelho et al. 2016), so our experimental plots were planted between mid-April to early May to increase the opportunity for natural infections to become established in our plots (OK1 planted on 15 April; OK2 on 20 April; CC on 8 May). Details are given in Mills et al. (2021; Chapter 2), and only a summary of the agronomic methods are given here. Plots were planted and managed by collaborators from the Asociación de Productores de Oleaginosas y Trigo (ANAPO) Agricultural Cooperative. Each location was planted with the susceptible

cultivar Atlax (CAICO, Santa Cruz de la Sierra, Bolivia) in six 27 x 27-m plots, with a 2-m border of sorghum between and on the edges of the plots. Row spacing was 20 cm, seeding rate was 80 seeds/m, and a single line of six plots was planted east to west in both OK1 and OK2, and six plots in a 2 x 3 arrangement were planted at CC. Agronomic practices for commercial wheat production in Bolivia, including weed management, fertilizer applications, and other recommendations were carried out by our local CAICO collaborators (ANAPO 2015).

Disease quantification. Primary spikes from the cultivar Atlax emerged asynchronously over approximately 10 to 14 days in Bolivia, with tiller spikes continuing to emerge after primary tillers reached Feekes Growth Stage 10.5.4 (watery ripe grain fill). Sampling, therefore, was limited to measuring disease severity on the primary tillers to reduce the effect of different growth stages on disease development at each rating. Each 27 x 27-m plot was split into a 10 x 10 grid with nodes (sampling locations) approximately 2.55 m apart. Disease assessments were made at each of the 100 nodes, where a handful of spikes (interquartile range of 14 to 20 spikes, average of 17 spikes per "handful") were individually rated for disease severity. Spike disease severity (SEV) was estimated as the amount of visibly diseased (bleached) tissue on the spike as a proportion of the total spike tissue. Disease incidence (INC) was calculated at each node in the plot as the proportion of spikes with any disease symptoms divided by the total number of spikes in the sample. Severity of blast symptoms on the flag leaves, referred to here as leaf severity (LEAF), was visually estimated as the average proportion of symptomatic tissue on four flag leaves at each node.

Spike emergence occurred first at OK1 (9 June), then OK2 (18 June), and finally at CC (16 July). Leaf ratings began on 18 June, so only the last three assessments at OK1 included both spike and leaf ratings, while all assessments at OK2 and CC included leaf ratings (Table 5.1.) Plots were rated every 3 to 4 days starting around initial spike emergence, weather permitting, and ending when the primary tillers reached Feekes growth stage 11.2 (soft dough). Wheat tissue at Feekes 11.2 begins to senesce and visual assessments of bleached spikelets are less reliable, although dark lesions characteristic of blast infection are still visible. The length of time between spike emergence and Feekes 11.2 varied among locations, so a different number of spike assessments were made across the locations (OK1 had 5 ratings, OK2 had 6, and CC had 7 ratings for spikes, and 9 ratings for leaf assessments). There was a big storm between June 28 and July 9 prevented three potential assessments from being made at OK2 because the field was inaccessible, and only two of the plots were included in the final assessment (see Chapter 2 for details). In addition, due to time constraints, only four of the six plots at CC were assessed throughout the epidemic. The total number of spike assessments (nodes x plots x number of assessments) varied by location, from 3,000 nodes (49,231 spikes) at OK1 (100 nodes x 4 plots x 5 ratings), 3,100 nodes (32,690 spikes) at OK2 (100 nodes x 2 to 6 plots x 6 ratings), and 3,600 nodes (46,027 spikes) at CC (100 nodes x 4 plots x 9 ratings) (Table 5.1.).

Data analysis. *Selection of data for spatiotemporal analyses.* To measure the spatial pattern of wheat blast over time on the 100-node lattices, there were minimum requirements for a node and/or a plot to be included in each assessment. A minimum of 8 spikes needed to be observed at a node for the data from that node to be included in the

plot, and the majority of the nodes (50 or more) needed to qualify with the 8-spike minimum for a plot to be included in SEV and INC analyses. Therefore, at early assessments some plots only qualified for LEAF analyses since not enough spikes had emerged across the plot, and at some later assessments, plots were disqualified because they lost too many nodes to lodging (that resulted from high levels of wheat blast, senescence, or other causes) or disease levels approached 100% disease . The plots that qualified for analyses at each location and rating are given in Table 5.1., with the total number of spikes included in each analysis.

Spatial analysis. In order to determine the degree of aggregation or clustering of the disease response variables (INC, SEV, LEAF), and to test whether disease was clustered or random in each plot, spatial analyses (Madden et al. 2007) were conducted using the VARIOGRAM procedure of SAS (SAS Institute, Cary, NC, U.S.A.). The SEV, INC, and LEAF values were logit-transformed prior to analyses. For instance, the logit of SEV is given by:

$$\text{logit}(\text{SEV}) = \ln\left(\frac{\text{SEV}}{1-\text{SEV}}\right) \quad (1)$$

Logits were used to approximately stabilize variances for different levels of disease and to provide a linear scale for the relation between transformed disease and its neighbors.

The SAS VARIOGRAM procedure was used to calculate the distribution of the distances between all possible pairs of points in the 27 x 27-m (100 x 100 node) data matrix for each rating time in each plot. The histogram showing the distribution of the pairwise

distances between nodes for each spatial lag class was used to select the lag distance (*lagd*) for spatial analyses. A *lagd* of 3.94 m was chosen because it defines nearest neighbors of a node as all the immediately adjacent nodes (within a row, column, or the diagonal). Moran's *I* spatial auto-correlation coefficient (Cochran 1936; Madden 1988; Madden et al. 2007; Moran 1950) was calculated for each combination of location x plot x rating x response variable as

$$I = \frac{n}{S_0} \frac{\sum_i \sum_j w_{ij}(x_i - \bar{x})(x_j - \bar{x})}{\sum_i (x_i - \bar{x})^2} \quad (2a)$$

in which i and j ($i \neq j$) are indices for locations in the plot, x_i and x_j are the response variable (SEV, INC, or LEAF on logit scale) at locations i and j, $\bar{x}$ is the mean of the response for the plot, n is the number of observations, w_{ij} is a weight for each i and j pair of locations, and S_0 is a scaling factor based on the sum of the weights (Madden et al. 2007; Reynolds et al. 1987). We used binary weights, where $w_{ij} = 1$ if the i and j pair were neighbors (less than 3.94 m away), and $w_{ij} = 0$ otherwise. Positive values of *I*, which is a type of weighted correlation coefficient, indicate clustering of disease (association of high values near high values, low values near low values, and so on), and values near 0 indicate a random pattern.

Observed Moran's *I* (eq. 2a) is compared to the expected Moran's *I* (equation 2b) under the null hypothesis of no spatial autocorrelation (i.e., complete spatial randomness).

$$E(I) = \frac{-1}{n-1} \quad (2b)$$

The standard deviation of *I* (*s*) under the null hypothesis was calculated using the formula found in *Spatial data analysis by example* (Upton and Fingleton 1985)based on the randomness assumption.

Significance was determined with a standard normal statistic (*Z*):

$$Z = \frac{I - \mathrm{E}(I)}{s} \qquad (2d)$$

One rejects the null hypothesis of random pattern in favor of the alternative of a clustered or aggravated spatial pattern if $|Z| \geq 1.96$.

Moran's *I* can be visualized graphically to show the relationship between each observation and its neighbors. This is done with a plot of standardized values of *x* (*x**; centered at 0 with a standard deviation of 1) versus the weighted (see w_{ij} above) average of neighbors (those less than *lagd* away). The regression slope of this line is strongly related to *I* and would exactly equal *I* if a slightly different set of weights ("row averaged") was used. Fig. 5.1. shows an example two Moran scatterplots for Cuatro Canadas, Plot 1, Rating 6. In the top image which shows the standardized SEV observations, the *I* value is -0.018 which is not significant, and there is no evidence of aggregation to neighboring values. In the bottom image which shows the standardized LEAF observations, however, there is a significantly positive (*p* value <0.001) slope to the regression line through the points and the *I* value is 0.259 indicating clustered or aggregated spatial pattern.

The distributions of Moran's *I* values were plotted in a box and whisker plot for each location and assessment type (INC, SEV, LEAF) to show the range of spatial autocorrelations that were achieved. The box plots were overlayed by violin plots (Blumenschein et al. 2020) which show the distribution of the *I* values and display peaks at certain Moran's *I* values where a relatively high frequency of values was found. Contour plots of the logit-transformed disease variables were plotted using the SGRENDER procedure of SAS with the ContourPlotParm template to visualize the patterns of disease and their associated *I* values. To observe the changes in spatial autocorrelation over time, individual Moran's *I* values, and the *I* averages across plots were plotted versus rating time. Mean logit values for SEV, INC, and LEAF for each plot, rating, and location were plotted against the observed *I* values. The differences in Moran's *I* values between logit-transformed INC and SEV, INC and LEAF, and SEV and LEAF were also plotted against the ratings to help identify if differences in magnitude of aggregation emerged between measures of disease or across time. The distribution of these differences in *I* values for assessment types were plotted as box plots.

The effects of location (*Loc*), rating time (*Rat*), disease response variable (*Dis*), and their interactions on the estimated Moran's *I* was quantified using a linear mixed model (Stroup et al. 2018). The following mixed model was fitted to the entire data set across three locations (k=1,2,3), multiple rating times (l=1, …; depending on the location and disease variable), three disease response variables (q=1,2,3; logits of SEV, INC, and LEAF); and plots within locations (*Plot*(*Loc*); l=1,…,6).

$$I_{klmq} = Loc_k + Plot(Loc)_{kl} + Rat_m + (Area \cdot Rat)_{km} + Rat \cdot Plot(Loc)_{klm} + Dis_q + (Loc \cdot Dis)_{kq} + (Rat \cdot Dis)_{mq} + (Loc \cdot Rat \cdot Dis)_{kmq} + Dis \cdot Plot(Loc)_{klq} + E_{klmq} \quad (3)$$

All terms involving plot and its interactions are random effects and other terms are considered fixed effects in the model. The E_{klmq} term is the residual, equivalent to *Loc*·*Rat*·*Var*·*Plot*(*Loc*). The *Plot*(*Loc*) random effects term (with a variance of $\sigma^2_{Plot(Loc)}$) represents the variation among plots within the three locations and also accounts for serial correlation of *I* values within plots. To accommodate the possible correlation structure for *I* within plots based on the three different disease response variables, the residual, *Dis*·*Plot*(*Loc*), and *Rat*·*Plot*(*Loc*) terms were combined into a row vector $\mathbf{D}_{klmq}$ with unstructured variance-covariance matrix of **Σ**. A Cholesky decomposition of **Σ** was used in model fitting to avoid ill-conditioned matrices (Madden et al. 2016).

Equation 3 was fitted using restricted maximum likelihood using the GLIMMIX procedure in SAS. Type 3 Wald *F* tests were used to test for significance of fixed effects. When a main effect or interaction was significant, least-squares means (LSMEANS) were compared using t-tests, with standard errors based on the variance and covariance parameters estimated for the mixed models (Stroup et al. 2018).

To determine if intensity of disease rather than rating time affected spatial aggregation, mean disease intensity per plot (logit scale) was substituted for Rating fixed effect (main effect and interactions) in equation 3. Rating was maintained in the model for all random effects to account for the variability of the sampling units. Also, disease intensity was considered a continuous variable rather than a factor in this latter analysis.

RESULTS

Disease development. Ratings began at each location weeks apart from each other, with OK1 rated from 9 to 29 June, OK2 from 18 June to 13 July, and CC from 10 July to 7 August (Table 5.1.). Although assessments generally occurred every three to four days, some assessment times were missed primarily due to weather events. In OK1, leaf ratings did not begin until the fourth rating (22 June) and were only observed for the final week of the epidemic. For both OK2 and CC, leaf ratings began before spike emergence, and were collected for the full duration of the epidemic.

Initial spike count was patchy across plots since emergence was asynchronous and occurred over approximately 10-14 days for primary tillers, and spikes on secondary tillers continued to emerge when primary tillers were in grain fill (Mills, Chapter 3). Since plots were only included in spatial analyses if 50 or more nodes had 8 or more spikes at an assessment time, some plots were eligible for spatial analysis sooner than others. For example, in OK2, at the first rating, the number of nodes with more than 7 spikes ranged from 2 to 27 in the six plots. By the second rating, this range increased to 16 to 34 nodes, and by the third rating all the plots were eligible to be included in the spatial analysis with a range of 63 to 83 nodes included in a plot. In OK1, all plots were eligible for inclusion from the second rating through the sixth rating, with a minimum of 88 eligible nodes and an average of 99 nodes included per plot. In CC, only half of the plots were included by the third rating with only 50 and 65 nodes eligible for inclusion. Spikes emerged more

synchronously in CC, and by the fourth rating, all plots were included with an average of 95 nodes per plot.

The number of spikes rated per plot was similar across all three locations with an average of 1,641 spikes rated/plot in OK1, 1,720 spikes/plot in OK2, and 1,770 spikes/plot in CC. The total number of individual spikes assessments that were included in the spatial analyses per location were 49,231 (OK1), 32,690 (OK2), and 46,027 (CC). For LEAF, all 100 nodes were included in every assessment for a total of 1,800 leaf severity assessments at OK1, 3,100 at OK2, and 3,700 at CC.

The temporal analysis of spike blast development at each location, plot, and rating time are evaluated in Mills et al. (2021, Chapter 3), and generally revealed trends of lower overall disease intensity at OK1 (INC 86%, SEV 57%, LEAF 37%), similar spike disease intensity at OK2 and CC (INC: 100% and 95% respectively, SEV: 74% and 71%), and much higher leaf severity at CC than at OK2 (87% vs 53%). Logit-transformed disease was used for all spatial analyses, and average logits for the final rating for INC, SEV, and LEAF were 2.64, 0.41, and -0.59 at OK1; 4.42, 1.24, and 0.32 at OK2; and CC 3.39, 0.98, and 2.48 at CC. Fig. 5.2. shows the average logit-transformed values for each location, plot, and rating. Logistic population growth models were previously fit to the INC and SEV development at each location (Mills et al. 2021, Chapter 3) and the rates for INC and SEV were significantly higher for OK2 than the other locations, while CC had a significantly higher rate for INC than OK1.

Distribution of Moran's I values. The distributions of *I* values for each measure of disease (INC, SEV, LEAF) are shown in Fig. 5.3. where a gray rectangle represents *I* values

that are not statistically significant ($p > 0.05$). Individual *I* values for each location, plot, and disease response variable are listed in Table 5.2.. There was a trend of increasing *I* values from INC to SEV to LEAF for each location, and a trend of higher *I* values at the fields that were planted and assessed earlier (OK1, then OK2, and CC). OK1 had the highest *I* values overall, followed by OK2, then by CC where many of the *I* values fell within the non-significant zone. In OK1, *I* values had a larger interquartile range for each response than at the other locations, but there were fewer outliers in OK1 than in OK2. Except for OK1, *I* values were relatively low, even when significant.

In Table 5.2., all of the individual estimated *I* values are listed for each location, plot, and rating. For the *I* values that were calculated for OK1, 95% of them were significant at ($P < 0.05$), in OK2 66% of the *I* values were significant, and in CC only 42% of them were significant. When this is broken down by disease variable, for OK2 and CC, the percent of *I* values that were significant were 29 and 21% for INC; 47 and 21% for SEV, and 100 and 67% for LEAF These comparisons show that there tended to be more non-random aggregation for all three disease variables at OK1 than at the other locations, and tended to have higher aggregation at OK2 than at CC..

Trends in I vs. time. Within a plot, non-random aggregation may be present for only some ratings and only some disease measurement variables. This trend of sometimes random, sometimes non-random aggregation was particularly common in CC. For example, Fig. 5.4 shows contour maps with in-set *I* values (significant ones at $P < 0.05$ are marked with an asterisk) for plot 3 at CC. In this case, spike assessments were made from ratings 3 through 9, and 13 out of the 21 contour plots show significant non-random

aggregation. In this example plot, there was a general trend of increasing *I* with rating time, and then a decline at the latest ratings when disease intensity was highest.

The individual *I* values are plotted versus rating time for each location in Fig. 5.5. Points that fall within the gray rectangle are not significantly different from random aggregation ($p > 0.05$). These graphs show the *I* values overlap across the plots at each location, but for the LEAF category, individual plots generally separate out for both OK1 and OK2, indicating that some plots at these locations had consistently higher or lower spatial aggregation than others for leaf disease severity. However, for most disease variables and locations, no plots were consistently high or low in terms of aggregation. The mean *I* values across plots are shown in Fig. 5.6 for each rating time. There was little evidence in Figs. 5 and 6 for a consistent increase or decrease in *I* with rating time for most variables and locations. The exceptions were SEV at OK2 (upward trend), LEAF at OK2 (downward trend), and possibly for LEAF at CC (upward followed by downward trend). It is important to note that in the example of rating 6 at OK2, that only two of the plots were rated at this final assessment instead of the six possible plots. While there also appears to be a positive trend for *I* values in OK1 with LEAF assessments, there are only three ratings with LEAF assessments, so there is not enough data to confirm this trend. This same limited data is seen for INC in OK2 where early ratings were not included due to too few spikes at the nodes, and later ratings nodes were either lodged or had almost 100% disease incidence in the plots so *I* values could not be calculated. The differences in Moran's *I* values between logit-transformed INC and SEV, INC and LEAF, and SEV and LEAF were also plotted against the rating times to help identify if differences in magnitude of

aggregation emerged between disease variables or across time (Fig. 5.7). No strong patterns were visible from the graphs, but this was further explored with a mixed-model analysis.

The fit of the linear mixed model in equation 3 indicated that location, rating time, and disease response variable all had significant effects on *I*. All main and interaction effects were significant ($P < 0.05$), except for the rating x disease response variable interaction, which was borderline at $P = 0.07$ (Table 5.3.). Overall, the least squares main-effect means of Moran's *I* for disease variable were 0.25, 0.16, and 0.10 for LEAF, SEV, and INC, respectively, and these were all significantly different from each other. The least squares means of *I* for location were 0.31, 0.14, and 0.07 for OK1, OK2, and CC, respectively, with the value for OK1 being significantly higher than the other locations. These means confirm the trends seen in the frequency distributions (Fig. 5.3) and the plots of individual *I* values (Fig. 5.5). However, because of the two- and three-way interactions, main-effect means can be misleading (Stroup et al. 2018).

The least squares means for the interaction of disease response variable and location is useful for determining the overall spatial patterns (across all rating times) for the locations and disease variables. The interaction results indicated that OK1 generally (but not always) had the highest *I* values and CC the lowest (Table 5.4.), as shown with the main effects. The highest three mean *I* values were for SEV and LEAF at OK1 and LEAF at OK2; the lowest means were for INC and SEV at CC (Table 5.4.). The three-way interaction indicates that the differences in location and disease measurement may depend on rating time. Least squares means are shown in Table 5.5 for ratings four, five, and six (earlier and later ratings had few levels of the other factors for relevant comparisons [and

for the later ratings, only observations from CC]). An example of the three-way interaction between location, rating, and disease measurement is visible at Rating 4, where for OK2 and CC, INC and SEV had similar means, but LEAF was significantly larger than them, while in OK1, SEV and LEAF have similar means and INC was significantly lower. CC had the lowest mean *I* values. At each location, LEAF had the highest or equal to the highest mean. This pattern was somewhat different in Ratings 5 and 6, although LEAF still had the highest or statistically equal to the highest mean *I* values, and the means were low and not significantly different from each other at CC. INC either had the lowest mean *I* within a location or was not significantly different from the lowest within a location. Comparing across the different rating times, the difference in *I* between SEV and LEAF was larger at rating 4 than the later ratings at CC and OK2. This is consistent with the slight visual trend in Fig. 5.7.

Moran's I versus disease intensity. Since there was great variation in disease levels at each plot rating, and location (see Fig. 5.2), *I* values were plotted against mean logit measurements for each plot to determine if differences in *I* can be attributed to differences in disease intensity (Fig. 5.8). Considerable variability was found among plots, locations, and disease response variables in the calculated *I* values. Although there was an upward trend in *I* with increasing intensity at OK2 for SEV, in most cases there was little or no evidence of a consistent trend in *I* with disease intensity within plots. There was a tendency, however, to see small *I* values at very low disease levels and more so at very high disease levels. The latter is exhibited by the final assessments of spike incidence (Fig. 5.8). The general lack of disease effect on *I* was confirmed by the fit of the mixed model (eq. 3,

where disease intensity as a continuous covariate was substituted for rating in all fixed-effect terms). Disease intensity was not significant ($P = 0.88$), and interactions were not significant ($p > 0.05$) in the fitted model (Table 5.6.). The test results quantify the effect of disease intensity after adjusting for effects of other factors and their interactions. Some locations had higher disease and higher *I* values (e.g., OK1),which may be due to disease or other factors.

DISCUSSION

Observing and quantifying the spatial patterns of a disease is a critical part of clarifying the underlying mechanisms of disease spread (Madden et al. 2007). There is a hierarchy of scale within a spatially structured environment, ranging from observations of plant tissues, to whole plant, field, region, and increasingly larger sizes of a location (Luan et al. 1996; Turechek and Madden 2001). While patterns of spatial data can be measured at many different scales, the actual mechanisms of disease expansion may not occur at the levels that are observed (Levin 1992; Turechek and Madden 2001).

Recently, wheat blast has been introduced to Asia and Africa as a seed-borne disease (Islam et al. 2020; Tembo et al. 2020). Wheat blast epidemics in South America may be expanded through seed contamination, but they are also initiated through spores that are present in the environment (Danelli et al. 2019). Sources of large spore loads that may infect wheat spikes may come from crop residue, weedy hosts that are susceptible to MoT, or be generated within wheat fields through foliar lesions (Cruz et al. 2015; Cruz and Valent 2017). It is critical that spatial analyses of wheat blast are conducted to ultimately elucidate the mechanisms of disease development (Sadat and Choi 2017). Cruz et al.

(2015) studied the spread of wheat blast lesions at the whole plant scale and observed the spatiotemporal spread of lesions and sporulation from the oldest leaves of the plant up to when spike infection can occur. Although several temporal analyses of wheat blast have occurred at the field-level (Gongora-Canul et al. 2020; Mills Chapter 4), this is the first study to explore the patterns of aggregation at the plot and field level for wheat blast during a natural epidemic.

There are many methods of collecting disease data for spatial analysis: intensive sampling conserves the locations and spatial arrangement of samples, while sparse sampling does not (Cochran 1936; Madden et al. 2007). If disease data (often incidence) are collected from of groups of plants or tissues, this is referred to as cluster sampling, which is a type of sparse sampling if the spatial locations are not preserved. Analyses for sparsely sampled (discrete) incidence data may include calculating the index of dispersion and intra-cluster correlations; comparing the distribution of disease frequencies to to theoretical frequencies for different models (binomal, β-binomal, Poisson, and negative binomial distributions); and other tests which also provide evidence of random or non-random aggregation (Madden et al. 2007). Kriss et al. (2012) analyzed a decade of sparsely sampled incidence data for Fusarium head blight of wheat in Ohio to quantify spatial aggregation and intra-cluster correlation of disease at county and state spatial levels. Rice blast spatial aggregation has been analyzed using ordinary run tests, doublet tests, and fitting disease frequency to the negative binomial distribution at different times during a natural epidemic (Suriya Rao et al. 2007).

Spatiotemporal patterns of disease aggregation can be analyzed with intensively sampled data when the locations of the observations are known and recorded, whether the disease observations are multiple clusters or individuals (Madden et al. 2007). Various forms of geostatistics have increasingly been used to describe spatial patterns for these types of data, whether collected at a single time or over time (Chellemi et al. 1988; Levin 1992; Madden et al. 1987). When locations are known, the disease status of a sampled plant can be compared with all other sampled plants using spatial autocorrelation or several other inter-related statistical methods (Chellemi et al. 1988; Turechek and Madden 2001; Reynolds et al. 1987). One of the earliest examples of using spatial autocorrelation in plant pathology was the study of virus disease of tobacco (caused by the potyviruses tobacco etch virus (TEV) and tobacco vein mottling virus (TVMV)) which characterized the aggregation or "patchiness" of diseased plants at different sampling times (Madden et al. 1987, 1988). Another advantage to knowing specific locations of disease is that Integrated Pest Management strategies can be targeted to specific areas in some cases, such as when Zhang et al. (2012) explored orchard location patterns of persea mites in avocado trees and citricola scale in citrus trees. Pathosystems with known spatial patterns can be compared with those of emerging diseases which may give insight into disease transmission in the emerging disease. For example, vector-borne viruses in vineyards have been spatially modelled for pests such as mealybugs (Naidu et al. 2014; Rosciglione et al. 1983) and dagger nematodes (Andret-Link et al. 2004); when a new pattern of disease clustering was observed in grapevine red-blotch associated virus the results suggested a new vector may be responsible (Cieniewicz et al. 2017). Spatial patterns of pathogens are important for

informing effective sampling practices, such as with soil-borne pathogens like plant parasitic nematodes (Noe and Campbell 1985).

Intensively sampled data may be analyzed using cross-product statistics (which include spatial autocorrelations), which evaluate the relationships between healthy and diseased plants within the sampled matrix (Madden et al. 2007). Disease aggregation, where diseased plants are in similar locations to each other, can be quantified through Moran's *I* (a weighted spatial-autocorrelation), semivariograms, and regression models (Reynolds et al. 1987; Madden et al. 2007). Diseases from many pathosystems have been spatially analyzed at different spatial hierarchies such as Phomopsis cane and leaf spot of grape which was analyzed at many levels including plant shoot, farm, and region (Nita et al. 2007) and leaf and panicle rice blast clusters at three different scales in China (Guo et al. 2016). This chapter analyzed patterns of wheat blast using Moran's *I* at the cluster (node) and plot scale across multiple plots and locations during a very favorable year for wheat blast development at the level of plant (spike severity and leaf severity), sampling node (spike incidence), field wide (across 4 – 6 plots), and location (OK1, OK2, and CC) using the Moran's autocorrelation coefficient (*I*). Spatial analyses using Moran's *I* have been used in many plant pathogen studies since the late 1980's, such as in Chellemi et al. (1988) who studied inoculum density patterns of pineapple heart rot; Mihail (1989) who used Moran's *I* to evaluate patterns of infection of *Euphorbia lathyrism*; Chiang and Huang (2005) who researched aggregation patterns in rice blast; and Dung et al. (2016) who analyzed the spatial patterns of ergot in perennial ryegrass.

In addition to calculating *I* values, this study used generalized linear mixed models (GLMMs) to evaluate the effects of multiple factors and their interactions on the resulting *I* statistic. This type of approach is unusual, since most studies on spatial patterns focus on individual fields with a more informal comparison of pattern results from different datasets. There are many advantages to using GLMMs, such as factors can be: count data or binary, discrete or continuous; their distributions can be non-normal and vary across them; and factor levels can be unbalanced (such as having different numbers of rating times or plots) (Madden et al. 2007; Stroup et al. 2018). Both fixed and random effects can be tested, and random effects can be used to account for experimental and sampling designs. Spatiotemporal analyses of Fusarium head blight have been analyzed using GLMMs (Kriss et al. 2012). Zhang et al. (2012) also used GLMMs for co-clustering which combined orchard and vector data to identify significant interaction terms.

Low to moderate levels of spatial autocorrelation were found at the three locations during very favorable conditions for leaf and spike blast development. The means of the final disease ratings for INC, SEV, and LEAF were 94%, 67%, and 59% (Mills et al. 2021, Chapter 3). Locations (OK1, OK2, CC), type of disease measurement (INC, SEV, LEAF), and their interactions were the most significant factors in overall trends of Moran's I values. Rating time was also significant as a main effect and interaction term, but there was not a monotonic effect of rating. The highest spatial aggregation was observed OK1 and much lower levels of aggregation, mostly non-distinguishable from random, were more common at CC which was planted three weeks after OK1 and developed blasted spikes about five weeks after OK1. The locations OK1, OK2, and CC represent different planting times,

spike emergence dates, and disease emergence dates during the natural wheat blast epidemic. Approximately 95% of the individual *I* values for each plot, rating, disease measurement, and location (Table 5.2.) were significant (at $P < 0.05$) in OK1, versus 66% in OK2, and only 44% in CC, which supports the idea of greater aggregation of disease at earlier periods in wheat blast epidemics at the regional scale, associated with overly higher levels of disease. At the smaller scale of individual plots and correlation between neighboring nodes within plots, there was no consistent trend in spatial aggregation over time (Fig. 5.5), other than several low values of *I* at very low and very high disease intensity (i.e., very early and late in the epidemics) for some disease measurements and locations, results confirmed by the mixed model analysis. This trend of low spatial aggregation at the beginning and end of epidemics is consistent with viral diseases of tobacco (Madden et al. 1988) and strawberry leather rot, where significant spatial aggregation did not occur until mid-way through the epidemics (Reynolds et al. 1987).

Spatial patterns may appear more aggregated or random at different times during an epidemic or at different locations during an epidemic due to environmental factors such as local microclimates; physical factors such as barriers to pathogen spread; field-level factors such as previous crops, tillage, and weed management; and inoculum distribution at the start of the epidemic and during an epidemic as new inoculum is produced (Kriss et al. 2012; Madden et al. 2007). There was variation in disease intensity and autocorrelation in all of the plots and ratings for each location (Figs 1 and 5). *I* values were plotted against the mean logit of disease levels for each plot and rating to account for differences in disease levels, and no patterns emerged, which supports the idea that disease intensity within plots

or locations during epidemics was not a significant factor in spatial aggregation. The linear mixed model which included disease level as a factor also showed that it was not significant by itself or in combination with other factors on spatial aggregation (Table 5.6.). However, there were substantial differences in *I* among locations.

The distributions of *I* values for each location and disease measurement (Fig. 5.3) showed greater spatial aggregation at the leaf scale of disease severity than at the spike scale in each location. This difference in aggregation among the disease measurements was more pronounced in OK1, which had higher levels of spatial aggregation in general. In OK2, the leaf disease assessments were conducted prior to spike emergence since foliar lesions were present and suggested patterns of spatial aggregation. Collaborators in Santa Cruz de la Sierra have anecdotally observed foci with high levels of leaf lesions early in epidemics, so-called hotspots, which expand before spikes emerge (*personal communication*). Visual observations of the plots in OK1 and OK2 during disease development were consistent with high spike severities co-occurring at the same nodes as high leaf severities (Mills, *unpublished*). Based on plots averages (across all locations, plots, and rating times), the correlation between logit of leaf severity and logit of spike severity was 0.79 ($P < 0.001$). The correlation of Moran's *I* between leaf severity and spike severity for the same dataset was lower at 0.53 but still significant ($P < 0.001$). This showed that both disease and aggregation are related for different wheat blast disease measurements. The pattern of expanding disease foci was not describable by the lattice data because of the distance between each of the 100 nodes in a plot, and sampling would have needed to occur at a finer resolution for more formal hotspot analyses. Skelsey et al.

(2015) conducted hotspot and coldspot analyses for blackleg of seed potatoes and collected samples at 5000 locations per year which is an unrealistic sampling size at the plot-scale for wheat blast. Quantifying the presence of disease foci and expansion of high disease surrounding the foci in future field studies will provide more information on the mechanism of MoT spore dispersal within a field.

In laboratory experiments, wheat blast spike severity has been shown to occur at high levels even when only one spikelet is exposed to spores in inoculations (Chapter 2). Additional growth chamber studies have shown that there is a strong, positive correlation between inoculum concentration and the speed and intensity of spike blast development (Chapter 3). These studies suggest that spike INC may reach higher levels than SEV across a field even when spore concentration is low or unevenly distributed since a single infection can completely blast a spike. In general, disease incidence will always be higher than severity (on the same plant unit, such as spikes) (McRoberts et al. 2003; Paul et al. 2005), but the degree of difference will depend on the level of disease severity and aspects of the epidemiology of the disease, such as the extension of secondary infections or colonization. Additionally, our previous studies suggest that if there are pockets of higher spore concentration (possibly from lesions on leaves), higher levels of disease severity of the spikes will be reached in those locations compared to others. In a side study to ascertain the potential role of hotspots of higher disease on epidemic development, leaf samples were collected from putative hotspots with actively sporulating lesions in OK1 plots and from locations with little to no visible leaf lesions (Mills, *unpublished*). The leaf tissues were washed to collect spores which were counted using a hemocytometer to estimate spore

concentrations. The samples of leaves with high severity had an average of 13 million spores/gram of leaf tissue. In comparison, plants that were collected and washed from outside of the visually distinct disease foci had an average of 125,000 spores/g of tissue.

Spatial and temporal statistics can provide information on whether a disease is a simple interest disease (monocyclic, one infection cycle per host cycle) or a compound interest disease (polycyclic, multiple infection cycles per host cycle), if the statistics are coupled with other knowledge about the disease (Madden et al. 2007; Ristaino and Gumpertz 2020). There is debate about whether wheat blast is monocyclic or polycyclic (Cruz and Valent 2017). Analyses which show wheat plants can produce spores in high concentration when spikes emerge (Cruz et al. 2015); temporal analyses that show good fits of logistic and Gompertz models to blast development over time (Gongora-Canul et al. 2020; Mills Chapter 3); and evidence of spatial aggregation of diseased leaves in fields before spikes emerge are all indicators that wheat blast is a polycyclic disease.

In conclusion, this research supports the ideas that earlier plantings of wheat in endemic wheat blast regions may have higher disease levels and greater aggregation of disease in both leaf and spike tissue. Leaf lesion aggregation was found to be generally higher than spike disease severity, and both disease and Moran's *I* were broadly higher in earlier plantings. There was no clear trend in aggregation over time within plots or locations. Additionally, the high spore counts found in the foliar clusters at the beginning of the epidemic in OK1 in combination with high aggregation of LEAF, may indicate that inoculum build-up can occur during a wheat season and potentially infect adjacent and distant plants through airborne dispersal (Del Ponte et al. 2003; Islam et al. 2020). It is

important that future intensive sampling studies are conducted at different spatial hierarchies to better understand the mechanisms of wheat blast progression and expansion.

REFERENCES

Anapo. Asociación de Productores de Oleaginosas y Trigo. 2015. Recomendaciones Técnicas para el cultivo de trigo. Santa Cruz, Bolivia.

Andret-Link, P. C., Laporte, C., Valate, L., Ritzenthaler, C., Demangeat, G., Vinge, E., Laval, V., Pfeiffer, P., Strussi-Garaud, C., and Fuchs, M. 2004. Grapevine fanleaf virus: Still a major threat to the grapevine industry. J. Plant Pathol. 86:183-198.

Barea, G. and Aguanta, G. 2012. Manual de Recomendaciones Técnicas: Cultivo de trigo. Asociación de Productores de Oleaginosas y Trigo ANAPO. Página 14.

Blumenschein, M., Debbeler, L. J., Lages, N. C., Renner, B., Keim, D. A., and El-Assady, M. 2020. V-plots: Designing hybrid charts for the comparative analysis of data distributions. Comp. Graph. Forum 39:565-577.

Chellemi, D. O., Rohrbach, K. G., Yost, R. S., and Sonoda, R. M. 1988. Analysis of the spatial pattern of plant pathogens and diseased plants using geostatistics. Phytopathology 78:221-226.

Chiang, K. S., and Huang, Y. T. 2005. Analysis of the spatial pattern of rice leaf blast. Plant Prot. Bull. Taipei 47:129-142.

Cieniewicz, E. J., Pethybridge, A. J., Gorny, A., Madden, L. V., McLane, H., Perry, K. L., and Fuchs, M. 2017. Spatiotemporal spread of grapevine red blotched-associated virus in a California vineyard. Virus Research 241:156-162.

Cliff, A., and Ord, K. 1970. Spatial Autocorrelation: A Review of Existing and New Measures with Applications. Economic Geography, 46, 269-292.

Cochran, W. G. 1936. The statistical analysis of field counts of diseased plants. Suppl. J. R. Statist. Soc. 3:49-67.

Cruz, C. D., Kiyuna, J., Bockus, W. W., Todd, T. C., Stack, J. P., and Valent, B. 2015. *Magnaporthe oryzae* conidia on basal wheat leaves as a potential source of wheat blast inoculum. Plant Pathol. 64:1491-1498.

Cruz, C. D., and Valent, B. 2017. Wheat blast disease: danger on the move. Trop. Plant Pathol. 42:210-222.

Danelli, A. L. D., Fernandes, J. M. C., Maciel, J. L. N., Boaretto, C., and Forcelini, C. A. 2019. Monitoring *Pyricularia* sp. airborne inoculum in Passo Fundo, Rio Grande do Sul – Brazil. Summa Phytopathol. 45:361-367.

de Oliveira Coelho, M. A., Torres, G. A. M., Cecon, P. R., and Santana, F. M. 2016. Sowing date reduces the incidence of wheat blast disease. Pesquisa Agropecuaria Brasileira 51:631-637.

Del Ponte, E. M., Shah, D. A., and Bergstrom, G. C. 2003. Spatial patterns of Fusarium head blight in New York wheat fields suggest role of airborne inoculum. Plant Health Prog. Online publication. doi:10.1094/PHP-2003-0418-01-RS.

Dung, J. K., Alterman, S. C., Walenta, D. L., and Hamm, P. B. 2016. Spatial patterns of ergot and quantification of sclerotia in perennial ryegrass seed fields in eastern Oregon. Plant Dis. 100:1110-1117.

Gongora-Canul, C., Salgado, J. D., Singh, D., Cruz, A. P., Cotrozzi, L., Couture, J., Rivadeneira, M. G., Cruppe, G., Valent, B., Todd, T., Poland, J., and Cruz, C. D. 2020. Temporal dynamics of wheat blast epidemics and disease measurements using multispectral imagery. Phytopathology 110:393-405.

Guo, F., Chen, X., Lu, M., Yang, L., Wang, S., and Ming Wu, B. 2018. Spatial analysis of rice blast in China at three different scales. Phytopathology 108:1276-1286.

Igarashi, S., Utiamada, C. M., Igarashi, L. C., Kazuma, A. H., and Lopes, R. S. 1986. *Pyricularia* em trigo, ocorrência de *Pyricularia* sp. no estado do Paraná. Fitopatol. Bras. 11:351-352.

Igarashi, S. 1990. Update on wheat blast (*Pyricularia oryzae*) in Brazil. Wheat for the nontraditional warm areas: a proceedings of the international conference. Foz do Igaçu, Brazil. 480-483.

Islam, M. T., Gubta, D. R., Hossain, A., Roy, K. K., He, X., Kabir, M. R., Singh, P. K., Khan, A. R., Rahman, M., and Wang, G. L. 2020. Wheat blast: a new threat to food security. Phytopathol. Research 2:28. Online publication. https://doi.org/10.1186/s42483-020-00067-6.

Kohli, M. M., Mehta, Y. R., Guzman, E., Viedma, L., and Cubilla, L. E. 2011. *Pyricularia* blast - a threat to wheat cultivation. Czech J. Genet. Plant Breed. 47:S130-S134.

Kriss, A. B., Paul, P. A., and Madden, L. V. 2012. Characterizing heterogeneity of disease incidence in a spatial hierarchy: A cast study from a decade of observations of Fusarium head blight of wheat. Ecol. and Epidemiol. 102:867-877.

Levin, S. A. 1992. The problem of pattern and scale in ecology: The Robert H. MacArthur award lecture. Ecol. 73:1943-1967.

Luan, J., Muetzelfeldt, R. I., and Grace, J. 1996. Hierarchical approach to forest ecosystem simulation. Ecol. Model. 86:37-50.

Madden, L. V., Hughes, G., and van den Bosch, F. 2007a. The study of plant disease epidemics. First. The American Phytopathological Society. Saint Paul, MN.

Madden, L. V., Paul, P. A., and Lipps, P. E. 2007b. Consideration of nonparametric approaches for assessing genotype-by-environment (G x E) interaction with disease severity. Plant Dis. 91:891-900.

Madden, L. V., Piepho, H. P., and Paul, P. A. 2016. Statistical models and methods for network meta-analysis. Phytopathology 106:792-806.

Madden, L. V., Reynolds, K. M., Pirone, T. P., and Raccah, B. 1987. Analysis of the spatial patterns of virus-diseased tobacco plants. Phytopathology 77:1409-1417.

Madden, L. V., Reynolds, K. M., Pirone, T. P., and Raccah, B. 1988. Modeling of tobacco virus epidemics as spatio-temporal autoregressive integrated moving-average processes. Phytopathology 78:1361-1366.

McRoberts, N., Hughes, G., and Madden, L. V. 2003. The theoretical basis and practical application of relationships between different disease intensity measurements in plants. Ann. Appl. Biol. 142:191-211.

Mihail, J. D. 1989. *Macrophomina phaseolina*: Spatio-temporal dynamics of inoculum and of disease in highly susceptible crop. Phytopathology 79:848-855.

Mills, K. B., Salgado, J. D., Cruz, C. D., Valent, B., Madden, L. V., and Paul, P. A. 2021. Comparing the temporal development of wheat spike blast epidemics in a region of Bolivia where the disease is endemic. Plant Dis, 105:96-107.

Mills, K. B., Madden, L. V., and Paul, P. A. 2020. Quantifying the effects of temperature and relative humidity on the development of wheat blast caused by the Lolium pathotype of *Magnaporthe oryzae*. Plant Dis. 104:2622-2633.

Mottaleb, K. A., Singh, P. K., Sonder, K., Kruseman, G., and Erenstein, O. 2019. Averting wheat blast by implementing a 'wheat holiday': In search of alternative crops in West Bengal, India. PLoS ONE. Online publication. doi:10.1371/journal.pone.0211410.

Moran, P. A. 1950. Notes on continuous stochastic phenomena. Biometrika 37:467-471.

Naidu, R., Rowhani, A., Fuchs, M., Golino, D., and Martelli, G. P. Grapevine leafroll: a complex viral disease affecting a high-value fruit crop. Plant Dis. 98:1172-1185.

Nicot, P. C., Rouse, D. I., and Yandell, B. S. 1984. Comparison of statistical methods for studying spatial patterns of soilborne plant pathogens in the field. Phytopathology 74:1399-1402.

Nita, M., Ellis, M. A., Wilson, L. L., and Madden, L. V. 2007. Evaluations of new and current management strategies to control Phomopsis cane and leaf spot of grape. Plant Health Prog. Online publication. doi:10.1094/PHP-2007-0726-06-RS.

Noe, J. P. and Campbell. 1985. Spatial pattern analysis of plant-parasitic nematodes. J. of Nematology 17:86-93.

Paul, P. A., El-Allaf, S. M., Lipps, P. E., and Madden, L. V. 2005. Relationships between incidence and severity of Fusarium head blight on winter wheat in Ohio. Phytopathology. 95:1049-1060.

Reynolds, K. M., and Madden, L. V. 1987. Analysis of epidemics using spatio-temporal autocorrelation. Phytopathology 78:240-246.

Rios, A., Debona, D., Duarte, H., and Rodrigues, F. 2013. Development and validation of a standard area diagram set to assess blast severity on wheat leaves. Eur. J. Plant Pathol. 136:603-611.

Ristaino, J. B., Gumpertz, M. L. 2000. New frontiers in the study of dispersal and spatial analysis of epidemics caused by species in the genus *Phytophthora*. Annu. Rev. Phytopathol. 38:541-576.

Rosciglione, B., Castellano, M. A., Martelli, G., P., Savino, V., and Canizzaro, G. 1983. Mealybug transmission of grapevine virus A. Vitis 22:331-347.

Sadat, A., and Choi, J. 2017. Wheat blast: A new fungal inhabitant to Bangladesh threatening world wheat production. Plant Pathol. J. 33:103-108.

Skelsey, P., Elphinstone, J. G., Saddler, G. S., Wale, S. J., and Toth, I. K. 2015. Spatial analysis of blackleg-affected seed potato crops in Scotland. Plant Pathol. Online publication. doi:10.1111/ppa.12455.

Stroup, W. W. Milliken, G. A., Claassen, E. A., and Wolfinger, R. D. 2018. SAS for Mixed Models: Introduction and Basic Applications. SAS Institute Inc., Cary, NC, USA.

Suriya Rao, a. V., Mukherjee, A. K., Mohapatra, N. K., and Nayak, P. 2007. Spatial distribution of rice blast disease under natural field epidemics. R. J. of Agric.and Biol. Sci. 3:615-620.

Tembo, B., Mulenga, R. M., Sichilima, S., M'siska, K. K., Mwale, M., Chikoti, P. C., Singh, P. K., He, X., Pedley, K. F., Peterson, G. L., Singh, R. P., and Braun, H. J. 2020. Detection and characterization of fungus (*Magnaporthe oryzae* pathotype Triticum) causing wheat blast disease on rain-fed grown wheat (*Triticum aestivum* L.) in Zambia. PLoS ONE 15(9): e0238724. Online publication. doi.org/10.1371/journal.pone.0238724

Turechek, W. W. and Madden, L. V. 2001. Effect of scale on plant disease incidence and heterogeneity in a spatial hierarchy. Ecol. Model. 144:77-95.

Uddin, W., Viji, G., and Vincelli, P. 2003. Gray leaf spot (blast) of perennial ryegrass turf: an emerging problem for the turfgrass Industry. Plant Dis. 87:880-889.

Upton, G. J., and Fingleton, B. 1985. Spatial data analysis by example. Volume 1: Point pattern and quantitative data. J. Wiley and Sons (eds) Chichester, New York.

Urashima, A. S., Grosso, C., Stabili, A., Freitas, E., Silva, D., Netto, D., Franco, I., Bottan, M. 2009. Effect of *Magnaporthe grisea* on seed germination, yield and quality of wheat. Wang, G. L., Valent, B. (eds) Advances in genetic, Genomics and Control of Rice Blast Disease. Springer, Netherlands, pp 267–277.

Yesmin, N., Jenny, F., Abdullah, H. M., Hossain, M. M., Kader, M. A., Solomon, P. S., and Bhuiyan, M. A. H. B. 2020. A review on South Asian wheat blast: The present status and future perspective. Plant Pathol. 69:1618-1629.

Zhang, Z., Jeske, D. R., Cui, X., and Hoddle, M. 2012. Co-clustering spatial data using a generalized linear mixed model with application to the integrated pest management. 2012. J. Agric. Biol. And Envir. Statistics 17:265-282.

Table 5.1. Summary of assessment dates, plots, and types of disease assessments (spike incidence, spike severity, leaf severity) at each research location in Santa Cruz de la Sierra, Bolivia (Okinawa 1, Okinawa 2, Cuatro Cañadas)

Okinawa 1						Okinawa 2						Cuatro Canadas					
Rating[a]	Dates[b]	DAE[c]	Plots[d]	Spikes[e]	Leaf[f]	Rating	Dates	DAE	Plots	Spikes	Leaf	Rating	Dates	DAE	Plots	Spikes	Leaf
1	9-Jun	0	NA	NA	NA	1	18-Jun	0	0	NA	Y	1	10-Jul	NA	0	NA	Y
NA	12-Jun	3	NA	NA	NA	2	21-Jun	3	0	NA	Y	2	13-Jul	0	0	NA	Y
2	16-Jun	7	6	9,048	N	3	24-Jun	6	6	6,459	Y	3	16-Jul	3	2	1,727	Y
3	19-Jun	10	6	10,467	N	4	27-Jun	9	6	7,787	Y	4	20-Jul	7	4	6,058	Y
4	22-Jun	13	6	9,791	Y	NA	30-Jun	12	NA	NA	NA	5	23-Jul	10	4	7,088	Y
5	25-Jun	16	6	10,202	Y	NA	3-Jul	15	NA	NA	NA	6	27-Jul	14	4	7,809	Y
6	29-Jun	20	6	9,723	Y	NA	7-Jul	19	NA	NA	NA	7	30-Jul	17	4	7,500	Y
						5	10-Jul	22	5	12,987	Y	8	4-Aug	22	4	7,940	Y
						6	13-Jul	25	2	5,457	Y	9	7-Aug	25	4	7,905	Y

[a]Disease assessment ratings by location. NA values refer to assessments that would fit the criteria of when a leaf or spike assessment did not occur.

[b]Dates when field assessments whould have occurred to be consistent with the pattern of rating disease progress every 3 to 4 days. Some plot x rating combinations did not have disease values collected at every rating because there were too few spikes present at early emergence, weather conditions interfered with ratings, or a majority of nodes were missing due to lodging or senescence.

[c]Days after spike emergence (DAE) refers to the number of days the rating occurred after initial spike emergence (DAE = 0). Spike assessments occurred when 50 or more nodes in a plot each had more than 7 spikes present in a sample.

[d]The count of plots that were included in the spike disease assessments, a maximum of 6, 6, and 4 plots for OK1, OK2, and CC respectively.

[e]The total number of spikes that were included in an assessment at each rating.

[f]If leaf severity ratings were assessed denoted with a ‘Y’ (yes, leaves were assessed) or a ‘N’ (no leaf assessments occurred).

Table 5.2. Moran's *I* autocorrelation values and significance levels (*p* values) at each location (Okinawa 1 [OK1], Okinawa 2 [OK2], Cuatro Cañadas [CC]), experimental plot at each location, and at each rating time for spatial analysis of logit transformations of wheat blast severity (SEV, mean proportion of diseased spikelets per spike), incidence (INC, mean proportion of diseased spikes divided by the total spikes), and flag leaf severity (LEAF, visual average of flag leaf severity).[a]

	RATING	2		3		4		5		6	
	PLOT	TYPE	*I*	p-value	*I*	p-value	*I*	p-value	*I*	p-value	*I*	p-value
OKINAWA 1	1	INC	0.266	<0.001	0.252	<0.001	0.192	<0.001	0.073	<0.001	0.108	<0.001
		SEV	0.372	<0.001	0.370	<0.001	0.287	<0.001	0.200	<0.001	0.282	<0.001
		LEAF	NA	NA	NA	NA	0.232	<0.001	0.276	<0.001	0.290	<0.001
	2	INC	0.449	<0.001	0.341	<0.001	0.353	<0.001	0.476	<0.001	0.086	<0.001
		SEV	0.430	<0.001	0.447	<0.001	0.310	<0.001	0.449	<0.001	0.512	<0.001
		LEAF	NA	NA	NA	NA	0.443	<0.001	0.587	<0.001	0.565	<0.001
	3	INC	0.116	0.016	0.222	<0.001	0.025	0.488	0.172	<0.001	0.188	<0.001
		SEV	0.283	<0.001	0.229	<0.001	0.067	0.137	0.259	<0.001	0.158	0.001
		LEAF	NA	NA	NA	NA	0.222	<0.001	0.296	<0.001	0.423	<0.001
	4	INC	0.234	<0.001	0.150	0.002	0.194	<0.001	0.195	<0.001	0.375	<0.001
		SEV	0.255	<0.001	0.512	<0.001	0.528	<0.001	0.298	<0.001	0.230	<0.001
		LEAF	NA	NA	NA	NA	0.321	<0.001	0.266	<0.001	0.295	<0.001
	5	INC	0.147	0.004	0.096	0.033	0.055	0.212	0.105	0.023	0.299	<0.001
		SEV	0.172	0.001	0.498	<0.001	0.302	<0.001	0.104	0.026	0.147	0.002
		LEAF	NA	NA	NA	NA	0.397	<0.001	0.378	<0.001	0.436	<0.001
	6	INC	0.078	0.116	0.290	<0.001	0.329	<0.001	0.203	<0.001	0.392	<0.001
		SEV	0.269	<0.001	0.505	<0.001	0.476	<0.001	0.396	<0.001	0.390	<0.001
		LEAF	NA	NA	NA	NA	0.547	<0.001	0.538	<0.001	0.527	<0.001

continued

Table 5.2. Continued.

	RATING	1		2		3		4		5		6	
	PLOT	TYPE	*I*	p-value	*I*	p-value	*I*	p-value	*I*	p-value	*I*	p-value	*I*	p-value
OKINAWA 2	1	INC	NA	NA	NA	NA	0.015	0.662	-0.062	0.413	NA	NA	NA	NA
		SEV	NA	NA	NA	NA	0.063	0.142	-0.050	0.531	NA	NA	NA	NA
		LEAF	0.295	<0.001	0.297	<0.001	0.187	<0.001	0.226	<0.001	NA	NA	NA	NA
	2	INC	NA	NA	NA	NA	0.052	0.296	0.238	<0.001	0.095	0.041	NA	NA
		SEV	NA	NA	NA	NA	0.183	0.001	0.127	0.012	0.047	0.266	0.301	<0.001
		LEAF	0.161	0.001	0.162	0.011	0.188	0.011	0.207	<0.001	0.104	0.026	0.092	0.048
	3	INC	NA	NA	NA	NA	-0.022	0.866	0.037	0.370	-0.019	0.866	NA	NA
		SEV	NA	NA	NA	NA	<0.001	0.802	0.096	0.043	0.237	<0.001	0.429	<0.001
		LEAF	0.304	<0.001	0.270	<0.001	0.226	<0.001	0.209	<0.001	0.216	<0.001	0.297	<0.001
	4	INC	NA	NA	NA	NA	0.140	0.025	0.129	0.017	-0.006	0.929	NA	NA
		SEV	NA	NA	NA	NA	0.025	0.531	-0.065	0.348	0.080	0.083	NA	NA
		LEAF	0.343	<0.001	0.346	<0.001	0.425	<0.001	0.307	<0.001	0.267	<0.001	NA	NA
	5	INC	NA	NA	NA	NA	-0.062	0.495	0.206	<0.001	-0.032	0.632	NA	NA
		SEV	NA	NA	NA	NA	0.112	0.058	0.069	0.147	0.156	0.002	NA	NA
		LEAF	0.209	<0.001	0.284	<0.001	0.304	<0.001	0.293	<0.001	0.217	<0.001	NA	NA
	6	INC	NA	NA	NA	NA	-0.014	0.980	0.040	0.405	-0.004	0.862	NA	NA
		SEV	NA	NA	NA	NA	0.080	0.104	0.089	0.110	0.199	<0.001	NA	NA
		LEAF	0.141	0.001	0.332	<0.001	0.377	<0.001	0.154	0.001	0.094	0.044	NA	NA

continued

Table 5.2.Continued.

CUATRO CANADAS

	RATING	1		2		3		4		5	
PLOT	TYPE	*I*	p-value	*I*	p-value	*I*	p-value	*I*	p-value	*I*	p-value
1	INC	NA	NA	NA	NA	NA	NA	-0.045	0.527	0.055	0.216
	SEV	NA	NA	NA	NA	NA	NA	-0.074	0.238	0.044	0.303
	LEAF	0.007	0.741	0.069	0.122	0.164	0.001	0.166	0.001	0.184	<0.001
3	INC	NA	NA	NA	NA	-0.007	0.898	0.024	0.521	0.096	0.044
	SEV	NA	NA	NA	NA	-0.020	0.945	0.160	0.002	0.116	0.016
	LEAF	0.106	0.017	0.082	0.049	0.088	0.043	0.111	0.019	0.096	0.040
5	INC	NA	NA	NA	NA	NA	NA	0.035	0.411	0.017	0.610
	SEV	NA	NA	NA	NA	NA	NA	-0.060	0.380	-0.084	0.165
	LEAF	0.019	0.561	0.072	0.111	0.225	<0.001	0.306	<0.001	0.087	0.062
6	INC	NA	NA	NA	NA	-0.009	0.904	0.115	0.018	0.034	0.402
	SEV	NA	NA	NA	NA	-0.083	0.447	-0.020	0.849	0.043	0.309
	LEAF	-0.017	0.882	0.070	0.064	0.211	<0.001	0.123	0.010	0.134	0.005

continued

Table 5.2. Continued.

CUATRO CANADAS

RATING		6		7		8		9	
PLOT	TYPE	*I*	p-value	*I*	p-value	*I*	p-value	*I*	p-value
1	INC	-0.002	0.877	0.040	0.333	0.137	0.004	0.100	0.035
	SEV	-0.018	0.884	0.103	0.029	0.184	<0.001	0.043	0.290
	LEAF	0.259	<0.001	0.157	0.001	0.022	0.541	0.056	0.209
3	INC	0.287	<0.001	0.177	<0.001	0.103	0.028	0.054	0.220
	SEV	0.231	<0.001	0.268	<0.001	-0.006	0.941	0.039	0.327
	LEAF	0.028	0.464	0.220	<0.001	0.118	0.012	0.106	0.025
5	INC	-0.003	0.897	0.026	0.489	-0.051	0.433	-0.012	0.976
	SEV	0.002	0.810	0.048	0.267	0.107	0.023	0.129	0.006
	LEAF	0.261	<0.001	0.099	0.034	0.119	0.013	0.039	0.342
6	INC	-0.075	0.214	0.106	0.024	0.031	0.428	-0.005	0.924
	SEV	0.011	0.686	0.157	0.001	0.004	0.776	0.204	<0.001
	LEAF	0.134	0.006	0.145	0.002	0.089	0.056	0.105	0.027

[a]Some plot x rating combinations did not have disease values collected at every rating because there were too few spikes present at early emergence, weather conditions interfered with ratings, or nodes were missing due to lodging or senescence.

Table 5.3. Statistics from fit of the linear mixed model (equation 3) to Moran's *I* values for the effects of location[a] , rating time, and logit-transformed disease response variable (measurement)[b], and their interactions on the spatial autocorrelation of wheat blast in Bolivia.

Factors	DF[c]	F Value[d]	*P* value
Location	2	24.39	<0.001
Rating	8	2.41	0.025
Location*Rating	8	3.72	0.001
Measurement	2	32.51	<0.001
Location*Measurement	4	3.38	0.014
Rating*Measurement	13	1.72	0.071
Location*Rating*Measurement	10	2.19	0.026

[a]Disease Locations include Okinawa 1 (OK1), Okinawa 2 (OK2), and Cuatro Cañadas (CC) in Santa Cruz de la Sierra, Bolivia

[b]Logit-transformed spike incidence (INC, mean proportion of diseased spikes divided by the total spikes), severity (SEV, mean proportion of diseased spikelets per spike),and average flag leaf severity (LEAF, visual average of flag leaf severity).

[c]Numerator degrees of freedom in the mixed model analysis for each effect.

Test statistic for effect of factor or interaction.

Table 5.4. Estimated least square means of Moran's *I* from mixed model analysis (equation 3) for combinations of research locations (Okinawa 1 [OK1], Okinawa 2 [OK2], Cuatro Cañadas [CC]) and disease measurement[a], with corresponding standard errors (SE), lower[c] and upper limits of the 95% confidence intervals around the estimates.

Location	Measurement[a]	Moran's *I*[b]	SE	Lower[c]	Upper	Grouping[d]
OK1	logit(INC)	0.214	0.029	0.155	0.274	C
OK1	logit(SEV)	0.322	0.030	0.260	0.384	B
OK1	logit(LEAF)	0.387	0.030	0.326	0.448	A
OK2	logit(INC)	0.049	0.033	-0.018	0.116	C
OK2	logit(SEV)	0.108	0.035	0.038	0.178	C D
OK2	logit(LEAF)	0.252	0.027	0.196	0.307	B
CC	logit(INC)	0.042	0.033	-0.027	0.111	D
CC	logit(SEV)	0.056	0.035	-0.016	0.127	D
CC	logit(LEAF)	0.118	0.029	0.054	0.182	C

[a]Disease assessment type: logit transformed spike incidence (INC, mean proportion of diseased spikes divided by the total spikes), severity (SEV, mean proportion of diseased spikelets per spike),and average flag leaf severity (LEAF, visual average of flag leaf severity).

[b]Least squares means for *I* that are adjusted for effects in the model.

[c]The lower and upper 95% confidence interval values for mean *I*.

[d]Tukey-Kramer grouping to identify least square means estimates that are significantly different from each other. Means followed by the same letters are not significantly different from each other at a *p* value of 0.05.

Table 5.5. Estimated least square means of Moran's *I* from mixed model analysis (equation 3) for combinations of research locations (Okinawa 1 [OK1], Okinawa 2 [OK2], Cuatro Cañadas [CC]) and disease measurements[a] at the 4th, 5th, and 6th assessments.

Location	Measurement[a]	Rating 4[b]	Grouping[c]	Rating 5	Grouping	Rating 6	Grouping
OK1	logit INC	0.191	DC	0.204	BC	0.249	BC
	logit SEV	0.328	AB	0.284	BC	0.287	BC
	logit LEAF	0.360	A	0.390	A	0.423	A
OK2	logit INC	0.098	DE	0.002	F		
	logit SEV	0.044	E	0.139	CDE	0.378	AB
	logit LEAF	0.233	BC	0.175	BCD	0.208	BCD
CC	logit INC	0.033	E	0.050	DEF	0.052	E
	logit SEV	0.002	E	0.030	EF	0.057	ED
	logit LEAF	0.177	DC	0.125	CDEF	0.171	CDE

[a]Disease assessment type: logit transformed spike incidence (INC, mean proportion of diseased spikes divided by the total spikes), severity (SEV, mean proportion of diseased spikelets per spike),and average flag leaf severity (LEAF, visual average of flag leaf severity).

[b]Least squares means for *I* that are adjusted for effects in the model.

[c]Tukey-Kramer grouping to identify least square means estimates that are significantly different from each other. Means followed by the same letters are not significantly different from each other at a *p* value of 0.05.

Table 5.6. Statistics from fit of the linear mixed model (equation 3) to Moran's *I* values for the effects of location[a] , logit-transformed disease response[b], disease measurement variable (INC, SEV, LEAF), and their interactions on the spatial autocorrelation of wheat blast in Bolivia.

Factors	DF[c]	F Value[d]	*P* value
Location	2	18.42	< 0.001
Disease	1	0.02	0.881
Disease*Location	2	0.39	0.679
Measurement	2	18.44	< 0.001
Location*Measurement	4	1.52	0.204
Disease*Measurement	2	2.55	0.085
Disease*Location*Measurement	4	1.22	0.310

[a]Disease locations include Okinawa 1 (OK1), Okinawa 2 (OK2), and Cuatro Cañadas (CC) in Santa Cruz de la Sierra, Bolivia.
[b]Logit- logit transformed spike incidence (INC, mean proportion of diseased spikes divided by the total spikes), severity (SEV, mean proportion of diseased spikelets per spike),and average flag leaf severity (LEAF, visual average of flag leaf severity).
[c]Numerator degrees of freedom in the mixed model analysis for each effect.
[d]Test statistic for effect of factor or interaction.

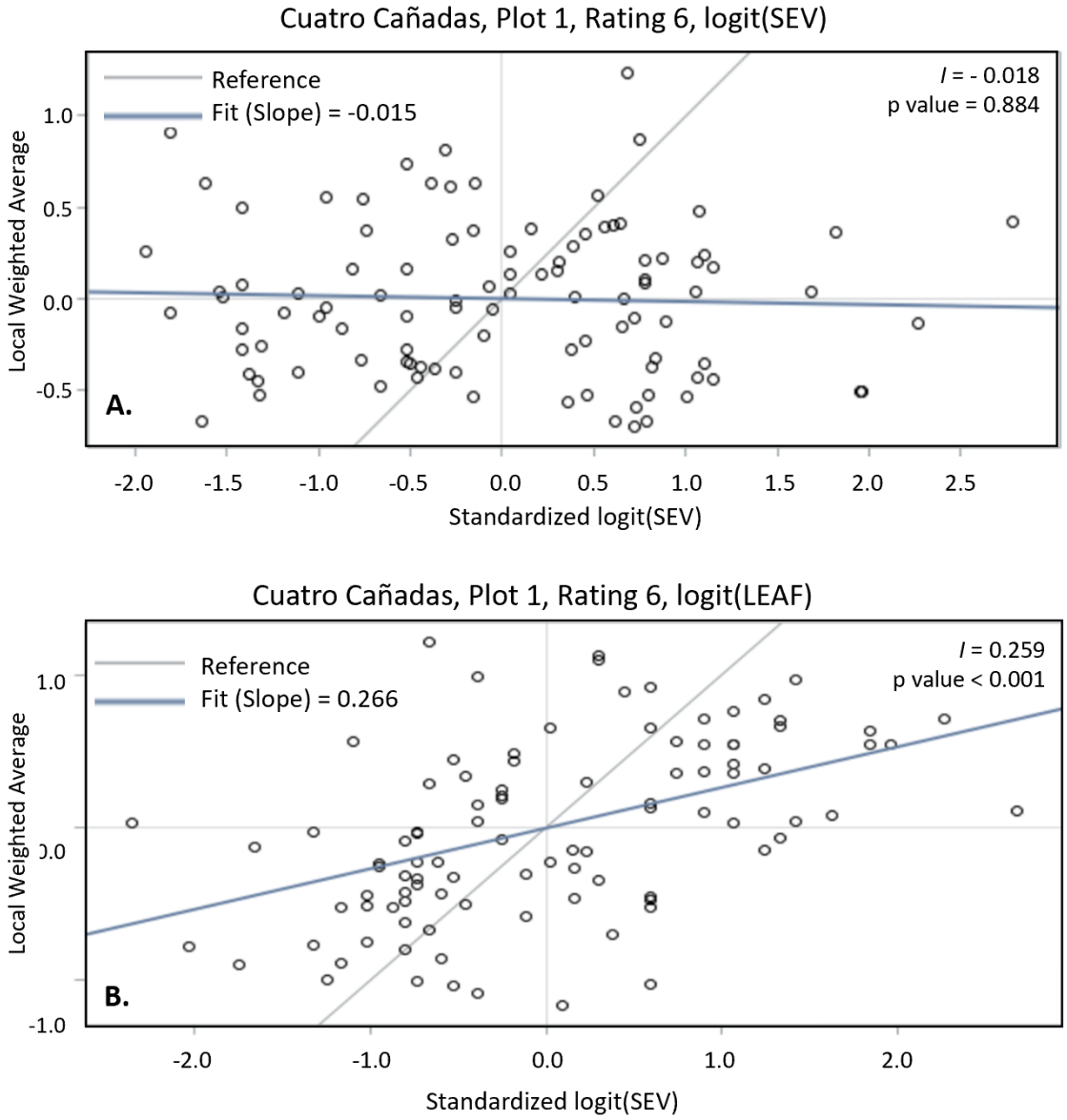

Fig. 5.1. Moran scatterplots showing the association of weighted average of neighboring sampling locations (nodes) < 3.94 m away from each node versus the standardized disease measurement (logit(SEV) and logit(LEAF) at each node for Cuatro Cañadas, Plot 1, rating assessment 6. The *I* value can be calculated from the slope of the regression line through these points, (A) shows an *I* value for logit(SEV) that is not statistically significant ($p > 0.05$), while (B) has an *I* value that is significant at $P < 0.001$ and indicates a positive spatial association of node values.

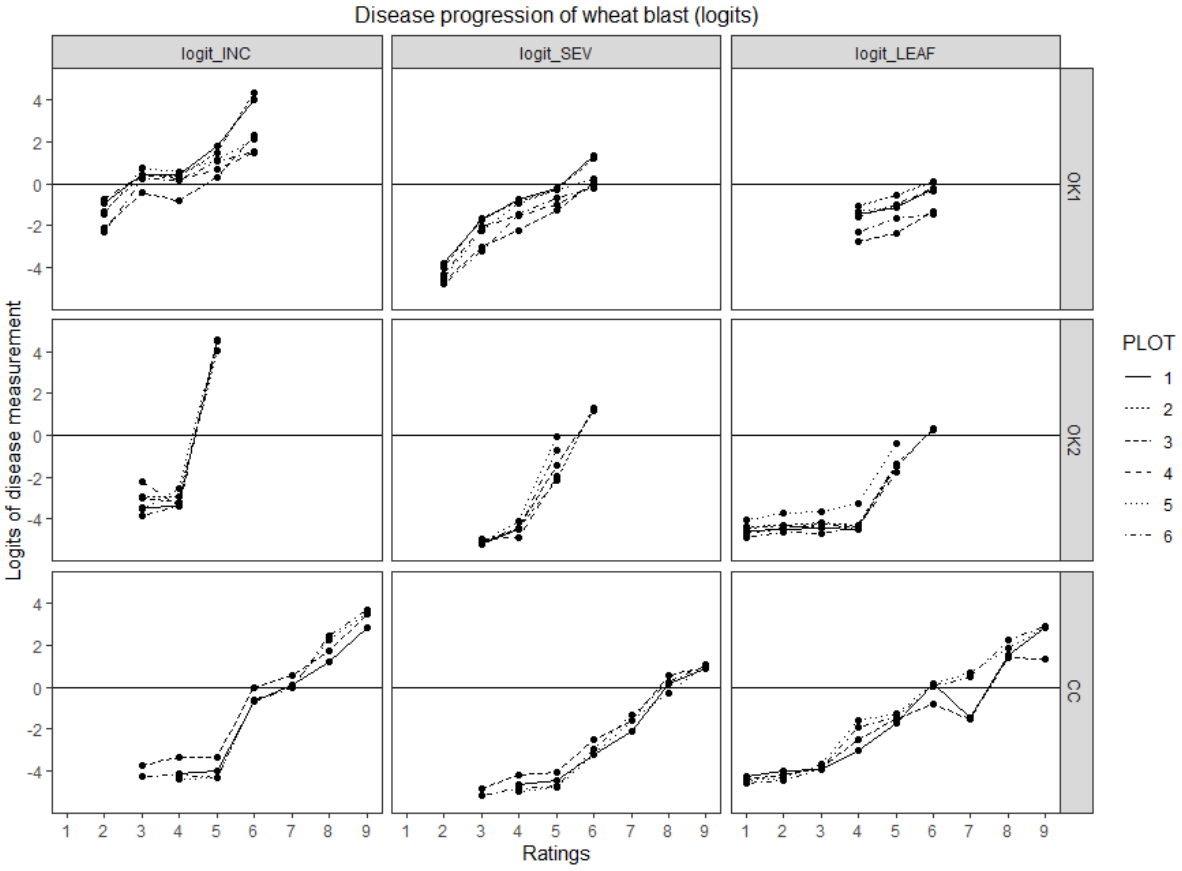

Fig. 5.2. Logit-transformed mean wheat blast disease measurements at each research location in Bolivia (Okinawa 1 [OK1], Okinawa 2 [OK2], Cuatro Cañadas [CC]) for spike severity (SEV, mean proportion of diseased spikelets per spike), incidence (INC, mean proportion of diseased spikes divided by the total spikes), and average flag leaf severity (LEAF, visual average of flag leaf severity) averaged at plot level for each rating where more than half of the nodes in a plot had greater than 7 spikes in a sample.

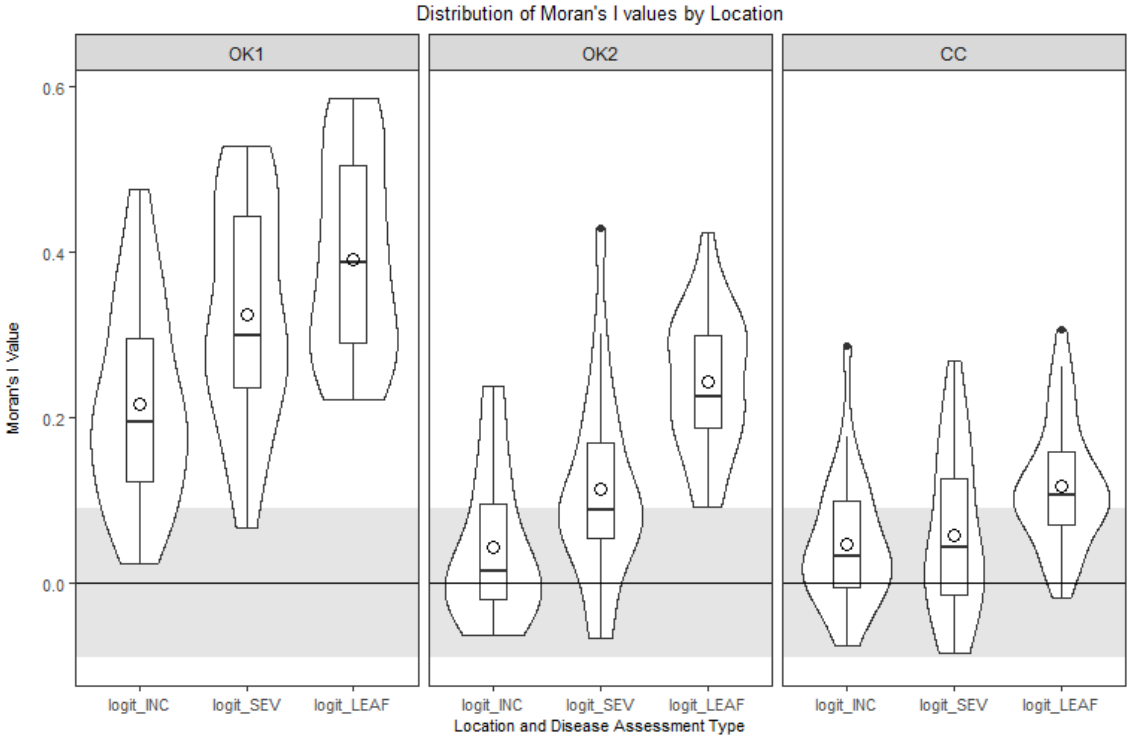

Fig. 5.3. Boxplots showing the distribution of Moran's *I* spatial autocorrelation values for the logit-transformed wheat spike blast incidence and severity (INC, SEV), and leaf severity (LEAF) at each location (Okinawa 1 [OK1], Okinawa 2 [OK2], Cuatro Cañadas [CC]) across all plots and rating assessments. Theses boxplots display a mirrored density to better present the proportion of *I* values. The empty circle and solid lines within each box represent means and medians, respectively. Vertical bars extending beyond the boxes represent the 5th and 95th percentiles, while filled circles represent outliers. The violin outline displays the distribution of response (the higher the frequency of points, the wider the display).

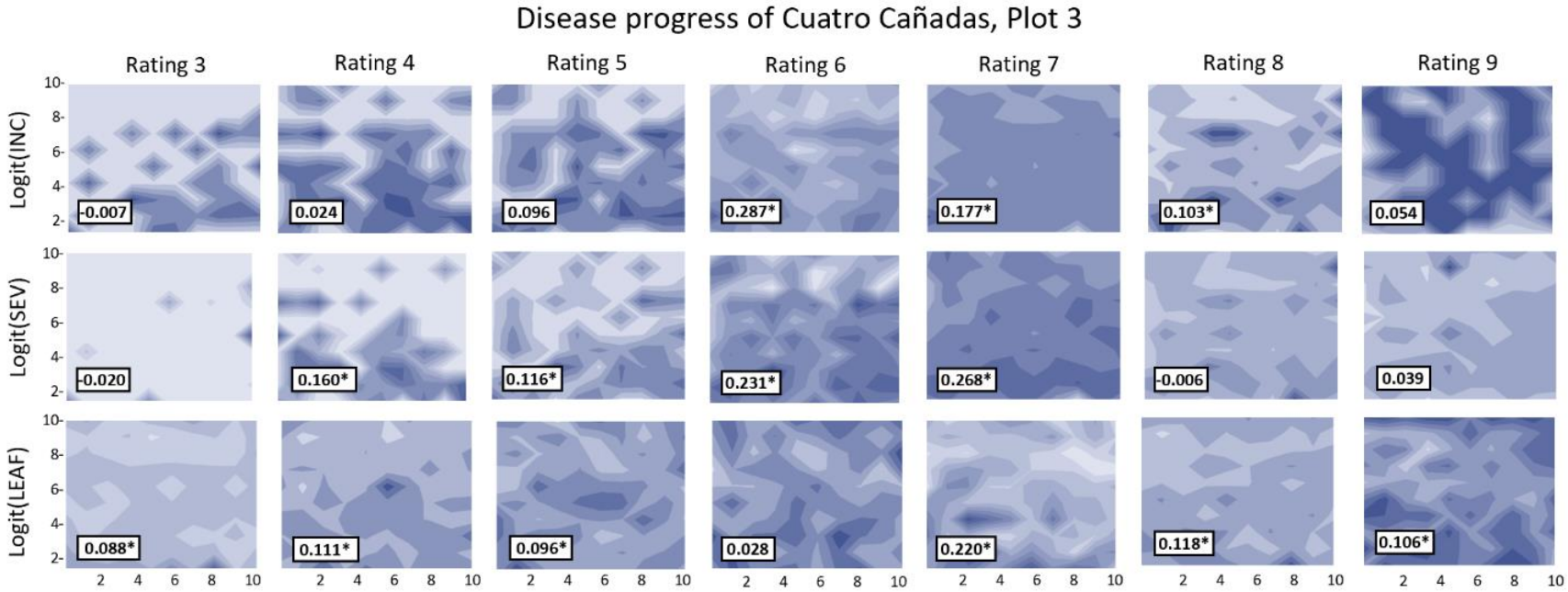

Fig. 5.4. Contour plots showing the logit transformed disease measurements spike severity (SEV, mean proportion of diseased spikelets per spike), incidence (INC, mean proportion of diseased spikes divided by the total spikes), and average flag leaf severity (LEAF, visual average of flag leaf severity) in plot 3 of Cuatro Cañadas over ratings 3 through 9. Moran's *I* values are located in the bottom left corner of each contour plot, and *I* values that are significant at p values < 0.05 are marked with an asterisk. The values of the shades vary by plot and the contour levels are calculated internally in SAS CONTOURPLOTPARM based on the range of data in the sample. -

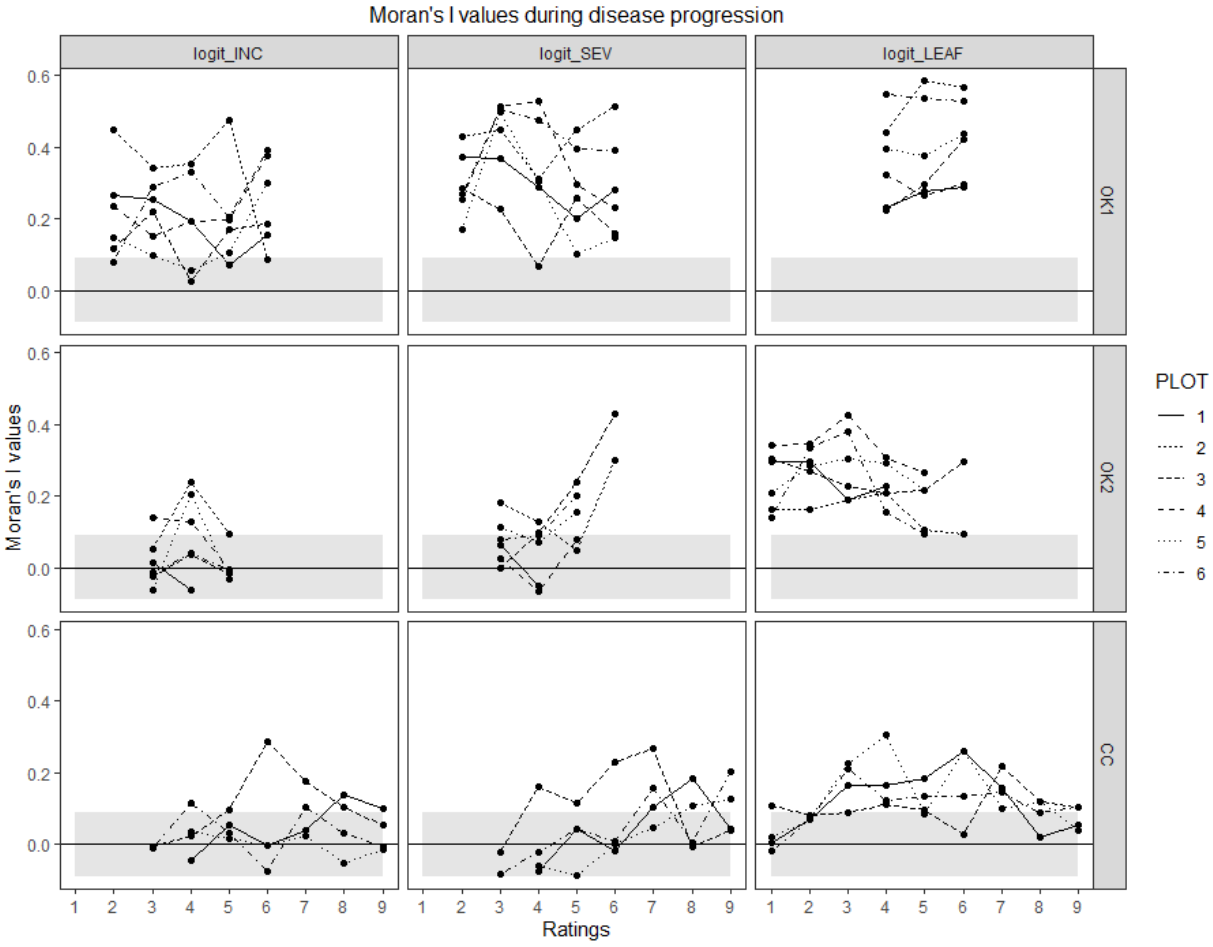

Fig. 5.5. The Moran *I* values for each combination of location (Okinawa 1 [OK1], Okinawa 2 [OK2], Cuatro Cañadas [CC]), plot, and rating. Points that are above the shaded rectangle are significant at $P < 0.05$ and represent positive spatial autocorrelation of disease (see equations 2a-2d).

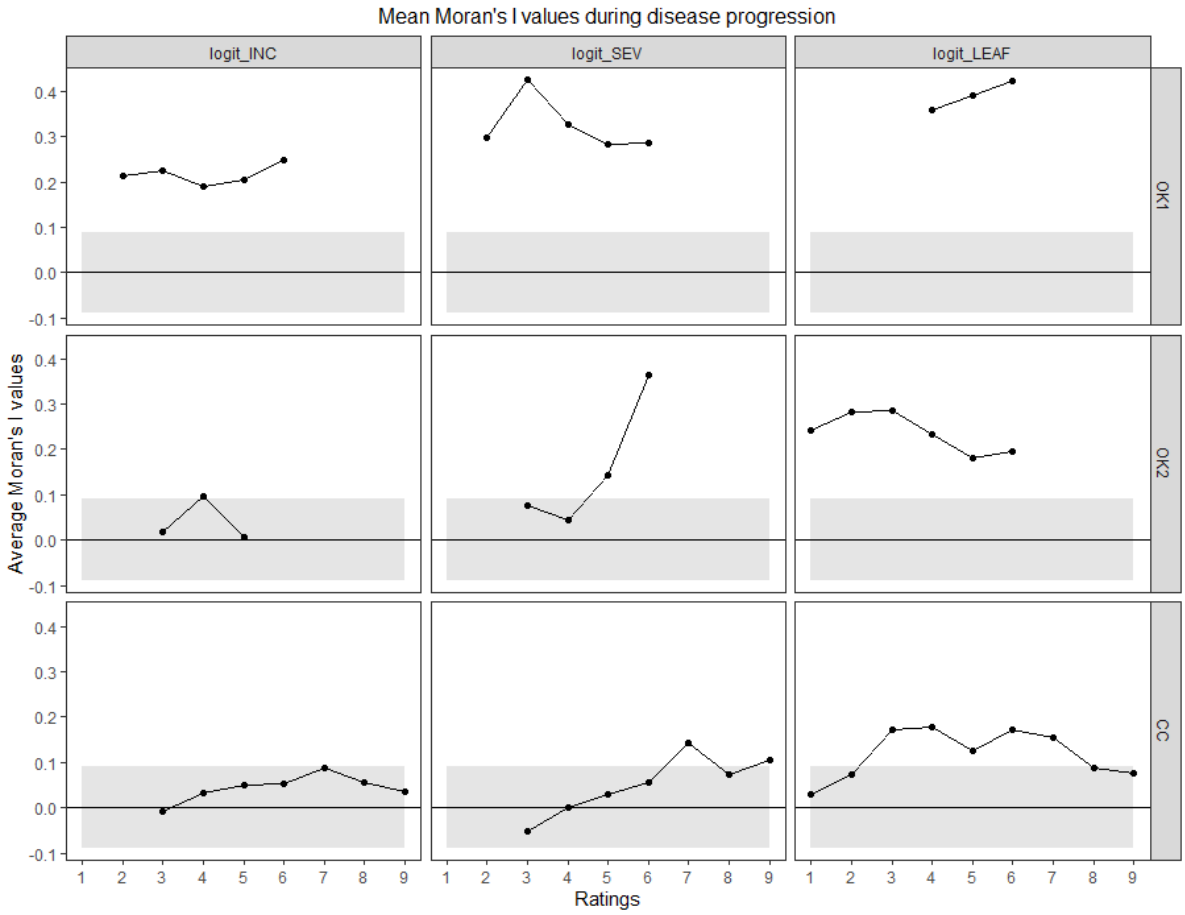

Fig. 5.6. The Moran *I* values for each combination of location (Okinawa 1 [OK1], Okinawa 2 [OK2], Cuatro Cañadas [CC]) and rating times averaged across the plots that were included at each rating. Shaded location indicates individual values of *I* that would be nonsignificant (see Fig. 5. 5). This region cannot be directly used for mean *I* values, but give guidance about the magnitude of *I*.

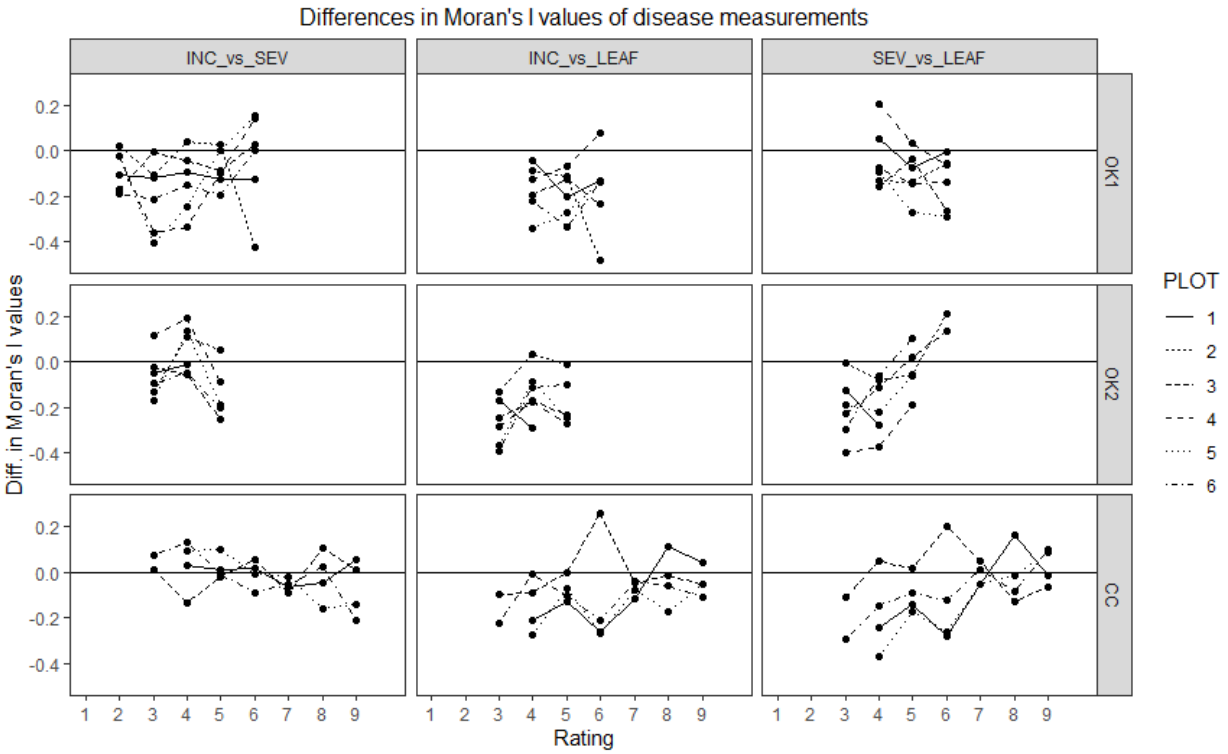

Fig. 5.7. Differences between measures of wheat blast (INC, SEV, LEAF) at each location (Okinawa 1 [OK1], Okinawa 2 [OK2], Cuatro Cañadas [CC]), plot, and rating, *I* values from the same plot and rating are subtracted from each other to generate each point.

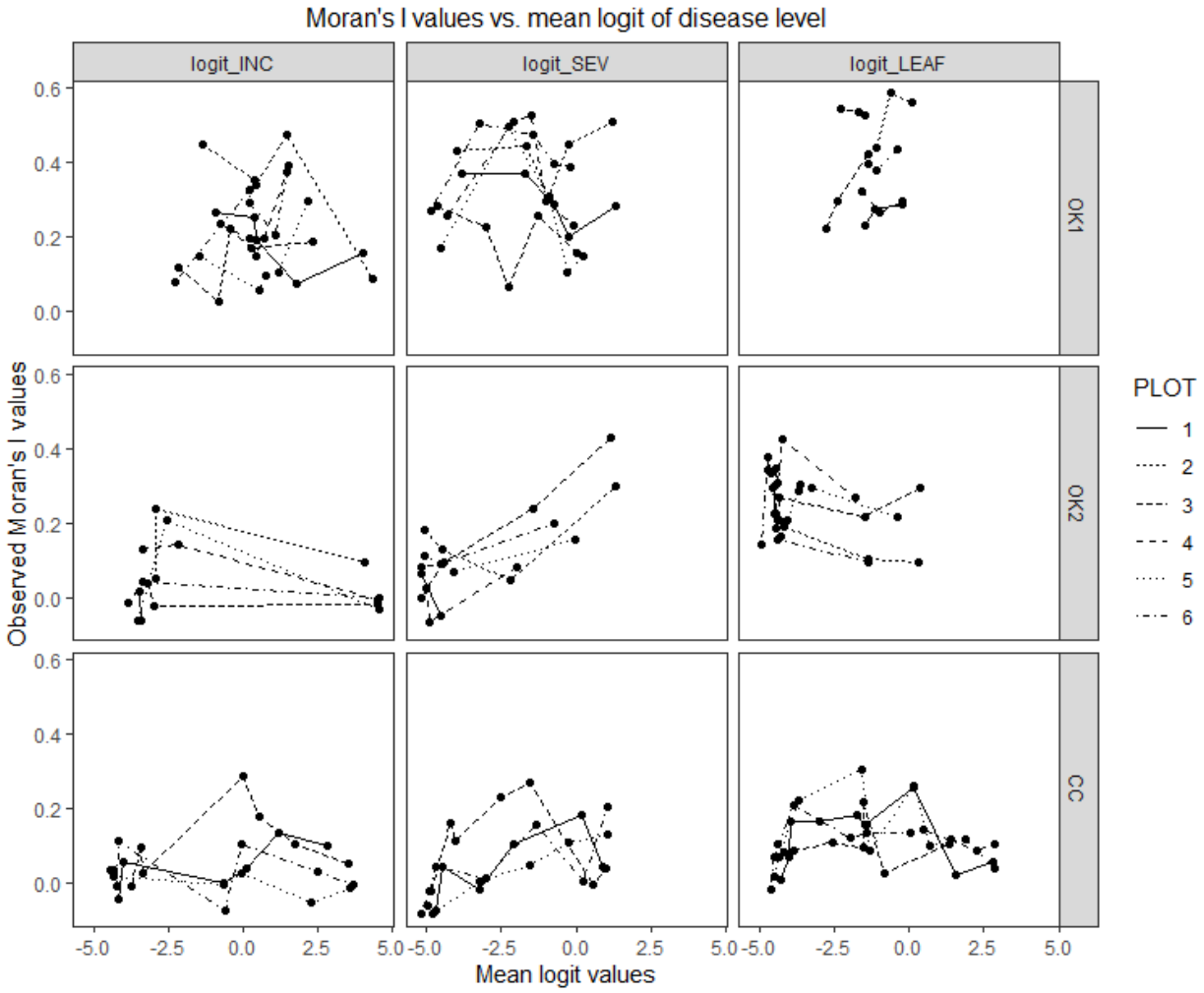

Fig. 5.8. Moran's *I* values versus mean logit values for SEV, INC, and LEAF for each plot, rating, and location (Okinawa 1 [OK1], Okinawa 2 [OK2], and Cuatro Cañadas [CC]) .

Bibliography

Allison, P.D. 2010. Survival Analysis Using the SAS® System: A Practical Guide, Second Edition. Cary, NC, SAS Institute Inc.

Alves, K. J., and Fernandes, J. M. 2006. Influência da temperatura e da umidade relativa do ar na esporulação de *Magnaporthe grisea* em trigo. Fitopatologia Brasileira 31:579-584.

Anapo. Asociación de Productores de Oleaginosas y Trigo. 2015. Recomendaciones Técnicas para el cultivo de trigo. Santa Cruz, Bolivia.

Andret-Link, P. C., Laporte, C., Valate, L., Ritzenthaler, C., Demangeat, G., Vinge, E., Laval, V., Pfeiffer, P., Strussi-Garaud, C., and Fuchs, M. 2004. Grapevine fanleaf virus: Still a major threat to the grapevine industry. J. Plant Pathol. 86:183-198.

Andersen, K. F., Madden, L. V., and Paul, P. A. 2015. Fusarium head blight development and deoxynivalenol accumulation in wheat as influenced by post-anthesis moisture patterns. Phytopathology 105:210-219.

Anderson, W. K. 2010. Closing the gap between actual and potential yield of rainfed wheat. The impacts of environment, management and cultivar. Field Crops Research 116:14-22.

Aucique Perez, C. E., Rodrigues, F. Á., Moreira, W. R., and DaMatta, F. M. 2014. Leaf gas exchange and chlorophyll a fluorescence in wheat plants supplied with silicon and infected with *Pyricularia oryzae*. Phytopathology 104:143-149.

Baker, C. K., and Gallagher, J. N. 1983. The development of winter wheat in the field. The control of primordium initiation rate by temperature and photoperiod. J. of Agric. Sci. 101:337-344.

Barea, G. and Aguanta, G. 2012. Manual de Recomendaciones Técnicas: Cultivo de trigo. Asociación de Productores de Oleaginosas y Trigo ANAPO. Página 14.

Barea G., Toledo J. 1996. Identificación y zonificación de piricularia o bruzone (*Pirycylaria oryzae*) en el cultivo del trigo en el dpto. de Santa Cruz. In: CIAT. Informe Técnico. Proyecto de Investigación Trigo, Santa Cruz, 76–86.

Berger R. D. 1981. Comparison of the Gompertz and logistic equations to describe plant disease progress. Phytopathology. 71: 716-719.

Berger, R. D., Bergamin Filho, A., and Amorim, L. 1997. Lesion expansion as an epidemic component. Phytopathology 87:1005-1013.

Bishnoi, S. K., Kumar, S., and Singh, G. P. 2021. Wheat blast readiness of the Indian wheat sector. Current Science 120:262.

Bland, J. M. and Altman, D. G. 2004. The logrank test. British Med. J. 1:328:1073.

Blumenschein, M., Debbeler, L. J., Lages, N. C., Renner, B., Keim, D. A., and El-Assady, M. 2020. V-plots: Designing hybrid charts for the comparative analysis of data distributions. Comp. Graph. Forum 39:565-577.

Breusch, T. S., and Pagan, A. R. 1979. A simple test for heteroskedasticity and random coefficient variation. Econometrica 47:1287-1294.

Brondani, C., Vianello, R. P., Garrido, L., and Elias, F. M. 2000. Development of microsatellite markers for the genetic analysis of *Magnaporthe grisea*. Gen. and Mol. Biol. 23:753-762.

Cabrera, M. and Gutiérrez, S. 2007. Primer registro de *Pyricularia grisea* en cultivos de trigo del NE de Argentina. Depto. Protección Vegetal, Facultad de Ciencias Agrarias, UNNE. Corrientes, Argentina.

Calvero Jr., S. B., Coakley, S. M., and Teng, P. S. 1996. Development of empirical forecasting models for rice blast based on weather factors. Plant Pathol. 4:667-678.

Campbell, C. L. and Madden, L. V. 1990. Introduction to Plant Disease Epidemiology. John Wiley & Sons, New York.

Cardoso, C. A. de A., Reis, E. M., and Moreira, E. N. 2008. Development of a warning system for wheat blast caused by *Pyricularia grisea*. Summa Phytopathol. 34:216-221.

Castroagudín, V. L., Ceresini, P. C., Oliveira, S. C., Reges, J. A., Maciel, J. L., Bonato, A. L., Dorigan, A. F., and McDonald, B. A. 2015. Resistance to QoI fungicides is widespread in Brazilian populations of the wheat blast pathogen *Magnaporthe oryzae*. Phytopathol. 105:3, 284-294

Castroagudın, V. L., Moreira S. I., Pereira D. A. S., Moreira, S. S., Brunner, P. C., Maciel, J. L. N., Crous, P. W., McDonald, B. A., Alves, E., and Ceresini, P. C. 2016. *Pyricularia graministritici*, a new *Pyricularia* species causing wheat blast. Persoonia 37:199-216.

Ceresini, P. C., Castroagudiin, V. L., Rodrigues, F. A., Rios, J. A., Aucique-P´erez, C. E., Moreira, S. I., Alves, E., Croll, D., and Maciel, J. L. 2018. Wheat blast: past, present, and future. Annu. Rev. Phytopathol. 56:427-456.

Ceresini, P. C., Castroagudiin, V. L., Rodrigues, F. A., Rios, J. A., Aucique-P´erez, C. E., Moreira, S. I., Croll, D., Alves, E., Carvalho, G., Maciel, J. L., and McDonald, B. A. 2019. Wheat blast: from its origins in South America to its emergence as a global threat. Mol. Plant Pathol. 20:155-172.

Chakraborty, M., Mahmud, N. U., Muzahid, A. N. M., Fajle Rabby, S. M., and Islam, T. 2020. Oligomycins inhibit *Magnaporthe oryzae* Triticum and suppress wheat blast disease. PLoS ONE. Online publication. doi:10.1371/journal.pone.0233665.

Chellemi, D. O., Rohrbach, K. G., Yost, R. S., and Sonoda, R. M. 1988. Analysis of the spatial pattern of plant pathogens and diseased plants using geostatistics. Phytopathology 78:221-226.

Chiang, K. S., and Huang, Y. T. 2005. Analysis of the spatial pattern of rice leaf blast. Plant Prot. Bull. Taipei 47:129-142.

Chuma, I., Zhan, S., Asano, S., Nga, N.T., Vy, T. T., Shirai, M., Ibaragi, K., and Tosa, Y. 2010. PWT1, an avirulence gene of *Magnaporthe oryzae* tightly linked to the rDNA locus, is recognized by two staple crops, common wheat and barley. Phytopathol. 100:436-443.

Cieniewicz, E. J., Pethybridge, A. J., Gorny, A., Madden, L. V., McLane, H., Perry, K. L., and Fuchs, M. 2017. Spatiotemporal spread of grapevine red blotched-associated virus in a California vineyard. Virus Research 241:156-162.

Cliff, A., and Ord, K. 1970. Spatial Autocorrelation: A Review of Existing and New Measures with Applications. Economic Geography, 46, 269-292.

Cochran, W. G. 1936. The statistical analysis of field counts of diseased plants. Suppl. J. R. Statist. Soc. 3:49-67.

Correa-Victoria, F. J., and Zeigler, R. S. 1993. Pathogenic variability in *Pyricularia grisea* at a rice blast “hot spot” breeding site in eastern Colombia. Plant Dis. 77:1029-1035.

Couch, B. C., Fudal, I., Lebrun, M., Tharreau, D., Valent, B., van Kim, P., Nottéghem, J., and Kohn, L. 2005. Origins of host-specific populations of the blast pathogen *Magnaporthe oryzae* in crop domestication with subsequent expansion of pandemic clones on rice and weeds of rice. Genetics 170:613-630.

Cowger, C., Beccari, G., Dong, Y. 2020. Timing of susceptibility to Fusarium head blight in winter. Wheat Plant Dis. 104:2928-2939.

Cruppe, G. 2019. Wheat blast management through identification of novel sources of genetic resistance and understanding of disease dynamics. Ph.D. Dissertation, Department of Plant Pathology, Kansas State University, Manhattan, KS.

Cruppe G. 2020. Novel sources of wheat head blast resistance in modern breeding lines and wheat wild relatives. Plant dis. 104:35-43.

Cruz, C. D. 2013. Wheat blast: quantitative pathway analyses for the Triticum pathotype of *Magnaporthe oryzae* and phenotypic reaction of U.S. wheat cultivars. Kansas State University.

Cruz, C. D., Bockus, W. W., Stack, J. P., Tang, X., Valent, B., Pedley, K. F., and Peterson, G. L. 2012. Preliminary assessment of resistance among U.S. wheat cultivars to the Triticum pathotypes of *Magnaporthe oryzae*. Plant Dis. 96:1501-1505.

Cruz, C. D., Kiyuna, J., Bockus, W. W., Todd, T. C., Stack, J. P., and Valent, B. 2015. *Magnaporthe oryzae* conidia on basal wheat leaves as a potential source of wheat blast inoculum. Plant Pathol. 64:1491-1498.

Cruz, C. D., Magarey, R. D., Christie, D. N., Fowler, G. A., Fernandes, J. M., Bockus, W. W., Valent, B., and Stack, J. P. 2016. Climate suitability for *Magnaporthe oryzae* Triticum pathotype in the United States. Plant Dis. 100:1979-1987.

Cruz, C. D., Bockus, W. W., Stack, J. P., Valent, B., Maciel, J. N., and Peterson, G. 2016. A standardized inoculation protocol to test wheat cultivars for reaction to head blast caused by *Magnaporthe oryzae* (Triticum pathotype). Plant Health Prog. 17:186-187.

Cruz. C. D., Peterson. G. L., Bockus, W. W., Kankanala, P., Dubcovsky, J., Jordan, K. W., Akhunov, E., Chumley, F., Baldelomar, F. D., Valent, B. 2016. The 2NS translocation from *Aegilops ventricosa* confers resistance to the Triticum pathotype of *Magnaporthe oryzae*. Crop Sci 56:990–1000.

Cruz, M. F. A., Prestes, A. M., Maciel, J. L .N., Scheeren, P. L. 2010. Partial resistance to blast on common and synthetic wheat genotypes in seedling and in adult plant growth stages. Trop Plant Pathol 35:24–31

Cruz, C. D., Santana, F. M., Todd, T. C., Maciel, J. L., Kiyuna, J., Baldelomar, D. F., Cruz, A. P., Lau, D., Seixas, C. S., Goulart, A. C., Sussel, A. A., Schipanski, C. A., Chagas, D. F., Coelho, M., Montecelli, T. D., Utiamada, C., Custódio, A. P., Rivadeneira, M. G., Bockus, W. W., and Valent, B. 2019. Multi-environment assessment of fungicide

performance for managing wheat head blast (WHB) in Brazil and Bolivia. Trop. Plant Pathol. 44**:**183–191.

Cruz, C. D. and Valent, B. 2017. Wheat blast disease: danger on the move. Tropical Plant Pathology 42:210-222.

Danelli, A. L. D., Fernandes, J. M. C., Maciel, J. L. N., Boaretto, C., and Forcelini, C. A. 2019. Monitoring *Pyricularia sp*. airborne inoculum in Passo Fundo, Rio Grande do Sul – Brazil. Summa Phytopathol. 45:361-367.

de Oliveira Coelho, M. A., Torres, G. A. M., Cecon, P. R., and Santana, F. M. 2016. Sowing date reduces the incidence of wheat blast disease. Pesquisa Agropecuaria Brasileira 51:631-637.

Del Ponte, E. M., Shah, D. A., and Bergstrom, G. C. 2003. Spatial patterns of Fusarium head blight in New York wheat fields suggest role of airborne inoculum. Plant Health Prog. Doi:10.1094/PHP-2003-0418-01-RS.

Derrick, B., Toher, D., and White, P. 2016. Why Welch's test is Type I error robust. Quantitative Methods for Psychology. 12:30-38.

Dung, J. K., Alterman, S. C., Walenta, D. L., and Hamm, P. B. 2016. Spatial patterns of ergot and quantification of sclerotia in perennial ryegrass seed fields in eastern Oregon. Plant Dis. 100:1110-1117.

Durbin, J., and Watson, G. S. 1950. Testing for serial correlation in least squares regression, I. Biometrika. 37:409–428.

Duveiller, E., Hodson, D., and von Tiedemann, A. 2010. Wheat blast caused by *Maganaporthe oryzae*: a reality and new challenge for wheat research. The 8th International Wheat Conference. St. Petersburg, Russia. Vavilov Research Institute of Plant Industry.

Economic Research Service (ERS), U.S. Department of Agriculture (USDA). Wheat data report – All years. Assessed May 2021. Available online. https://www.ers.usda.gov/data-products/wheat-data/.

Engle, J. S., Madden, L. V., and Lipps, P. E. 2003. Evaluation of inoculation methods to determine resistance reactions of wheat to *Fusarium graminearum*. Plant Disease, 87:1530-1535.

FAO. FAOSTAT. Wheat crop production. Assessed May 2021. Available online. http://www.fao.org/faostat/en/#search/wheat.

Farman, M., Peterson, G., Chen, L., Starnes, J., Valent, B., Bachi, P., Murdock, L., Hershman, D., Pedley, K., Fernandes, J. M., and Bavaresco, J. 2017. The Lolium pathotype of *Magnaporthe oryzae* recovered from a single blasted wheat plant in the United States. Plant Dis. 101:684-692.

Ferreira, J. R., Vancini, C., Deuner, C. C., Torres, G. A. M., Consoli, L., Seixas, C. D. S. 2018. Absence of 2NS/2AS in wheat resistance sources to *Magnaporthe oryzae* in Brazil. Boletim de Pesquisa e Desenvolvimento. Online publication. https://www.embrapa.br/busca-de-publicacoes/-/publicacao/1095170/absence-of-2ns2as-in-wheat-resistance-sources-to-magnaporthe-oryzae-in-brazil.

Gigot, C., Turechek, W., and McRoberts, N. 2017. Analysis of the spatial pattern of strawberry angular leaf spot in California nursery production. Phytopathology 107:1243-1255.

Gladieux, P., Condon, B., Ravel, S., Soanes, D., Maciel, J.L.N., Nhani, A., Chen, L., Terauchi, R., Lebrun, M.-H., Tharreau, D., Mitchell, T., Pedley, K.F., Valent, B., Talbot, N. J., Farman, M., and Fournier, E. 2018. Gene flow between divergent cereal- and grass-specific lineages of the rice blast fungus *Magnaporthe oryzae*. mBio, 9: e01219-17. https://doi.org/10.1128/mBio.01219-17.

Goddard, R., Steed, A., Chinoy, C., Ferreira, J. R., Scheeren, P. L., Maciel, J. L. N., and Nicholson, P. 2020. Dissecting the genetic basis of wheat blast resistance in the Brazilian wheat cultivar BR 18-terena. BMC Plant Biol. 20:1-15.

Godfrey, L. G. 1978a. Testing for Higher Order Serial Correlation in Regression Equations When the Regressors Include Lagged Dependent Variables. Econometrica 46: 1303–1310.

Godfrey, L. G. 1978b. Testing for Higher Order Serial Correlation in Regression Equations When the Regressors Include Lagged Dependent Variables. Econometrica 46: 1303–1310.

Goel M.K., Khanna P., and Kishore J. 2010. Understanding survival analysis: Kaplan-Meier estimate. Int J Ayurveda Res. 1:274-8.

Gomes, D. P. 2012. Incidêcia de *Pyricularia grisea* em genótipos de trigo em função da quantidade de inóculo inicial no campo: availaçao de danos e métodos de detecção nas sementes. Viçosa Minas Gerais, Brasil.

Gomes, D. P., Rocha, V. S., Pereira, O. L., and De Souza, M. A. 2017. Damage of wheat blast on the productivity and quality of seeds as a function of the initial inoculum in the

field. [Danos da brusone do trigo na produtividade e na qualidade das sementes em função do inóculo inicial no campo] Journal of Seed Science 39:66-74.

Gomes, D. P., Rocha, V. S., Rocha, J., de Souza, M. A., and Pereira, O. L. 2019. Temporal progression of wheat blast as a function of primary inoculum, fungicide application and genotype resistance. [Progresso temporal da brusone do trigo em função do inóculo primário, da aplicação de fungicida e da resistência dos genótipos] Summa Phytopathol. 45:50-58.

Gongora-Canul, C., Salgado, J. D., Singh, D., Cruz, A. P., Cotrozzi, L., Couture, J., Rivadeneira, M. G., Cruppe, G., Valent, B., Todd, T., Poland, J., and Cruz, C. D. 2020. Temporal dynamics of wheat blast epidemics and disease measurements using multispectral imagery. Phytopathology 110:393-405.

Gongora-Canul, C., Salgado, J. D., Singh, D., Cruz, A. P., Cotrozzi, L., Couture, J., Rivadeneira, M. G., Cruppe, G., Valent, B., Todd, T., Poland, J., and Cruz, C. D. 2020. Temporal dynamics of wheat blast epidemics and disease measurements using multispectral imagery. Phytopathology 110:393-405.Goulart, A. C. P., and Paiva F. A. 1992. Incidência da brusone (*Pyricularia oryzae*) em diferentes cultivares de trigo (Triticum aestivum) em condições de campo. Fitopatol. Bras. 17:321-325.

Goulart, A. C. P., Sousa, P. G., Urashima, A. S. 2007. Danos em trigo causados pela infecção de *Pyricularia grisea*. Summa Phytopathologica 33:358-363.

Greer, C. A., and Webster, R. K. 2001. Occurrence, distribution, epidemiology, cultivar reaction, and management of rice blast disease in California. Plant Dis. 85:1096-1102.

Guo, F., Chen, X., Lu, M., Yang, L., Wang, S., and Ming Wu, B. 2018. Spatial analysis of rice blast in China at three different scales. Phytopathology 108:1276-1286.

Harmon, P. F., and Latin, R. 2003. Gray leaf spot of perennial ryegrass. Plant Health Progress. Online publication. doi.org/10.1094/PHP-2003-1223-01-DG.

Igarashi, S., Utiamada, C. M., Igarashi, L. C., Kazuma, A. H., and Lopes, R. S. 1986. Pyricularia em trigo, ocorrência de Pyricularia sp. no estado do Paraná. Fitopatol. Bras. 11:351-352.

Igarashi S. 1990. Update on wheat blast (*Pyricularia oryzae*) in Brazil. In: Saunders DA (ed) Wheat for the nontraditional warm areas: a proceedings of the international conference. Foz do Iguaçu, Brazil, pp 480–483.

Igarashi, S., Utiamada, C. M., Igarashi, L. C., Kazuma, A. H., and Lopes, R. S. 1986. *Pyricularia* em trigo, occurrence de *Pyricularia* sp. no estado do Paraná. Fitopatol. Bras. 11:351-352.

Inoue, Y., Vy, T. T., Yoshida, K., Asano, H., Mitsuoka, C., Asuke, S., Anh, V., Cumagun, C. J., Chuma, I., Terauchi, R., Kato, K., Mitchell, T., Valent, B., Farman, M., and Tosa, Y. 2017. Evolution of the wheat blast fungus through functional losses ni a host specificity determinant. Science 357:80-83.

Islam, M.T., Croll, D., Gladieux, P., Soanes, D.M., Persoons, A., and Bhattacharjee, P. 2016. Emergence of wheat blast in Bangladesh was caused by a South American lineage of *Magnaporthe oryzae*. BMC Biology, 14. Online publication. https://bmcbiol.biomedcentral.com/articles/10.1186/s12915-016-0309-7.

Islam, M. T., Gubta, D. R., Hossain, A., Roy, K. K., He, X., Kabir, M. R., Singh, P. K., Khan, A. R., Rahman, M., and Wang, G. L. 2020. Wheat blast: a new threat to food security. Phytopathol. Research 2:28. Online publication. https://doi.org/10.1186/s42483-020-00067-6.

Kaplan, E. L., and Meier, P. 1958. Nonparametric estimation from incomplete observations. J. Amer. Statist. Assoc. 53:457–481.

Kemler, M., Kohn, L. M., Lebrun, M-H., Stajich, J. E., Talbot, N. J., Terauchi, R., Tharreau, R., and Zhang, N. 2019. *Pyricularia graminis-tritici* is not the correct species name for the wheat blast fungus: response to Ceresini et al. (MPP 20:2). Mol. Plant Pathol. 20:173-179.

Kohli, M. M., Mehta, Y. R., Guzman, E., Viedma, L., and Cubilla, L. E. 2011. *Pyricularia* blast - a threat to wheat cultivation. Czech J. Genet. Plant Breed. 47:S130-S134.

Kriss, A. B., Paul, P. A., and Madden, L. V. 2012. Characterizing heterogeneity of disease incidence in a spatial hierarchy: A cast study from a decade of observations of Fusarium head blight of wheat. Ecol. and Epidemiol. 102:867-877.

Large, E. C. 1954. Growth stages in cereals illustration of the Feekes scale. Plant Pathol. 3:128-129.

Levin, S. A. 1992. The problem of pattern and scale in ecology: The Robert H. MacArthur award lecture. Ecol. 73:1943-1967.

Lima, M. 2004. Giverela ou brusone? Orientações para indentificação correta dessas enfermidades em trigo e em cevada. Embrapa Trigo Documentos online, 40. http://www.cnpt.embrapa.br/biblio/do/p_do40.pdf

Luan, J., Muetzelfeldt, R. I., and Grace, J. 1996. Hierarchical approach to forest ecosystem simulation. Ecol. Model. 86:37-50.

Maciel, J. L. N., Ceresini, P. C., Castroagudin, V. L., Zala, M., Kema, G. H. J., and McDonald, B. A. 2014. Population structure and pathotype diversity of the wheat blast pathogen *Magnaporthe oryzae* 25 years after its emergence in Brazil. Phytopathology 104: 95-107.

Madden, L.V., and Hughes, G. 1995. Plant disease incidence: distributions, heterogeneity, and temporal analysis. Annu. Rev. Phytopathol. 33:529-564.

Madden, L. V., Hughes, G., and van den Bosch, F. 2007a. The study of plant disease epidemics. First. The American Phytopathological Society. Saint Paul, MN.

Madden, L. V., Paul, P. A., and Lipps, P. E. 2007b. Consideration of nonparametric approaches for assessing genotype-by-environment (G x E) interaction with disease severity. Plant Dis. 91:891-900.

Madden, L. V., Piepho, H. P., and Paul, P. A. 2016. Statistical models and methods for network meta-analysis. Phytopathology 106:792-806.

Madden, L. V., Reynolds, K. M., Pirone, T. P., and Raccah, B. 1987. Analysis of the spatial patterns of virus-diseased tobacco plants. Phytopathology 77:1409-1417.

Madden, L. V., Reynolds, K. M., Pirone, T. P., and Raccah, B. 1988. Modeling of tobacco virus epidemics as spatio-temporal autoregressive integrated moving-average processes. Phytopathology 78:1361-1366.

Malaker, P. K., Barma, N. C. D., Tiwari, T. P., Collis, W. J., Duveiller, E., Singh, P. K., Joshi, A. K., Singh, R. P., Braun, H. J., Peterson, G. L., Pedley, K. F., Farman, M. L., and Valent, B. 2016. First Report of Wheat Blast Caused by *Magnaporthe oryzae* pathotype Triticum in Bangladesh. Plant Disease 100:2330-2330.

Martínez, S. I., Sanabria, A., Fleitas, M. C., Consolo, V. F., and Perelló, A. 2019. Wheat blast: Aggressiveness of isolates of *Pyricularia oryzae* and effect on grain quality. Journal of King Saud University - Science 31:150-157.

McRoberts, N., Hughes, G., and Madden, L. V. 2003. The theoretical basis and practical application of relationships between different disease intensity measurements in plants. Ann. Appl. Biol. 142:191-211.

Mehta, Y. R., Riede, C. R., Campos, L. A. C., and Kohli, M. M. 1992. Integrated management of major wheat diseases in Brazil: An example for the southern cone region of Latin America. Crop Protection, 11: 517-524.

Miedaner, T., Schneider, B., and Geiger, H. H. 2003. Deoxynivalenol (DON) content and Fusarium head blight resistance in segregating populations of winter rye and winter wheat. Crop Breeding, Gen. & Cytology 43:519-526.

Mihail, J. D. 1989. *Macrophomina phaseolina*: Spatio-temporal dynamics of inoculum and of disease in highly susceptible crop. Phytopathology 79:848-855.

Milazzo, J., Pordel, A., Ravel, S. and Tharreau, D. 2009. First scientific report of *Pyricularia oryzae* causing gray leaf spot disease on perennial ryegrass (*Lolium perenne*) in France. Plant Dis. 103:1024.

Mills, K. B., Madden, L. V., and Paul, P. A. 2020. Quantifying the effects of temperature and relative humidity on the development of wheat blast caused by the Lolium pathotype of *Magnaporthe oryzae*. Plant Dis. 104:2622-2633.

Mills, K. B., Paul, P. A., Madden, L. V., and Peterson, G. L. 2015. Preliminary assessment of differential susceptibility of northern soft red winter wheat cultivars to Lolium and Triticum pathotypes of *Magnaporthe oryzae*. Phytopathology 105:S4.96.

Mills, K. B., Salgado, J. D., Cruz, C. D., Valent, B., Madden, L. V., and Paul, P. A. 2021. Comparing the temporal development of wheat spike blast epidemics in a region of Bolivia where the disease is endemic. Plant Dis. 105:96-107.

Moran, P. A. 1950. Notes on continuous stochastic phenomena. Biometrika 37:467-471.

Mottaleb, K. A., Singh, P. K., Sonder, K., Kruseman, G., and Erenstein, O. 2019. Averting wheat blast by implementing a 'wheat holiday': In search of alternative crops in West Bengal, India. PLoS ONE. Online publication. doi:10.1371/journal.pone.0211410.

Murakami, J., Tosa, Y., Kataoka, T., Tomita, R., Kawasaki, J., Chuma, I., and Mayama, S. 2000. Analysis of host species specificity of *Magnaporthe grisea* toward wheat using a genetic cross between isolates from wheat and foxtail millet. Phytopathology 90: 1060-1067.

Naidu, R., Rowhani, A., Fuchs, M., Golino, D., and Martelli, G. P. Grapevine leafroll: a complex viral disease affecting a high-value fruit crop. Plant Dis. 98:1172-1185.

NC State Extension. 2018. Gray leaf spot on the rise in North Carolina. Assessed May 2021. Available online. https://turfpathology.ces.ncsu.edu/2018/10/gray-leaf-spot-on-the-rise-in-north-carolina/.

Nicot, P. C., Rouse, D. I., and Yandell, B. S. 1984. Comparison of statistical methods for studying spatial patterns of soilborne plant pathogens in the field. Phytopathology 74:1399-1402.

Nita, M., Ellis, M. A., Wilson, L. L., and Madden, L. V. 2007. Evaluations of new and current management strategies to control Phomopsis cane and leaf spot of grape. Plant Health Prog. Doi:10.1094/PHP-2007-0726-06-RS.

Noe, J. P. and Campbell. 1985. Spatial pattern analysis of plant-parasitic nematodes. J. of Nematology 17:86-93.

Nesi, C. N., Shimakura, S. E., Ribeiro Junior, R. J., and De Mio, L. L. 2013 Survival analysis in plant pathology. IDESIA (Chile). 31:017-110.

Ojiambo P. S., and Scherm, H. 2005. Survival analysis of time to abscission of blueberry leaves affected by Septoria leaf spot. Phytopathology 95: 108-113.

Pagani, A. P. S., Dianese, A. C., and Café-Filho, A. C. 2014. Management of wheat blast with synthetic fungicides, partial resistance and silicate and phosphite minerals. Phytoparasitica 42: 609-617.

Paul, P. A., Bradley, C. A., Madden, L. V., Lana, F. D., Bergstrom, G. C., Dill-Macky, R., Wise, K. A., Esker, P. D., McMullen, M., Grybauskas, A., Kirk, W. W., Milus, E., and Rudin, K. 2018. Effects of pre- and postanthesis applications of demethylation inhibitor fungicides on Fusarium head blight and deoxynivalenol in spring and winter wheat. Plant Dis. 102:2500-2510.

Paul, P. A., El-Allaf, S. M., Lipps, P. E., and Madden, L. V. 2005. Relationships between incidence and severity of Fusarium head blight on winter wheat in Ohio. Phytopathology. 95:1049-1060.

Paul, P. A., and Munkvold, G. P. 2005. Influence of temperature and relative humidity on sporulation of *Cercospora zeae-maydis* and expansion of gray leaf spot lesions on maize leaves. Plant Dis. 89:624-630.

Paul, P. A., Salgado, J. D., Bergstrom, G., Bradley, C. A., Byamukama, E., Byrne, A. M., Chapara, V., Cummings, J. A., Chilvers, M. I., Dill-Macky, R., Friskop, A., Kleczewski, N., Madden, L. V., Nagelkirk, M., Stevens, J., Smith, M., Wegulo, S. N., Wise, K., and Yabwalo, D. 2019. Integrated effects of genetic resistance and Prothioconazole + Tebuconazole application timing on Fusarium head blight in wheat. Plant Dis. 103: 223-237.

Pieck, M. L., Ruck, A., Farman, M. L., Peterson, G. L., Stack, J. P., Valent, B., and Pedley, K. F. 2017. Genomics-Based Marker Discovery and Diagnostic Assay Development for Wheat Blast. Plant Dis. 101:103-109.

Prabhu, A. S.; Filippi, M. C., and Castro, N. 1992. Pathogenic variation among isolates of *Pyricularia oryzae* affecting rice, wheat, and grasses in Brazil. Journal of Tropical Pest Management 38:367-371.

Prestes, A.M., Arendt, P.F., Fernandes, J.M.C., and Scheeren, P.L. 2007. Resistance to *Magnaporthe grisea* among Brazilian wheat genotypes. Buck H.T., Nisi J.E., Salomón N. (eds) Wheat Production in Stressed Environments. Developments in Plant Breeding, vol 12. Springer, Dordrecht.

Reynolds, K. M., and Madden, L. V. 1987. Analysis of epidemics using spatio-temporal autocorrelation. Phytopathology 78:240-246.

Rios, A., Debona, D., Duarte, H., and Rodrigues, F. 2013. Development and validation of a standard area diagram set to assess blast severity on wheat leaves. Eur. J. Plant Pathol. 136:603-611.

Rios, J. A., Rios, V. S., Paul, P. A., Souza, M. A., Araujo, L., and Rodrigues, F. A. 2016. Fungicide and cultivar effects on the development and temporal progress of wheat blast under field conditions. Crop Prot. 89:152-160.

Rios, J. A., Rios, V. S., Paul, P. A., Souza, M. A., Neto, L. B. M. C., and Rodrigues, F. A. 2017. Effects of blast on components of wheat physiology and grain yield as influenced by fungicide treatment and host resistance. Plant Pathol. 66:877-889.

Ristaino, J. B., Gumpertz, M. L. 2000. New frontiers in the study of dispersal and spatial analysis of epidemics caused by species in the genus *Phytophthora*. Annu. Rev. Phytopathol. 38:541-576.

Rosciglione, B., Castellano, M. A., Martelli, G., P., Savino, V., and Canizzaro, G. 1983. Mealybug transmission of grapevine virus A. Vitis 22:331-347.

Sadat, A. and Choi, J. 2017. Wheat blast: A new fungal inhabitant to Bangladesh threatening world wheat production. Plant Pathol. 33:103-108.

Saharan, M. S., Bhardwaj, S. C., Chatrath, R., Sharma, P., Choudhary, A. K., and Gupta, R. K. 2017. An overview Journal of Wheat Research 8:1-5

Scherm, H. and Ojiambo, P. S. 2004. Applications of survival analysis in botanical epidemiology. Phytopathology 94:1023-1026.

Schmale III, D. G., and Bergstrom, G. C. 2003 Fusarium head blight in wheat. The Plant Health Instructor. Online publication. doi:10.1094/PHI-I-2003-0612-01.

Shafer, M., Ojima, D., Antle, J. M., Kluck, D., McPherson, R. A., Peterson, S., Scanlon, B., and Sherman, K. 2014. Great Plains. Climate change impacts in the United States: the third national climate assessment. U. S. Global Change Research Program, Washington, D. C.

Silva, G. B., and Prabhu, A. S. 2005. Quantificação de conídios de *Pyricularia grisea* no plantio direto e convencional de arroz de terras altas. Fitopatologia Brasileira, Brasília 30:569-573.

Skelsey, P., Elphinstone, J. G., Saddler, G. S., Wale, S. J., and Toth, I. K. 2015. Spatial analysis of blackleg-affected seed potato crops in Scotland. Plant Pathol. Doi:10.1111/ppa.12455.

Stroup, W. W. Milliken, G. A., Claassen, E. A., and Wolfinger, R. D. 2018. SAS® for Mixed Models: Introduction and Basic Applications. SAS Institute Inc., Cary, NC, USA.

Suriya Rao, a. V., Mukherjee, A. K., Mohapatra, N. K., and Nayak, P. 2007. Spatial distribution of rice blast disease under natural field epidemics. R. J. of Agric.and Biol. Sci. 3:615-620.

Surovy, M.Z., Mahmud, N.U., Bhattacharjee, P., Hossain, M.S., Mehebub, M.S., Rahman, M., Majumdar, B. C., Gupta, D. R., and Islam, T. 2020. Modulation of nutritional and biochemical properties of wheat grains infected by blast fungus *Magnaporthe oryzae* Triticum pathotype. Frontiers in Microbiol. 11:1174.

Suzuki, H. 1975. Meteorological factors in the epidemiology of rice blast. Annual Review of Phytopathology 13:239-256.

Tembo, B., Mulenga, R. M., Sichilima, S., M'siska, K. K., Mwale, M., Chikoti, P. C., Singh, P. K., He, X., Pedley, K. F., Peterson, G. L., Singh, R. P., and Braun, H. J. 2020. Detection and characterization of fungus (*Magnaporthe oryzae pathotype* Triticum)

causing wheat blast disease on rain-fed grown wheat (*Triticum aestivum L*.) in Zambia. PLoS ONE 15(9): e0238724. https://doi.org/10.1371/journal.pone.0238724

Torres, G., Santana, F., Fernandes, J., and Só E Silva, M. 2009. Doenças da espiga causam perda de rendimento em trigo nos estados do Paraná, São Paulo e Mato Grosso do Sul. Emprapa Trigo. Comunicado Técnico online, 255. https://www.infoteca.cnptia.embrapa.br/bitstream/doc/821793/1/pco255.pdf

Tosa, Y., Hirata, K., Tamba, H., Nakagawa, S., Chuma, I., Isobe, C., Osue, J., Urashima, A. S., Don, L. D., Kusaba, M., Nakayashiki, H., Tanaka, A., Tani, T., Mori, N., and Mayama, S. 2004. Genetic constitution and pathogenicity of Lolium isolates of *Magnaporthe oryzae* in comparison with host species specific pathotypes of the blast fungus. Phytopathology 94:454-462.

Turechek, W. W. and Madden, L. V. 2001. Effect of scale on plant disease incidence and heterogeneity in a spatial hierarchy. Ecol. Model. 144:77-95.

Uddin, W., Serlemitsos, K., and Viji, G. 2003 (a). A temperature and leaf wetness duration-based model for prediction of gray leaf spot of perennial ryegrass turf. Phytopathology 93:336-343.

Uddin, W., Viji, G., and Vincelli, P. 2003 (b). Gray leaf spot (blast) of perennial ryegrass turf: an emerging problem for the turfgrass Industry. Plant Dis. 87:880-889.

Upton, G. J., and Fingleton, B. 1985. Spatial data analysis by example. Volume 1: Point pattern and quantitative data. J. Wiley and Sons (eds) Chichester, New York.

Urashima A. S. 2010. Wheat blast. In: Bockus W.W., Bowden R.L., Hunger R.M., Murray T.D., Smiley RW (eds) Compendium of wheat diseases and pests. American Phytopathological Society Press, St. Paul, pp 22–23.

Urashima, A. S., Grosso, C. R. F., Stabili, A., Freitas, E. G., Silva, C. P., Netto, D. C. S., Franco, I., and Merola Bottan, J. H. 2009. Effect of *Magnaporthe grisea* on seed germination, yield, and quality of wheat. Wang, G. W., and Valent, B. (eds) Advances in genetics, genomics and control of rice blast disease. Springer, Netherlands, pp 267-277.

Urashima, A. S., Igarashi, S., and Kato, H. 1993. Host range, mating type, and fertility of *Pyricularia grisea* from wheat in Brazil. Plant Dis. 77:1211-1216.

Urashima, A. S., Lavorent, N. A., Goulart, A. C. P., and Mehta, Y. R. 2004. Resistance spectra of wheat cultivars and virulence diversity of *Magnaporthe grisea* isolates in Brazil. Fitopatologia Brasileira 29:511-518.

Valent, B., Farman, M., Tosa, Y., Begerow, D., Fournier, E., Gladieux, P., Islam, M. T., Kamoun, S., Kemler, M., Kohn, L. M., Lebrun, M.-H., Stajich, J. E., Talbot, N. J., Terauchi, R., Tharreau, R., and Zhang, N. 2019. *Pyricularia graminis-tritici* is not the correct species name for the wheat blast fungus: response to Ceresini et al. (MPP 20:2). Mol. Plant Pathol. 20:173-179.

Viji, G., Wu, B., Kang, S., Uddin, W., and Huff, D. R. 2001. *Pyricularia grisea* causing gray leaf spot of perennial ryegrass turf: Population structure and host specificity. Plant Disease 85: 817-826.

Villari, C., Mahaffee, W. F., Mitchell, T. K., Pedley, K. F., Pieck, M. L., and Peduto Hand, F. 2017. Early detection of airborne inoculum of *Magnaporthe oryzae* in turfgrass fields using a quantitative LAMP assay. Plant Disease, 101:170-177.

Vincelli, P., and Dixon, E. 2002. Resistance to QoI (strobilurin-like) fungicides in isolates of *Pyricularia grisea* from perennial ryegrass. Plant Dis. 86:235-240.

Waggoner, P. E. 1986. Progress curves of foliar diseases: Their interpretation and use. Plant Disease Epidemiology. Vol. 1, Population Dynamics and Management. Leonard, K. J. and Fry, W. (eds) Macmillan, New York, pp 3-37.

Welch, B. L. 1947. The generalization of 'student's' problem when several different population variances are involved. Biometrika 34: 28–35.

White, H. 1980. A heteroskedasticity-consistent covariance matrix estimator and a direct test for heteroskedasticity. Econometrica 48:817–838

Wilson, R. A., and Talbot, N. J. 2009. Under pressure: investigating the biology of plant infection by *Magnaporthe oryzae*. Nat Rev Microbiol. 7:185-95.

Yasuhara-Bell, J., Pedley, K. F., Farman, M., Valent, B., and Stack, J. P. 2018. Specific detection of the wheat blast pathogen (*Magnaporthe oryzae* Triticum) by loop-mediated isothermal amplification. Plant Dis. 102: 2550-2559.

Yesmin, N., Jenny, F., Abdullah, H. M., Hossain, M. M., Kader, M. A., Solomon, P. S., and Bhuiyan, M. A. H. B. 2020. A review on South Asian wheat blast: The present status and future perspective. Plant Pathol. 69:1618-1629.

Yoshida, K., Saunders, D.G.O., Mitsuoka, C., Natsume, S., Kosugi, S., Saitoh, H., Inoue, Y., Chuma, Y., Tosa, Y., Cano, L. M., Kamoun, S., and Terauchi, R. 2016. Host specialization of the blast fungus *Magnaporthe oryzae* is associated with dynamic gain and loss of genes linked to transposable elements. BMC Genomics 17:1.

Zhang, Z., Jeske, D. R., Cui, X., and Hoddle, M. 2012. Co-clustering spatial data using a generalized linear mixed model with application to the integrated pest management. 2012. J. Agric. Biol. And Envir. Statistics 17:265-282.